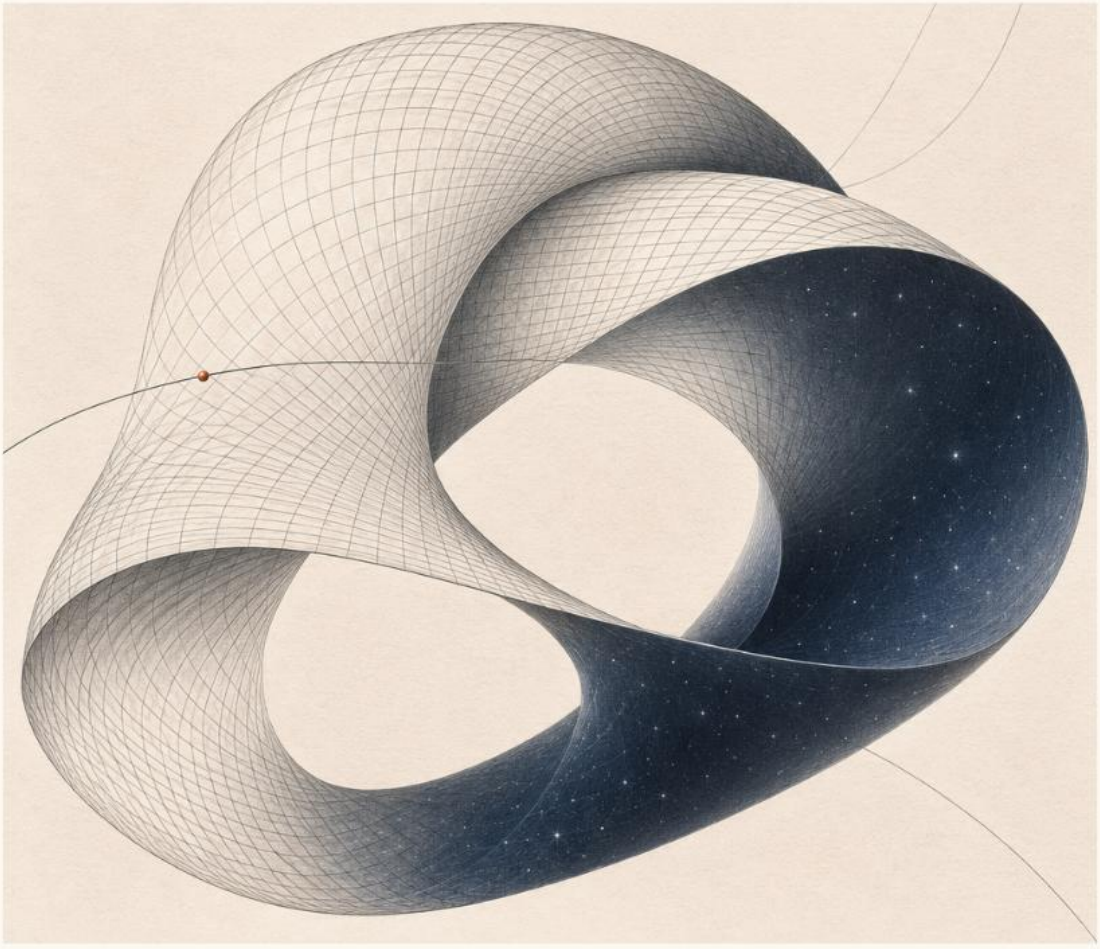
# The World Has Nowhere to Fit



Eudgene Brenev
Mira Veyran

2026

*Eudgene Brenev*
*Mira Veyran*

# The World Has Nowhere to Fit

*The Origin and Structure of the Universe at the Frontier of Scientific Knowledge*

*2026*

# Contents

Illustrations ..... 4
Preface ..... 5

**I Observable Universe**

1 The world has nowhere to fit ..... 7
2 How to see the past ..... 13
3 What's expanding ..... 18
4 Thermal history ..... 24
5 The Universe before the first stars ..... 33

**II Invisible components**

6 Invisible mass ..... 42
7 Why matter remained ..... 48
8 Accelerating Universe ..... 54
9 How much does emptiness weigh? ..... 62
10 Where the measurements diverge ..... 69

**III Before the usual start**

11 Where did the structure come from? ..... 78
12 Was the origin of cosmic structure quantum? ..... 85
13 Before the hot start ..... 92
14 Why does time have a direction? ..... 98

**IV Underlying Structure**

15 What is the “where” made of? ..... 106
16 Additional dimensions ..... 114
17 Can space close on itself? ..... 120
18 Other universes ..... 126
19 When Gravity Goes Quantum ..... 132

**V Open future**

20 Several futures of one Universe ..... 138
21 How to pose a question to nature ..... 145
22 Cosmology with AI ..... 151

Epilogue ..... 160
Appendix A Calculations and limits of their applicability ..... 162
Appendix B Research programs ..... 175
Appendix C Computational tasks and reproduction ..... 184
Glossary ..... 187
References ..... 193

# Illustrations

Engravings accompany explanations and help present models, analogies and experimental design. Calculation graphs and diagrams are indicated separately in the text as figures.

## Engravings

1. Geometry can be measured from inside ..... 8
2. The observed area depends on the observer ..... 10
3. The last scattering opens the way for light ..... 15
4. Distances grow, but bound systems maintain scale ..... 21
5. When early plasma leaves light nuclei ..... 26
6. From neutrino target to electronic signal ..... 30
7. Frequency reveals different layers of the past ..... 36
8. Radio observation from the far side of the Moon ..... 40
9. Light reveals invisible mass distribution ..... 43
10. Moving boundary between two phases ..... 51
11. Cosmological field and laboratory clock ..... 58
12. Void inside the complete installation ..... 65
13. Two routes to expansion scale ..... 71
14. From small inhomogeneities to the space network ..... 79
15. One statistical trail and different explanations ..... 86
16. The rebound hypothesis and the fate of disturbances ..... 94
17. Entropy and the removed restriction ..... 99
18. Condensation of matter and outgoing energy ..... 100
19. From quantum connections to geometric description ..... 109
20. Quantum simulator and geometric interpretation ..... 112
21. Direction hidden by resolution ..... 114
22. Short distance force measurement ..... 118
23. Two portraits of one source ..... 122
24. Areas of different field states ..... 128
25. Counting order of infinite ..... 129
26. Save quantum state ..... 136
27. General history and various sequels ..... 140
28. New measuring angle ..... 147
29. Fast calculation and accurate standard ..... 153
30. Checking on deferred data ..... 159

## Calculation drawings and diagrams

1. Cosmological distances ..... 22
2. Space history observation windows ..... 35
3. Reconstruction of the scalar potential ..... 57
4. Redshift drift ..... 59
5. General parameters of three observation channels ..... 76
6. Topology of a two-dimensional flat torus ..... 121
7. Spatial branches of two masses ..... 133
8. Two futures with a common past history ..... 143
9. Map of distinguishability of two models ..... 156

# Preface

Every scientific answer has a domain of applicability. This is easy to forget when the question concerns everything that exists. Measuring the ages of stars does not yet measure the age of time. Describing the hot early universe leaves its origin an open question. Establishing a boundary to the signals we can receive is only the beginning of understanding what that boundary tells us about the structure of the world.

This book explores cosmology from its observational foundations to problems that still lack generally accepted answers. We will consider space, time, matter, the early history of the universe, and its possible future. As we proceed, the degree of confidence changes: a precise measurement gives way to an inference within a model, followed by competing theoretical descriptions and proposals for new tests.

The title concerns a habit that has long helped us understand the things around us. Every object is somewhere, surrounded by other objects. Applied to all of space at once, this habit produces a demand for yet another place. Physics allows us to ask the question differently: what relationships make distance and direction possible, how are they measured, and do we need external coordinates to describe them? Attention to the wording becomes part of the investigation.

We will start with what actually reaches our instruments: light, particles, and changes in physical quantities. We will then examine how expansion and the early hot history are reconstructed. These foundations are needed to keep discussions of dark matter, extra dimensions, or the universe's prehistory connected to observation. Theoretical imagination is especially valuable when the commitments of already tested physics are understood.

Later chapters will repeatedly return to one requirement. A proposed general mechanism must have consistent consequences across different observations. The properties of new particles connect to the origin of matter. The geometry of additional directions connects to their spectrum and possible interactions. The dynamics of dark energy connect to expansion, the growth of structure, and, in some models, laboratory measurements. These connections expose a hypothesis to results that could contradict it.

Individual chapters address the era before the first stars, the gravity of the vacuum, and the testability of the quantum origin of structure. These subjects connect different levels of explanation: an unknown initial spectrum, the dynamics of already existing fields, and the conditions under which geometry itself becomes a physical object. Finally, we will consider how computation and artificial intelligence can help compare such explanations while preserving the ability to check every important step independently.

Each chapter includes a section on physical tests. It describes measurable quantities, existing or possible apparatus, principal sources of interference, and the limits of inference. Sometimes the next task is to reanalyze data. Sometimes a more precise laboratory experiment is needed. In other cases, we must first calculate a prediction that the hypothesis does not yet provide. A question about technology is meaningful only alongside a question about how explanations can be distinguished.

The main narrative addresses readers willing to engage with new concepts without already knowing all the mathematics of cosmology. A few formulas are needed directly to understand the relationships. More detailed conventions and reproducible examples appear in the appendices, along with

specific research programs, a glossary, and sources. The book allows two reading paces: following the ideas in sequence and returning to the calculations on which particular conclusions depend.

The computational examples have a defined status. They show how a model works, test a mathematical consequence, or demonstrate the ambiguity of a familiar inference. Their parameters should not automatically be treated as measured properties of the cosmos. The proposed joint tests develop existing scientific research directions; establishing priority for a particular new idea would require a dedicated comparison with the literature. Where an analysis of observational data has not yet been performed, this is stated explicitly.

Cosmology continues to develop. The value of an argument is not determined solely by the latest number in a table. What matters also includes how that number was obtained, how it depends on assumptions, and whether its necessary consequences can be tested by the same physical method or another one.

At the frontier of science, the difference between a question that sounds profound and one that can already be investigated is especially clear. Moving from the former to the latter often requires rebuilding the language itself. That is the task of this book: to make open problems clear enough for the next step to be described by an equation, an observation, or an experimental design.

**I Observable Universe**

**Chapter 1**

# The world has nowhere to fit

Let's put the box on the table. There is a stone inside, there is air around, and the city continues outside the walls of the room. Each object occupies part of the space, and each has an environment. We are so accustomed to this arrangement of things that we transfer it to the whole world. If the Universe exists, it also needs to be somewhere. If it expands, space should be freed up next to it. If it had a beginning, some other countdown must have preceded it.

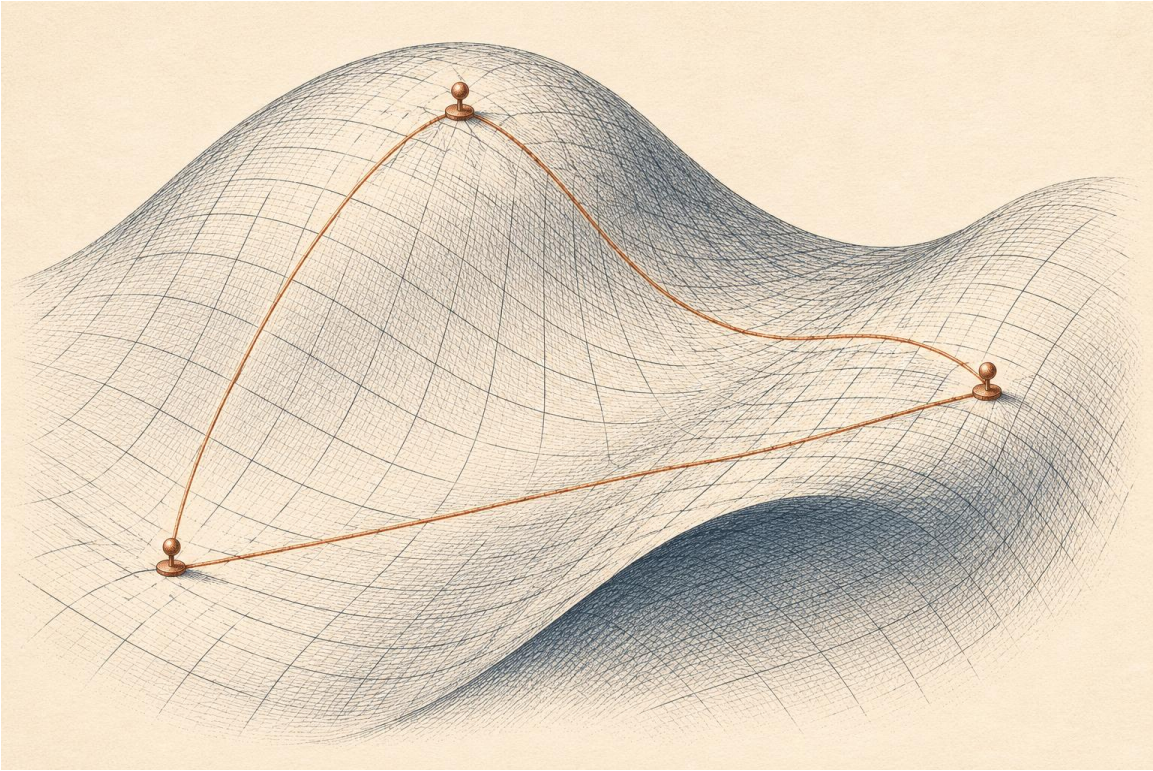
Thus arises the question that gives this book its title. It is difficult to resist him because in everyday life he almost never lets us down. But the word “Universe” changes the scale of the argument. We begin to ask about the conditions within which place, size and distance make sense at all. Rules that are appropriate for the box may not be sufficient for the space itself.

This is not the answer yet. You cannot simply ban the question of the external world by calling it wrong. Another thing we can do is figure out what assumptions we have already made to the question, which ones are necessary, and what observable consequences they lead to. It is this path that will allow us to move from the familiar picture of the sky to ideas that so far exist only in the form of mathematical models.

## Space without an outer box

Let's imagine a researcher who can measure distances, angles and travel times of signals, but cannot look at his world from the outside. He builds triangles from the shortest paths, compares their angles, and monitors the divergence of neighboring trajectories. These measurements tell him about geometry, even if there is no external scene in his description.

On a plane, the sum of the angles of a triangle composed of shortest paths is equal to two right angles. On a sphere you can go from the North Pole to the equator, turn at a right angle, go a quarter of the equator and, turning again, return to the pole along another meridian. You will get a triangle with three right angles. The traveler discovered the curvature without ever leaving the surface. The image of a sphere in three-dimensional space helps our imagination, but the result of the measurement is written in the language of the surface itself.



Engraving 1. Geometry can be measured from the inside. Measurements of distances and directions can be made within the space itself. The curved surface serves as a two-dimensional analogy here: the researcher learns about curvature from the routes and their relative positions. External perspective is necessary for the drawing, but is not a necessary part of the physical description; The exact metric is not given by this engraving.

This is where the useful part of the familiar balloon analogy ends. It shows how distances between points can increase without a designated center on the surface. But the rubber, the air inside and the room around the ball relate to the arrangement of the model on the table. It is impossible to transfer them to cosmology without an additional physical basis. To describe three-dimensional space, an external room is not necessary.

In the general theory of relativity, the geometry of space-time is included in the physical description. It determines how gaps are measured and what events can exchange signals. Matter and geometry are related by equations. Coordinates help indicate events, but they are not physical rods and clocks in themselves. They can be changed while maintaining the observed distances and times.

It does not follow from this that a more comprehensive structure is impossible. Theories with extra dimensions offer just such constructions. But this is an additional hypothesis that requires its own equations and tests. We do not yet have a logical requirement to place any physical world into another physical world. The endless chain of outer boxes comes from our original habit, not from a dimension.

## Three meanings of the word Universe

In conversation, the word “Universe” often serves several purposes at once. Sometimes it refers to all of physical reality. Sometimes - the space-time of a specific cosmological model. Sometimes - the area from which signals managed to arrive to us. These meanings overlap, but give different answers to the question of boundaries.

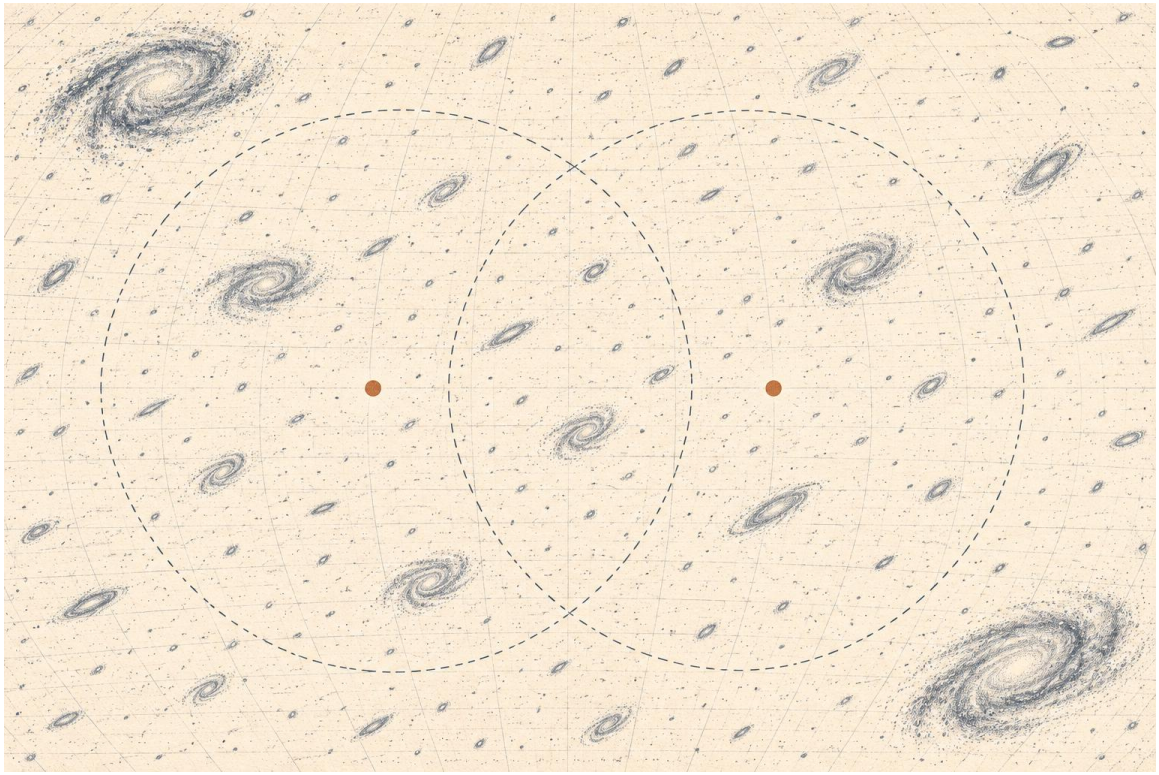
The observed area is limited by the history of signal propagation. Light has a finite local speed, but cosmic geometry changes. Therefore, information has reached us only about part of the events. The boundary of such access does not have to coincide with a physical wall, the end of a substance, or a break in space. A person far enough away would have a different observable area. Our position at its center expresses the way the map is constructed around the observer.

Standard cosmological geometry distinguishes between the particle horizon, the future event horizon, and the Hubble sphere. The first is related to the accessible past. The second limits the area from which a signal emitted at a selected moment can ever reach the observer; it depends on the entire subsequent expansion history and does not exist in every model. The third is determined by the current rate of expansion. Their radii generally differ. The Hubble sphere itself is not the absolute limit of visibility. [1]

To get a sense of the scale of the difference, consider a tutorial flat model with nonrelativistic matter, radiation, and a positive cosmological constant. The matter here includes ordinary and dark components; We will talk about the second in detail in chapter 6. With the chosen parameters close to standard cosmological values, the age is about 13.8 billion years, and the current particle horizon radius is about 46.1 billion light years. This is our calculation for the declared model; formulas and parameters are given in the appendix. The radius is not equal to age times the speed of light because distances changed as light traveled.

The number 46.1 billion already contains a method of comparison: the distances are recalculated for one current slice of cosmic time. The telescope itself does not see such a slice. The further we look, the earlier the state of the source we observe. The border of the accessible past and the map of distances today are connected by calculation, and do not coincide in the finished photograph.

By extending the model beyond the observational limit, we assume that its rules apply there as well. Such extrapolation may be well motivated, but it is different in meaning from measurement. The phrase “there is a similar Universe beyond” expresses a simple continuation of the model. The phrase “we see what lies next” requires a signal that we do not have.



Engraving 2. The observed area depends on the observer. Two conditional observation areas are built around different observers. They partially overlap, and the depicted environment continues beyond them. The outline denotes a restriction of access to signals, rather than a wall or the end of a substance. This is a clear analogy; the dimensions of the horizons and today's distances are determined by a separate cosmological calculation.

## Finiteness without a wall

The finitude of space is also not identical to the presence of an edge. You can define a geometry in which a traveler, moving long enough in a certain direction, returns to the starting point. In another space such a return is impossible. In small neighborhoods, these worlds may have the same geometric properties, but differ in the way they connect distant regions.

This connection method is studied by topology. Geometry is responsible, in particular, for distances and curvature; topology - for more general properties of connectivity. Therefore, the proximity of the observed spatial curvature to zero does not establish the infinite size of all space. There are flat compact models in which the volume is finite. The possibility of such a construction is a mathematical fact; The belonging of our Universe to this class must be decided by observations. [2]

But what if we assume a real physical border? Then you will need to describe the behavior of the substance and signals near it. Can light reach the border? What determines the state of the fields on it? Does it change the available vibrations and energy distribution? The word “edge” becomes a physical hypothesis only after such conditions appear. Drawing a wall in emptiness does not automatically define them.

One can also consider a region whose boundary simply lies outside causal accessibility. Its very remote existence then does not guarantee any measurable effect here. Verification will require additional connections - for example, the predicted impact on the overall history or on the state of the observed fields. If two models in the entire accessible region give the same probabilities of all

outcomes, the name of the outer region will not allow one to experimentally choose between them. This is the limit of formulated comparison, and not a prohibition on looking for more meaningful models.

For now, it is useful to hold on to one thought. The question “where is the edge” has an answer only after we have determined what object we are discussing and what we consider to be the edge. Sometimes the answer is a measurable horizon. Sometimes - a property of the selected topology. Sometimes a question requires new physics, because the very familiar description of space approaches the limit of applicability.

## From an imaginary world to a physical model

Cosmology allows for bold constructions, but the meaning of the word “allows” is limited here. We can write down a mathematically consistent geometry and still not know whether there is a process that can create it. We can obtain a solution to the equations and then find that small disturbances destroy it. We can find a stable model that predicts observed effects that have already been excluded by experiment. Each subsequent step introduces an additional requirement.

Therefore, the book will contain statements of varying strength. The spectrum recorded by the instrument refers to the data after calibration. The age obtained from a cosmological model depends on its assumptions. The possible additional dimension remains a hypothesis. A numerical example that shows the ambiguity of the derivation can be rigorous even if the parameters chosen for it do not describe real space.

We will distinguish between these cases in the argument itself. Sometimes the words “in this model” are more important than the number that follows them. Sometimes the absence of a signal narrows the parameters, but does not eliminate the entire class of explanations. Sometimes an idea doesn't yet have a calculated prediction, and the first necessary step is working with equations rather than building a more powerful telescope.

This discipline has practical meaning. If the question is posed too broadly, any observation can easily be declared compatible with the hypothesis. For example, beyond the horizon one can imagine almost any structure in the world. As long as the device does not affect the available data and is not related to the theory being tested, the observer has nothing to compare with its predictions. To advance, you need to find a specific consequence that might turn out to be false.

The possibility of verification also has several levels. The installation may lack precision. The desired epoch may be hidden by the opacity of early material. Several different mechanisms can produce the same signal. Finally, two descriptions may be physically equivalent over the entire accessible region. Solutions to these problems vary. Magnifying the telescope mirror does not help in all cases.

## How to check it

Let's start with the assumption on which the simple cosmological picture rests: on sufficiently large scales, space is described by a single homogeneous and isotropic geometry. Galaxies and voids make the real Universe inhomogeneous, so we are talking about a large-scale approximation and its accuracy. This approximation itself can be checked through the consistency of different distances and expansion rates.

Physically, two types of measurements are needed. The angular sizes of statistical structures in the distribution of galaxies provide transverse scales. The redshift distribution of the same structures carries information about the radial expansion. Additional estimates of time can be obtained from differences in the ages of stellar populations, although here one must take into account their evolutionary models. No channel is free from assumptions, so it is useful to make them explicit and compare independent calibration methods.

In Friedmann-Lemaître-Robertson-Walker geometry, distances and expansion rates are related so that data from different eras should restore the same value of today's curvature parameter. The physical curvature of spatial slices may change during expansion; the parameter reduced to the general normalization is compared. This is what the Clarkson, Bassett and Lu test is based on. Its violation after error control would call into question the accepted set of geometric assumptions. The fulfillment of the condition in itself does not prove complete homogeneity. [3]

Real analysis will require galaxy selection models, precise spectroscopic calibration, control of the influence of intrinsic velocities, consistent handling of covariances, and checking whether the desired result has not already been built into the way the distances are reconstructed. You cannot first calculate all the distances for a fixed geometry and then declare their agreement to be an independent proof of the same geometry.

The next research product here is quite specific: analyzing artificial catalogs with known geometries in advance, including controlled deviations from homogeneity, and then applying the same method to the observations. This establishes which deviations the procedure is actually capable of recognizing. The agreement obtained will limit the available violations of the model; a disagreement will indicate which part of the overall chain needs to be re-examined.

The properties of space can be explored from the inside. Let's see how information about a distant event turns into instrument readings.

Chapter 2

# How to see the past

The telescope does not obtain an image of the Universe in a single present. Each detected photon completes its own propagation history. Some signals came from nearby star systems, while others left their source when the region of space around us looked completely different. The sky map connects events separated not only by distances, but also by eras.

This circumstance makes cosmology possible. We cannot go back to the early Universe, but we can explore its surviving traces. At the same time, it requires caution: the brightness of a distant galaxy, its age and distance to it are not read from the photograph as a signature under the exhibit. Between the instrument and the output is a sequence of measurements and physical assumptions.

## What does the light say?

In the simplest case, the detector registers the energy flow or the number of incoming photons. To turn the reading into a property of the source, it is necessary to know the sensitivity of the instrument, exposure time, noise, atmospheric influence for ground-based observations, and radiation along the line of sight. The space telescope removes the atmosphere, but retains its own limitations: finite resolution, thermal effects, calibration, and partial frequency range.

The image answers the question of where the radiation comes from. The spectrum shows how it is distributed across wavelengths. Atoms and molecules leave characteristic lines in the spectrum. If a recognizable sequence of lines is shifted in a consistent manner, the ratio of the observed wavelength to its value in the source system can be determined. This ratio is usually expressed in terms of redshift z.

$$1 + z = \frac{\lambda_{\mathrm{obs}}}{\lambda_{\mathrm{em}}}$$

For example, at z=2 the observed wavelength is three times longer than the original one. Such a measurement does not mean that the source is moving away at a speed of 2c. At high redshifts, conversion to velocity requires determination of the velocity itself and the geometry model. Near objects may have noticeable motions of their own; the strong gravitational field also affects frequencies. For cosmological problems, these contributions are separated from the average expansion. [4]

Line recognition is also a verifiable operation. One striking feature of the spectrum allows for multiple identifications. Several lines connected by known atomic transitions provide a more stable solution. Photometric redshift reconstructed from broad color bands is useful for large surveys, but is usually more dependent on the spectral model. Therefore, clarifying spectroscopy can change the conclusion about the distance and age of a particularly unusual object.

Theoretically, the quantities on which the atomic transitions themselves depend can also change. The simultaneous comparison of different lines then becomes a test of fundamental physics. This complicates the interpretation, but gives a new observable consequence: changing the constants does not have to bias all transitions equally. In the future, we will connect this possibility with cosmological fields and laboratory atomic clocks.

## Multiple distances to one source

Let's ask how far away the galaxy is. We can mean the distance at the moment of emission of light, the distance between comoving points at present, or the time of propagation of light multiplied by c. In changing geometry these are different quantities. Mixing definitions creates seeming paradoxes, even when the calculation itself is correct.

Astronomical measurements add two more useful definitions. If the luminosity of the source is known, the luminosity distance can be entered from the received flux. If the transverse physical dimension is known, the distance along the angular diameter can be entered using the angular dimension. These definitions are designed so that the usual formulas for brightness and angle remain convenient, and the influence of cosmological geometry passes into the corresponding distance. [4]

A distant source dims for several reasons. The radiation is distributed over a larger area, the energy of each photon decreases due to the red shift, and the intervals between their arrivals stretch. Therefore, the reconstructed luminosity depends on how these effects are taken into account. In addition, some of the light may be absorbed by dust or redistributed by gravitational lensing.

An object of standard size does not have to become smaller in the sky as redshift increases. The distance along the angular diameter in the usual expanding models has a maximum. This is a consequence of the fact that we are observing the source in an earlier state of the geometry. The angular size itself therefore does not yet give an unambiguous distance. What is needed is a redshift and a consistent way to interpret the data.

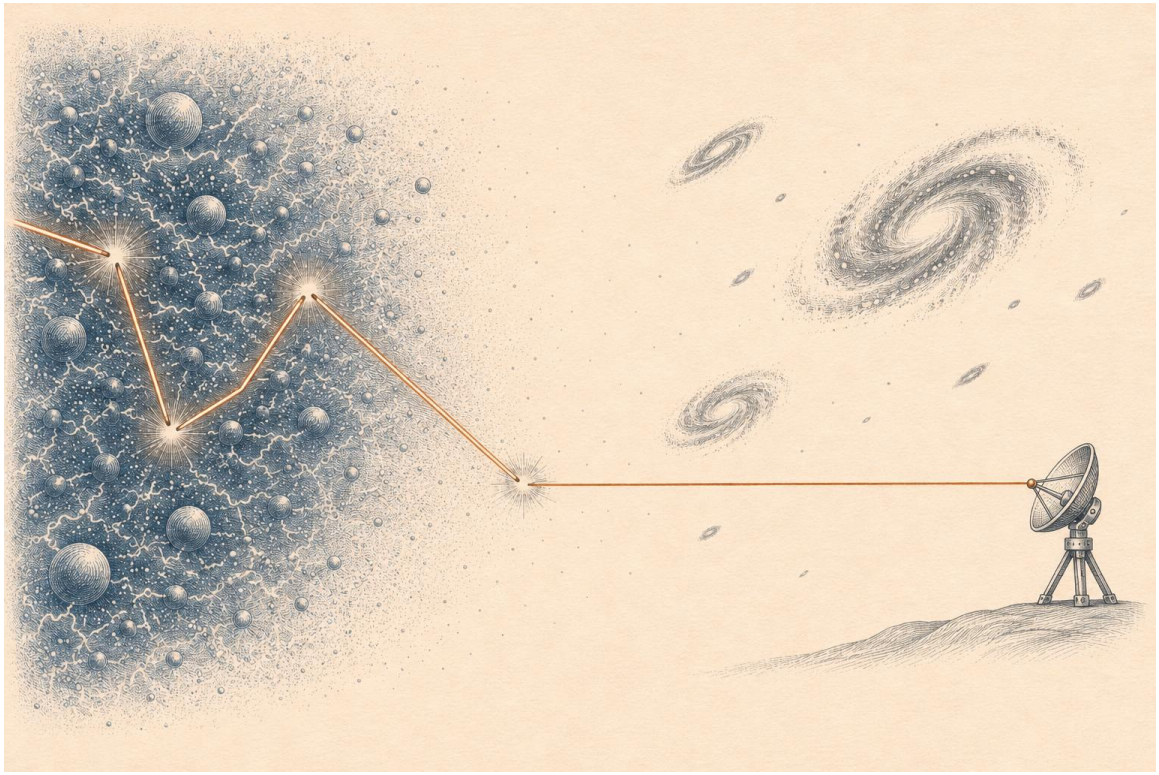
The “today’s distance” to a distant galaxy is also a reconstruction. We do not observe her current state directly. It is calculated on a selected slice of cosmic time in a model that matches the available signals. This reconstruction can be very accurate within the model, but must be distinguished from the actual time of arrival of the detected photon.

## CMB radiation as a visibility surface

Early matter was opaque to the free propagation of light: photons interacted repeatedly with charged particles. As the electrons cooled, they began to bond with nuclei, and a significant portion of the radiation was able to travel great distances. Today we observe this radiation in the microwave range. Its average temperature is close to 2.725 kelvin. [5]

The CMB map shows slight differences in temperature and polarization. They arise from the history of matter, gravitational disturbances and photon propagation. In the standard cosmological model, the last scattering epoch, which left the bulk of this picture, dates back to about 380 thousand years after the start of hot evolution. The most recent scattering is distributed over a certain time interval, and later processes additionally change the signal. [6]

Therefore, this is not a photograph of the first moment of the world’s existence. Earlier events can only be reconstructed by how they influenced the subsequent picture. The conditions before the opaque age are sometimes accessible indirectly, although the light from there has not reached us directly. This is an important example of cosmological inference: the observed trace and the event that we reconstruct from it belong to different times.



Engraving 3. The last scattering opens the way for light. In an opaque plasma, photons repeatedly changed direction during interactions. After the formation of neutral atoms, a significant part of the radiation was able to propagate freely. The engraving conventionally connects these stages: the transition has a finite duration, and the observed cosmic microwave background radiation is not a direct image of the first moment of the world's existence.

## What does measurement error mean?

Most cosmological models predict the statistics, rather than the exact location, of each galaxy in our sky. In such a model, random initial disturbances give rise to different realizations of the cosmos. We compare the observed implementation to the distribution of possibilities and ask how typical it is under the chosen parameters.

Even an ideal telescope sees a finite number of available large-scale modes. Increasing the accuracy of measuring an already observed mode does not create new independent examples of the same magnitude. The limited sampling in cosmology is called cosmic variance. It should be distinguished from instrument noise: some limits of accuracy are determined by the amount of information available. [7]

This does not make cosmology untestable. Different statistics, polarization, matter distribution, and other physical media can provide additional constraints. But reusing the same sky requires taking into account correlations. Two analyzes of the same map do not become independent observations just because they were performed by different programs.

It is also useful to distinguish between random and systematic errors. For independent measurements with the same variance, the random error of the mean decreases as the square root of the number of measurements. For example, if the error of each is two arbitrary units, the average of one hundred measurements has a random error of 0.2 units. The overall scale shift of one unit will remain a shift of one unit. Therefore, a thousand additional objects do not correct the incorrect gray scale; a different instrument or method with a different calibration may detect the problem.

An anomaly claim therefore requires a description of the entire path from raw data to output. How were the objects selected? What signals might not have made it into the catalog? What parameters were recorded? How many different features were you looking for before you noticed one? These questions are especially important at the frontiers of science, where an unusual result can easily be mistaken for an indication of new physics.

Let's look at a simple selection example. Let sources of different luminosities occur at equal distances. Close we detect almost everything, but far away we detect mainly the brightest ones. If you compare the average brightness of two catalogs without taking into account the detection threshold, you get an artificial evolution of the population. In this case, each recorded flow can be measured completely correctly. An error will occur when moving from detected objects to a conclusion about all existing ones.

To evaluate this effect, researchers add signals with known parameters to real or artificial data and test which of them the search procedure recovers. This is how the selection function is determined. It also needs to be checked: artificial objects must reproduce the essential properties of real ones quite well. For a hypothesis about a rare unusual class of objects, the standard source model is sometimes not enough.

There is also an inverse problem. If certain objects are not in the catalog, this may mean their physical absence, small numbers, low brightness, or the inability of the algorithm to recognize the desired signal. A statement about the limit on a hypothesis requires estimating the probability of detecting its prediction. The empty area of the drawing turns into a scientific limitation only with such an assessment.

## How to check it

One way to check the entire chain is to compare two definitions of distance to the same epoch. When light propagates along the null geodesics of metric space-time and the number of photons is conserved, the distances in luminosity and angular diameter are related by reciprocity. In the accepted notation it looks like:

$$D_L(z) = (1+z)^2 D_A(z)$$

This relationship does not select a particular dark energy model. It tests more general conditions for light transfer. Practical comparisons require objects or statistical scales with known properties: for example, standardized supernovae for brightness and an acoustic scale in galaxy distributions for angular distances. Acoustic observations give primarily the ratio of distance to the size of the sound line. Its length and the absolute luminosity of supernovae must be calibrated independently or included as common unknown parameters. Their calibrations must be taken into account together, including dependencies that came from the same input data. [4] [8]

A simple example shows what is being checked here. Let some photons be lost, and a fraction exp(−τ) of the flux reaches the observer, where τ characterizes the transparency of the path. If the loss is not taken into account, the source will appear further away: the luminosity distance will be overestimated by exp(τ/2) times. This follows from the inverse proportionality of the flow to the square of the distance. But the same attenuation of all sources can be confused with an error in their absolute luminosity. Therefore, it is necessary to check the dependence of the effect on redshift and wavelength, while maintaining the general calibration parameters. The very disagreement between the two distances does not yet indicate the reason for the loss of light.

A possible discrepancy does not indicate a single cause. Dust reduces the flux, the sources' own evolution changes the estimated luminosity, and lensing redistributes brightness. In itself, ordinary gravitational lensing does not violate reciprocity for a consistent light beam while preserving its premises; errors may arise due to the selection of objects and the method of averaging. New photon interactions could also influence the result. Observations at different ranges, independent calibrations, and the predicted dependence of the effect on redshift help to separate the causes. A model that claims to explain must reproduce the entire pattern of deviations.

Another test uses the time course of an observed event. At cosmological redshift, the intervals between successive stages of the event increase by a factor of 1+z. It is possible to compare changes in the spectra of nearby and distant supernovae, determining their physical stage based on spectral features. This check has already been carried out and is consistent with the expected stretch; it rules out specific redshift explanations that do not predict time stretching. [9]

To strengthen this test, we need repeated spectra of the same events, control for differences between supernova populations, and a predetermined procedure for comparing their stages. Agreement with the expected stretch supports the signal transfer property being tested. It does not separately establish all other provisions of cosmology. The lack of expected stretch or other discrepancy should first be compared with the specific prediction and the entire measurement chain.

We can thus ask the light not only about a distant source, but also about the rules by which information about it reached us. The next step is based on these rules: restoring how distances changed in space itself.

Chapter 3

# What's expanding

If the distances between distant galaxies grow, I would like to imagine flying fragments of an explosion. Then there must be a center from which they scattered, and empty space into which they move. This picture is useful for the explosion of a substance in an already existing environment. Cosmological expansion is described differently: the geometric ratio of the distances between points participating in the general movement of cosmic matter changes.

Let us imagine a network of ideal observers, each of whom, on average, is at rest relative to the surrounding space environment. They can have the same age according to the cosmological clock, exchange signals and compare distances. In a homogeneous approximation, the ratio of distances between any pair of such observers changes according to a general law. This general dependence is determined by the scale factor a.

## Expansion clock

Usually today's value of a is taken equal to one. This is a normalization choice rather than measuring the absolute size of the entire world. If at some epoch a was equal to half, the corresponding cosmological distances in the homogeneous model were half as large as today's ones. The rate of relative change in the scale factor is denoted by H.

Let's see why such a movement does not have to have a dedicated center. Let's take three comoving objects in a small area on the same line with equal intervals. At the selected moment, the derivative of the distance between the first and second is equal to H multiplied by one interval, and between the first and third - H multiplied by two. If we go to the description of the relative middle object, the one closest to the left and the one closest to the right will move away from it equally quickly in opposite directions.

All participants see the same law depending on distance and distance. This simple example uses uniform motion on a global cosmological slice and a locally applicable comparison method. He explains why the observer's position at the center of his own map does not make him the center of the entire physical system. For distant objects, the full calculation additionally takes into account the different emission times of the observed light.

The law can be violated in a specific group of galaxies, where their own velocities and gravity are significant. Such a local violation does not cancel the large-scale expansion: one must compare the observation with the model at the scale for which its approximations are stated.

$$H(t) = \frac{\dot{a}(t)}{a(t)}$$

The dot above means the derivative with respect to cosmic time. The quantity H has the dimension of inverse time. Astronomers often record it in kilometers per second per megaparsec: such a notation shows how, to the appropriate approximation, the speed of removal changes with distance. A megaparsec is approximately 3.26 million light years.

By calling the modern value of H the Hubble constant, we do not assume that it was the same in all eras. The number $H_0$ refers to today. H itself changes during cosmic evolution. Moreover, it can

decrease even as expansion accelerates. Acceleration refers to the positive second derivative of a, while H describes the relative rate of its change. These two questions are mathematically different.

In a simple example, the distance increases faster and faster, but the scale already achieved increases even more significantly. In this case, the ratio of speed to scale can fall. Therefore, the expression “acceleration of expansion” cannot be automatically replaced by the words “increase in the Hubble constant.” To restore the dynamics, you need to know the entire H function in time or redshift.

Consider a mathematical example: the scale factor is proportional to time to the power of three halves. Its first derivative grows as the square root of time, so expansion accelerates. But the ratio of that derivative to the scale factor itself equals three divided by twice the time, and decreases. This example does not describe the established history of our Universe. It shows that the distinction between acceleration and a change in H already follows from the definitions of the quantities, before any particular cosmological theory is chosen.

Acceleration has another subtlety. In relativistic cosmology, dynamics are affected by pressure, not just the density of matter. Therefore, a positive component density does not necessarily mean deceleration. Sufficiently negative pressure can maintain accelerated mode. This pressure does not need to be imagined as a substance that pushes the outer walls of the world: it enters into the equations of the internal dynamics of geometry.

How exactly a component acquires this property is an independent physical question. The cosmological constant gives one answer at the level of equations. A moving scalar field may give a different story. Changing the law of gravity requires a third description. The coincidence of expansion in a certain range does not yet make these mechanisms identical: their differences can manifest themselves in the growth of inhomogeneities or laboratory interactions.

For a source participating in the overall expansion, the ratio of the observed and emitted wavelengths is equal to the ratio of the scale factors at the ends of the path. With today's normalization this gives a=1/(1+z) at the moment of emission. This relationship links the spectroscopic measurement with cosmic history. Additional movements and gravitational shifts require separate corrections. [4]

## The composition of matter shapes the history

In general relativity, the rate of expansion is related to the content of the Universe and spatial curvature. For a model in which radiation, nonrelativistic matter and the cosmological constant are present, it is convenient to write the equation in terms of their present shares:

$$\frac{H^2(a)}{H_0^2} = \Omega_r a^{-4} + \Omega_m a^{-3} + \Omega_k a^{-2} + \Omega_\Lambda$$

Here $\Omega_r$ refers to radiation, $\Omega_m$ to matter, and $\Omega_\Lambda$ to the cosmological constant. The parameter $\Omega_k$ describes the contribution of spatial curvature and is not a fraction of a special substance. When a=1 the sum of these four quantities is equal to one. The entry assumes the specified properties of the components; the transition of particles from relativistic to slow motion or the exchange of energy between sectors requires a more detailed description.

The density of slowly moving matter falls approximately as the inverse volume. The number of particles in the expanding region is maintained, but the volume grows like a cube a. In free radiation, the energy of each quantum is further reduced, so its density drops faster. The density of the cosmo-

logical constant is preserved in this model. Due to different dependencies, components can sequentially determine the overall dynamics.

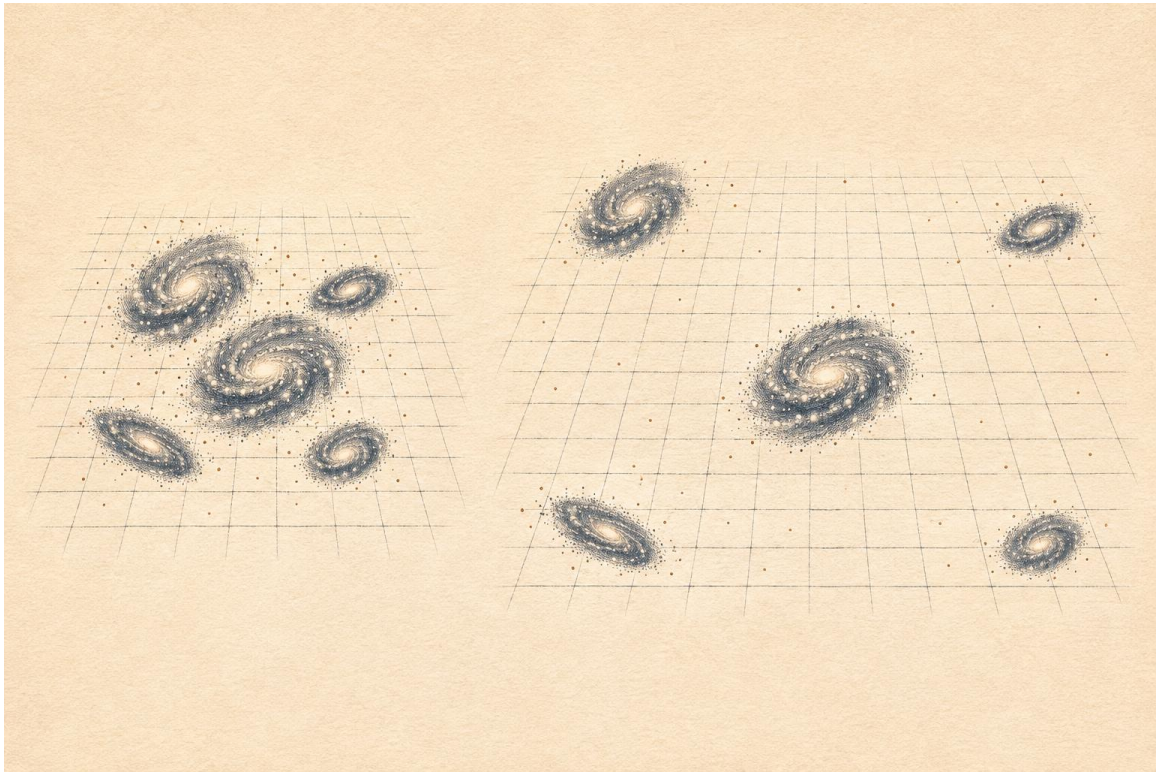
In early epochs, radiation is especially significant. Later, matter plays a big role. With a positive cosmological constant, its relative value increases as other components become rarefied. This sequence makes it possible to connect epochs of very different temperatures with one dynamic description. The observational success of the standard model lies in the reconciliation of many traces of this history, and its parameters are determined by joint analysis of the data. [6]

Measuring one $H_0$ is not enough to find out the age. The reciprocal $H_0$ sets the characteristic time scale, but the age depends on the entire history of H. In our illustrative model, the reciprocal $H_0$ is about 14.5 billion years, and the calculated age is about 13.8 billion. The difference expresses the cumulative result of the change in expansion rate.

## Why doesn't everything stretch?

The homogeneous cosmological model is an approximation to large-scale dynamics. An atom, a planetary system, and a gravitationally bound galaxy require consideration of the forces that hold them together. They are not required to follow a common comoving network of observers. To describe their sizes, a local dynamic problem is solved on the appropriate background.

This can be understood using the example of two particles. If they are practically free and participate in the general cosmic movement, the distance between them is associated with expansion. If they enter a stable bound state, their distance is determined by the interaction and the state of the system. The cosmological impact is estimated as part of the complete problem and is extremely small in conventional coupled systems. We don't get the right to multiply the size of each item by a.



Engraving 4. Distances grow, but bound systems maintain scale. The two illustrative states show increasing distances between comoving regions. The dimensions of the depicted bound systems are preserved to emphasize the role of their own dynamics. Cosmological expansion does not mean that all objects are stretched equally. The engraving conveys the principle and does not specify the exact ratio of scales or the real history of individual galaxies.

The recession velocity of a distant object also requires careful determination. In a homogeneous model, the derivative of the proper distance between distant comoving points can exceed c. This is not the local speed of an object flying near the observer. The limitation of special relativity relates to local measurements and signal transmission. Analysis of cosmological horizons shows why the superluminal value of such a derivative does not automatically turn into a prohibition on observing the source. [1]

Now we can return to distances. In our illustrative model, the light from the comoving source at z=1 propagated about 7.95 billion years. The distance between the corresponding points today is approximately 11.09 billion light years, and at the time of emission - about 5.55 billion. All three numbers refer to the same model and source. Their difference is associated with the definition of the measured quantity.

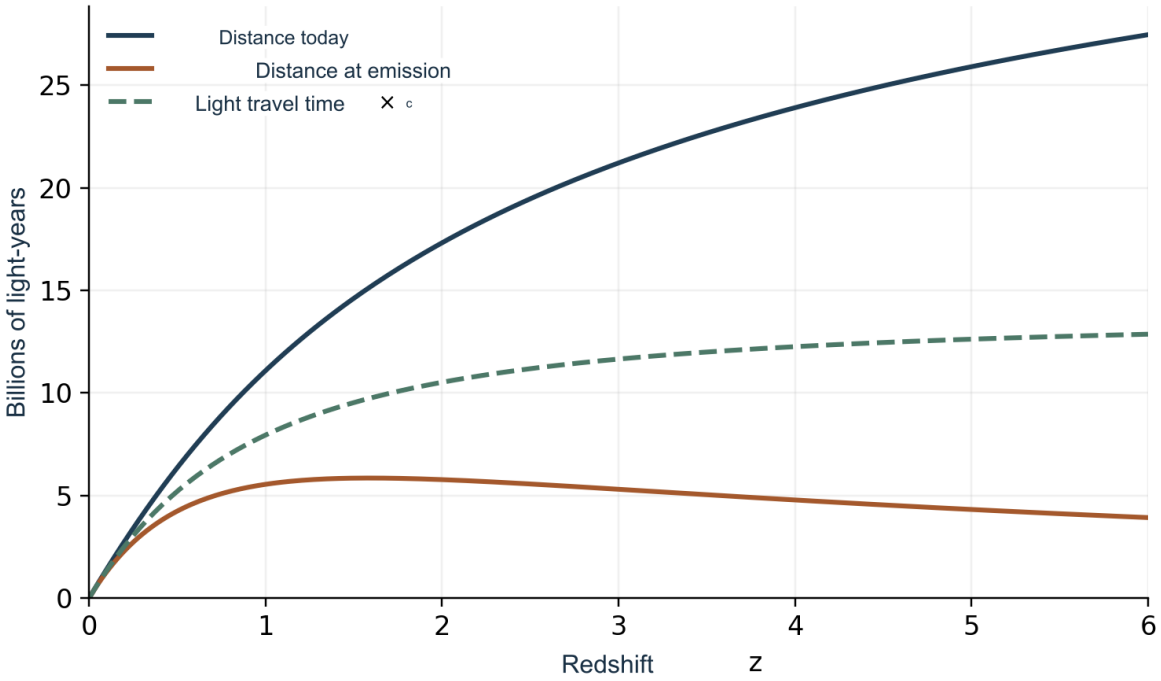



Figure 1. Different distance measures in an illustrative spatially flat model with radiation, matter and cosmological constant. The parameters and calculation method are given in the mathematical appendix. The curves are model calculations and do not represent new observational data.

The change in radiation energy raises the following natural question: where does the energy of reddening photons go? In general relativity, local conservation of energy and momentum has an exact mathematical form. But transferring the familiar concept of total conserved energy to an arbitrary dynamical space-time requires additional conditions, such as suitable symmetry in time. For the entire expanding Universe, such a global energy account may not exist in its usual form.

For a homogeneous component, the local conservation equation relates the change in its density to expansion and pressure. It is consistent with the indicated laws of rarefaction of matter and radiation. The additional statement that the lost energy must accumulate in a separate cosmic reservoir does not follow from it. For the same reason, the popular phrase about the exactly zero total energy of the Universe needs to define the model and the energy itself.

## How to check it

Most expansion measurements compare objects from different eras: we reconstruct history from light coming from different sources. A more direct task could be to re-measure the redshift of the same cosmological source many years later. Over the past time, the geometry has changed, which means that the ratio of scale factors at the ends of the path of the world should also change slightly.

In the homogeneous model for the comoving source, the redshift drift is expressed in terms of today's $H_0$ and the value of H at the emission epoch. The physical idea of such a measurement has been developed for the spectra of distant quasars: many absorption lines in intergalactic gas create a detailed pattern that can be compared between observation epochs. [10]

$$\frac{dz}{dt_0} = (1+z)H_0 - H(z)$$

Time $t_0$ is measured by the observer's clock. The formula involves two ends of the path of light: while we are waiting for the next spectrum, both the moment of reception and the moment of emission of the photons that reach us changes. Therefore, the sign of the drift cannot be attributed to the acceleration of the source alone. For comparison with a spectrograph, a small change in z is converted into an equivalent velocity shift by multiplying it by c/(1+z). In chapter 8 we will calculate such a signal for two dark energy histories.

The effect is very small. Success depends on long-term stability of the wavelength scale, sufficient photons, and control of the observer's movements. Accurate frequency standards, repeatable processing of spectra, and verification of changes in the gas itself will be required. The intrinsic accelerations of individual systems can mask the cosmological contribution, so the ensemble of objects and the consistent dependence of the signal on redshift are essential.

Measuring expansion in this way is part of the scientific mission of the ANDES spectrograph being developed for ESO's Extremely Large Telescope. On the official project page, long-term stability of the 0.02 m/s calibration over ten years is listed as a goal, not an achieved performance. For such work, a frequency comb connected to an atomic standard and other calibration sources are needed: they allow you to monitor changes in the device itself. [11] [12]

The first series of observations already show the scale of the task. In work 2026, the ESPRESSO group compared three epochs of spectroscopy of the quasar J052915.80−435152.0 over an interval of about two years. The resulting drift −3.5 ± 3.6 m/s per year is consistent with zero. The error is much larger than the expected cosmological effect; This is a test of the measurement procedure, not a detection of expansion by this method. [13]

Further work begins with calculating the shifts for the compared models and transferring them to artificial spectra with noise, calibration and astrophysical distortions. Then you need to determine which sources and observation intervals allow you to reconstruct the difference. Estimates of campaign duration depend on the brightness of objects and the number of photons collected; The twenty-year interval chosen in the training calculation does not itself promise detection within twenty years. [14]

The result is useful in any case when its sensitivity is predetermined. The discovered consistent relationship will allow the extension reconstruction to be verified in another way. The absence of the expected effect in the available range will raise the question of a specific model or measurement control. Already here, the future of cosmology looks like a certain physical work: two carefully compared observations, separated by time, are able to study the change of the cosmic scale itself.

Chapter 4

# Thermal history

If you trace the expansion backwards, the matter on average becomes denser and the radiation gets hotter. But simply moving the equations in the opposite direction is not enough to restore the past. We need preserved traces. In the case of the early hot Universe, such traces are found in the composition of matter, in the spectrum of the cosmic microwave background radiation and in the structure of its inhomogeneities.

The strength of this painting lies in the connection between different eras through verifiable physics. Nuclear reactions, atomic transitions, and the propagation of light have left various observable effects. They can be compared. Extrapolation increases as we delve deeper into the past, so it's helpful to separate a well-tested hot history early on from hypotheses about what made it possible.

## Radiation remembers temperature

Thermal radiation in equilibrium has a certain spectrum. Its shape is related to temperature and the fundamental laws of statistical physics. When such radiation propagates through the expanding Universe without significant new energy release, the wavelengths increase in a consistent manner. The spectrum retains its thermal form, and the temperature decreases in inverse proportion to the scale factor.

The early hot stage therefore predicts more than a faint background glow. It connects the spectral shape, present-day temperature, and temperatures at earlier epochs. Today's cosmic microwave background temperature is measured from its spectrum; Fixsen's analysis gave a combined estimate of $2.72548 \pm 0.00057$ kelvin. This is a specific temperature measurement, rather than an independent measurement of the age of the Universe. [5]

Is it possible to check whether this radiation was hotter before? This does not require sending the thermometer into the past. In distant gas clouds, molecules interact with surrounding radiation. The populations of their energy levels affect the absorption lines in the light of the more distant quasar. If collisions and local radiation are taken into account, such levels can serve as a cosmic thermometer.

It is this principle that was used in observations of the excitation of carbon monoxide molecules in distant absorption systems. The results are consistent with the standard temperature increase with redshift. The method has its own astrophysical uncertainties, but it tests temperature history through different physics than today's whole-sky microwave measurements. [15]

## How did the first light nuclei appear?

In early plasma, reactions were fast enough that particles could interact repeatedly during a noticeable change in conditions. As it expanded, density and temperature decreased. There came moments when a certain reaction no longer had time to maintain the previous equilibrium. Its trace was preserved in the form of the composition of matter or the distribution of particles.

Here two physical times are compared. One is the average time between the required reactions for a particle, the other is the time of noticeable expansion of the medium, on the order of $1/H$. While the first is much shorter than the second, the collisions have time to adapt the composition to the chang-

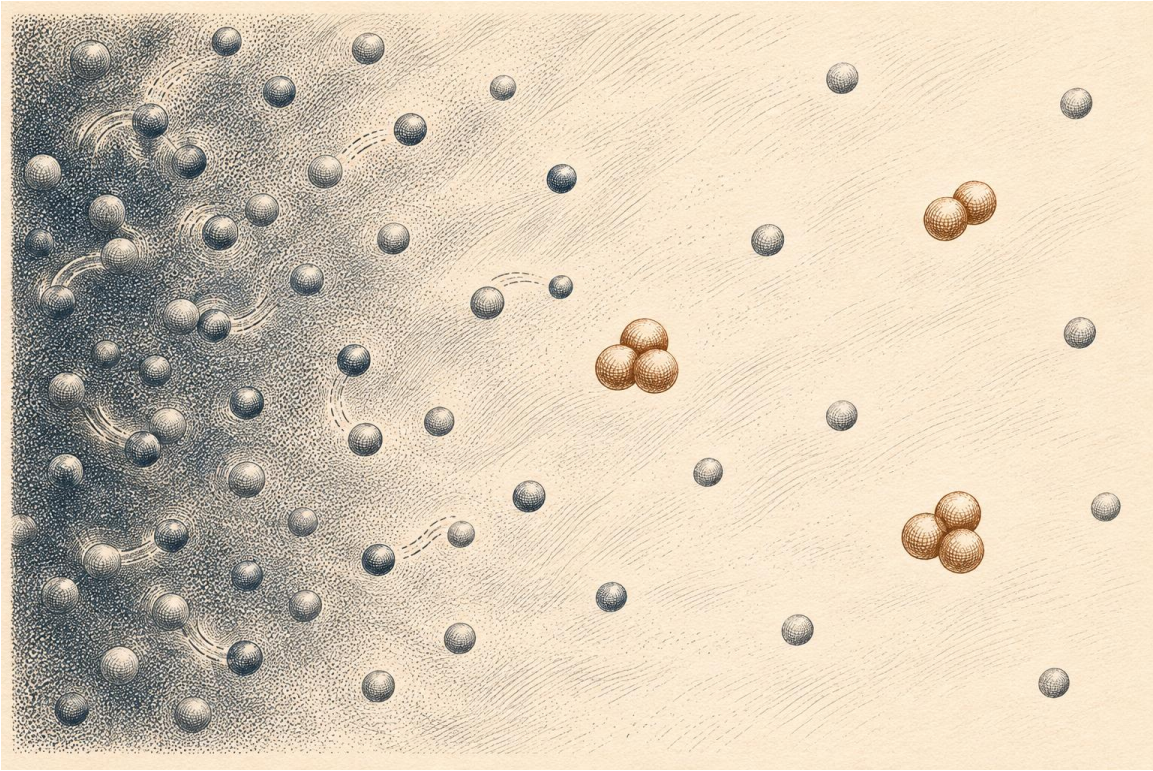
ing temperature. When they become too rare, the previous balance is disrupted. The so-called freezing of a reaction does not mean that the particles stop moving or that all reactions are turned off at the same time. Each process has its own speed and leaves its own mark. [16]

In the first seconds of the hot history, the ratio of neutrons and protons was of particular importance. Weak interactions transferred some particles into others, then began to lag behind the expansion. Free neutrons continued to decay. The steady accumulation of deuterium and the main synthesis of light nuclei date back to the first minutes of the hot history. Modern calculations of this sequence use a network of reactions, measured cross sections and neutron lifetimes. [16]

Why did nuclei not appear immediately as soon as the average energy of particles became less than their binding energy? The thermal distribution has a high-energy tail. In addition, there are many more photons than baryons. Therefore, even a small fraction of sufficiently energetic photons could destroy the newly formed deuterium. Only after further cooling was the synthesis chain able to continue effectively.

Almost all the neutrons preserved by this time ended up in helium nuclei-4. A simple assessment reveals the reason for the large amount of primordial helium. If there are approximately seven protons per neutron, then two neutrons together with two protons form one helium nucleus from the original sixteen nucleons. Helium accounts for about a quarter of their mass. A more accurate result depends on the actual reaction rates and neutron decay time.

The Universe did not turn all matter into heavy elements. Expansion quickly reduced density, and the properties of light nuclei limited the paths for further synthesis. The formation of many heavy elements is associated with the subsequent evolution of stars and other astrophysical processes. Particularly valuable for cosmology are residual quantities of light nuclei that are sensitive to early conditions.



Engraving 5. When early plasma leaves light nuclei. As expansion progressed, the density, temperature, and the ratio of reaction time to the time of evolution of the medium changed. After overcoming the deuterium obstacle, the effective formation of light nuclei became possible. Only a qualitative transition from particles to small connected groups is shown here; the composition, reaction rates and yield of elements are calculated using the nuclear network.

## Two ways to measure the same contents

The deuterium content depends on the density of ordinary matter in the early Universe. The more often the corresponding nuclear reactions occur, the differently its residual fraction changes. But primary deuterium has to be measured much later. The gas could have passed through stars, mixed with other matter, or ended up in a complex absorption system.

Therefore, observers look for relatively little processed gas clouds and examine several lines of the same absorber. The isotopic shift allows one to distinguish between hydrogen and deuterium. It is necessary to check whether the weak deuterium line does not imitate hydrogen from another component at a different speed. Accurate spectroscopy and a unified cloud model here determine the quality of the cosmological inference. The one percent estimate obtained by Cook, Pettini, and Steidel in 2018 provides an example of how a small, carefully studied sample can be powerfully limiting. [17]

Another physical channel for determining the density of ordinary matter is provided by cosmic microwave background radiation. Before the last scattering, photons and charged matter formed a bound medium in which vibrations propagated. The number of baryons influenced their dynamics. Therefore, the characteristic structure of temperature and polarization spectra carries information about the same physical quantity that participated in nuclear reactions much earlier. When rigorously testing nucleosynthesis itself, it is also necessary to take into account whether the fraction of helium predicted by it was previously used in the analysis of the cosmic microwave background radiation. Independent verification is carried out by allowing this proportion to vary and maintaining the overall uncertainties. [6]

Comparing the two eras requires a coordinated transition from the densities then to today's parameters. If there had been a significant addition of energy between them, a change in composition, or an unusual violation of the accepted law of evolution, this could spoil the agreement. This test connects nuclear physics with cosmological geometry and makes it possible to search for new components that are almost inaccessible to direct observation.

Imagine an additional light particle that barely interacts with ordinary matter. If many such particles existed in the early Universe and moved relativistically, their energy would help determine the expansion rate. Nuclear reactions would have a different amount of time to proceed at each temperature. Other conditions held fixed, faster expansion could, for example, change when effective neutron-proton interconversion ceases and alter the subsequent helium yield.

Thus, a particle can leave a trace without even hitting our detector. But the size of the trace depends on its early population. The mere existence of a particle species does not tell us how much energy it carried. For a cosmological constraint, it is necessary to specify the birth mechanism, the temperature of the corresponding sector, and possible decays. This explains why the laboratory constraint on the interaction and the cosmological constraint on density are different parts of the same test.

Comparison with the CMB adds a temporal distinction. The component could exist during nucleosynthesis and decay before the last scattering or transition to another mode of motion. For this version to become an explanation, it is necessary to calculate both eras with the same particle history. The freedom to choose independent densities for them would destroy the predictive relationship.

## Where the established history ends

There remain real difficulties in this picture. A known problem with lithium is the discrepancy between the standard prediction and the lithium abundance inferred from observations of some old, heavy element-poor stars. Interpretation requires taking into account changes in stellar composition, material transfer, and uncertainties in spectral analysis. The possibility of a new physics is discussed, but the mere fact of disagreement does not automatically select it. [16]

The accuracy of deuterium predictions also depends on nuclear data. Improvement in one response does not guarantee the disappearance of other uncertainties. As an astronomical measurement becomes more precise, a previously subtle error in the speed of another reaction can begin to determine the outcome. The early space verification program therefore involves conventional laboratory nuclear physics in which the experimenter controls the particle beam and target composition.

The earlier the era under consideration, the more important the limits of applicability of the theory. The accelerator can confirm the interaction properties at high energy. But the cosmological use of this result additionally assumes a certain density, composition of the medium and expansion history. A specific process is reproduced in the laboratory. The entire cosmological situation is restored through the model and the preserved observational traces.

If we continue the classical solution far back, we can arrive at a regime of extremely high density and curvature. This indicates a limit where it is necessary to check the applicability of the equations used. The very existence of such a limit is not an observation of the absolute birth of time. The earlier stage, quantum transition or other description remains a subject of independent research.

The term “Big Bang” is therefore convenient to use with clarification. The hot history implies expansion and cooling of the early plasma, supported by several observational tests. The assumption of an absolute beginning is a stronger statement. Data on light elements retain their value under different hypotheses about how the hot stage arose, if these hypotheses reproduce the necessary conditions at the time of nucleosynthesis.

## First second trace

The hot history must have one more witness - the cosmic neutrino background. Neutrinos are also born in the Sun, supernovae and terrestrial installations, but here we are talking about particles that inhabited the early hot environment. Their cosmological meaning is determined precisely by the origin and subsequent evolution of distribution. The detection of any neutrino is not the detection of this background, just as the registration of an ordinary radio photon does not mean the measurement of cosmic microwave background radiation.

In early plasma, weak interactions supported the exchange of energy between neutrinos and other particles. As it cooled, this exchange could no longer keep up with the expansion. The characteristic epoch refers to the first seconds of the standard hot history, at temperatures on the order of megaelectronvolts. This is not an instantaneous shutdown of one reaction, nor is it a measurement of the absolute age of space. The background stores information about release conditions and subsequent influences that may have changed particle numbers, momentum, or motion.

The simplest estimate of temperature comes from the conservation of entropy. After an idealized instantaneous decoupling, the annihilation of electrons and positrons predominantly heats the photons relative to the already separated neutrinos. In a photonic-electronic medium, the effective number of degrees of freedom involved in entropy changes from 11/2 to 2. Temperature scales as the inverse cube root of this number, in addition to cosmological cooling. We get the well-known relation:

$$T_{\nu,0} = \left(\frac{4}{11}\right)^{1/3} T_{\gamma,0} \simeq 1.945 \text{ K}.$$

For the numerical example, $T\gamma,_0$ = 2.72548 kelvins from the above measurement are used; the calculated coefficient is approximately 0.71377. This is an idealized estimate and not a direct measurement of modern neutrino temperature. For massive particles that have become nonrelativistic, the value $T\nu,_0$ denotes the scale of the retained momentum distribution. Without additional recalculation, it cannot be understood as the usual kinetic temperature of a gas, determined by the average energy of motion.

Accurate calculation of decoupling requires kinetic equations, taking into account collisions, oscillations between flavors and plasma properties. Photons and neutrinos do not separate completely instantly, so the simple temperature law has corrections. In the calculation of Froustey, Pitru and Volpe 2020, the effective number of relativistic neutrino degrees of freedom $N_{eff}$ = 3.0440 was obtained. The difference from three describes a correction to the energy density, not the discovery of a fractional number of particles. [18]

The parameter $N_{eff}$ is generally convenient as a single measure of the energy of the relativistic sector relative to photons. Different sets of particles and temperatures can give the same value. Therefore, measuring only this quantity will not determine the interaction of neutrinos. To learn more, we

need to use not only the average density, but also the behavior of the perturbations: how matter transferred energy between regions and changed the surrounding gravitational field.

Freely propagating relativistic neutrinos move differently than bound photon-baryon plasma. Their disturbances change gravitational potentials, which affect the acoustic vibrations of this plasma. A characteristic phase shift of oscillations occurs. This is different from simply changing the angular size of the entire painting due to geometry. Bashinsky and Seljak derived the corresponding physical mechanism and showed its diagnostic value under given adiabatic initial conditions. [19]

In 2015, Fallin, Knox, Millea and Pan reported the discovery of the expected phase signature in the temperature spectrum of the CMB. This is an example of indirect evidence of the behavior of cosmic neutrinos: the detector measures photons, and the neutrino is inferred through gravitational influence. This result should be distinguished from both the measurement of neutrino mass and the direct capture of a relic neutrino in the laboratory. [20]

For the next study, two specific stories can be compared. In the first, neutrinos propagate freely after standard weak decoupling. In the second, the additional elastic interaction between them maintains collisions longer, maintaining a similar average energy density. Such options have been studied for a long time. For example, Cyr-Racine and Sigurdson considered the effective neutrino self-interaction strength $G_{\text{eff}}$ and its reflection in cosmological perturbations. [21]

In the regime of contact interaction with a heavy mediator for relativistic neutrinos, the characteristic collision rate has a temperature dependence $\Gamma\nu \propto G_{\text{eff}}^2 T\nu^5$ in units where c, ħ and $k_B$ are equal to unity. The coefficient and angular response depend on the adopted microscopic model. To calculate it, it is not enough to arbitrarily move the decoupling time: you need to set the collision term, check the applicability mode of the approximation, and trace the hierarchy of angular disturbances of the distribution. [21]

This formulation does not assume that strong self-interaction is now required by the data. In work published in 2025 by Camarena and Cyr-Racine, a joint consideration of selected CMB data and galaxy distributions significantly constrained a simple version of such a cosmology. The result refers to the studied model and datasets. It shows why the new version should be tested by several observables at once, rather than presenting a successful fit to a separate spectrum. [22]

It is especially useful to select stories in advance with a similar average energy of the relativistic sector. The difference in phase and polarization then tests the nature of the motion, not just the addition of new energy. At the same time, changes in standard cosmological parameters and the helium fraction should be allowed. Otherwise, a rigidly fixed auxiliary value can artificially increase the visibility of the difference. The final task is to find collision parameters that remain distinguishable after such joint comparison.

Direct examination of the background requires a different instrument. One of the ways being studied is the capture of neutrinos by tritium with the formation of helium-3 and an electron:

$$\nu_e + {}^3\mathrm{H} \longrightarrow {}^3\mathrm{He} + e^-.$$

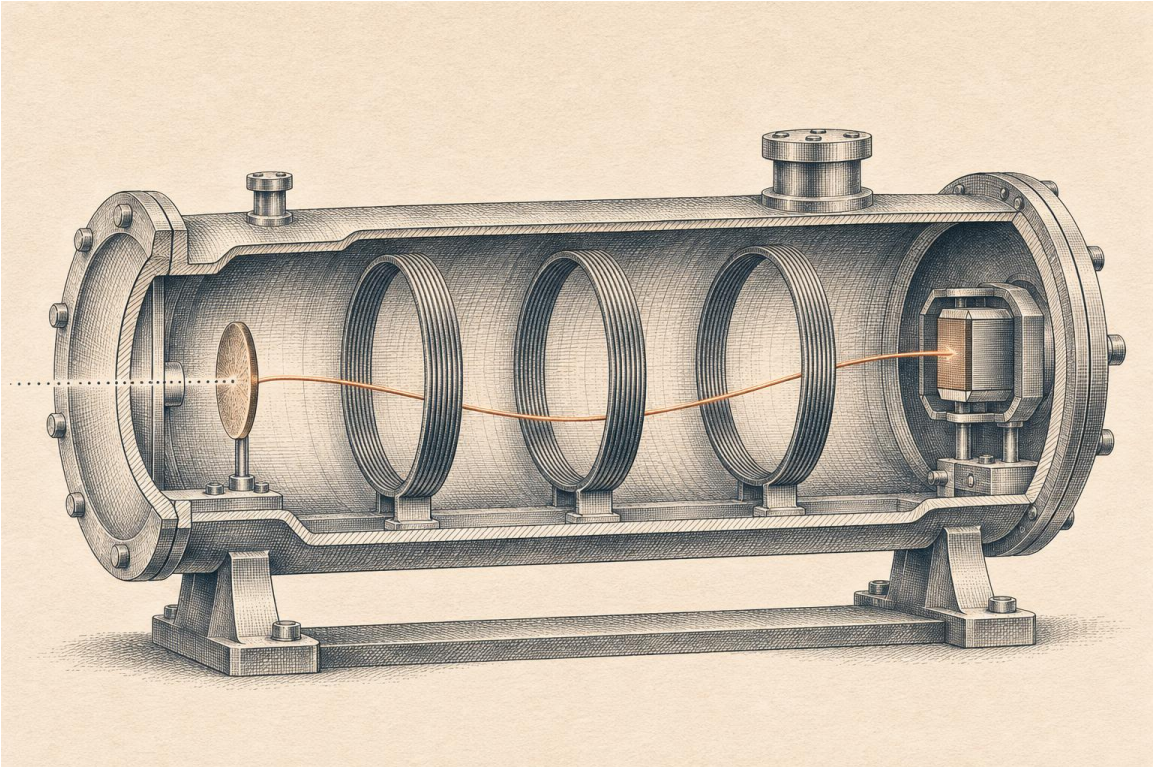
Capture is capable of producing an electron with an energy above the end of the normal beta spectrum. For almost identical nonrelativistic masses, the characteristic distance between the signal and the beta end is approximately $2mvc^2$. For different masses, it is necessary to calculate several contributions with mixing weights. The frequency of events also depends on the local density, helicity and

nature of the neutrino; these dependencies are analyzed in detail by Long, Lunardini and Sabancilar. [23]

The PTOLEMY research program is considering the development of a setup for such capture. Published estimates relate its capabilities to target mass, energy resolution, and background. Between a physically resolved reaction and a reliable cosmological measurement lies a test of the actual response: how tritium binds to the material, what broadens the electron line, how electrons lose energy, and how stable its scale is determined. Project estimates do not constitute a report of the detection of relic neutrinos. [24]

The PTOLEMY white paper used shows the construction of a prototype magnetic system and electromagnetic filter. The immediate engineering goal is to verify the selection and measurement of electrons with the desired properties. This phase should be taken into account separately in the study plan and not replaced by a design assessment of the feasibility of the full installation. [25]

Even a successful capture will not provide an unconditional photograph of the first second. A modern gravitational accumulation of neutrinos can change the density near the Earth, and the properties of the masses can transform this density into the capture rate. Therefore, the laboratory and cosmological channels are valuable together: the first tests particles directly, the second limits early energy and propagation. Their disagreement will become interesting only after calculating the entire chain connecting both measurements.



Engraving 6. From a neutrino target to an electronic signal. In the direct search method being studied, a neutrino is captured by tritium, and the energy of the resulting electron is measured. The conventional arrangement connects the target, electron transfer and detector. It does not reproduce the design of a specific project: the ability to isolate the relic-neutrino signal is determined by the energy resolution, background, target properties and calibration stability.

## How to check it

The first path goes through the laboratory. In the reaction of proton capture by deuterium, helium-3 is formed and a gamma quantum is emitted. By measuring the probability of a reaction at the desired energies, it is possible to reduce the uncertainty in the calculation of primordial deuterium. The LUNA experiment used a proton beam, a gas target, and gamma ray recording in an underground laboratory where the cosmic background is significantly attenuated. This is a concrete example of how a measurement on Earth refines the conclusion about the first minutes of cosmic history. [26]

Further challenges include concerted improvement of the entire critical reaction network, control of target properties, detector efficiency and energy scale. The updated network must then be compared with independent observations of deuterium and helium, without fitting each reaction to the desired cosmological density. It is especially useful to publish error correlations: a few well-measured quantities may retain a common systematic uncertainty.

The second way examines the deviations of the spectrum of the cosmic microwave background radiation from the thermal form. Additional energy release in the early environment can leave a spectral trace if the processes of restoring equilibrium are no longer effective enough to completely erase it. Based on the shape and magnitude of the distortion, the time and mechanism of energy release can be limited. However, one spectral component can have several sources, including ordinary astrophysical processes.

Physically, you need an absolute spectrometer with an accurate internal reference source, wide frequency coverage and control of the device’s own radiation. Multi-frequency observations allow separation of galactic dust and other foregrounds. The PIXIE instrumental concept shows how spectroscopy and polarimetry can be combined in such a task; published design capabilities should be distinguished from already obtained operational mission sensitivities. [27]

A specific research work begins with the choice of a process: for example, the decay of a particle with a given lifetime and energy fraction. Next, changes in the composition of the plasma, primary elements and radiation spectrum are calculated. The model must pass these tests with the same parameters. A signal in one channel with a prohibited effect in another does not provide a consistent explanation.

A positive result will require checking the spectral shape, frequency calibration and alternative sources. The absence of distortion will limit the energy release only in those epochs and channels to which the experiment is sensitive. A very early process could have been thermalized; too weak will remain beyond the threshold of the device. It is the calculation of these boundaries that turns the promise of “seeing the beginning” into a definite task.

The neutrino part of the program begins by reproducing the standard calculation and one published collision model. Then, on a common grid of parameters, the temperature, polarization and cross spectra of the CMB are calculated, maintaining the connection with nucleosynthesis. If a hypothesis with a fixed non-zero interaction requires a phase and polarization pattern that does not fit into the data after changing the allowed parameters, this version is rejected. A null result limits the range of interaction; it does not prohibit any hidden neutrino interaction.

For direct capture, the first result must be a measured distribution of the response to electrons of known energy, together with background and scale stability. It is convolved with the predicted lines and beta spectrum for specific masses and local densities. This is how verifiable requirements for the

next device are obtained. Without sufficient resolution, the absence of a separate line does not refute the cosmic neutrino background. Both branches of work can produce a meaningful result before detection: an acceptable history of free streaming and a reasonable bound on the achievability of direct registration.

The hot history links nuclear reactions, radiation and the movement of weakly interacting particles. After the formation of neutral atoms, another possible source of information appears - cosmic hydrogen itself before the birth of the first stars. His radio signal is able to continue this story to the era when the future structure of the world begins to take shape from early heterogeneities.

**Chapter 5**

# The Universe before the first stars

After the formation of neutral atoms, the Universe survived for a long time without starlight. Inhomogeneities already existed in it, the gas moved in gravitational fields, and the densest regions were gradually preparing for further compression. Between the well-studied cosmic microwave background radiation and the observed galaxies lies an epoch, a significant part of which is still being reconstructed according to theory. This is where you can try to see the growth of the structure before the stars began to heat and recycle the surrounding matter.

The name "dark ages" describes the absence of numerous luminous objects. It does not mean the absence of radiation or physical processes. Relict photons continued to fill space. Neutral hydrogen could change their flux in a narrow spectral line. The principle of studying this signal before the appearance of the first stars was quantitatively developed, in particular, by Loeb and Zaldarriaga. Therefore, a new research step should be sought in some testing of models and its feasibility, and not in declaring hydrogen itself an unknown space probe. [28]

This chapter connects the hot history to the question of the nature of dark matter. Is it possible to determine from early gas why there are few inhomogeneities at some scale? Were they weak from the very beginning, or did the pattern that had already emerged smooth out the movement of the particles? To discern the causes, one will have to consistently understand the atomic signal, its cosmological change, and the limitations of the measurement itself.

## The atom as a radio transmitter

The ground state of hydrogen has two sublevels that are close in energy, associated with the mutual orientation of the spins of the electron and proton. The transition between them corresponds to a wavelength of about 21 centimeters in the rest frame of the atom. In a cosmological problem, the collective effect of a huge number of atoms is important: their interaction with background radiation creates a weak change in radio brightness at a certain frequency.

The three temperatures play different roles here. Kinetic temperature characterizes the movement of gas particles. The temperature of the CMB describes the surrounding photon field. The spin temperature is given by the ratio of the populations of two sublevels of hydrogen. It shows how atoms absorb and emit photons of this line, and does not have to coincide with the temperature of motion of the atoms. The temperature ratio changes due to competition between collisions and interaction with radiation.

In a simple homogeneous region, if the background is the cosmic microwave background radiation, the observed difference in brightness temperatures can be written in terms of the spin temperature $T_s$, the background temperature $T_\gamma$ and the optical thickness of the line $\tau_{21}$. The latter characterizes the probability of interaction of radiation with gas along the path under consideration. This notation follows from the transfer of radiation through the layer and takes into account the cosmological decrease in brightness temperature:

$$\delta T_b = \frac{T_s - T_\gamma}{1+z}\left(1 - e^{-\tau_{21}}\right).$$

A negative difference means absorption relative to the background, a positive difference means additional brightness. When $T_s$ and $T_\gamma$ are equal, the gas can exist and have inhomogeneities, although the average line contrast disappears. Therefore, the absence of a strong average signal does not yet measure the amount of hydrogen. The exact calculation also takes into account inhomogeneities in optical thickness, velocities and temperature; a linear analysis of such transfer was carried out by Lewis and Challinor. [29]

After the thermal connection with relict photons is weakened, the gas is able to cool faster than radiation. As long as collisions couple the spin temperature well enough to the gas temperature, absorption occurs. With further rarefaction, collisions become less effective, and the difference between the spin temperature and the background temperature decreases. So ordinary atomic physics creates a time-varying radio signal even before the stars appear. [28]

When the first sources light up, the picture becomes more complicated: their radiation changes the populations of the levels, heats the gas and gradually ionizes it. This stage is called cosmic dawn. It is also interesting, but it already answers additional questions about the properties of sources. For our task, we need to specify in advance the interval in which their contribution can be considered small, and check this assumption when changing the model.

## Frequency becomes an epoch indicator

Atoms interacted with photons at a known frequency, but they arrived at the observer after cosmological stretching of the wavelength. If we neglect the gas's own velocities, the relationship is simple:

$$\nu_{\text{obs}} = \frac{\nu_{21}}{1+z}, \qquad \nu_{21} \simeq 1420.4\ \text{MHz}.$$

At redshift z = 30 the result is about 45.82 megahertz, at z = 50 - 27.85, at z = 100 - 14.06. These values are actually calculated for the book using the given formula. They show the desired frequency range; Antenna sensitivity, observation time, or detection probability cannot be deduced from them. Neither the foreground stream nor the device noise participates in this conversion.

By observing different frequencies, you can access different layers of the past. The angular position on the sky gives two coordinates, and the frequency adds information about the redshift. The transition to distance requires a cosmological model, natural velocities introduce a correction, and the finite channel width mixes neighboring layers. The resulting volume refers to our past light cone: more distant regions are observed in an earlier state.

This feature is both useful and dangerous. It allows you to compare the statistics of the structure in several epochs, but prohibits considering the entire observed volume as one snapshot without corrections. If the average temperature and growth rate of disturbances change noticeably within a wide

band, the processing must take into account the evolution. Otherwise, part of the temporary change will mistakenly fall into the spatial structure.

The hydrogen signal's place among other cosmic traces is now becoming clearer. The neutrino background is associated with a much earlier cessation of effective exchange with plasma; relict photons carry a picture of the era of the last scattering; the hydrogen line adds subsequent layers to the stars. These observables are not three photographs of the same type. Each channel remembers its own processes, and its connection with the era is determined by its own transfer physics.

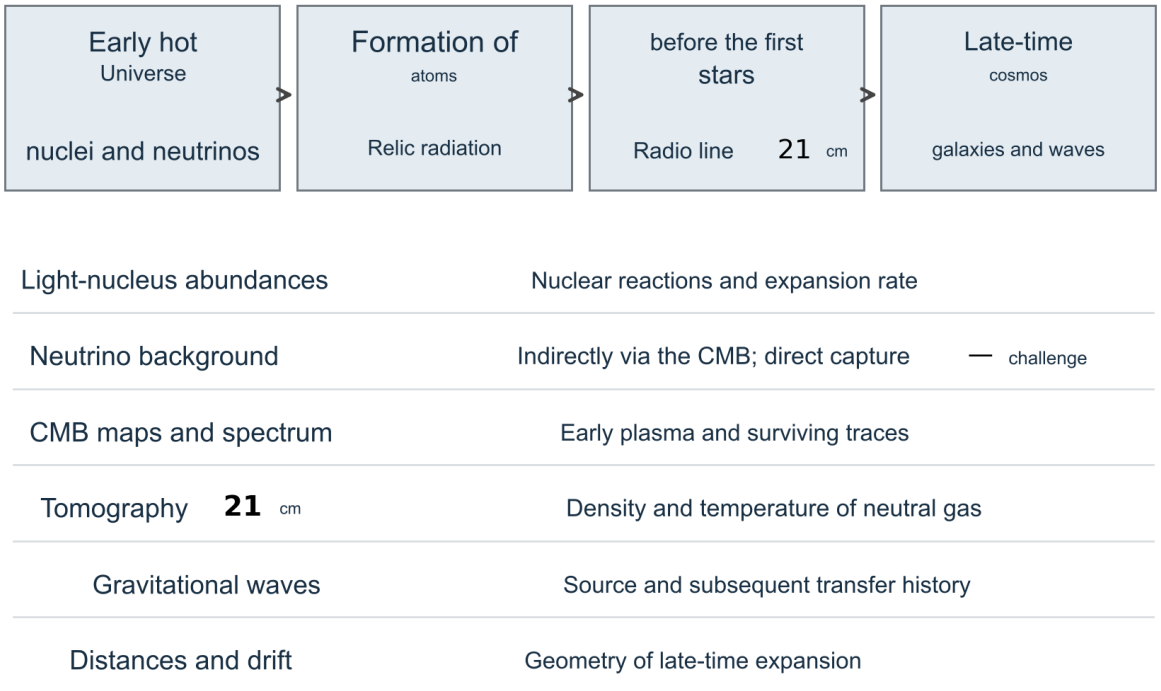



Figure 2. Carriers of information about different stages of space history. The diagram shows the sequence and physical roles, not the exact durations or sensitivity achieved. The neutrino background has indirect evidence; Direct capture and tomography of the Dark Ages remain challenges. Gravitational waves can carry information about different eras depending on the source and transport.

## From mean brightness to spatial structure

In the first version of the experiment, the spectrum averaged over the sky is measured. It talks about the average thermal history and composition of the gas. In the second, the differences between directions and frequencies are restored. They allow one to study the statistics of inhomogeneities. Modern calculations of dark age prospects consider these two modes separately: obtaining an accurate map requires different dimensions and setup capabilities than searching for an average spectral profile. [30]

The mean and the range answer different questions. Two gases may have the same average temperature, but a completely different distribution of dense and rarefied regions. Therefore, the detec-

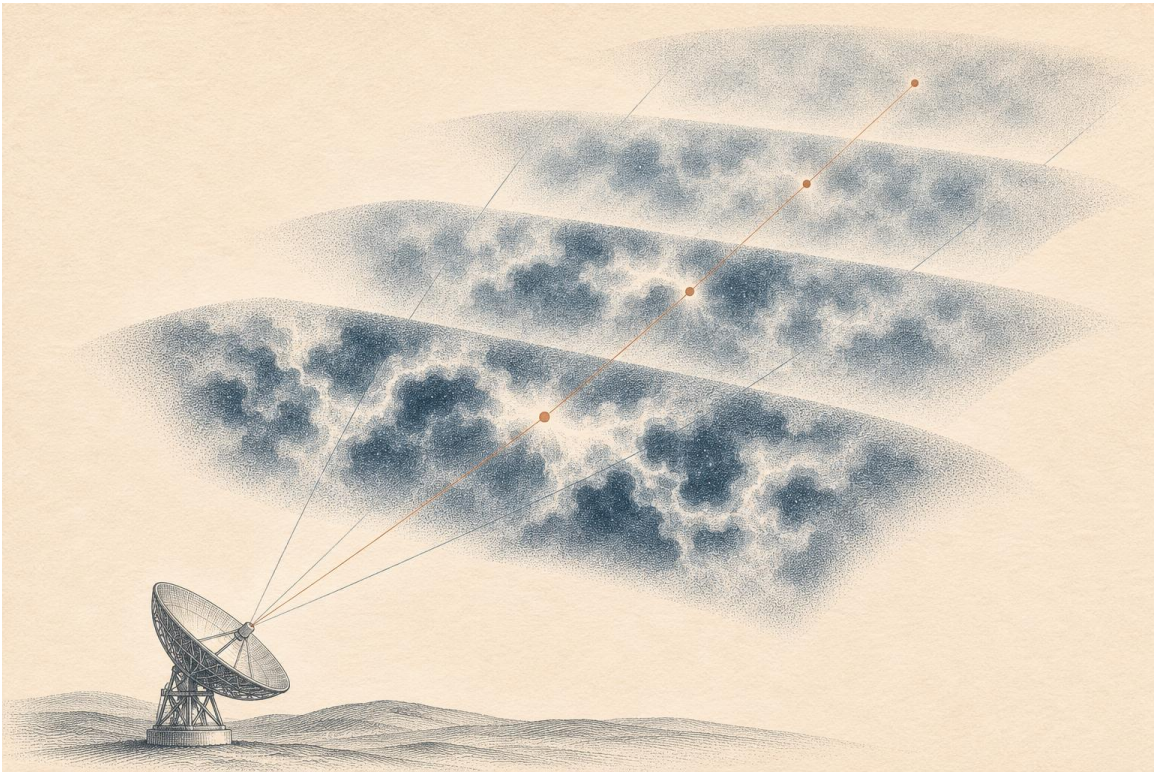
tion of average absorption in itself does not yet provide a spectrum of small perturbations. To measure it, it is necessary to establish how consistently the radio brightness changes when moving between points with a certain spatial separation.

A convenient statistic for such a figure is the power spectrum $P_{21}$. It distributes the average magnitude of brightness variations across spatial scales. A large comoving wavenumber k corresponds to a small scale. Additionally, a dependence on the direction relative to the line of sight arises: the movement of the gas changes the observed frequency and thereby the apparent radial location of the inhomogeneities. The same physical structure can therefore appear different along and across the beam.

Let q denote the cosine of the angle between the wave vector and the line of sight, and ζ the primary curvature perturbation. In a limited linear description with one adiabatic initial mode, the brightness is proportional to ζ. If we use the same Fourier normalization, it follows:

$$P_{21}(k, q, z) = |\mathcal{R}_{21}(k, q, z)|^2 \, P_\zeta(k).$$

The value $R_{21}$ combines the increase in density, movement and thermal response of the gas; its units are specified by the selected brightness temperature units. The formula expresses the usual property of linear response. With several independent initial components, instead of one product, a sum with mutual correlations is needed, and with significant nonlinearity, additional terms arise. Even a simple recording shows the main difficulty: one measured product does not separately determine the initial pattern and subsequent dynamics.



Engraving 7. Frequency reveals different layers of the past. In the idea of centimeter line 21 tomography, the direction in the sky and frequency are associated with the distribution of radio brightness. The conditional layers refer to different eras of our past light cone. They cannot be combined into a snapshot without corrections: the transition to distance requires a model, and gas velocities and finite channel widths change the reconstruction.

## Gas has its own history

Early hydrogen is attractive because it does not require describing a complex set of radiation sources before the stars. But it cannot be considered a stationary screen for dark matter. Gas has pressure, residual ionization and thermal inertia. Different densities affect collisions, and therefore affect the relationship between spin temperature and particle motion. Therefore, even the same gravitational inhomogeneity does not always give the same brightness.

The relative speed of ordinary matter and cold dark matter after recombination is especially significant. It changes the growth of small disturbances and relates their statistics to larger regions. Ali-Haimud, Meerburg and Yuan showed that this effect is reflected in the 21 centimeter signal at different scales. Exotic power suppression should be sought after including such a common contribution into the basic calculation. [31]

For our setting, this means that we need to compare entire physical states. Density matches alone are not enough: velocities, gas temperatures, and their mutual correlations must be checked. If the two versions agree only on density, further divergence may result from an incomplete initial condition. It will be the actual result of the calculation, but not the difference in mechanisms that the researcher intended to test.

You can also turn to triple correlations - the bispectrum. They describe the couplings between the three modes that form a triangle of wave vectors and add information to the conventional power spectrum. However, the nonlinear growth and the very dependence of the brightness on the properties of the gas create triple correlations even with a Gaussian primary field. The work of Muñoz, Ali-Haimud and Kamionkowski shows the need to take this secondary contribution into account when searching for primary non-Gaussianity. [32]

Therefore, the promise to “add a bispectrum and solve degeneracy” requires a separate calculation. It is necessary to show which of its components connects the models differently than power, and whether this difference remains after estimating the gas parameters. If the two versions specify the same available full state statistics and then follow the same equations, the new name of the statistic will not itself create missing information.

## Two origins of one deficiency

Let's define a limited project. In version A, dark matter is cold and the primordial spectrum is smoothly suppressed at small scales. For the first calculation, you can specify a positive phenomenological form:

$$P_{\zeta}^{A}(k) = P_{\zeta,0}(k)\,\exp[-(k/k_c)^{p}]\,, \qquad k_c > 0, \quad p > 0.$$

Here $k_c$ determines the position of the cut, p is its sharpness, and $P\zeta,_0$ is the selected smooth reference spectrum. This is a convenient research parameterization, not a new theory of the origin of disturbances. It does not yet explain what early mechanism created the slice. The test first determines whether the observation channel itself is able to distinguish between such an initial condition and another reason for the loss of small structure.

In version B, the primary spectrum is left smooth, but a specific thermal dark matter relic with a given momentum distribution is selected. The rapid movement of particles smoothes out small inhomogeneities. This physical mechanism has long been studied in models of warm dark matter; the

work of Bode, Ostriker and Turok serves as one primary example. Here the mass, distribution and contribution of the component must be related by the chosen model, rather than being fitted independently for each redshift. [33]

First, the parameters of both versions are chosen so that their measured power is close in the same reference epoch and in a prespecified range of scales. Then the remaining epochs, the direction of oscillation relative to the line of sight and, with sufficient theoretical accuracy, triple correlations are compared. The assumption being tested is that the continued difference in dynamics will leave an additional trace that cannot be absorbed by the permitted parameter change.

This assumption may turn out to be incorrect. If by the available epoch the residual motion of the warm component is no longer significant, and its action has been reduced to an almost constant change in the transfer function, a specially selected primary spectrum is capable of reproducing the same result. Multiple redshifts do not guarantee separation: equal subsequent growth carries the coincidence from one epoch to the next. The exponential form given above may be too rigid for an exact fit; then it is this form that is tested, and not the whole idea of primordial suppression.

This outcome is useful for science. It will determine that the radio map is measuring a combination of initial spectrum and carryover, and will indicate what additional assumption is needed for the separation. It may be necessary to limit the primary spectrum to another channel or to observe an epoch when residual dynamics are still noticeable. You may need to test the particle yourself. The choice should follow from the structure of degeneration, and not from the desire to obtain a positive answer at any cost.

The first test of degeneracy can be made particularly transparent. With one linear initial mode, the ratio of powers in two epochs with the same comoving k and values of the angular parameter q reduces the primary power. If both responses are non-zero, it follows directly from the previous formula:

$$\frac{P_{21}(k,q,z_1)}{P_{21}(k,q,z_2)} = \left|\frac{\mathcal{R}_{21}(k,q,z_1)}{\mathcal{R}_{21}(k,q,z_2)}\right|^2 .$$

Therefore, changing the initial power alone will not falsify an arbitrary change in this ratio. But if the response ratios are the same in versions A and B, this test does not separate them. This is an algebraic consequence of a limited linear description, and not a universal law of dark matter identification. In real observation, statistics from different layers are compared, rather than repeated images of the same area; their covariance, different resolutions, and overall geometric model must be taken into account.

Such control is also useful for artificial intelligence, which is tasked with searching for distinguishing features. First, he is given pairs where the relation is analytically identical, then pairs with a known transfer difference. If the algorithm confidently distinguishes the first group based on unmeasurable details of the simulation, it has found a feature of the data preparation. Returning to the analytical example allows us to detect this error before interpreting the result as new physics.

If the outcome is positive, the next step is to check the stability. The difference must survive changes in standard cosmological parameters, gas temperature and the allowable residual stellar contribution. A prediction that is noticeable only with perfectly fixed covariates may disappear in real analysis. Therefore, the result of the project will be a region of distinguishability in parameter space, and not a single spectacular pair of theoretical curves.

## Radio silence and device operation

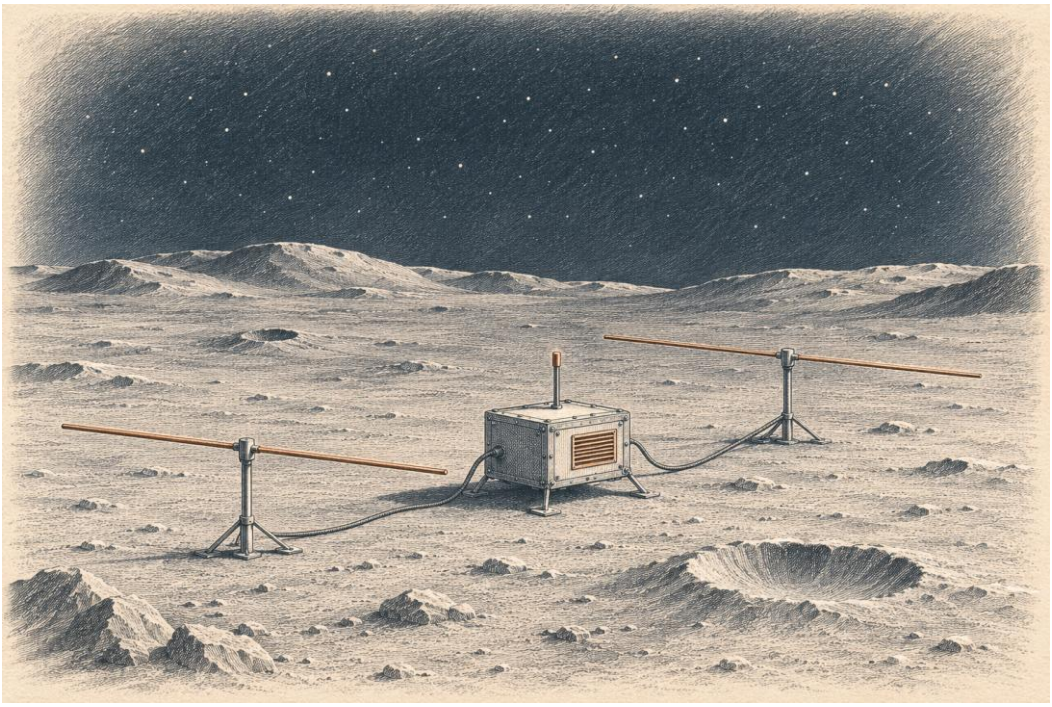
The low frequencies required make the task engineering difficult. The Earth's ionosphere changes the propagation of radio waves, and human transmitters create powerful interference. The far side of the Moon is seen as a place where Earth's radio pollution can be mitigated. The official description of LuSEE-Night defines it as a precursor experiment for exploring the radio environment and mastering such an observation window. This status is not equivalent to the already completed tomography of the Dark Ages. [34]

The LuSEE-Night design includes a low-frequency receiver and mutually oriented antennas; The team's published work describes autonomous observations on a lunar night. For the book, the physical step itself is important: check the reception, calibration and operation of the installation in the desired environment. The delivery schedule is not proof of the sensitivity achieved, so conclusions about cosmology must be based on the measured performance of a particular instrument. [35]

The lunar site does not eliminate the galactic radiation, the inherent noise of the electronics, or the inaccuracy of the antenna model. The dependence of its directional response on frequency is especially dangerous. If the instrument mixes bright areas of the sky differently at different frequencies, a spectrally smooth foreground can produce a structure similar to the signal of interest. It is necessary to measure not only the gain of the receiver, but also how much of the sky it is weighing.

For an interferometer, this problem also manifests itself in mixing of spatial modes. The connection of the smooth foreground with the frequency response of the installation is capable of contaminating the wedge-shaped region in the transverse and longitudinal wave number coordinates. Statistical analysis of this effect was developed in studies of the 21 centimeter line of the reionization epoch. For the dark ages, it is necessary to re-substitute the frequencies, geometry and noise of the future array; the ready-made sensitivity of another experiment is not automatically transferred. [36]

This implies a specific requirement for the project: to calculate the distinguishability of models only on those modes that actually remain after cleaning and selection. If the main discrepancy lies in a distant region, it cannot be considered an observational advantage. A machine learning algorithm can predict latent values from the adopted model, but such reconstruction does not add an independent measure of the removed modes.



Engraving 8. Radio observation from the far side of the Moon. The far side of the Moon is considered as a site for low-frequency measurements with attenuated terrestrial radio interference. The image shows a conventional antenna installation, not a finished project of a telescope. Lunar shielding does not eliminate galactic foreground, intrinsic noise, or antenna frequency dependence; future sensitivity must be determined by measurement and calculation.

## How to check it

The first result can be obtained before the construction of a large observatory. For a given pair of A and B, a reproducible calculation of densities, velocities, temperatures and radio brightnesses in several layers should be produced, for example around z = 30, 50 and 100. These values serve as a reference grid rather than a universal star-free boundary. Lower layers are excluded or supplemented with sources if the chosen model predicts a significant stellar contribution there.

Then a measurement model is built. For the mid-spectrum, it includes frequency response, antenna pattern, and calibration standard. Spatial correlations require array geometry, a set of distances between antennas, frequency channels, and observation duration. The parameters are taken from a specific project or explicitly specified as options for a future design. Only after this the difference between the theoretical signals receives observational meaning.

Each of the two models along with celestial foregrounds and instrumental errors are introduced into the artificial data. Reconstruction is carried out blindly for the analyzing algorithm, changing the allowed nuisance parameters in both versions. One part of the simulation sets the threshold for the model to be falsely selected, the other tests how often the correct version passes the selection. Independent code implementations must reproduce key transfer functions on a common mesh.

A particular test concerns an erroneous basic calculation. One must alternately vary the residual ionization, gas pressure, relative component velocities, and foreground frequency shape within reasonable uncertainties. If the small standard correction simulates the stated effect of warm matter, the experiment is still limited by the combination of causes. It is such a test that will indicate which atomic, cosmological or engineering uncertainty is more profitable to reduce.

The selected version A will be rejected if, after general fitting, its resolved parameters do not reproduce the available statistics of several layers under a predetermined criterion. The same rule applies for B. The absence of a difference due to insufficient sensitivity does not reject both versions. The detected low-power deficit also does not automatically establish the particle: other initial spectra, dynamic mechanisms, and possible transfer errors remain.

The final product of the study is a map of for what parameters and observed modes the two given versions differ, where the foreground interferes, where the theory constrains, and where degeneracy persists even in the absence of instrumental noise. It compares the benefits of additional bandwidth, larger array base and better calibration. Such a result could change the design of the telescope even before it is manufactured and give the next group a narrower, testable task.

The Dark Ages provide an opportunity to trace the transition from early disturbances to the structure of matter. Their scientific value is determined by what causes of this structure can be separated by physical measurement. Now the question about the invisible gravitating component can be posed more precisely: what properties of dark matter are required by observations and what independent traces will allow us to verify its nature?

**II Invisible components**

**Chapter 6**

# Invisible mass

Through a telescope, the galaxy looks like a cluster of luminous objects. If you take the photo deeper, fainter stars and clouds will appear. A natural expectation arises: it is enough to collect all the light, add a mass of invisible gas, and we will find out how much matter is in front of us. But the movement of the galaxy tells a different story. The mass needed to explain the observed velocities is often noticeably greater than the mass of ordinary matter found.

This discrepancy relates to a specific connection between observations and the law of gravity. We measure the spectra, positions and distortions of the images, then reconstruct the mass distribution. Therefore, from the very beginning, the problem has two solutions: an additional source of gravity and a change in its description. One has to choose between them based on the totality of phenomena. The explanation for one rotation curve still has to stand the test of light, hot gas, and the history of the structure's formation.

Dark matter is a component whose presence is judged primarily by its gravitational effect. The name does not identify the particle, mass, or mechanism of creation. It denotes a place in the physical description that is already limited by observations, but has not yet been filled by established microphysics. The gravitationally bound extended structure of such a substance is called a halo. In the standard picture, the visible galaxy occupies only part of this structure.

## Mass by motion and light

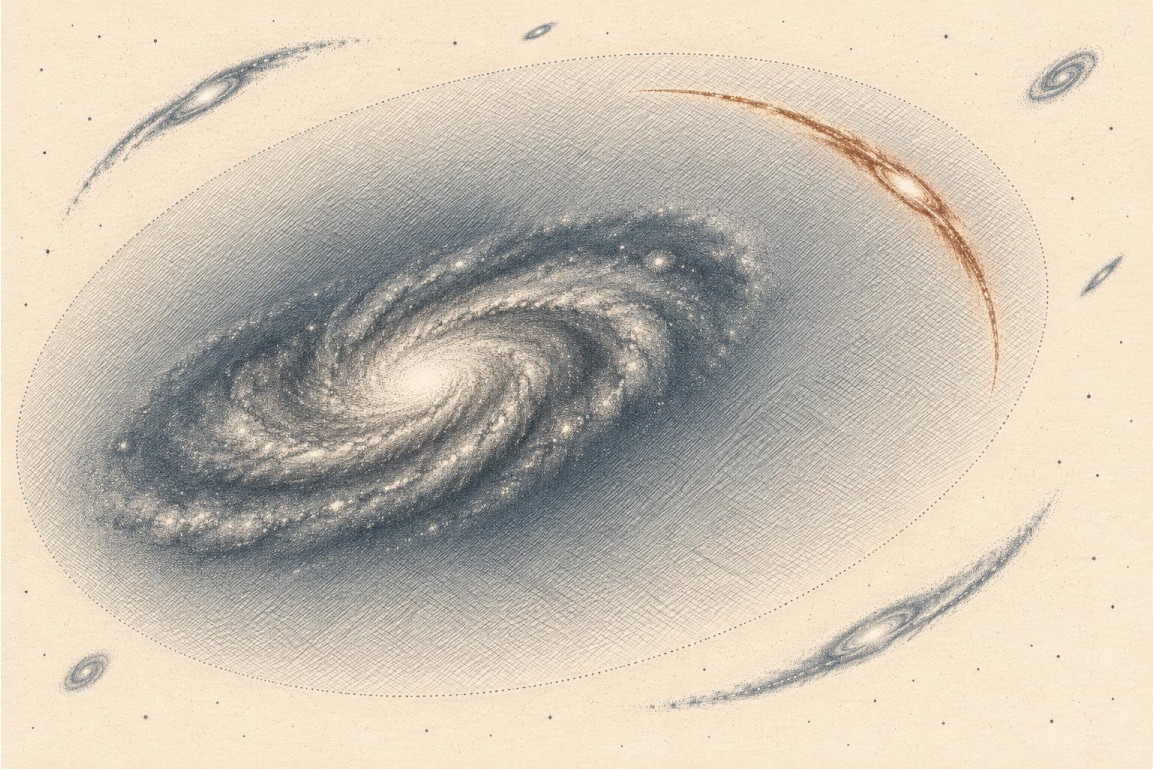
Let's imagine a star in an almost circular orbit around a spherically symmetric distribution of matter. In the Newtonian approximation, its speed is related to the mass inside the orbit by a simple relation:

$$v^2(r) = \frac{GM(<r)}{r}.$$

Here r is the distance to the center, G is the gravitational constant. When almost all the mass has already remained inside the orbit, the speed should decrease with distance. If the speed remains approximately constant, the required enclosed mass continues to increase. A real disk galaxy is not spherical, so an accurate reconstruction requires a different geometry, corrections for gas motion and the contribution of the stellar disk. A simple formula only explains why distant orbits are sensitive to the invisible distribution of matter.

Even the speed of a star is not included in the calculation as a ready-made number. The spectrum shows the component of motion along the line of sight. To obtain the rotation speed, you need to know the inclination of the disk. For a galaxy visible almost from the face, a high velocity in the plane of the disk may produce a small spectral shift; the tilt error will significantly change the reconstructed mass. Therefore, a good check uses a spatial motion map and independent geometry constraints. This way we can distinguish the halo property from the error that our position relative to the object created.

Distortions of distant images provide another route. Light travels through curved spacetime, and nearer mass acts as a gravitational lens. Its distribution can be estimated even when it emits very little light. Comparing such maps with X-ray emission is particularly revealing in colliding clusters. In the Bullet Cluster, hot gas containing most of the visible ordinary matter is spatially separated from the mass peaks reconstructed by lensing. This is strong evidence for an additional gravitating component. The image itself, however, does not identify the particle making up that component. [37]



Engraving 9. Light reveals an invisible distribution of mass. Gravitational lensing changes images of distant sources and allows us to reconstruct the distribution of mass in front of them. The halo is shown in the engraving with conventional shading to make the subject of the calculation visible: such a glow is not directly observed. This method relates mass to the geometry of light, but does not itself establish a dark matter particle.

There is also an early cosmological argument. Before the formation of neutral atoms, ordinary matter participated in acoustic vibrations along with radiation. A component that interacts weakly with light had a different effect on gravitational inhomogeneities. The ratio of peak heights in the CMB spectrum therefore helps distinguish between the densities of ordinary matter and cold dark matter. In the basic flat ΛCDM model, Planck analysis gives a ratio of these densities of about five. Here, the weight of the invisible component is determined by its influence on early oscillations, taking into account other parameters of the model. [6]

It is the diversity of evidence that gives stability to the task. An attempt to replace dark matter with a modified law of gravity should predict motion, lensing, and early acoustic vibrations. The model with new particles assumes the same obligations. Comparisons become meaningful when both sides calculate the same observables and honestly account for errors.

The word “cold” in the name of the standard component characterizes its movement during the stages of structure formation. It means that the random velocities are small enough and do not erase inhomogeneities on the scales of interest. This name has nothing to do with the temperature of the

surface of a dark cloud. Different particles may behave similarly in large structures, but differences will only appear on smaller scales or in laboratory interactions.

## How to Hear a Rare Collision

One experimental approach is to wait for a putative dark matter particle to collide with ordinary matter. The detector is hidden from cosmic rays, surrounded by protection, and the radioactive background is carefully measured. If a galactic stream of new particles passes through the facility, it can sometimes transfer energy to a nucleus or electron. We need properties of the signal that allow us to distinguish it from already known processes.

In the LZ biphasic xenon detector, the interaction creates a flash of light and releases electrons. The electric field transports electrons to the liquid-gas interface, where an additional light signal appears. The combination of the two signals helps to reconstruct the energy and position of the event and distinguish between types of interactions. For the selected standard spin-independent scattering of weakly interacting massive particles, or WIMP, scenario, the 4.2 ton-year analysis published in 2025 found no excess above background. With a particle mass of 40 $GeV/c^2$, the upper limit of the cross section was $2.2 \times 10^{-48}$ $cm^2$ at a confidence level of 90 percent. This is a conditional limit for this interaction and the galactic flow model. [38]

The cross section relates the flow of particles to the expected frequency of their collisions in the target. A zero result cuts off those combinations of mass, cross-section and density that should have produced a detectable excess of events. For a particle of a different mass, interacting primarily with electrons, or another type of communication, the calculation of the signal changes. It also changes when the desired particles make up only a small fraction of dark matter. Therefore, the boundary in such a graph tests a specific mode of interaction, rather than exhausting all candidates.

Axion searches have a different logic. In a magnetic field, the putative axion can be converted into an electromagnetic excitation; The resonator amplifies the response in a certain frequency band. Such a setup is sensitive both to the particle’s coupling with photons and to its local density. A laboratory experiment involving passage through an opaque wall tests the production and subsequent conversion of a new particle back into light without requiring its presence in the galactic halo. Therefore, the discovery of a light particle in the laboratory in itself would not determine its cosmological fraction. [39] [40]

The lower the background becomes, the more noticeable are processes that could previously be ignored. A separate LZ analysis found evidence of coherent scattering of solar neutrinos. The significance of the 4.5 standard deviation given there applies precisely to neutrinos under the accepted hypothesis of the absence of a dark matter signal. It is not the significance of the discovery of a new substance. The spectral similarity of neutrino events to some putative signals adds complexity, but leaves room for other nuclear targets, energy ranges, and additional event characteristics. [41]

The theory also needs to explain the number of new particles. In the early hot environment they could be born and destroyed in reactions. As the reaction cooled, the rate of reactions became insufficient to maintain the previous equilibrium, and a residue remained. Mechanisms are also possible in which equilibrium was not established at all, or the field arose as a general initial state. These options relate modern density to different parameters. Therefore, even the accurately measured mass of a new particle does not yet allow us to calculate its share in the Universe without knowledge of interactions and early history.

## What changes do collisions inside dark matter make?

Scattering by an ordinary nucleus and the collision of two dark matter particles are different interactions. A weak connection with the detector does not exclude noticeable communication between particles. This allows us to consider dark halos as systems with their own internal evolution, which can be studied by mass distribution.

In self-interacting dark matter, collisions transfer energy between particles. If heat flows from the outer regions to the center, the central region expands and becomes less dense. At a later stage the flow may reverse. Losing energy, the self-gravitating center contracts; At the same time, the characteristic velocities of particles increase, and the heat outflow can increase. This sequence allows one law of interaction to create both sparse and very dense centers: different halos can be at different stages of evolution. This relationship has already been studied for small galaxies and dense objects detected by lensing. [42]

The dependence of interaction on speed is important. Small galaxies and large clusters have different characteristic velocities, and one constant number may not be a good description. In the illustrative calculation of this book, a law is chosen in which the transport cross section per unit mass decreases from approximately 8.9 to 0.0073 $cm^2/g$ when the relative speed changes from 30 to 1000 km/s. These parameters are chosen to demonstrate the effect and are not declared as permitted observations. Moreover, the transport section with a certain angular weight still needs to be correctly related to the heat transfer in the real velocity distribution.

There is a verifiable risk to such an idea. Some parameters must be suitable for the entire population under consideration. An analysis of the SPARC catalog galaxies, updated in 2026, shows how difficult it is to fulfill this condition: in the family considered, the authors did not find a single cross-section model that satisfactorily describes all galaxies. The reconstructed parameters also degenerate with the age and stage of halo evolution. Good individual descriptions therefore do not yet establish general microphysics. [43]

The same work identifies a general L-shaped region of preferable parameters: both an almost constant small cross-section and a strong dependence on speed are acceptable. This does not contradict the previous conclusion. In section 4.2, the authors separately warn: the best joint compromise does not yet provide a satisfactory description of each galaxy, and the narrow range of parameters cannot be overestimated. The next check should compare not only the position of the general minimum, but also the distribution of residuals across objects, while maintaining uncertainties in age, baryonic history and evolutionary stage. [43]

The main astrophysical competitor is nearby. Star formation bursts, gas emissions and changes in the central gravitational potential can rearrange the distribution of ordinary cold dark matter. Such effects are reproduced in numerical models with baryon feedback. Two models with comparable freedom of description of ordinary matter should be compared; otherwise, the advantage will be given to the one that was simply allowed more adjustments. [44]

## Wave the size of a star system

The quantum properties of a particle become noticeable at the scale of its de Broglie wavelength. For a sufficiently light field, this scale can be astronomical. Then it is more convenient to talk about a

distributed field with a changing phase and interference, and not about independent point objects moving along trajectories. For nonrelativistic motion, the characteristic length has the form:

$$\lambda = \frac{h}{mv}.$$

In this notation, h is Planck's constant, m is mass, v is characteristic velocity. At rest energy $2\times10^{-20}$ eV and speed 20 km/s, the own dimensional calculation gives about 30 parsec. If we use the reduced Planck constant, the corresponding scale will be 2π times smaller. Both quantities may appear in the literature, so the definition of length must be checked before comparing numbers.

Wave properties can suppress the formation of small structures. The trace is sought in the spectra of quasars: light passes through intergalactic hydrogen, which leaves many absorption lines. They measure how transmittance changes along the spectrum at different scales and compare it with artificial spectra from models of gas and dark matter. The thermal motion of the gas also smooths out small details, so its history must be determined together with the field properties. The published lower mass bound $2\times10^{-20}$ eV/$c^2$ with 95 percent Bayesian confidence refers to a specific model where the field constitutes all dark matter. A separate calculation is required for a mixture of components. [45]

The same field creates the changing gravitational environment of stars. A system with a small internal velocity spread is called cold here. The almost identical acceleration of all stars changes the motion of the system as a whole and may have almost no effect on this scatter. Differences in acceleration between stars are important for its internal heating. The system's own gravity, the structure of the central region of the field, and the tidal action of neighboring objects determine whether it will expand and survive to this day. Modern calculations show the need to take all these effects into account. [46]

## How to check it

For a self-interacting model, two samples can be defined in advance. The first contains small galaxies in which the velocities of gas and stars are measured at different points. Radio observations of neutral hydrogen and optical spectroscopy provide a motion map; imaging and star formation history constrain the contribution of ordinary matter. In the second, there are strong gravitational lenses, in the images of which they look for disturbances from small dark concentrations. To isolate their contributions, the main lens, the background source, and the material along the line of sight are simultaneously modeled.

From the first sample, acceptable parameters of the general scattering law are obtained, and then the number and profiles of detectable disturbances in the second are predicted. The probability of their detection is measured by adding artificial condensations to the image model and repeating the entire search procedure. The age and orbit of an individual halo may be unknown, but the distributions of these quantities must have a general physical basis. The version being tested is rejected if no valid set of parameters reproduces the second sample, taking into account selection and errors. Competing cold matter with the influence of ordinary matter is tested in the same way.

For a wave field, the general parameters are mass and cosmological fraction. The feasible region is first obtained from the quasar spectra along with uncertainties in temperature and gas ionization. Then, for the same parameters, the sizes and internal velocity dispersion of old stellar systems are calculated after evolution in a changing field. Repeated spectroscopy helps to separate the motion of

binary stars; Additionally, estimates of age, former compactness, and tidal orbits are needed. The local field density in each object should follow from the same mixed model, and not become a new free means of matching.

A decisive result occurs if the parameters required by one channel are inconsistent with the other under tested uncertainties. The preservation of the old cold system can eliminate the field that was sure to destroy it; the absence of early suppression of structure is a field to which late dynamics attributes too large ripple effects. If the differences lie below the sensitivity, the result will be a map of an area that has not yet been tested. The next computational step here is quite defined: a general model of structure formation and late dynamics with a forecast for data that did not participate in the selection of parameters.

Chapter 7

# Why matter remained

The atoms that make up the Earth and stars contain protons, neutrons and electrons. These particles have antiparticles. In a hot environment, sufficiently energetic interactions can produce pairs, and the meeting of a particle with an antiparticle can convert their energy into other forms. The question then arises before the formation of stars: why was there so much ordinary matter left after the early hot epoch?

Explaining the appearance of particles and explaining their excess are different tasks. You can get huge amounts of matter and antimatter without changing the difference between them very much. Subsequent annihilation will destroy most of the pairs, maintaining a small initial advantage. It is this preponderance that needs to be associated with physical processes.

The problem does not require that antimatter not exist anywhere: antiparticles are being created today. We need to explain the observed cosmological baryon excess. Particles like protons and neutrons are called baryons; in early plasma the corresponding charge was distributed between quarks. Cosmological history should relate this charge to the present amount of ordinary matter without destroying successful predictions of the formation of light nuclei.

## Small excess with big consequences

To compare different epochs, the excess of baryons over antibaryons is expressed relative to another quantity, which is rarefied during expansion. We can take the ratio of the numerical densities of the excess and photons. Another choice is the entropy density: the resulting ratio is called the baryon yield. It is especially convenient when the entropy in the comoving volume is conserved:

$$Y_B = \frac{n_B - n_{\bar{B}}}{s}.$$

The numerator contains the numerical densities of baryons and antibaryons, and s denotes the entropy density. The Planck reference cosmology with standard late thermal history gives a baryon yield of about $8.7\times10^{-11}$; the ratio of the excess to the number of photons is about $6.1\times10^{-10}$. This specifies the order of magnitude that the mechanism must reproduce. The transition between the two ratios depends on the thermal history; a constant number of photons cannot be transferred through any early particle transformations. [6]

Baryon excess should be distinguished from electric charge. A proton and an electron have opposite electrical charges, but an electron is not an antiproton. Therefore, an ordinary neutral atom is capable of containing a positive baryon number while remaining electrically neutral. Confusing these two accounts creates a false mystery about why excess matter does not make the entire Universe a giant charged body. Every physical interaction must be checked to ensure that the charge in question is maintained.

Creating a small advantage is only part of the task: it must survive further cooling. The number of pairs of particles and antiparticles varies, and some reactions can both create and erase asymmetry. Therefore, the calculation tracks the remaining charge. A rapid reaction that effectively produces an excess is sometimes just as effective in returning the system to equilibrium and destroying the result.

For the usual scenario, starting with a symmetric plasma, Sakharov's conditions bind three requirements. Changing the baryon number makes it possible to shift the initial balance altogether. The

breaking of symmetries between particles and antiparticles makes it possible to prefer one sign of excess. Deviation from thermal equilibrium allows this preference to persist: under standard assumptions, reverse processes in equilibrium compensate for the directional accumulation of charge. Conditions specify the necessary properties of the mechanism; the amount of remaining substance is determined by the rates of specific reactions. [47]

C symmetry replaces particles with antiparticles; P changes spatial orientation, like a mirror image. For many mechanisms, their combination of CP is essential. The ability to distinguish a process from the corresponding process with antiparticles and reflected coordinates opens the way to different probabilities. However, measured CP violation in one interaction does not automatically determine all the necessary differences in another, early system.

Cosmological expansion creates a natural possibility of moving away from equilibrium. Particles have a characteristic time of interaction, and a changing Universe has a time of change in temperature and density. If reactions do not keep pace with changes in the environment, some equilibrium relationships cease to hold. For the researcher, this is a comparison of measurable or calculated speeds. It allows you to specify exactly when the desired charge can arise and which late reactions must turn off in order to maintain it.

## Neutrinos as a connection between eras

One research line is adding heavy neutral leptons to known particles. They can mix weakly with ordinary neutrinos. This mixing links processes observed at low energies to possible early plasma dynamics. The minimal version considers two new states, their masses, and a single matrix of interactions with three types of ordinary leptons.

The interaction matrix is a table of coefficients relating each new state to ordinary leptonic species. The same table is involved in calculating the masses of light neutrinos, the birth and decay of a new particle in the installation, and the reactions of early plasma. Thanks to this, the laboratory can test the cosmological explanation. However, a single experiment usually measures only some combinations of coefficients, so the results of different channels have to be combined.

In oscillatory leptogenesis, asymmetry arises due to the quantum evolution of mixing neutral states and CP-violating interactions. During production in the plasma, their relative phases and the distribution of leptonic charges change. Interactions transfer the asymmetry to ordinary leptons, and electroweak processes link it to the baryon excess. This is how the mechanism proposed by Akhmedov, Rubakov and Smirnov works; For him, it is the evolution of mixing states in a hot medium that is essential. [48]

Quantum coherence means that for calculations it is sometimes not enough to know only the number of particles of each type. The relative phases of states are also important. Collisions with plasma can destroy this information, and free evolution can change the interference pattern. Therefore, the usual scheme of independent births and decays may miss a significant effect. Matrix kinetics equations allow you to take into account both the numbers of particles and the correlations stored between states, and then check how much the simplification changes the final charge.

The connection between the baryon and lepton excesses is ensured by sphaleron processes—collective transitions of electroweak fields. They change the baryon and lepton numbers, maintaining their difference. Therefore, the asymmetry that arises in ordinary leptons affects the final baryon charge. The transfer must take place while these processes are fast enough compared to cosmological evolution. When cooled they become ineffective. Their moment of switching off depends on the

properties of the fields and the expansion history; a change in the scalar sector or cosmological background requires a new calculation. [49]

The laboratory picture can be quite visual. A new neutral particle is born during the decay of a meson or W-boson, flies for some distance and decays into visible products. The apex of its decay turns out to be displaced relative to the collision site. Based on geometry and energies, the mass and lifetime are reconstructed, and based on the composition of products, connections with various leptonic species are reconstructed. ATLAS searches of this type already constrain specific mass and mixing regions; the boundaries have the form of contours depending on the adopted scenario. [50]

Even after a particle is discovered, some complex interaction parameters will remain poorly determined by the available decays. The resulting asymmetry also depends on the initial population of new states and the late release of entropy. For our test, we fix a sufficiently high heating temperature, after which the expansion is controlled by radiation; the initial asymmetry and initial population of new states are equal to zero, there is no late dilution by entropy. These are the conditions of the chosen version of the mechanism: changing them after an unsuccessful result would mean testing a different version.

An independent search for double beta decay without neutrino emission is useful. Its observation would test for lepton number violation, but converting the signal into parameters requires taking into account possible exchange mechanisms and nuclear calculations. In the model with heavy neutrinos, the contributions can enhance or suppress each other. Collaborative studies show how such data, early nucleosynthesis limitations, and accelerator searches are narrowing the region in which the desired baryon yield is possible. [51]

## Matter on a moving boundary

Another way connects asymmetry with an electroweak phase transition. During a first-order transition, new bubbles may appear in the old phase. Their boundaries move through the plasma, changing the properties of particles and the conditions of interactions. A spatially inhomogeneous, nonequilibrium environment arises in which the physical source of CP violation is capable of redistributing charges.

In the familiar Standard Model with the observed mass of the Higgs boson, the electroweak change of state is a smooth transition rather than the required bubble pattern. Therefore, such a mechanism requires additional physics. Lattice calculations help determine the conditions and speed of sphaleron processes in the standard case; When adding new fields, their results cannot be transferred without verification. [49]

As a specific hypothesis, one could add a single real scalar field and a separate CP-violating interaction between that field, the Higgs field, and the top quark. A scalar by itself is not enough: the source of the difference between particles and antiparticles must be stated explicitly. From one potential it is necessary to obtain the structure of the phases, the probability of bubble birth, the development of the transition, and plasma heating. Only then can the charge transfer at the moving wall be calculated.

The wall velocity is of particular interest. Slow and fast movement give particles different times to transport and react. At the same time, this speed affects the motion of the plasma and possible gravitational radiation. If you choose one speed for the formation of matter and another for a beautiful wave spectrum, you end up with a set of incompatible calculations. The model must use a single physical wall, with general uncertainty about its speed and thickness.



Engraving 10. A moving boundary between two phases. In the considered extension of the model, the boundary of the bubble of the new phase passes through the plasma and changes the conditions of interactions. The same wall is involved in the transfer of charges and the movement of the medium. This is an illustration of the hypothesis: the bubble transition requires additional physics, and the speed, wall thickness and amount of asymmetry are subject to general calculation.

This expansion also predicts laboratory effects. An additional scalar state can change the properties of the Higgs or appear in decays. The source of CP violation is capable of influencing electric dipole moments. In the singlet model studied by Ellis et al., there are regions with sufficient baryon yield, but with gravitational waves that are not available in their prediction. Therefore, the absence of waves does not exclude the entire mechanism of electroweak asymmetry formation. [52]

A permanent electric dipole moment along the spin would manifest itself in a certain dependence of the particle energy on the electric field. In molecular spectroscopy, the corresponding frequency shift is sought under controlled reversal of fields and other setup parameters. However, the molecular response may depend on several CP-violating interactions. The limit derived under the assumption of one contribution cannot be automatically transferred to their arbitrary combination. Comparing multiple measurements helps separate these contributions and test for a common source of asymmetry. [53]

## What can you learn from a gravitational wave?

The movement of boundaries and excited plasma during a phase transition can generate a stochastic gravitational wave background. Its spectrum carries information about the characteristic size of the sources, duration and energy of the process. Unlike light from stars, such a signal could reveal the state of matter long before the appearance of atoms. But it is possible to reconstruct a single history from it only with a sufficiently definite physical model.

A simple calculation shows the problem. According to the published calibration of the sound source, the transition at a temperature of about 100 GeV and the transition at a temperature of about 1000 GeV could have the same peak frequency today - about 1.50 millihertz, if the duration of the process relative to the expansion time differs. Here, specially selected parameters are used, rather than found solutions to a specific scalar potential. The calculation illustrates the dependence of frequency on several quantities; amplitude and detectability were not determined. [54]

Even a convincing detection of such a background will require finding out which sector created it. A latent matter transition may produce a similar spectrum and not be involved in baryon production at all. To establish a connection, one must find consistent laboratory signatures and derive the correct charge from the overall dynamics. The very position of the peak in the sensitive range of the future device does not yet answer either the question of the source or the question of the possibility of detection.

The similar order of densities of ordinary and dark matter also motivates general models. In theories of asymmetric dark matter, interactions can bind the charges of two sectors, and then their history leads to different residual densities. However, the ratio of mass densities depends on masses, and on numerical asymmetries, and on subsequent reactions. The proximity of two cosmological numbers does not in itself prove a single origin. [55]

## How to check it

The neutrino program tests two new states with a common interaction matrix and the initial conditions fixed above. Accelerator data constrain the masses, lifetimes, and couplings to ordinary leptons; neutrino measurements and double beta decay add other constraints. For the entire jointly feasible region, the achievable baryon excess is calculated. The version is rejected if the observed value with the correct sign is unattainable under any set of parameters, taking into account calculation errors. The failure of one chosen point is not enough for this.

The next calculation should reproduce published benchmark solutions of quantum kinetics, evaluate the influence of approximations, and enumerate phases that have not yet been measured. It needs to be associated with a specific detector model. The lifetime determines how many particles will decay inside the sensitive volume; geometry and thresholds - which products will be registered. Artificial events, together with background decays, will show how much of the cosmologically feasible region the setup will actually test. So the absence of found particles receives a certain physical meaning.

For the bubble scenario, the sequence starts with the common potential. It is necessary to verify that the transition actually completes and the created charge is not erased. Further, some parameters determine the bubble wall, charge transfer, properties of new particles, dipole moments and wave spectrum. The test must preserve common parameter values and in places where different observations would prefer different values. The laboratory search includes new scalar birth and decay channels, changes in Higgs interactions, and molecular measurements with independent controls.

Failure here can have various physical reasons: the transition does not occur, the asymmetry is too small, subsequent reactions destroy it, or the required region has already been excluded by the laboratory. The absence of waves is only critical where a consistent calculation predicts a detectable signal. If its level is lower than real noise and backgrounds, such an experiment does not yet verify this point. If the result is successful, you will need to compare the shape of the spectrum with alternative sources.

Complete new kinetic or thermal calculations for these programs have yet to be performed. Its result should be a general region of parameters that allows the desired baryon excess and all independent measurements. Then the explanation of the ancient history of the substance will be associated with laboratory conditions under which it will have to be abandoned.

Chapter 8

# Accelerating Universe

The expansion history can be reconstructed from objects whose light was emitted at different epochs: measure their redshifts and distances, then find the dynamics compatible with them. Another way is to monitor the change in redshift of one source for years. It requires an extremely stable frequency scale. Let's start with the first path that led to the discovery of acceleration, and then ask what independent measurements can be used to verify its physical cause.

At the end of the twentieth century, measurements of distant Type Ia supernovae provided evidence that cosmic expansion was accelerating. After their light-curve properties were taken into account, the supernovae appeared fainter than expected in the models under consideration, which contained only decelerating matter. The relationship between brightness, distance, and redshift therefore pointed to a different cosmic history. The original papers already considered alternative explanations, including dust, source evolution, selection effects, and calibration. [56]

The modern challenge goes deeper than the detection of acceleration itself. We need to establish what physical description is behind it. The term "dark energy" brings together possible ways to describe the corresponding contribution to cosmological dynamics. It does not mean that a substance of an unknown type has already been caught and studied in the laboratory.

## Constancy as a physical hypothesis

In general relativity, expansion is affected by both energy density and pressure. Therefore, knowing only the amount of energy is not enough. It is convenient to introduce the parameter w—the ratio of pressure p to energy density ε:

$$w = \frac{p}{\varepsilon}.$$

For a slowly moving substance, the pressure is small compared to its energy density. For radiation it is positive and essential. A component with sufficient negative pressure is able to support accelerated expansion. Pressure here denotes the energy and momentum tensor components; The mechanical picture of gas pushing against the outer wall does not apply to the Universe as a whole.

The cosmological constant Λ provides a particularly parsimonious description. Its energy density is not rarefied during expansion, and the parameter w is equal to −1. As the density of ordinary and dark matter decreases, the relative value of the constant contribution increases. This allows us to obtain a sequence of epochs without assigning a separate push to each galaxy.

If the density of such a component is constant, the energy inside the expanding comoving volume increases. This does not contradict the local conservation equations: they take into account the work of pressure, which in this case is negative. The idea of one unchanging total energy of the entire Universe requires additional conditions of space-time symmetry and is not automatically transferred from the mechanics of an isolated system. Therefore, the cosmological constant cannot be estimated from an everyday picture of a substance, the amount of which remains the same as the vessel increases.

This simplicity has a price. The measured value of the constant does not yet explain its origin. Quantum fields and possible constant terms of the fundamental theory contribute to the gravitational-

ly significant energy of the state. Why the overall result has the observed small scale is an independent theoretical problem. Substituting a suitable number into cosmological equations reliably describes the dynamics, but does not solve the question of why nature chose it.

One can check a simple consequence of this description. For a separately conserved component with constant w, the density changes during expansion in a predictable manner. When w=−1 it remains constant, and when it deviates from this value it changes. Actual distances depend on the accumulated expansion history. Therefore, even the variable w cannot be read directly from one supernova: it has to be reconstructed from integral observations along with other parameters.

The boundary w=−1 also requires careful interpretation. The value below it is called phantom. In some simple field models it is associated with unacceptable kinetics, but the parameter recovered from observations can be an effective characterization of a more complex system. The first step is to establish what has been subtracted from the total density and what interactions have been excluded by the chosen model.

## How convincing is the hint of change?

For data analysis, a two-parameter form is often used, in which the current value and the change over time are specified separately:

$$w(a) = w_0 + w_a(1 - a).$$

The scale factor a is today assumed to be equal to unity. This form is convenient for comparing results, but does not represent an independent field theory. Even the statistical preference for such a curve still leaves the question of what dynamics are capable of creating it and where its applicability ends.

DESI measures the spectra of many galaxies and quasars and reconstructs the large-scale distribution of matter. The acoustic scale in this distribution serves as a cosmological ruler. In the DR2 analysis, the distance measurements themselves allow a good description of the flat ΛCDM. The preference for changing dark energy emerges from the combined analysis: for the combination of DESI with the CMB it was 3.1 standard deviation, and with the addition of different sets of supernovae it was from 2.8 to 4.2. Numbers refer to the specified two-parameter alternative and specific data sets. [8]

Further observations need not consistently strengthen the initial hint. In the DESI analysis of 2026, using additional information from the Lyman-α forest, the significances for the combinations considered changed. This demonstrates the dependence of the result on the available observables. When combining analyses from the same survey, their shared data must be taken into account: reusing correlated information without appropriate covariance would artificially increase confidence. [57]

A combination of different observations from the Dark Energy Survey itself also tests for variable dark energy. In the year 2026 work, significance depended on the inclusion of CMBs and supernovae; revision of supernova calibrations changed it. However, a separate analysis without supernovae retained a moderate preference for dynamics. Therefore, explaining all the results by a single photometric error is still as premature as declaring established evolution. [58]

The specified number of standard deviations characterizes the result of a particular statistical comparison; it is not the probability of the truth of the physical picture. Robustness checks to alternative parameterizations, biases, and prior distributions are needed. Forecasting is especially useful for

new data: a model selected from one combination of observations must predict another in advance. Then the added flexibility of the curve has a real chance of being wrong.

## Field behind the drawn curve

A scalar field is given by one value at each point in space-time. Its change in time is related to the kinetic energy density K, and the potential V specifies a part of the energy density that depends on the field value itself. For a homogeneous field in the usual canonical description we obtain:

$$\varepsilon_\varphi = K + V, \qquad p_\varphi = K - V.$$

When the field changes slowly and the potential contribution dominates, the pressure is close to the minus energy density. As you move, the ratio of contributions may change. Expansion affects the speed of the field, and its energy affects the expansion; both histories must be calculated together.

The sum of pressure and energy density in these formulas is equal to twice K. For the canonical field, K is non-negative, therefore, with a positive total energy density, w does not fall below −1. A curve crossing this boundary will require different physics or a different interpretation of the reconstructed parameter.

To see this connection, consider the illustrative calculation of the book. Let us set a positive bell-shaped deviation 1+w with a maximum 0.25 near the redshift 0.5 and a width 0.2 in the variable ln a. Today, the fraction of matter is taken to be 0.3, the fraction of field is 0.7; space is flat, radiation in the late interval from the present epoch to z=3 is neglected. The parameters are hand-selected and are not the result of fitting observations.

The bell-shaped profile remains above the −1 boundary. It illustrates the dynamics of a canonical field and differs from the two-parameter description favored by some DESI data combinations. The compatibility of this particular profile with observations remains to be tested.

The given function allows you to restore the field density, the rate of its change and the potential along the trajectory. Then the found potential is substituted into the equation of motion and solved independently. The coincidence of the two histories verifies the physical consistency of the reconstruction. The method itself has well-known scientific predecessors. [59]

In this example, an independent calculation reproduces the original history with high numerical accuracy. The potential has a minimum, which the field passes at approximately redshift 0.199. Today it is already rising on the other side, using up the accumulated kinetic energy. The picture of a continuous downward slide would be incorrect, although the solution itself is canonical. This is a simple illustration of why a convenient image needs to be tested by equations.

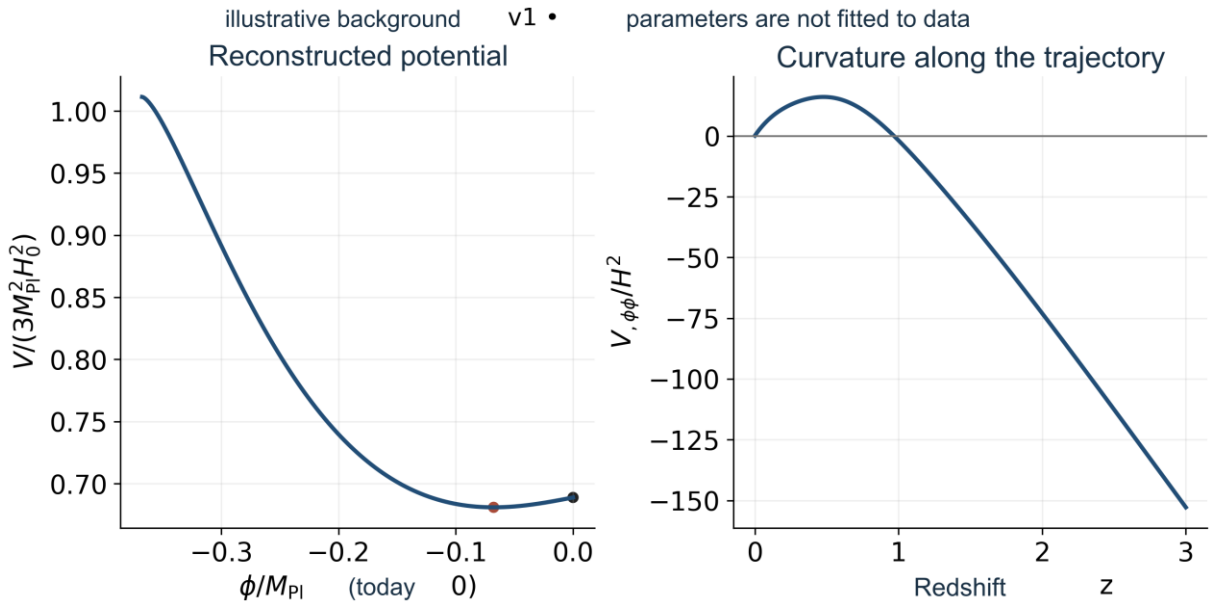



Figure 3. Reconstruction of the training scalar profile and independent verification of its dynamics. The minimum potential is in the already passed section of the trajectory. The graph describes the selected example; Agreement with observational data was not tested here.

Small changes in homogeneous initial conditions produce small changes in the later result in the studied neighborhood. Spatial inhomogeneities require separate verification. On part of the trajectory, the curvature of the potential is negative: here we mean the shape of the field energy graph, and not the curvature of space. It affects the growth or decay of disturbances, but the sign alone is not enough for a conclusion. Spatial gradients and connections to gravity must be taken into account; the accuracy of a homogeneous solution does not ensure this.

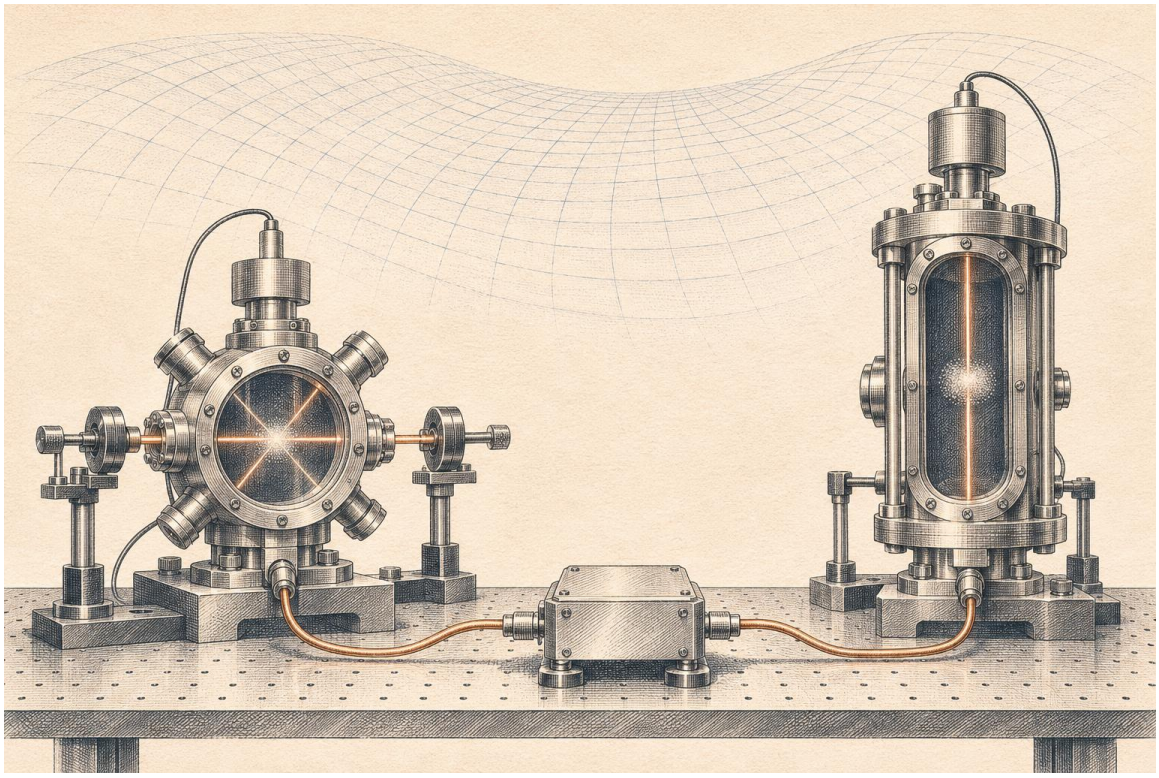
There is also a limit to continuation into the future. With infinite extrapolation of the same bell-shaped function, the field approaches a finite value, and the second derivative of the potential increases in magnitude indefinitely. It is impossible to extend the potential through this point with a continuous second derivative. It is achieved only in an infinite time, therefore the calculation does not establish a finite cosmological catastrophe. It indicates where the selected profile will require a physically based extension.

## From atomic clocks to the extra dimension

If the field is associated with electromagnetism, its movement can change the dimensionless characteristics of interactions, such as the fine structure constant. Then the cosmological idea receives a laboratory channel of verification. Different atomic transitions are sensitive to microphysics parameters in different ways; Comparing clocks allows one to look for relative changes in their frequencies.

But the measurement usually limits the product of coupling strength and field velocity. A nearly constant frequency ratio may mean little motion, weak coupling, or a combination of both. It is impossible to separate them without additional prerequisites. The reconstructed cosmological trajectory helps to relate quantities, but must itself withstand observational constraints. It is the dependence of the conclusions on such premises that is studied in detail in works on the changing fine structure constant. [60]

The same connection can give rise to differences in the accelerations of bodies of different compositions. Therefore, a test of the equivalence principle is added to the clock: the prediction depends on how the field interacts with the constituent atoms and their binding energies. A separate difficulty is the stability of a very light field to quantum corrections. A law convenient for the cosmological graph must still be compatible with the rest of microphysics. [61] [62]



Engraving 11. Cosmological field and laboratory clock. A comparison of different atomic transitions links the cosmological hypothesis to a laboratory measurement. If the field interacts with the electromagnetic sector, changing the frequency ratio can limit the combination of coupling strength and field speed. Instrument components are shown conventionally; the engraving does not specify the design of the clock and does not claim that such a connection has already been discovered.

In the Dark Dimension direction, a connection appears with geometry: the radius of the additional dimension changes along with the scalar field, affecting the mass states of dark matter. A paper published in November 2026 examines such dynamics. To describe it with familiar components, the authors subtract from the total density the hypothetical matter that would be stored separately, and attribute the remainder to effective dark energy. Moreover, the normalization of subtracted matter was set in an early era. The remainder may correspond to w below −1, although the kinetic energy of the field itself remains ordinary: part of the effect arises from the accepted separation of the interacting components. [63]

One geometric mechanism here links the expansion and properties of dark matter. This is a testable hypothesis, but the existence of an additional dimension has not yet been established. To predict the growth of structures, equations of the interacting sector are needed; formulas for separately conserved matter are not applicable to it.

## Measure change over twenty years

A given field history has another observable consequence. In chapter 3 we discussed re-measuring the redshift of one absorber. Now we can calculate its drift and compare it with a model where dark energy is constant. Let's take the same Gaussian profile, $H_0$=70 km/s/Mpc, the current fraction of matter 0.3 and the interval between observations of twenty years. Twenty years here sets the scale of calculation; The duration of the actual experiment has yet to be justified.

At redshift z=0.5, the cosmological constant gives a spectral shift equivalent to +5.48 cm/s, and the selected field is +4.00 cm/s. The largest difference is about 1.82 cm/s at z≈0.78. At z=3 both models give a negative shift, and the difference decreases to approximately 0.37 cm/s. The sign refers to the change in redshift converted to velocity units; the formula and other values are given in the appendix.

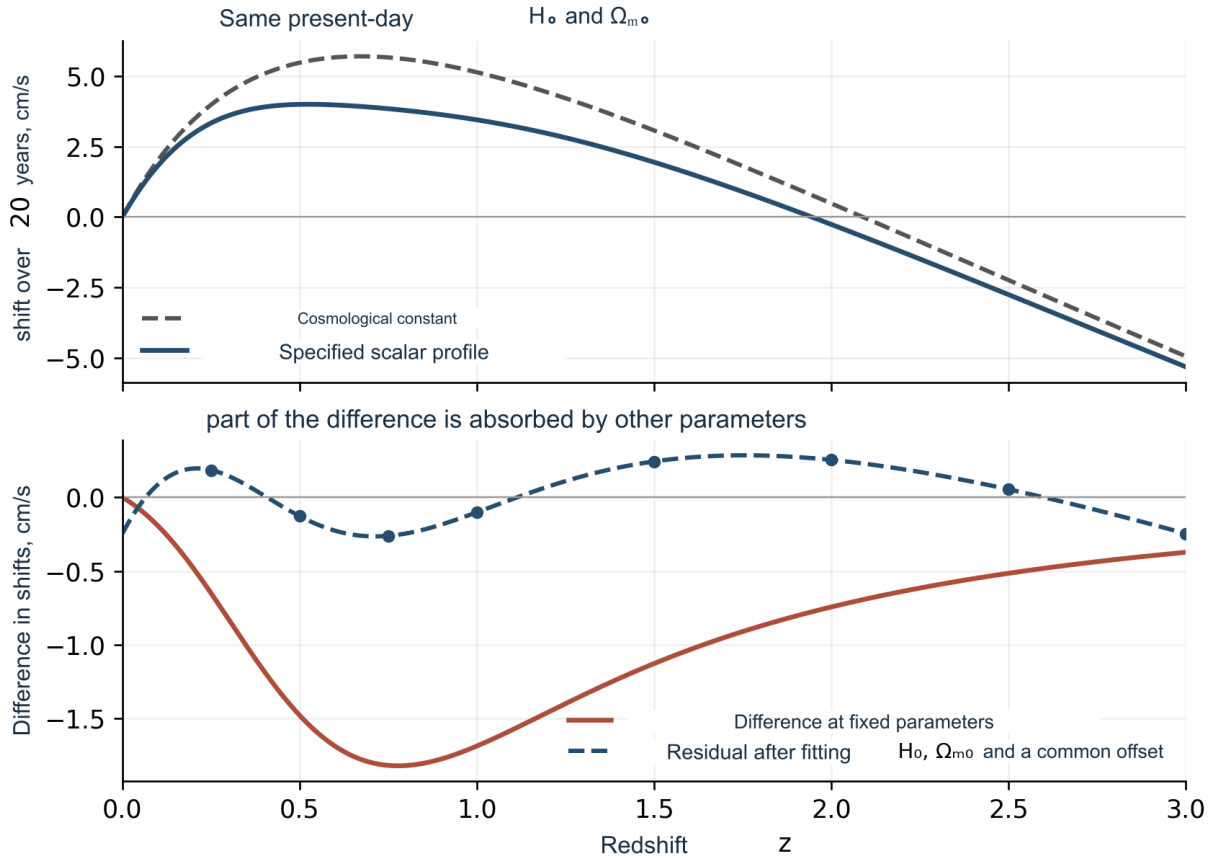



Figure 4. Redshift drift for a given scalar profile and cosmological constant over twenty years. From above, $H_0$=70 km/s/Mpc and $\Omega_{m0}$=0.3 are the same. Below are the initial difference and the remainder after fitting $H_0$, $\Omega_{m0}$ and the total calibration shift in the model with a constant. The dots represent the eight arbitrary redshifts for the fit. This is a calculation of two models; There are no observational data or predictions of the accuracy of a specific device in the figure.

However, comparison with fixed parameters overestimates the independent discriminative ability of this channel. Let us allow the model with the cosmological constant to change $H_0$ and the fraction of matter. At eight conventional redshifts, its curve approaches the scalar one so that each remainder becomes less than 0.3 cm/s. To do this, it requires $H_0$ about 57.1 km/s/Mpc. We do not claim that this value is consistent with the real cosmos: no independent observations were included in this fit. The

example shows which parameters will need to be constrained by other measurements before assessing the discriminability of two mechanisms.

The available spectral lines must also be taken into account. The largest difference in our fixed models occurs at a relatively small redshift. Ground-based optical observations of the Lyman-α forest are designed for more distant absorbers, where the ultraviolet line has already shifted into the accessible range. Therefore, the proposed grid does not describe the capabilities of a single spectrograph. It is necessary to separately calculate the sensitivity of optical and radio observations and check what their combination gives after taking into account general and individual calibrations. [14] [13]

The next step is determined by the calculation itself: replace the conditional errors with a real observational model and add independent constraints on the cosmological parameters. Here we compare different expansion histories in the available past. In chapter 20 a more rigorous difficulty will appear - different future continuations, whose past coincides exactly in a given approximation; this drift example by itself does not remove it.

## How to check it

Let's start with a specific field model: define its action, connections and area of applicability, and calculate the expansion and spatial disturbances. Supernovae and acoustic scale limit distances. The fall of galaxies into concentrations of matter adds their own velocities and distorts their distribution in redshift space; this effect, together with weak lensing, tests the growth of the structure. The initial amplitude is limited to early observations, and the continuation of the model is consistent with them. Then the same initial perturbations and substance parameters are used in all late channels, without new normalization for each.

Taking into account these initial restrictions on geometric measurements, we obtain an acceptable range of parameters and predict growth for a predetermined sample. Let's take into account redshift errors, proper orientations of galaxies, the influence of ordinary matter and neutrino mass. If the region fitting the distances does not reproduce growth under the tested uncertainties, the model is rejected. Adding a free change in gravity would mean a new hypothesis.

The required accuracy will be determined by artificial catalogs for the cosmological constant and the selected field. They reproduce feature selection, noise, and general systematic biases, and then apply real data processing. Given a pre-selected acceptable false discovery rate, it is calculated which field parameters can be distinguished from a constant. The result is a sensitivity map that includes yet indistinguishable versions.

Atomic clocks add an independent channel when the field is related to electromagnetic parameters. Several transitions with different sensitivities are compared, external fields are controlled, and the result is compared with experiments on the universality of free fall. Zero frequency change limits the combination of field velocity and field coupling. The version that predicts exceeding the reached limit is excluded; a field almost unrelated to ordinary matter may remain accessible only to cosmological tests.

For an additional dimension, the overall radius, spectrum, and couplings must simultaneously determine the cosmology, the laboratory force at short distances, and astrophysical energy transfer. The first step is to independently reproduce one complete implementation along with its perturbations. The absence of a general permissible region, taking into account measurement and theoretical errors, will exclude this particular implementation.

The next research result should combine the calculated dynamics with observations and show which parameters are simultaneously tested by distances, growth and available laboratory measurements. The completed reconstruction is the source material for such work; its observational viability has not yet been established.

**Chapter 9**

# How much does emptiness weigh?

Let's imagine a laboratory from which air, light, thermal radiation and residual particles are sequentially removed. The devices become colder, the pressure drops, but the question is “what’s left?” does not boil down to the answer “nothing.” The physical description remains of the fields, their interactions and permissible states. Vacuum is the name of the state of the system, and not the absence of laws and the system itself. Therefore, the question of its gravity arises before any speculation about the origin of the world from absolute nothing.

The title of this chapter is deliberately reminiscent of everyday weighing. However, the cosmologist does not put emptiness on the scale. He asks what contribution the state of the fields makes to the equations of geometry and whether the magnitude of this contribution can be explained while preserving the rest of the successes of physics. The late acceleration of expansion makes the issue observational. But even an ideal reconstruction of the expansion will not yet tell which part of the measured effect is associated with the vacuum, and which part is due to a new field or a change in the law of gravity.

There are two different difficulties hidden here. First: why is the constant contribution allowed by the equations so small compared to many scales in particle physics? Second: why should its smallness remain when the calculation is refined? The number can be selected once. The explanation must withstand new amendments. It is between the successful selection of numbers and a stable mechanism that a significant part of the leading edge of this problem lies.

## Why does the zero mark become physical?

In ordinary mechanics, you can add a constant to potential energy. The force depends on its change with position, so the trajectory of the particle will remain the same. You can also change the zero height mark without changing the difference between floors. This freedom often suggests the wrong answer: it is enough to declare the vacuum energy to be zero, and the question will disappear. In gravitational theory, adding a constant to the energy density requires a closer look at the action.

It is also necessary to clarify what kind of vacuum is meant. In a changing geometry, the choice of field state may require additional conditions, and its energy-momentum tensor does not have to consist only of a constant term. Therefore, below we first highlight the constant part of the action. This allows us to pose a clear problem without declaring all energy of quantum fields a cosmological constant. Dynamic excitations, thermal contributions and geometry-dependent polarization require their own calculations.

Let's take the metric signature −+++ and units in which the speed of light is equal to one. The constant term in the action of matter is written as minus the energy density multiplied by the four-dimensional volume element. The volume element depends on the metric. Consequently, even a spatially homogeneous additive participates in the variation of the action according to geometry. From this we directly obtain the energy-momentum tensor and equation of state:

$$T^{\text{vac}}_{\mu\nu} = -\rho_{\text{vac}} g_{\mu\nu}, \qquad p_{\text{vac}} = -\rho_{\text{vac}}.$$

Negative pressure here does not mean that the empty space is filled with invisible gas with unusual molecules. This is a characteristic of the energy response to a change in volume. If the uniform density remains constant, the energy of the selected expanding comoving volume increases in proportion to the volume itself. In the local conservation law, this behavior is consistent with the work of pressure. It is impossible to transfer the law of conservation of energy from a stationary laboratory box to the entire expanding Universe without specifying the conditions.

Let's consider an extremely simple case: there are no other sources, gravity is described by general relativity, all constant contributions are already collected into one physical density ρΛ. Let us denote the reduced Planck mass by $M_{\text{Pl}}$, so that $M_{\text{Pl}}^2=1/(8\pi G)$. Taking the trace of Einstein's equation gives:

$$M_{\text{Pl}}^2 G_{\mu\nu} = -\rho_\Lambda g_{\mu\nu} \quad \Longrightarrow \quad R = \frac{4\rho_\Lambda}{M_{\text{Pl}}^2}.$$

This is a small conclusion, not a new formula for gravity. It shows where the mechanical analogy with zero height breaks down: constant density determines curvature. In the presence of matter and inhomogeneities, the number R alone is no longer sufficient to describe space-time, but the constant source does not disappear from the equations. You can move it from the right side to the left, calling it the cosmological constant. This movement changes the recording, not the physical content.

Suppose now that one wants to replace this constant with an arbitrary function of time in order to improve agreement with observations. Then an additional condition arises. The geometric part of the equations satisfies the Bianchi identity, so the total source must be covariantly conserved. If an ordinary substance is kept separately, simply substituting a "constant" variable would break consistency. A field, energy exchange, or other explicitly specified change in theory will be needed. A flexible curve on a graph by itself does not cause such a change.

## What exactly adds up to the measured quantity?

Quantum calculation requires separating intermediate quantities from the observed result. In the integrals, infinities or strong dependence on the introduced energy limitation may appear. This is not permission to plug any resulting huge number into cosmology. The action parameters and field contributions are determined in a consistent renormalization procedure. The observations refer to their final sum, not to each term individually.

A schematic notation is convenient, where μ denotes the renormalization scale:

$$\rho_{\Lambda,\text{phys}} = \rho_{\Lambda,\text{ren}}(\mu) + \rho_{\text{fields}}(\mu), \qquad \frac{d\rho_{\Lambda,\text{phys}}}{d\ln\mu} = 0.$$

The last equality refers to the agreed upon full settlement; when the series is truncated, a higher order dependence remains. By changing μ, we change the way the result is distributed between the terms. This is not a physical change in vacuum density over time. The running parameter cannot be

identified with the automatically predicted evolution of dark energy: such evolution requires a separate dynamic justification.

Let's look at one specific quantum contribution. For one real scalar field with positive squared mass $m^2$, in a flat background and a modified minimal subtraction scheme, the one-loop term of the effective potential is as follows. This standard formula follows from a quantum calculation; its generalized presentation is given, for example, in the work of Stephen Martin. [64]

$$\Delta V_1 = \frac{m^4}{64\pi^2}\left[\ln\left(\frac{m^2}{\mu^2}\right) - \frac{3}{2}\right].$$

What is important here is the scale $m^4$ and the need to coordinate the correction with the action parameters. The coefficients for other fields and schemes may differ, fermion contributions have their own structure, and additional geometric terms appear in curved space. Therefore, this line is not a numerical prediction of the entire vacuum energy of the Universe. It shows why adding a heavy sector can change the conditions under which a small finite value persists.

Often the problem is illustrated by one giant mismatch number. It depends on what scale and method of assessment are chosen. What is more important for the argument is that once the theory has been agreed upon at one level, the next physically permissible contribution should not force us to re-arrange extremely precise compensation. Even if we discard the rough estimate with the maximum possible cutoff, the question of sensitivity to known mass thresholds remains meaningful.

You can see the logic in the invented arithmetic example. Let two contributions of about a million should give a difference of the order of unity. It's easy to find them. But if independent refinement changes one contribution to a thousand, the result is no longer small. The explanation of smallness should explain why the other contribution will change or why the new addition will not fall into the measured amount at all. By itself, re-adjusting the numbers does not contain such a message.

This leads to a useful rule for comparing models. You need to ask not only how many free parameters allowed you to get a good result, but also what connections between the parameters are required. If compensation follows from symmetry or constraint, the refinement must preserve this relationship in the specified region. If two numbers are independent, the requirement that they coincide with high accuracy remains an additional condition. The presence of a small parameter does not mean the presence of a mechanism for its smallness.

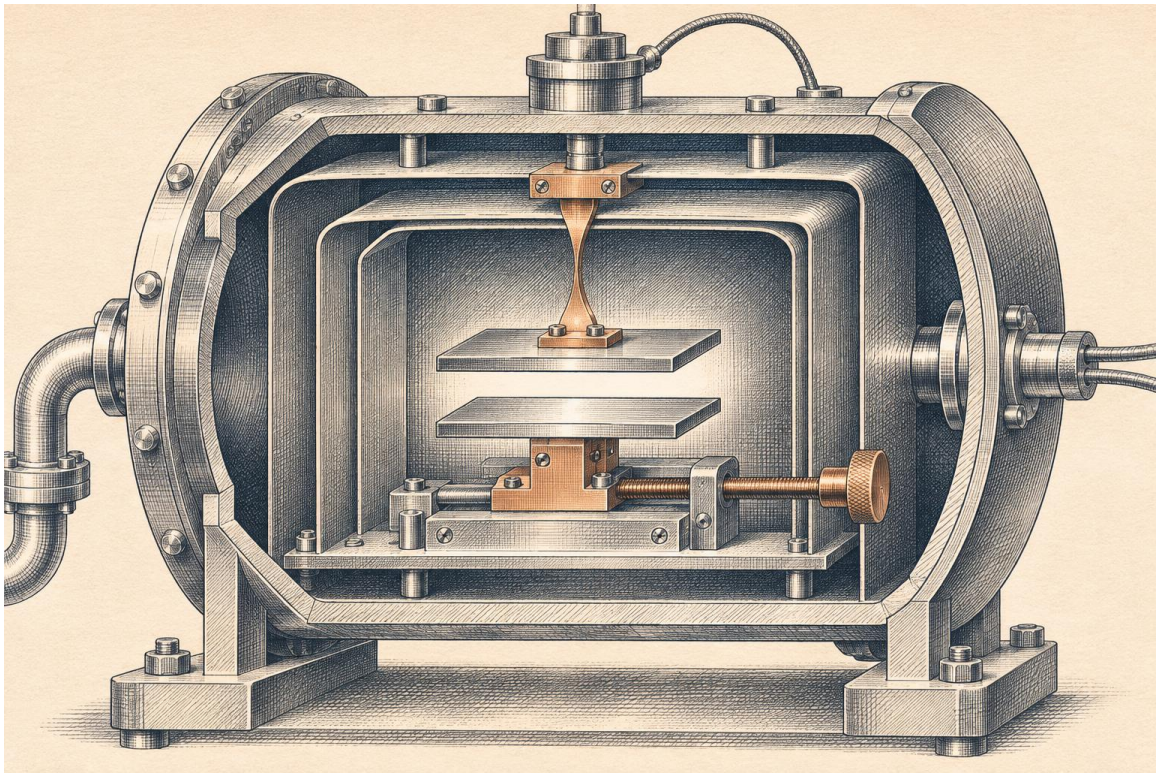
There is also a separate question about time: why are the densities of the permanent component and the densities of the diluting substance comparable at some epoch? Even an explanation of a stable small constant does not have to answer it automatically. Conversely, a model linking the transition to acceleration with a change in the composition of the Universe must still explain its own sensitivity to vacuum corrections. Separation of concerns allows one to evaluate the contribution of a theory without demanding that everything be solved immediately and without discreetly appropriating unnecessary successes.

## What does the laboratory void say?

Vacuum has measurable manifestations, but each experiment has its own observable quantity. The force between material surfaces depends on their properties and distance. In his analysis of the Casimir effect, Robert Jaffe showed the possibility of description through the interactions of charges and

currents without resorting to the absolute sum of zero-point energies. Therefore, the measured force by itself does not determine the gravitational effect of a homogeneous cosmological vacuum. [65]

It is useful to formulate the difference as a task for the experimenter. If an installation measures the change in force when moving plates, its result must be compared with the derivative of the energy of the entire installation with respect to this movement. If it is intended to measure the change in its gravitational mass, it is necessary to take into account the plates, stresses, fastenings, thermal conditions and the source of the work done. It is impossible to subtract inconvenient parts of the system in words. Otherwise, we will compare different physical objects and call the difference “the weight of emptiness.”



Engraving 12. Emptiness inside a complete installation. By varying the distance between surfaces, the response of the entire physical installation is measured. For the question of its gravitational mass, fastenings, stresses, heat and work done are also significant. The plates and chamber are shown conditionally. The measured force between surfaces does not by itself determine the gravitational contribution of a homogeneous cosmological vacuum.

This does not make laboratory tests useless. They can test a specific prediction about how the total energy of a bound system contributes to gravity. But the path from such a result to the cosmological constant must pass through an explicit theory. A local change in boundary conditions and a homogeneous addition to the action throughout space-time are different operations. Distinguishing between them protects the research program from the false promise of one decisive experiment.

## The mechanism must survive refinement

Let's assume that instead of a constant we introduced a slowly varying scalar field. Its potential can be adjusted to obtain a suitable extension. However, a constant can still be added to the potential, and field interactions generate corrections. This means that explaining the dynamics of dark energy

and explaining the stability of its absolute level are two related problems. The solution of the first should not automatically be considered the solution of the second.

Approximate symmetry can constrain allowable corrections. For example, if shifting a field leaves the action nearly unchanged, some potential shapes are better protected than arbitrary ones. But the word "symmetry" does not complete the calculation. The symmetry-breaking interactions, the sizes of their parameters, and the corrections introduced by matter and gravity must be specified. A computational assistant can help search for overlooked allowed operators. A mechanism can be declared stable only after their effects have been checked.

One specific research path was proposed by Nemanja Kaloper and Antonio Padilla. In the original global sequestration design, additional variables introduce constraints that cause the constant vacuum contributions of matter loops to cancel out in the gravitational equations. The scope of the statement is important: we are talking about a protected sector of matter, without a complete solution to the problem of graviton loops. The initial design has global conditions, including a finite four-dimensional volume. This is a strong change in the structure of the theory, and not a new designation of the old constant. [66]

In the subsequent local version, Kaloper, Padilla and co-authors used additional fields and four-form field strengths. The constancy of some quantities becomes a consequence of local equations. The requirement for a finite four-dimensional volume is removed in this version, and the residual constant contribution includes integration constants. The authors obtain stability under the matter vacuum corrections considered, but the value of the final residue needs to be measured. Prediction of stability and prediction of a specific observable quantity must be distinguished here. [67]

These examples are useful even to the reader who is not ready to consider the mechanism correct. They ask a rigorous question: what exactly needs to be changed in the equations so that a uniform energy shift does not destroy the observed geometry, while maintaining the gravity of ordinary excitations? If you remove all the energy from the right side, the explanation for the movement of the planets will disappear. If you compensate for only one pre-selected constant, the question of the next correction remains. A successful design must move between these extremes.

## How to check it

It is proposed to start with an open computational task that can be completed before the new telescope becomes available. A completely specified action, a sector of matter, a renormalization procedure, and a set of boundary or global conditions are selected. Then two consistent cases are calculated: the original case and the case with an additional constant contribution to the matter Lagrangian. The parameter matching rule is fixed in advance. Otherwise, manual retuning of the cosmological term will reproduce the desired response under any mechanism.

In the simple vacuum example of general relativity discussed above, with other parameters fixed, the change in curvature is equal to $4\Delta\rho/M_{Pl}^2$. For an alternative design, you must independently derive the corresponding response, including restrictions. If the constant contribution cancels out, the next step is to add allowed interactions and perform at least the first non-trivial quantum correction. The test should show a reduction in the measurable value, not just the disappearance of the selected character from one action line.

This shift serves as a diagnostic of the theory, not as an instruction to instantly change the vacuum of the laboratory. A real phase transition is much more complex: the state of the substance, energy

distribution, temperature and, possibly, the number of effective degrees of freedom change. For cosmological verification, the transition should be included in a single history, preserving the laws of energy exchange. You can't just switch the constant in the Friedman equation and ignore where the energy difference went.

The next step is to associate the background with the disturbances. The model must predict not only H(z), but also the growth of inhomogeneities, the propagation of light, and the properties of gravitational disturbances where it changes them. The existence of a solution, the absence of unacceptable fast instabilities, and the range of applicability of the approximation are checked. The coincidence of one expansion curve does not compensate for the incorrect sign of the kinetic energy of the additional degree of freedom.

Only after this does it make sense to build an observational forecast. Predicted distances and structure growth are compared together, with common parameters and systematic errors. If the mechanism appreciably changes the early expansion, constraints from the hot history are added, including primordial nucleosynthesis. If it acts only on a constant contribution and leaves the usual dynamics, it is necessary to directly indicate what data are generally capable of distinguishing it from general relativity with a chosen cosmological constant.

It may turn out that in the accessible region the two constructions are observationally equivalent. This is a meaningful negative: it prohibits existing measurements from being sold as evidence of an internal mechanism. The program then splits between checking the mathematical consistency and finding a new effect that actually differentiates the models. Such an effect should follow from an already given design. Adding an arbitrary signal specifically for a convenient device will not test the original idea.

A specific format is suitable for working with AI here. The researcher defines the action and controlled approach, and the system automatically derives equations, checks dimensions, compares independent calculation methods, and builds a failure map. The person checks the choice of observable, the reduction conditions, and the admissibility of approximations. The useful outcome is a reproducible set of cases where the mechanism survives the disturbance and cases where it breaks. Generating hundreds of similar potentials without this check does not bring the answer much closer.

In practice, such a set can be started small. One free massive field, one chosen regularization and one family of cosmological solutions are sufficient. Then one interaction is added, followed by a second mass threshold. At each stage, intermediate expressions and a comparison with an independent output are stored. Consistent expansion prevents an implementation error from being confused with a physical mechanism failure. The discrepancy found must be accompanied by a minimal example that can be reproduced by another group.

The most difficult cases will be those where the mechanism depends on conditions throughout the history of space-time. For them, it is not enough to present a local solution on a short interval. It is necessary to check whether it admits a continuation that satisfies the original constraint, and how sensitive the output is to this continuation. If different admissible continuations produce the same observables today, such ambiguity must enter into the result. It connects the problem of vacuum with the question of the limits of inference from a finite observable region.

The refutation criterion should be written down in advance. For the claimed mechanism, this could be a non-cancelling allowed quantum contribution, inevitable rapid instability in the desired region, or incompatibility of related observables under one set of parameters. Each such outcome re-

futes a certain construction and its area of assertions. It does not prove that any future vacuum theory is impossible. This chapter suggests a research order; the new sequestration model and its fit to the data are not calculated here.

The problem of the weight of the void connects cosmology with the structure of quantum theory in a particularly tight way. It is not enough to explain why the Universe is accelerating today. What we need to understand is why its large-scale geometry remains consistent with what we learn about the microscopic world. This makes the small constant contribution not the last fitted number in the table, but the place where one can look for the missing rule of connection between energy and spacetime.

**Chapter 10**

# Where the measurements diverge

The contradiction between measurements attracts attention more than their agreement. This is understandable: it is the discrepancy that may indicate physics that is not yet in our equations. But the observations do not directly argue. Between the recorded light and the cosmological parameter there is a chain of calibrations, corrections and model connections. To understand the meaning of the divergence, it is necessary to find out at which link the two routes diverge.

Let's imagine two groups of surveyors measuring one area. One determines the length by direct comparison with a ruler, the other calculates it from the angles of the triangle. A discrepancy may indicate an incorrect ruler, an angular error, or a failure of the flat surface assumption. In cosmology, the role of the surface is played by the history of expansion and growth of the structure. The very presence of several routes makes it possible to test these assumptions.

According to the state of research discussed in this book, it is impossible to reduce all cosmological stresses to one universal breakdown. The Hubble constant, irregularity amplitudes, and early galaxies have different observed values and major uncertainties. Linking them into one new theory would be valuable, but each link must first become a quantitative prediction.

## Two paths to today's expansion

The parameter $H_0$ describes the current relative expansion rate. For a nearby galaxy, the distance is compared with the redshift, taking into account its own motion relative to the general flow. The distance is constructed using a chain of overlapping methods. Geometrically measured nearby objects define the absolute scale; stars of known types transfer it to other galaxies, and brighter sources continue measurements further.

For Cepheids, the pulsation period is related to luminosity. Once calibrated, this relationship allows one to know from the period how much light the star is emitting, and from the observed brightness to determine the distance. Other stellar methods use different physical properties. However, common supports, galaxies, and brightness standards link their errors. Ten assessments with one common calibration do not provide ten independent tests of that calibration; such relationships are taken into account by the covariance matrix.

The joint local distance network received $H_0=73.50\pm0.81$ km/s/Mpc. Here 0.81 is the standard error obtained from the general covariance matrix in the adopted Gaussian approximation. The authors tested the robustness to removal of individual indicators and took into account overall calibrations. But the word “consensus” in the title of the paper describes the result of the participating collaboration, and not the final agreement of all research groups. [68]

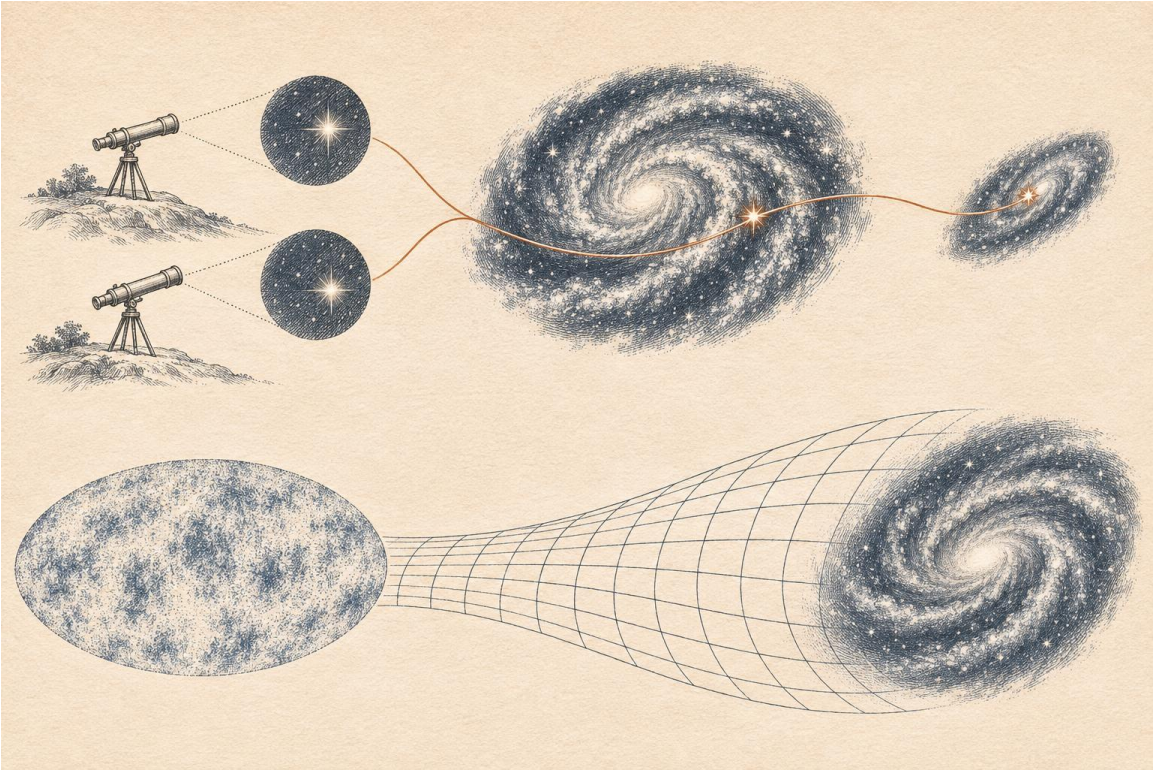
Another route begins with the cosmic microwave background radiation. The angular pattern of early irregularities is measured; the physical model relates it to the sound scale and the subsequent distance to the corresponding epoch. In the basic flat ΛCDM, the Planck analysis gives today's value $H_0=67.4\pm0.5$ km/s/Mpc at the 68 percent confidence level. This is not a direct measurement of today's expansion in the early Universe. The meaning is obtained after running the model through its history. [6]

The tip of the red giant branch method uses the sharp edge of the luminosity distribution of old stars before the start of helium burning in their cores. After calibrating the absolute luminosity, the position of the boundary gives the distance. JAGB uses the properties of another selected stellar population. Different stages of stellar evolution are differently sensitive to age, chemical composition and environment. Therefore, the agreement of methods is valuable precisely as a physical control, although common geometric supports may preserve the correlation of their errors.

The position between the two numbers is occupied by several other routes. CCHP, which uses the tip of the red giant branch, or TRGB, and selected asymptotic giant branch, or JAGB, stars, reports lower central estimates than the local network and wider uncertainties. Its most accurate reduced estimate according to TRGB is 70.39 km/s/Mpc. The authors share errors: ±1.22 from statistics, ±1.33 from systematics, and an additional contribution of ±0.70 for residual uncertainties of supernovae, including their photometric calibration and proper motions of galaxies. The statistical part corresponds to the central 68 percentage interval of the marginal distribution; the other two contributions are given separately. This is a sufficient reason to consider the local scale structure in more detail. [69]

A strong lens produces multiple images of a single source. If a source changes brightness, the same pattern of changes arrives along different light paths with a delay. It depends on the geometry and gravitational potential of the lens and allows us to determine the cosmological scale. In the TDCOSMO 2026 analysis, the authors report $H_0$=71.1 km/s/Mpc with asymmetric uncertainty estimates +2.4 and −2.3. This result was obtained with a flat ΛCDM with an external constraint on the density of matter from the DES-Dovekie supernova sample. The mass distribution of the lens is further limited, in particular, by stellar kinematics. The resulting accuracy does not yet clearly select between the main routes. [70]

This is where degeneracy arises: different distributions of lensing mass and source position are able to preserve the observed image geometry but predict different time delays. Therefore, even precisely measured image positions do not determine the distance unambiguously. The movement of stars in the lens and information about matter along the line of sight reduce this freedom. The uncertainties of these additional models contribute to the resulting cosmological-scale error.



Engraving 13. Two routes to scale expansion. The local scale connects geometric supports, properties of stars and more distant sources. Another route links the CMB pattern to today's expansion through a cosmological model. This is a conditional mapping of inference methods, not a distance map. Common calibrations can relate the errors of even different observational methods.

## When a small correction becomes cosmology

Models of new early physics may change the sonic scale by which the cosmological ruler is calibrated. Then the same observed angular pattern will correspond to a different combination of late distances and $H_0$. But the changes must preserve the rest of the spectrum of the cosmic microwave background radiation, the formation of light nuclei and the subsequent growth of the structure. It is usually impossible to freely replace the length of the ruler while leaving all other consequences the same.

Later explanations change another part of the chain: expansion after the formation of the primary scale, dark sector interactions, or light propagation. They are tested by a combination of acoustic measurements, supernovae and growth. Therefore, successfully fitting one number $H_0$ is just an initial filter. The model must survive the data that did not participate in the selection of its parameters.

Taxonomy may be of comparable scale. In the controversy over supernova analyses, a relative shift of about 0.04 magnitude between subsamples has been discussed. Through the definition of the grayscale, this corresponds to approximately 1.86 percent in distance. With modern precision, this effect is significant. However, the fact of a shift does not determine which directory requires correction and how exactly it should be changed. [71]

The DES team's response showed that the differences were related to patterns of dispersion and selection functions, among other things. The same supernovae, after various reasonable corrections, are not required to have identical published distances. To test the source of the difference, we need to

go back to light curves, brightness standards, and modeling of what objects might have been included in each view. Simply subtracting a convenient step from the final catalog does not replace this work. [72]

The difference between random and general error is clearly visible in a simple example. Let us add new supernovae, each with its own random variation in brightness. Averaging them will improve the score. But if they are all measured relative to one slightly incorrect standard, the overall shift will remain for any number of objects. Even a different telescope will not create a completely independent verification if its calibration is tied to the same standard. Therefore, it is useful to increase not only the sample, but also the number of physically independent ways to relate measurements to an absolute scale.

For a mental experiment, let’s divide the data not according to the result, but according to the physical circumstances of registration: instrument, wavelength range, type of host galaxy, selection conditions. Cosmological change is primarily organized by redshift and geometry. The calibration effect can follow the apparatus or the source population. These dependencies sometimes overlap, but it is their comparison that suggests what additional observations can separate the explanations.

## How heterogeneous is the Universe?

The next question is how strongly the substance is collected into heterogeneous structures. For comparison, use $S_8$: this quantity is convenient to measure by gravitational lensing, and it connects the average fraction of matter with the amplitude of its linear inhomogeneities:

$$S_8 = \sigma_8 \sqrt{\frac{\Omega_m}{0.3}}.$$

Let us imagine the calculated density field smoothed by identical spheres. The value $\sigma_8$ characterizes the root-mean-square relative spread of the densities of such regions around the average in the linear model extended to the present epoch. The radius of the spheres is 8 $h^{-1}$ megaparsecs; h — $H_0$ in units of 100 km/s/Mpc. Weak lensing often better constrains the combination of $\sigma_8$ with the matter fraction $\Omega_m$ than each quantity separately, so $S_8$ is used. The coincidence of this number does not yet guarantee the coincidence of the structure on all scales and in all eras.

Weak lensing is measured statistically. An individual galaxy has its own shape, which we do not know in advance. Therefore, correlations of multiple images distributed by directions and distances are analyzed. It is necessary to restore optical and atmospheric blur, calibrate the shape measurement, and take into account that nearby galaxies may be oriented in a similar way even before lensing.

The full six-year DES analysis gives $S_8=0.789\pm0.012$ in a flat ΛCDM at 68 percent confidence level. The difference with the considered combination of CMB data is 2.6 standard deviation in the projection onto $S_8$, but 1.8 in the full parameter space. Univariate comparison tests the difference of one quantity; the joint one takes into account the entire set of parameters and the correlations of its errors. These are different statistical questions, so the answers expressed in standard deviations do not have to be the same. [73]

The completed KiDS-Legacy received $S_8=0.815$ with asymmetric errors +0.016 and −0.021. This entry shows the position of the maximum of the one-dimensional posterior distribution and its 68-percentage interval of the highest density. The result is consistent with Planck in the comparison used. The authors attribute the change in estimate relative to earlier analyzes primarily to improved

redshift estimates, calibration, area, and image processing. Therefore, the idea of a single, unchanging "crisis $S_8$" does not adequately describe the current state of measurement. [74]

Condensing complex observations into a single number is useful for first comparison. However, two models with the same $S_8$ may produce different relative strengths of heterogeneities at large and small scales or different growth between epochs. Matching only the central values will lose this information. The full test returns to correlations between images and galaxy positions, their dependence on angle and redshift. It is there that signs of new physics that disappeared after statistical compression can be preserved.

At small scales, astrophysics is added to instrumental issues. The gas cools, forms stars and is ejected from galaxies, changing the distribution of mass. Neutrinos also affect the scale dependence of growth. Robust testing first uses areas where the description is sufficiently controlled, then checks for robustness when more complex modes are included. Discarding some of the data may reduce accuracy, but it helps to understand what physics is actually causing the discrepancy.

## Early galaxies and the cost of luminosity

The James Webb Telescope observes distant sources in the infrared. Some of them turned out to be brighter or more massive than expected by certain models of early galaxy formation. At this point it is easy to mix several statements: the object is bright, it has many stars, its dark halo is massive, and cosmology does not allow for a sufficient number of such halos. Between neighboring statements there are different measurements and physical models.

Young massive stars can produce greater luminosity per unit stellar mass. The spectrum is influenced by age, star formation history, chemical composition, dust, and a possible active nucleus. The redshift estimated using several wide filters requires verification with spectral lines. The distance obtained after spectroscopy helps, but does not automatically eliminate all mass uncertainties.

Krishnan and Abazajian's paper 2026 examined how systematic errors in stellar masses and scatter change conclusions about the efficiency of galaxy formation. At the rare massive end of the distribution, more numerous moderate objects may fall into the top category more often than rare true giants fall out of it. Such asymmetry must be included in comparison with theory. [75]

Another analysis of 2026 jointly varied the cosmology and baryon-to-star conversion efficiency of selected CEERS and FRESCO objects. The release of the dark energy parameter and spatial curvature did not eliminate the requirement for high efficiency for the spectroscopic sample studied. This result points to the need to study the astrophysics of galaxy formation in more detail, but is specific to the data and extensions of cosmology considered. [76]

The size of the view is also part of the physics problem. A small field may randomly cross an area of high galaxy density and give the appearance of an overabundance of rare objects. On the other hand, extremely deep observation allows one to see weak systems that are not accessible to a wide view. To check the abundance, both modes are needed: depth specifies the composition of the population, area limits its spatial dispersion. Artificial sources with known properties added to images help measure the detection probability of each class.

The new early physics remains subject to testing. Its essential feature would be a consistent change in the number of haloes, their clustering and other observable quantities, which cannot be reproduced by permissible changes in star formation and selection. An impressive image alone is not

enough to reach this conclusion. And even a revision of the standard model of structure formation would not automatically cancel the evidence for an early hot stage: these are different levels of cosmological description.

## How to check the law of gravity itself

So far we have compared ways to determine cosmological parameters. A stronger question can be posed: does the chosen theory describe expansion, the movement of matter, and the propagation of gravitational waves in the same way? To check this, we need observations that respond to different aspects of the same law. Distances primarily limit geometry. Galactic velocities and lensing add information about gravitational field perturbations. The merger signal also allows us to check the transfer of waves from the source to us.

For two theories, one can select a similar history of H(z) and then compare their perturbations. The coincidence of the background function does not require the coincidence of the equations for the growth of the structure. In terms of gravity modifications, the attenuation of the gravitational wave amplitude at cosmological distances also changes. This effect is possible even at a propagation speed equal to the speed of light. In this case, the usual distance derived from the amplitude under the assumption of general relativity needs to be reconsidered. [77]

A convenient value for observational verification is the ratio of the gravitational-wave and electromagnetic luminosity distances at one redshift:

$$\Xi(z) = \frac{d_L^{\rm GW}(z)}{d_L^{\rm EM}(z)}.$$

In general relativity, with standard propagation of photons and waves, a correct source model and the same consideration of lensing, this ratio is equal to unity. Both estimates have the dimension of length, but are obtained by different physical methods. The emitted power and observed brightness determine the electromagnetic path. Changing the frequency and shape of the gravitational signal limits the properties of the binary system; together with the orientation and response of the detector, they allow the amplitude scale to be reconstructed. The designation $d_L$ itself does not make these procedures independent of theory.

The joint registration of GW170817 and a gamma-ray burst in the year 2017 made it possible to strictly limit the difference in the speeds of light and the gravitational signal in the studied regime, taking into account assumptions about the emission time. But speed and amplitude evolution are different properties of the equation. The success of the first test does not replace the second. And testing at low redshift does not automatically measure the accumulated effect at cosmological distances. [78]

To understand the mechanism, consider a limited example with two tensor polarizations, velocity c and a positive effective Planck scale $M_*(t)$. Ordinary matter is minimally related to the metric by which hours and distances are determined. On a uniform background in units of c=1, each free mode obeys the equation:

$$\ddot{h} + (3+\alpha_M) H \dot{h} + \frac{k^2}{a^2} h = 0, \qquad \alpha_M = \frac{d\ln M_*^2}{d\ln a}.$$

The dots here mean derivatives with respect to cosmic time, k is the comoving wave number. If the wavelength is small relative to the scale of the background change, its envelope changes approx-

imately as $1/(aM_*)$. In a homogeneous transport model, this gives an additional multiplier in distance. The change in $M_*$ may be confounded with the $H_0$ estimate: a smaller recorded amplitude may indicate a different distance or a different transfer. Such degeneracies were studied, in particular, in the work of Lagos et al. [79]

A short example with a given $\alpha_M(a)$ is given in the mathematical appendix. It calculates the pass-through effect under the stated assumptions. To obtain a full-fledged theory, you still need to select an action, match its background with disturbances, check stability and calculate conditions around the source and observer. Arbitrarily assigned $H(z)$, growth and function $\Xi(z)$ may not belong to the same physical model at all.

## From source to detector

The homogeneous calculation has a significant limit. The real binary system is in a dense environment, and the detector is inside the galaxy. Some theories use shielding: an additional field acts in space, but its influence is suppressed in dense regions. Dalang and Lombriser's research shows that in the class of models they examined, consistent shielding at both ends of the path can restore normal distance. Therefore, it is impossible to leave the effect of cosmological transfer and at the same time declare all local physics standard without calculation. [80]

In geometric optics for a certain class of Horndesky theories, with the specified neglect of additional scalar radiation and mode conversion, the observed amplitude effect is associated with local values of the effective Planck scale at the places of emission and reception. This leads to a specific requirement for the program: to trace the field through transitions between the cosmological background and the environment of the source. The coincidence of speed with c in itself does not solve this problem. [81]

Even with standard gravity, the distance along a single merger is uncertain. Orbital inclination changes apparent amplitude and mixes with distance. Lensing enhances or weakens the signal. Vivid and well-oriented events are included in the sample more often. If the theory of wave generation changes, the wave form must also be recalculated. For the electromagnetic route, its calibrations, possible absorption and standard source model remain. The set of corrections must describe the same selected catalog, not an arbitrary average Universe.

The following thought experiment is useful. Let two models give the same distances to supernovae at the selected interval. If the first predicts $\Xi=1$, and the second predicts a certain deviation, wave events can distinguish them. However, allowing freedom to change orientations, photometric calibration, or propagation parameters will reduce the difference. Therefore, we first need to establish which part of the second forecast is mandatory and which disappears when reconfiguration is allowed. We have already encountered this logic in the calculation of redshift drift.

## Shared parameters for three channels

The proposed task begins with two explicitly written actions and general rules for handling the substance. For each action, feasible background solutions, linear disturbances, and wave transport are calculated. Then pairs of solutions with close $H(z)$ are selected. This proximity is determined by the range of measurements and their covariance, and not by the coincidence of the curves drawn by eye. The next step is to check whether the overall parameter range is maintained after adding growth, lensing and standard sirens.

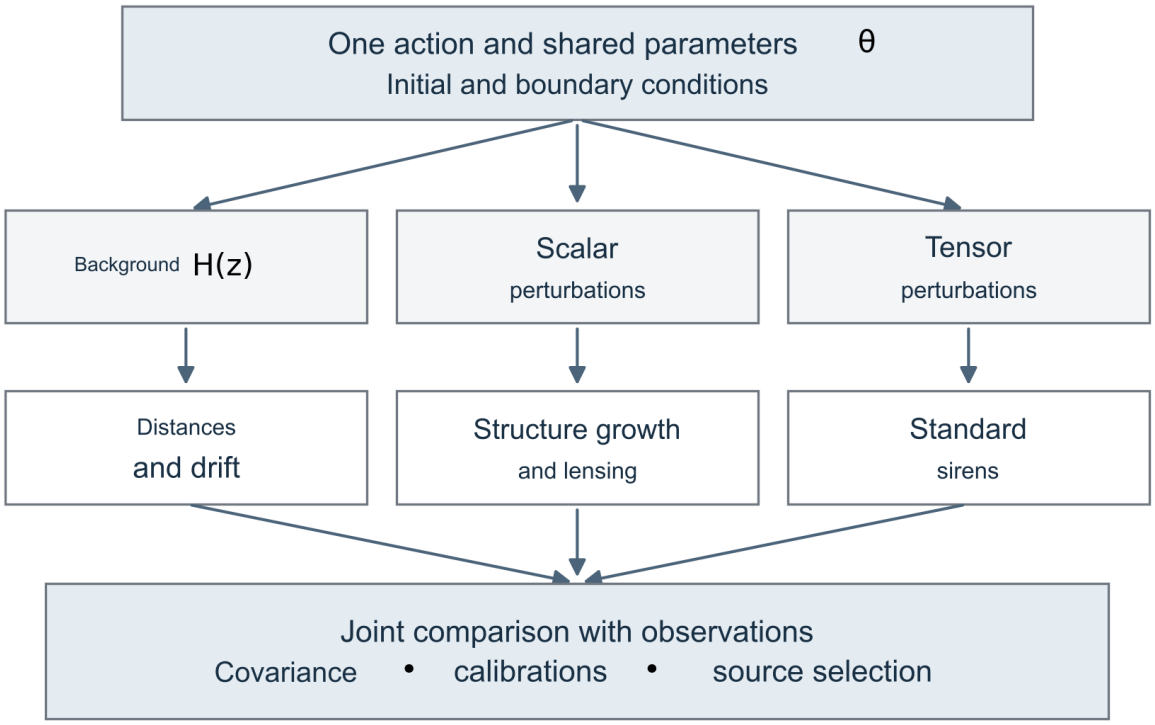



Figure 5. Three observation routes connected by one physical model. General parameters and initial conditions set the background and disturbances; Each channel goes through its own measurement model. The scheme does not assume that any arbitrarily given triple of functions can be obtained from a coordinated action.

A strong result will be an area where the same theory passes all three tests, but the chosen competitor does not. An equally meaningful negative result: shielding or freedom of parameters can make the channels in question almost identical. Then the degeneracy map will show whether a different redshift range is needed, more precisely a known orientation of the sources, a laboratory test of the field, or a new physical channel. It is impossible to promise in advance that the sirens will solve the problem of dark energy.

The deviation of Ξ from unity is also not the name of the discovered theory. It indicates that the selected joint description does not agree with the observation. The reason may be wave transport, source model, photon route, or general calibration. To favor a change in the law of gravity, one would need to reproduce the particular redshift dependence of the effect and test it with independent observables. Two consistent fits do not replace one overall prediction.

## How to check it

Let's start with the local scale: measure the distances to common galaxies using Cepheids and TRGBs with the same geometric supports. Independent groups will process the images with a prefixed selection. Artificial stars added to frames will allow us to measure displacements from mixing sources. We will check the difference in estimates for dependence on the density of stars, color and position of the region in the galaxy. Its predictable change as resolution improves will indicate a specific measurement error. The general error of the supports themselves must be checked in another, physically independent way.

This method is provided by standard sirens - gravitational waves from mergers. The shape and amplitude of the signal allows one to deduce the distance in a given theory of gravity, and electromagnetic tracking helps to find the host galaxy and measure its redshift. The feasibility of this combination was demonstrated at GW170817. We need control of the orbital inclination, amplitude calibration of interferometers, selection of detected events and the natural velocities of nearby galaxies. [82]

For an event without an identified host, a probabilistic set of galaxies is used, taking into account the completeness of the catalog. The next calculation would create artificial merger samples for the expansion histories being compared, run them through the specific network's noise and selection model, and reconstruct the distances using the same method as in the real data. Repeating the experiment will show how often the difference can be recognized and how often interference creates a false discrepancy. This determines the required number of events and calibration accuracy; a predetermined percentage of accuracy does not replace this calculation.

Geometry is also checked by the Clarkson, Bassett and Lu test. From the independently reconstructed distances and expansion rates at different redshifts, the current value of the spatial curvature parameter is calculated. In a homogeneous isotropic model, each such calculation should give the same parameter, regardless of the form of dark energy. The physical curvature of a spatial slice changes with expansion; The test compares values reduced to one, today's normalization. One cannot derive one observable relationship from another using the testable relationship itself. Derivatives, common calibrations, and correlated errors require control. If inconsistency remains after these checks, the basis of the accepted geometric model will require revision. [3]

For early galaxies, the next physical step is different: spectroscopy, expanding the wavelength range and viewing area, independent constraints on stellar masses, and measuring spatial clustering. Models must predict recorded images and spectra after full selection, not just ideal masses. As a result, the scientific result takes the form of a map: which general physical parameters are supported by different routes, which are excluded and which are still indistinguishable. It is such a map that can show where the lack of accuracy ends and the need for a new picture of the world begins.

To test gravity together, they first create artificial merger catalogs from each selected theory and run them through the same screening network of detectors. Lensing and growth are calculated using the same parameters. Part of the catalog is saved to check the forecast; common calibrations and large-scale modes are counted as dependencies rather than as independent replicates. If the required relationship between channels is not reproduced under any acceptable parameters, this version of the model is rejected. Such joint analysis is posed here as a research task; a new limit on Ξ based on observational data is not declared.

**III Before the usual start**

**Chapter 11**

# Where did the structure come from?

A galaxy map has one thing that's easy to take for granted: it has a pattern at all. The substance gathers into extended threads, nodes and clusters, between which sparse areas remain. Gravity helps to understand how a small initial heterogeneity turns into a noticeable structure. The denser area attracts additional substance, the difference intensifies. But this explanation has a beginning: the site should already be slightly different from its neighbors. If you specify a strictly homogeneous classical system and equations preserving its symmetry, words about attraction alone are not enough for the appearance of the original picture.

The question of the first inhomogeneities connects cosmology with quantum physics. It allows us to get closer to eras from which we do not receive direct images. To do this, it is necessary to trace a long causal chain: the early state of the fields, the appearance of disturbances, their development in a hot plasma, the formation of atoms and the subsequent growth of the structure. The observed sky is at the end of this chain. The way back to its beginning requires checking every link.

## Small differences, big consequences

It is convenient to parse early disturbances into waves of different sizes. This is a mathematical representation of a spatial pattern, similar to the decomposition of sound into frequencies. A wave here can mean a slight deviation in the density or curvature of space from a uniform background. Its length determines the scale, amplitude determines the magnitude of the deviation, and phase determines the location of the ridges and troughs. Such a wave component with a given length and direction is called a mode. It serves as an element of description of the general field, and not as a separate subject.

The power spectrum shows how strong disturbances of different scales are in a statistical sense. It does not report the coordinates of every future galaxy. One spectrum corresponds to many possible spatial patterns. This is an important difference between predicting a distribution and predicting a single outcome. A cosmological theory can correctly describe the statistics of the sky without specifying in advance which direction a particular cold spot will be.

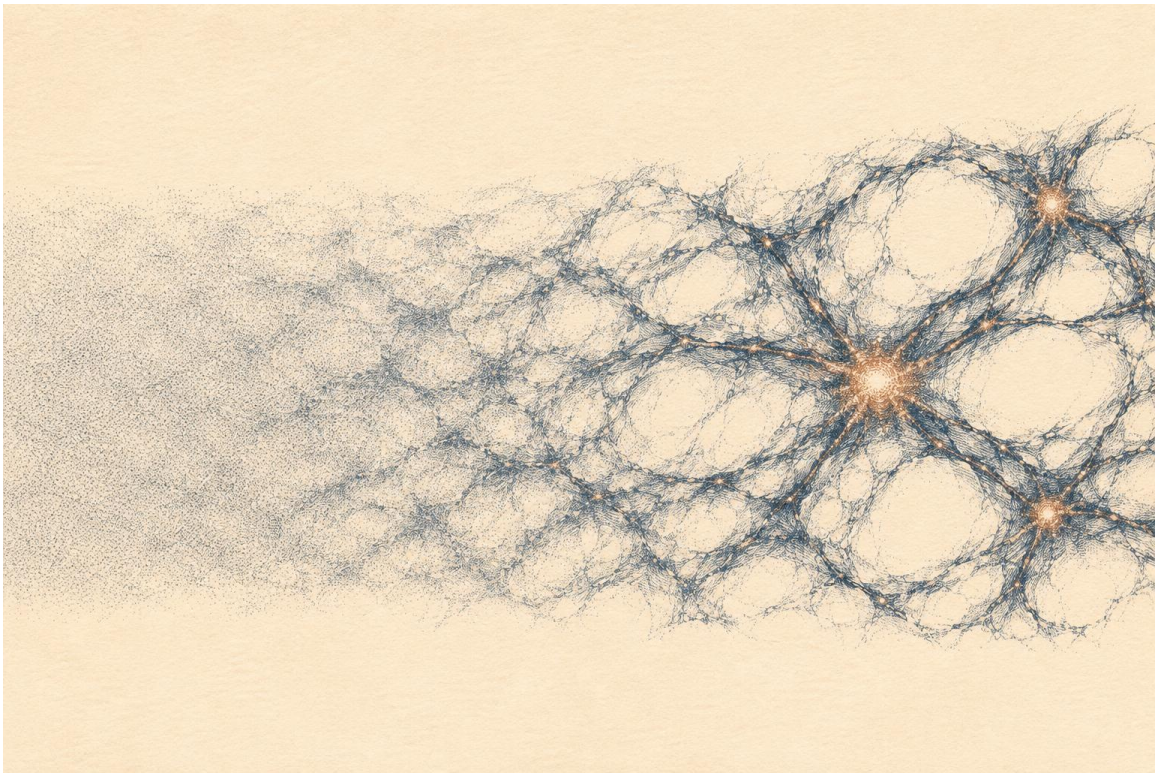
In a simple approximation, the dimensionless primary power is written as a power law:

$$\mathcal{P}_\zeta(k) = A_s \left( \frac{k}{k_*} \right)^{n_s - 1} .$$

The letter k denotes the wave number: the larger it is, the smaller the spatial scale. The index ζ indicates that a curvature perturbation is being described. The value $A_s$ specifies the amplitude at the selected reference scale $k_*$, and $n_s$ specifies the slope. For $n_s$ equal to one, equal logarithmic intervals contribute equal power: what is important is the same proportion between the boundaries of the intervals, not the same difference. This distribution is called scale-invariant.

On the way to the observer, some disturbances manage to oscillate in the plasma, others grow under the influence of gravity, and others are partially smoothed out. Therefore, the peaks in the temperature spectrum of the cosmic microwave background radiation cannot be read as direct peaks in

the inflationary potential. The measured pattern contains both the initial conditions and the history of the environment. Likewise, the distribution of galaxies depends on how the matter collected in the halo and where the luminous objects formed. The restoration of the beginning is always based on the model of this transference.



Engraving 14. From small inhomogeneities to the cosmic network. Small initial differences go through the evolution of the environment and gravitational growth before becoming a cosmic network. A conditional transition from a faint grainy pattern to threads and knots conveys this chain. The engraving is not the result of a numerical simulation and does not show the only possible outcome of a given power spectrum.

## How inflation connects the quantum and the cosmic

Inflation is the name given to the accelerated expansion of the early Universe. What is important here is the nature of the change in the scale factor, and not just the large numerical value of the expansion rate. With inflation, the comoving Hubble length decreases: the physical length c/H is divided by a scale factor a to compare it with distances on a stretched coordinate grid. Therefore, the wavelength can become much larger than c/H, even if it was originally smaller. This transition is important for the evolution of disturbances; the Hubble sphere itself cannot be identified with all causal horizons.

A sufficient inflationary stage allows the observed region to be linked to a smaller region within which a causal interaction may have previously occurred. It also reduces the relative salience of spatial curvature. It was the problems of homogeneity and proximity to the plane that motivated the classic work of Alan Guth. However, the specific mechanism for completing the original model proved problematic; The name of a program does not make all its implementations equally successful. [83]

As in the description of late acceleration, inflationary dynamics are often associated with a scalar field and its potential energy. It is a general mathematical tool; it does not establish that the early and

late accelerations are caused by the same field. When the potential part predominates and the field changes slowly enough, the energy density decreases much less than the density of an ordinary expanding gas. The energy must then be converted into particles and radiation, from which the hot stage develops. This transition, called reheating, links the inflationary model to subsequent cosmic history.

Against such a background, quantum field disturbances can stretch to enormous physical wavelengths. In simple adiabatic regimes, where there are no independent perturbations of the relative composition of the medium, the long-wavelength curvature perturbation preserves statistical information for the hot epoch. Classical calculations have shown how this mechanism is capable of creating almost scale-invariant density perturbations. In this case, the amplitude depends on the field dynamics: the general idea must be brought to a quantitative prediction. [84]

The phrase “galaxies grew from quantum fluctuations” compresses several physical transitions. It requires a chosen quantum state, equations of evolution, and an explanation of the applicability of classical statistics. The stretching of the wavelength itself does not mean that the particle moves through space faster than light. And the increase in cosmic scale does not eliminate the question of the origin of the initial state. Inflation can explain the properties of the observed area, leaving open the question of why this particular stage began.

There is also practical uncertainty: one current scale is associated with a certain moment of inflation throughout the subsequent history of expansion. By changing the duration of reheating or the properties of the substance during it, we change this correspondence. Therefore, comparing the potential shape with the data requires taking into account intermediate epochs. The potential figure in itself does not yet provide a ready date of origin for each observed heterogeneity.

## What exactly is the sky testing?

In the Planck 2018 analysis, temperature, polarization and lensing data yielded $n_s = 0.9649 \pm 0.0042$ at the 68 percent level in the adopted model. This is a historical published reference: the spectrum is close to scale-invariant, but has a slight slope. This result helps limit inflationary scenarios. Its meaning depends on the background cosmology and the chosen set of parameters; the number is not a direct measurement of the shape of the fundamental field. [85]

Temperature and polarization provide different types of information. Polarization occurs when radiation with a certain angular inhomogeneity is scattered and therefore in its own way reflects the early state of the plasma. The general theory must simultaneously describe temperature correlations, polarization correlations, and the connection between them. The spectra of ACT DR6 provide another set of temperature and polarization measurements with published statistical descriptions. Working with them requires taking into account foreground radiation and instrumental uncertainties. [86]

An additional question concerns primordial gravitational waves. They could leave a special component of polarization - B-modes. This pattern is also created by gravitational lensing and polarized radiation from our Galaxy. In the published BICEP/Keck analysis of observations prior to the 2018 season, a coupled model of these contributions yielded a limit of $r < 0.036$ at the 95 percentage level and the inverse megaparsec reference wavenumber 0.05. Here r is the ratio of the primary tensor power related to gravitational waves to the scalar power of curvature perturbations. This is the result of specific work, and not a stated current sensitivity record. [87]

If the model requires a tensor signal above the reliable upper limit, it faces an observational contradiction. However, different inflation models allow for different values of r. Improving the limit consistently narrows the space of possibilities without automatically turning into a refutation of the entire program. If detected, the spectrum shape and alternative sources will also have to be checked, since one type of observed pattern can arise in different ways.

Statistics can be explored deeper than through power. The bispectrum describes the correlations between triplets of wave modes. With statistical homogeneity, their wave vectors close into a triangle; We are talking about the relationship between the scales and directions of waves, and not about a triangle on a sky map. The dependence of the bispectrum on its shape is sensitive to the interactions of early fields. Such correlations make it possible to look for deviations from Gaussian statistics, which are completely specified by the mean and two-point correlation. In the Planck analysis of primary non-Gaussianity, no significant signal was found among the studied patterns. The results are limited precisely by the forms of correlations tested. [88]

## One event and several traces

Let us imagine a short change in the conditions for the propagation of disturbances during inflation. For example, their effective speed of sound decreases slightly and returns to its previous value. We are talking about the speed of propagation of a certain field mode, and not about sound in the air. For some effective descriptions, such an episode creates associated features of the power spectrum and bispectrum. The connection has already been established in the scientific literature and provides a meaningful test of the mechanism. [89]

An event has general parameters: position in time, duration and strength. They are connected by action - a single mathematical expression from which equations of fields and their interactions are derived. Once selected, one episode determines several observable consequences. Therefore, the power feature and the correlation pattern cannot be shifted independently. In this case, the transfer functions of temperature and polarization differ. A common physical scale does not require that the visible peaks of two graphs be in the same locations. [90]

This can be thought of as reconstructing one brief exposure using multiple sensors with different response times. True agreement means that after taking into account the properties of the sensors, one source history is obtained. If each device requires its own event time, the explanation loses its main content. In cosmology, the role of sensors is played by various statistics and observed fields, and their response has to be calculated through the evolution of the Universe.

A competing explanation changes the initial quantum state: in some modes additional excitations are allowed relative to a chosen vacuum field reference. This state is also capable of creating features and enhancing three-point correlations, in particular for close to elongated configurations. Therefore, power oscillation by itself does not establish an early mechanism. Even the preference for the excited state is not proven by the previous rebound: a separate physical model is needed that actually prepares this state. [91]

Conjoint verification has the advantage of limiting freedom of explanation. Each new measurement must test a necessary consequence of the already chosen model. If the parameters are expanded each time just enough to accommodate the next deviation, the number of matches increases and the discriminating power disappears. A meaningful result begins where it is clear in advance which combination of observations will become difficult for the mechanism.

## What does the wave learn along the way?

The primary tensor spectrum depends on the mechanism of perturbation generation, but the gravitational wave background observed today also bears a trace of subsequent expansion. A wave of a certain comoving scale goes through different regimes relative to the Hubble radius. After returning to a region where its length is significantly less than this radius, it oscillates, and its amplitude changes with expansion. Therefore, the spectrum is able to store information about both the source and the reentry epoch.

In the general theory of relativity for the linear tensor mode, we can write the equation in conformal time at c = 1:

$$h_k'' + 2\mathcal{H}h_k' + k^2 h_k = 16\pi G a^2 \Pi_k^{\mathrm{TT}}.$$

Here $h_k$ is the amplitude of one polarization, primes denote derivatives with respect to conformal time, the calligraphic H is equal to a'/a, and $\Pi_k^{TT}$ is the corresponding transverse traceless part of the anisotropic stress in the accepted normalization. Even after the wave generation ceases, the medium influences the transport through expansion and stress. Boyle and Steinhardt investigated how such effects enter into the transfer function of the primary background. [92]

A useful extreme example illustrates the meaning of this relationship. Let the waves re-enter the epoch with a constant ratio of pressure to energy density w, with w > −1/3. For sub-Hubble freely propagating waves, the amplitude decreases as 1/a. If the initial dimensionless tensor power is proportional to the power k with exponent $n_t$, then far from the boundaries of the epoch we obtain a well-known power-law dependence:

$$\Omega_{\mathrm{GW}}(f) \propto f^{\,n_t + 2(3w-1)/(3w+1)}.$$

Here $\Omega_{GW}$ is the fraction of the modern critical energy density per logarithmic frequency interval. An additional indicator is derived from the input condition k = aH: at constant w, the input scale factor is proportional to $k^{-2/(1+3w)}$. Substitution into the energy spectrum, proportional to $k^2$, the primary power and the square of this factor, gives the written power. This conclusion assumes averaging of oscillations, the absence of an additional source and noticeable anisotropic stress, as well as a constant number of effective degrees of freedom in the considered interval.

At the radiative value w = 1/3 the additional degree is zero; for w = 0 it is equal to −2. Therefore, even a smooth primary spectrum can acquire a kink if different frequencies were included in different epochs. However, the same slope in a limited band can arise due to the shape of the source. A single observed kink does not establish either the heating temperature or the existence of a new particle.

The actual basic transfer function already contains singularities. The number of relativistic degrees of freedom changes; free propagation of neutrinos affects tensor perturbations. Watanabe and Komatsu calculated such changes within the framework of standard physics. Before searching for an unusual epoch, it is necessary to reproduce this background and evaluate the accuracy of its calculation. Otherwise, a standard transition can be erroneously declared as evidence of a non-standard history. [93]

The combination of cosmic microwave background radiation with the gravitational wave spectrum as a way to limit early epochs and additional entropy production was studied by Kuroyanagi, Rengeval and Takahashi. This idea already exists in the literature. Our addition is to make a limited

comparison: which two preselected histories remain distinguishable after a permitted change in source, standard transfer, and the actual response of the future measurement? [94]

In the first version, the selected reheating is followed by a standard radiation history. The second adds a finite epoch with a fixed w that ends early enough to accommodate nucleosynthesis. Termination temperature, duration, and possible entropy production are linked by one model of the component and its disappearance. You cannot independently assign a convenient break and separately maintain standard densities without checking the energy balance.

For both histories, one constrained class of primary tensor spectra consistent with the selected large-scale perturbation data is first calculated. Then the transport equation is solved and the modern spectrum is obtained. Some parameters can be selected so that the versions almost coincide in the same frequency band. The testable question is whether the obligatory divergence will remain in the other available band or in the associated cosmological constraints.

It is especially important not to confuse observation frequency with source temperature. To turn the position of the kink into the transition temperature, you need to know the relationship of the scale factor with temperature and the change in entropy between the transition and the present day. Additional decay can change this relationship. Therefore, the temperature inference is always relative to the full model, even if the frequency is measured very accurately. As a first step, it is safer to estimate the observed amplitudes, slopes and positions of the features, and obtain the physical parameters from the joint transport.

A practical intermediate product is a library of transfer functions for a resolved mesh of durations and state equations. It is tested at analytical levels far from transitions and numerically refined in the transition regions themselves. Only then can a fast approximate computer be trained. The error of such a computer is compared to the difference between two histories: a small average error over the entire grid is useless if it systematically smoothes out precisely the distinguishing kink.

The freedom of the source must be declared before comparison. If both its form and the transfer history are allowed to change arbitrarily, one observable function will not restore both. In contrast, a fixed physical class of sources can make some spectral relationships predictive. The negative result of such a study is also specific: it shows how much prior knowledge about the source is required before the spectrum begins to measure the expansion history.

## How to check it

You can start with two limited models: one with a brief change in the speed of sound and the other with a given excited state against a general inflationary background. For each, the action, initial conditions and acceptable range of parameters are fixed. In the first model, interactions with three disturbance factors are derived from the same action that determines power; in the second, the initial three-point correlations are also specified. Then the positivity of the kinetic coefficients, the applicability of the approximations, and the fact that the excitation energy does not destroy the accepted background are checked.

The first calculation should give the primary power and bispectrum for different triangle sizes and shapes. The following transfers them to temperature and polarization observables. Published Planck data and ACT temperature and polarization spectra in the ranges for which statistical models have been prepared are suitable for pilot testing. Galactic surveys can add information, but will require

separate calculations of nonlinear growth, the connection of galaxies with matter, and the geometry of the surveyed volume.

A physical apparatus does not directly measure a ready-made primordial correlation. Polarimeters receive radiation in several frequency bands, helping separate dust and synchrotron foregrounds. The beam shape, polarization angle, calibration, and noise must be controlled. Artificial maps with these properties are generated on a computer, injected with a known signal, and passed through the entire processing chain. This establishes the detection probability for a specified model, including cases where contaminants hide its signature.

The parameters are estimated on part of the data, and a conditional forecast is built for the remaining information. For example, a feature found in temperature should predict a certain polarization pattern. Both quantities are related by the initial disturbances, so their joint covariance is taken into account—the statistical relationship between fluctuations and errors. At the same time, the background cosmology and interference parameters are varied. The frequency search range for the feature is set in advance, and the detection threshold is calibrated on artificial data, taking into account the entire search. This protects against choosing a spectacular random fluctuation among many attempts.

A particular non-null version of a mechanism fails testing if the power-explaining parameters require a measurable bispectrum that is inconsistent with the data. If the expected additional signal is too weak, its absence leaves the versions indistinguishable at a given precision. The next result is a map of detection probability depending on the strength, duration and time of the episode with a preselected acceptable false detection rate. It has yet to be built for the selected pair after taking into account the interference and the permitted changes in other parameters. Such a map will show which extra dimension actually separates the models.

The tensor branch requires first calculating the absolute amplitude, then selecting the appropriate range and instrument. The presence of a theoretical break does not promise detection of the usual inflationary background by a cosmic interferometer. The measurement model includes instrumental noise and astrophysical background, and when compared with polarization, foregrounds and lensing contributions. A particular non-standard epoch is excluded if all of its parameters allowed by other tests predict a measurable spectral ratio that is inconsistent with the data. The immediate result is the calculation of the area where such a ratio retains its discriminative ability after adjusting the source and interference; where it does not exist, the reason for the degeneration should be indicated, and not the complete early history should be declared restored.

**Chapter 12**

# Was the origin of cosmic structure quantum?

Galaxies grew from small irregularities. In inflationary models, their origin is often described by quantum fluctuations of fields. The words are so familiar that it is easy to miss the next question: what observation will establish the quantum nature of this origin? A successful quantum calculation and an experimental exclusion of the classical explanation are different results. A testable difference in predictions should appear between them.

We see late traces of a process to the beginning of which we cannot return with laboratory equipment. It is impossible to repeat the birth of the same Universe, choose the moment of preparation of its state and switch the interaction on command. But you can compare related statistical features, transfer them through known dynamics, and check whether a competing model still has the ability to reproduce them. It is precisely this formulation that makes the question scientific.

The purpose of the chapter is to separate several levels of assertion. Quantum theory provides a natural mechanism for the formation of disturbances. A certain classical statistical model can reproduce part of his results. Interactions can destroy this coincidence. But detecting a difference in the sky can only be done after calculating signal transmission, observational errors and the freedom of an alternative explanation. Every transition is important here: a missing link turns a measurement program into a beautiful story.

## One pattern and several ways to get it

Let the two measured values correspond to the deviations $x_1$ and $x_2$. We can estimate their variances and correlations by collecting a covariance matrix C. If it is positive definite, there is an ordinary positive Gaussian distribution that reproduces these second moments. In the two-dimensional case it is written as follows:

$$P(\mathbf{x}) = \frac{\exp[-\mathbf{x}^{\mathsf{T}} C^{-1} \mathbf{x}/2]}{2\pi\sqrt{\det C}}.$$

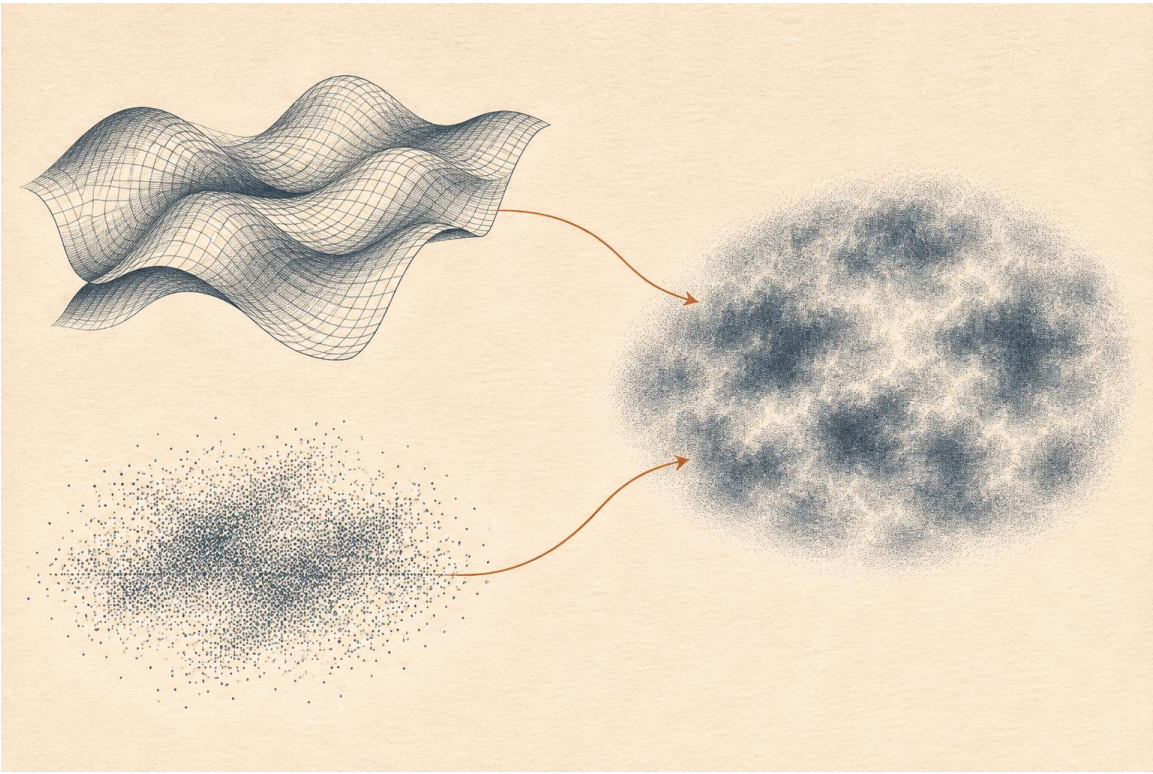
This formula does not describe the entire cosmology. It establishes a narrow logical fact: the measured set of Gaussian second moments alone does not force one to choose the quantum interpretation. It is possible to construct classical random variables with the same matrix. For a singular matrix, the distribution is specified on a smaller subspace; the essential conclusion about incompleteness of information remains the same.

In cosmology, the role of a set of such quantities is played by the amplitudes of spatial modes of disturbances. The power spectrum describes their two-point correlations. Its success is extremely important for testing the expansion model and shaping the structure. However, the question “where did the distribution come from?” contains more information than asking "what is its covariance?" A single statistical slice can be compatible with different state preparation mechanisms.

The quantum description also differs in the algebra of observables. Coordinate and momentum are represented by operators that do not commute. Their symmetrized products can be compared with ordinary statistical moments, but permutation of operators cannot certainly be replaced by permuta-

tion of numbers. If a calculation uses only a set of quantities for which the difference is hidden, good agreement with the data does not test the inaccessible part of the algebra.

It is important to name your classic opponent in advance. This could be a free field with Gaussian initial conditions, an interacting field with a given distribution, or a much freer model with specially selected nonlocal correlations. Excluding the first does not automatically exclude the third. The more freedom allowed to an alternative, the stronger the assumptions must be or the more independent observations required.



Engraving 15. One statistical trail and different explanations. Different state preparation methods can match the available two-point correlations. Therefore, a successful description of the power spectrum does not exclude all classic competitors. The engraving serves as an analogy for the ambiguity of the inverse problem: distinguishability must be sought in additional observables and verified after taking into account signal transfer and the freedom of each alternative.

## How a quantum state becomes like a random field

During expansion, the relationship between the amplitude of the mode and its canonical conjugate variable changes. In a suitable description, a strong compression arises: the uncertainty is distributed between the directions of the phase space extremely unevenly. Large uncertainty of one quantity and small uncertainty of another does not mean that the quantum law has ceased to apply. They mean that the available observations can preferentially see a certain part of the state.

Polarski and Starobinsky investigated how neglecting the strongly damped mode allows one to obtain a classical stochastic description of cosmological perturbations in the regime under consideration. Marten and Vennan later worked out which correlations and quantum properties were lost with various classical substitutions. In particular, reproducing certain two-point functions does not repro-

duce the entire quantum state. These results require preserving the approximation conditions and do not provide a general prohibition on searching for other observables. [95] [96]

Let's imagine a long narrow cloud of points on the phase plane. If the instrument is sensitive only to its long direction, two different models of cloud thickness may look the same. This is a useful geometric analogy for limiting measurements. But the shape of the cloud does not in itself indicate that each point is simultaneously the determined values of all quantum observables. It is here that a statistical picture can imperceptibly replace the physical meaning.

Another part of the transition has to do with the environment. To describe the selected long-wave modes, the remaining degrees of freedom can be excluded from explicit consideration by taking a partial trace from them. The resulting reduced density matrix no longer contains all the correlations of the full system. If the available interference terms are suppressed, the observed part begins to behave like a statistical mixture. No conscious observer is required for this operation.

Elliot Nelson showed a specific mechanism for such decoherence during inflation, arising from gravitational nonlinearities and the connection of the modes in question with other modes. The significance of the work lies in the explicit interaction and the calculated reduced dynamics. This result should not be translated into a statement that every cosmological model decoheres at the same rate or that all measurement issues are thereby resolved. [97]

Suppression of visible interference does not erase the difference between the laws of motion. Even if the initial description assumes a positive classical distribution, subsequent nonlinear evolution may change its moments differently. Let's test this idea on a system small enough for independent calculations. Such an example will not replace the observation of the Universe, but it will help not to confuse the initial coincidence with the eternal equivalence.

## Control calculation of nonlinear dynamics

Let's take one coordinate q and momentum p with the Hamiltonian $H=p^2/(2m)+\lambda q^4/4$. We choose the initial quantum state to be coherent with respect to the auxiliary harmonic oscillator. Its Wigner function is positive and Gaussian. We will set the same positive distribution as the initial conditions of the classical ensemble. Then at the initial moment the symmetrized moments coincide, including those needed below. The Hamiltonian itself, along which the movement begins, is the same in both calculations.

Moyal's formalism writes quantum dynamics in phase space. For a given potential, the classical Liouville equation is supplemented with a term with the third derivative with respect to momentum; higher derivatives of the potential vanish here. This is a well-known consequence of quantum mechanics. [98]

$$\partial_t W = -\frac{p}{m}\partial_q W + V'(q)\partial_p W - \frac{\hbar^2}{24}V^{(3)}(q)\partial_p^3 W, \qquad V = \frac{\lambda q^4}{4}.$$

Now let's multiply the equation by $p^3$ and integrate over phase space. For the initial Gaussian state, the boundary terms disappear. Three integrations by parts give a positive sign for the quantum correction. With the same initial distribution, we get:

$$\left.\frac{d\langle p^3\rangle_Q}{dt}\right|_0 - \left.\frac{d\langle p^3\rangle_C}{dt}\right|_0 = \frac{\hbar^2}{4}\langle V^{(3)}\rangle_0 = \frac{3}{2}\hbar^2\lambda\langle q\rangle_0.$$

The book has undergone independent numerical verification. In conventional units $\hbar$=m=1 we take λ=0.2, averages $q_0$=0.7 and $p_0$=0.2, both variances are equal 1/2. The classical derivative is calculated by Gaussian-Hermite quadrature, the quantum derivative is calculated through the matrix commutator $(i/\hbar)\langle[H,p^3]\rangle$. −0.451332 and −0.241332 were obtained, respectively. Their difference +0.21 coincides with the derived expression.

During numerical verification, the size of the oscillatory basis increased from 24 to 48 and 96 states. The maximum absolute difference with the formula was 1.67 × 10−16; control with a quadratic potential gave the difference 2.22 × 10−16. The source code, parameters and results are given in the computational kit. This is a test of the initial derivative of one moment, and not of the entire subsequent evolution.

The example shows exactly what is included in it: the coincidence of the initial symmetrized moments does not guarantee the coincidence of nonlinear dynamics for this classical comparison. It does not establish the magnitude of the cosmological signal, nor does it rule out all conceivable classical models with different initial conditions or laws. A useful direction for future work is to find a similar controlled difference in the primary disturbance model and trace it to an observable value.

## Where interactions leave a mark

For a free Gaussian field, many statistical properties are determined by the two-point function. Interactions link modes, and then higher order correlations become informative. Bispectrum refers to three modes whose wave vectors form a closed triangle. Its dependence on the sides and angles of this triangle helps distinguish mechanisms. However, the word “non-Gaussian” does not in itself mean “proven quantum”: nonlinear classical dynamics also creates non-Gaussian distributions.

It is necessary to compare two fully defined evolutions. Let us denote the difference between the predicted bispectra by ΔB. This is our designation of a diagnostic quantity, and not a new law of nature:

$$\Delta B_\zeta(k_1,k_2,k_3;\tau_0) = B_\zeta^Q(k_1,k_2,k_3;\tau_0) - B_\zeta^C(k_1,k_2,k_3;\tau_0).$$

In both parts, the action, parameters, initial comparison time $\tau_0$ and the rule for setting initial statistics are recorded. Otherwise, a difference can be obtained simply because different system preparations are compared. If the classical description is allowed to re-select the initial bispectrum for each result, this is a different research task. It requires assessing what additional assumptions make such freedom physically permissible.

Daniel Green and Rafael Porto proposed looking for signatures of quantum origins through an analytical framework of correlations, including features in stacked pulse configurations, under certain assumptions about locality and classical alternatives. This formulation is important because it con-

nects a philosophical-sounding question with the form of the function being calculated. The conditions of the argument are included in the statement itself and cannot be discarded when moving on to observations. [99]

In the paper "Classical and quantum evolution of inflationary fluctuations" by Guillermo Ballesteros, Jesús Gambin Ejea and Alejandro Pérez Rodríguez, version v2 from November 4 2026, the comparison is made at a finite initial time. The authors explore the differences in the tree scalar bispectrum and the one-loop tensor spectrum. An essential caveat: classical evolution in this formulation is not obliged to produce folded poles. The result depends on the interactions and the moment of comparison of the initial conditions. The work is not a prediction of guaranteed observability of the effect. [100]

This is a good example of how the cutting edge is evolving. The strong idea about the sign of quantumness becomes more precise when the formulation of the initial problem changes. Therefore, the book design should not fix one waveform as universal. One should construct a set of comparisons with explicitly stated premises and find out which differences survive acceptable changes in the description. Even the absence of a universal sign narrows the following search.

## Why is it not enough to just mention Bell?

Laboratory tests of Bell's inequalities compare correlations of results across different measurement settings. For cosmology, a particular difficulty arises: early conditions cannot be switched in the same way as the directions of analyzers in the laboratory. A single late sky image does not automatically contain all the alternative measurements required for the selected test. Before writing an inequality, you need to determine the physical meaning of its input variables and assumptions.

Maldacena constructed a special inflationary model in which cosmological correlations allow a formulation associated with Bell's inequalities. This is a proof of principle possibility in a given design. It cannot be transferred to an arbitrary CMB map as a ready-made measurement procedure. [101]

In addition, a test of the quantum properties of modern photons answers the question about the state of these photons and the chosen experiment. To connect it with primary disturbances, it is necessary to trace the preparation, interactions, transfer of correlations and the availability of the necessary observables. The last quantum stage of a long chain does not automatically establish the quantum nature of the very first link. This transition needs to be proven separately.

In the proposed program, it is more useful to first search for a specific distinguishable prediction in a limited class of models. The universal exclusion of all classical explanations is a stronger goal. If the first paper honestly refutes only certain classical dynamics with certain initial conditions, it may still be important. The size of the result is determined by the completeness of the output, not the volume of the title.

## From test case to research program

The first stage of the proposed work is a reproducible free limit. For the chosen inflationary action, quantum symmetrized correlators and the classical evolution of the consistent Gaussian ensemble are calculated. Where the theory predicts a match, the program must show it. Without such controls, the interaction-on difference can easily be confused with incompatible normalizations, Fourier transform conventions, or initial state error.

At the second stage, one explicitly recorded weak interaction is included. Quantum and classical contributions of the same order are calculated, with the same cutoff and renormalization rules where required. The parameters are selected in the region in which the discarded corrections are less than the difference under study. A large divergence outside this area is not a strong signal: it may indicate a loss of control over both calculations.

The third stage is the time dependence of the initial comparison. It should be varied along with the physical justification of the initial state. It is necessary to establish which result reflects the chosen preparation of the system, and which remains stable for the family of valid preparations. If the difference disappears when this premise is changed, it should be published. This way it becomes clear what exactly a future experiment potentially measures.

Next, a mapping of the primary signal into observables is constructed. Cosmological disturbances occur through hot plasma, structure formation, and light propagation. These processes can mix the forms of correlations and create their own non-Gaussianity. Therefore, comparison with the primary field ΔB data directly is usually not sufficient. It is necessary to calculate transfer functions and late contributions under the same set of conventions.

For AI, there is a job here with a clear criterion for success. It can compare independent implementations of integrals, look for unaccounted-for triangle configurations, test limiting cases, and identify combinations of observables that are less sensitive to interfering parameters. You cannot entrust him with choosing the “most quantum picture” without a predetermined comparison. Optimization will then find the feature of the simulator or dataset, rather than the physical evidence.

A useful first result would be an open package with several constrained models, benchmark solutions, and a list of indistinguishability regions. Such a package does not claim to be a new fundamental theory. Its value is the ability to check which part of the supposed cosmological feature survives independent calculation. This chapter's oscillatory example shows the control format; a full-fledged inflation package has not yet been created here.

## How to check it

Physical testing must begin with the selection of an observable and a family of alternatives. For example, a researcher can specify the shape of the primary bispectrum, allowed initial states, and a limited set of interactions. After transfer to observables, predictions are made for the temperature and polarization of the cosmic microwave background radiation or for the distribution of matter. The choice of channel depends on the calculated waveform, and not on the usual list of future telescopes.

The performance of a particular measurement is then modeled: available sky area, resolution, noise, masks, astrophysical interference, and calibration errors. These conditions can erase the interesting part of the triangular configurations or make it degenerate with a late effect. Until such a calculation is performed, detectability cannot be asserted even with a non-zero theoretical difference. A non-zero signal and a measurable signal are two different criteria.

The proposed analysis must be tested on artificial data where the true model is known. The classical signal, the quantum signal of the selected model, and the intended interference are separately added to the data. If a procedure systematically declares an ordinary nonlinear contribution to be quantum, it should be corrected before working with the real sky. The training and testing parameters are separated so that the algorithm does not recognize the simulator based on extraneous features.

When using multiple surveys together, common space modes and common sources of error must be taken into account. Two studies of one area of the sky do not provide two independent copies of the Universe. The coincidence of the result in different observables is useful when it is calculated in advance what kind of relationship between them the model predicts. The ability to select an independent amplitude for each channel weakens this check.

Failure conditions should be recorded before significance can be assessed. A theoretical program fails its own control if the difference turns out to be a numerical error, depends on incompatible initial conditions, or is less than an uncontrollable next order. An observational hypothesis is rejected if the predicted set of correlations is inconsistent with the data under the stated assumptions. The absence of a signal may limit the interaction or initial state, but does not prove the classical nature of the entire early world.

And the opposite result requires precise formulation. If the detected form contradicts the chosen classical model, the conclusion applies to that model and the tested alternatives. To make a statement about primary quantumness, it is necessary to show which additional classical explanations are excluded and on what physical grounds. Such carefulness does not weaken the prospect of discovery. It makes it possible to understand what exactly has been discovered.

The question of the quantum origin of the cosmic pattern fits particularly well with the intent of the book. It leads from an understandable coincidence of statistics to an actually performed small calculation, then to interacting fields and a project for future measurement. At each step you can get a certain result, including a negative one. From this chain arises a research direction that can be continued by the collaboration of theorists, observers and computing systems.

**Chapter 13**

# Before the hot start

Having established that the Universe has passed the hot dense stage, we are able to ask earlier questions. Due to what process did this condition arise? Was it preceded by inflation? Could expansion have been preceded by contraction? Did the usual time itself arise along with the history that we are restoring? These questions relate to different levels of description. The answer to one of them does not automatically carry over to the others.

It is especially easy to confuse the beginning of the hot stage with the absolute beginning of existence. The first is associated with a certain physical regime. The second requires statements about all possible regimes, including those for which the current description has not yet been constructed. To explore the background, it is useful to first replace the general word "beginning" with a precise question: what quantity, geometry, or causal relationship ceases to continue in the chosen model?

## The limit of the model and the beginning of the world

When tracing the expansion back, ordinary matter becomes denser and the temperature rises. In some classical solutions, this path leads to a singularity. The mathematical description here is subtler than the image of an infinitesimal ball. A geodesic—the trajectory of a freely moving particle or light in a given geometry—may not be extendable beyond a finite proper time of the particle or a finite affine parameter along the light ray. The affine parameter is consistent with the equation of free motion; it is not light's own time, which light does not have. Incompleteness means that the model stops answering where to continue the path.

This is not yet a description of the physical event at which the world was created. An interrupted trajectory may indicate the incompleteness of the selected region of space-time, the significance of other dynamics, or the boundary of the classical concept of geometry itself. To distinguish between options, you need to build a continuation and check its consistency. Declaring the boundary final does not replace such work; its arbitrary elimination with the words “there was another world there” also does not define physics.

The Bordet-Guth-Vilenkin theorem limits certain attempts to continue inflation indefinitely into the past. When the condition of positive averaged expansion along a suitable geodesic is satisfied, the corresponding description turns out to be incomplete in the past. Today's expansion in itself does not provide this condition: history along the path in question is essential. The argument is kinematic and does not require the usual condition of positive energy. Its outcome relates to the trajectories and assumptions of the model; he does not select a mechanism on the past boundary and does not prove the emergence from absolute nothing. [102]

Therefore, the model with previous compression must be checked for compliance with the conditions of the theorem throughout the proposed continuation. The name “cyclical” alone is not enough to consider the problem solved. Likewise, the presence of a quantum word in a description does not guarantee that the classical boundary has actually been eliminated. There must be certain variables, a law of their variation, and a region in which the observable cosmology is again obtained from the new description.

It is useful to distinguish between the local continuation of history and the explanation of the entire resulting chain of states. The first removes an obstacle at a specific location; the second must also justify the conditions of the previous phase. The scientific value of the continuation is given by the connection of these conditions with observed consequences. If a new epoch changes the initial statistics of disturbances, a subject of comparison with the sky appears. If it only receives a name, the explanation has not yet advanced.

## The bounce must withstand perturbations

In the rebound model, contraction gives way to expansion when the scale factor reaches a nonzero minimum. The space can remain infinite. The expansion rate H is initially negative, passes through zero and becomes positive. This simple sequence already imposes a limitation on the dynamics. In a spatially flat homogeneous model of general relativity, if the speed of light is taken to be unity, the following relation applies:

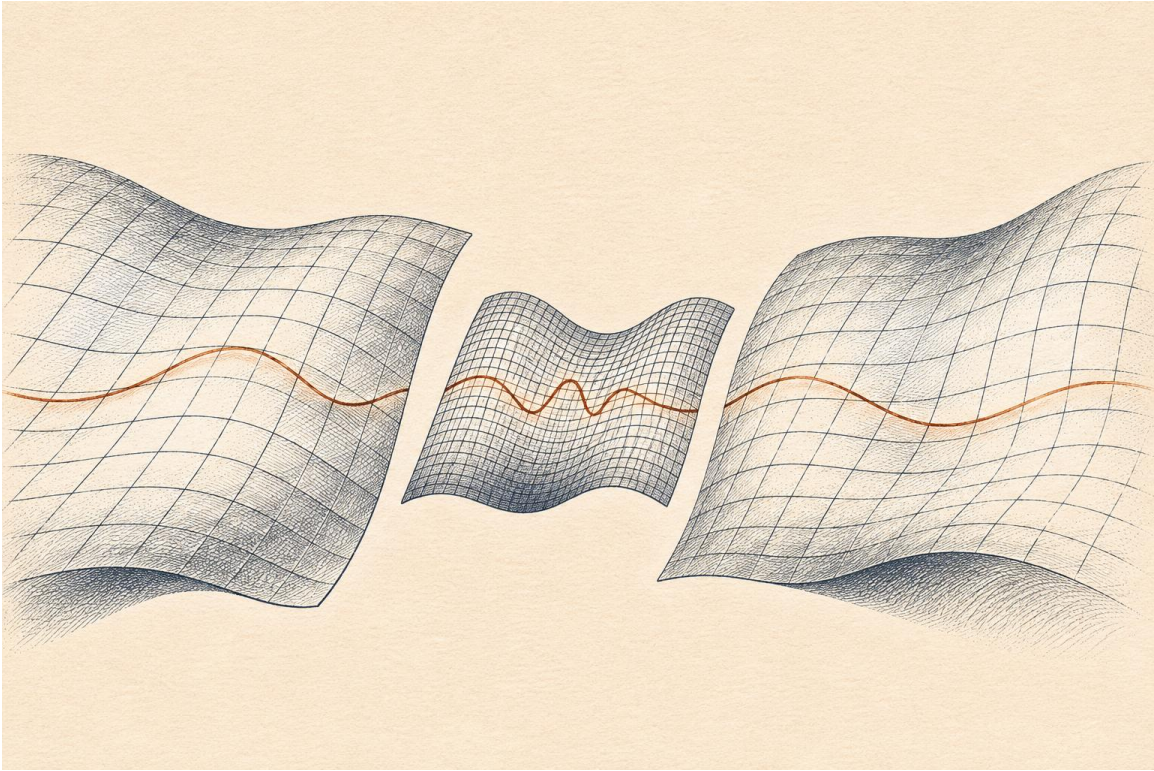
$$\dot{H} = -\frac{\rho + p}{2M_{\mathrm{Pl}}^2}.$$

Here ρ is the total energy density, p is the pressure, and $M_{Pl}$ is the reduced Planck mass. If the sum of density and pressure is non-negative, H cannot increase through zero. Consequently, a rebound in such a formulation requires changing at least one essential prerequisite. A different geometry, a different composition of matter, or altered gravitational dynamics are possible. Each option has its own price and its own conditions of applicability.

In the loop quantum cosmology of Ashtekar, Pavlovsky and Singh, the singularity was replaced by quantum rebound for a spatially flat isotropic model with a massless scalar field. The field was used as internal time: its changing value is used to number states without introducing an external clock. Evolution was studied analytically and numerically. This is a concrete result of a quantum model with a greatly reduced set of degrees of freedom; transferring the conclusion to the real inhomogeneous Universe requires separate work. [103]

The next step is especially important: small deviations from ideal uniformity must pass through the rebound. A pretty scale factor plot can hide instability. Some disturbances may grow rapidly, while others may cease to obey the approximation used. It is necessary to check the sign of the kinetic energy, the distribution of spatial inhomogeneities, and the influence of the disturbances themselves on the background. If they become comparable to the background, the linear calculation no longer confirms the smoothness of the transition.

You can't take a convenient background curve from one quantum theory and add perturbations from another just because they're easier to calculate. They must follow from a compatible description. Consistency is also needed when moving to the hot stage: the way particles are formed and energy transferred to them can change the predicted scales. It is here that the idea of a prior world turns into a set of difficult but concrete physical problems.



Engraving 16. The rebound hypothesis and the fate of disturbances. In the rebound scenario, compression gives way to expansion at a nonzero minimum scale factor. The images depict conventional areas of space, and not the external size of the entire Universe. The thin, inhomogeneous line reminds us of the main condition: the disturbances must undergo a transition within the framework of consistent dynamics. The existence of such a stage in our history has not been established.

There is a meaningful example of a joint constraint. In the considered single-field class of rebounds after dust-like compression, an attempt to reduce the ratio of tensor to scalar power by increasing scalar perturbations was accompanied by an increase in non-Gaussianity. The correction of one observational difficulty created another. The result depends on the initial vacuum, the chosen matter and the dynamics; it does not prohibit all bounces. But it shows why power, tensors and three-point correlations need to be checked together. [104]

Bouncing isn't necessarily part of an infinite loop either. One transition from compression to expansion does not say anything about the next turn of history. For repetition, additional conditions are needed, and the transfer of energy and entropy through successive phases requires a separate calculation. The ability to continue the scale factor through a minimum solves one problem out of several.

## Boundary state and the question of time

There are approaches in which searching for the usual previous epoch is not enough. In quantum cosmology, geometry itself becomes part of the quantum description. Then the usual time can appear only in a region where an approximately classical history is acceptable. The question of a more fundamental state remains meaningful, but it is no longer possible to translate it into a sequence of events on an external clock without additional justification.

The Hartle-Hawking proposal defines the wave function of the Universe through summation over suitable compact geometries. The wave function determines the quantum amplitudes of possible ge-

ometries and field states; from them, given the rules, the probabilities are obtained. In its original formulation, this is a method for choosing a quantum state, studied using simplified models. The geometries involved in the calculation do not have to be sequential frames of the real process. Therefore, the absence of the usual past boundary in such a construction is not equivalent to a registered transition from non-existence to existence. [105]

An observational forecast arises when a dynamic theory, admissible configurations, a method for calculating amplitudes, and a rule for transition to observation probabilities are selected. Then we need to find out under what conditions approximately classical space-time appears. Then you can compare, for example, the weights of stories with different disturbances. A boundary proposition becomes testable to the extent that it limits these weights and, through them, the statistics available to us.

This is where a useful discipline of language arises. The expression "emergent time" can denote the appearance of a convenient variable in some regime, rather than an event that occurs before all other events. A mathematical relationship between more fundamental quantities need not be a relationship of temporal cause and effect. To preserve the meaning of the word "before", we first need to establish whether there is a general order in the model that links the states being compared.

Even a successful boundary proposal need not produce a single classic story. It can specify a probability distribution. The test then concerns this distribution and its observed consequences. Choosing the most attractive outcome after looking at the sky would weaken the test: the theory must also explain how natural it is to obtain exactly the data given the predetermined rules.

## How much of the past remains in the present

The disturbance that arose before the hot stage goes through subsequent evolution and appears in the range of scales accessible to us only under suitable conditions. Long enough inflation can stretch the trace of interest beyond the observable region. Some features are smoothed out during transfer, others are mixed with later processes. Therefore, the absence of a trace is a property of the story itself, and not a defect of the detector.

For the scalar linear contribution to the temperature and E-polarization spectra, before lensing corrections, the relationship with the primary power is:

$$C_\ell^{XY} = 4\pi \int d\ln k\, \mathcal{P}_\zeta(k)\, \Delta_\ell^X(k) \Delta_\ell^Y(k), \qquad X, Y \in \{T, E\}.$$

Here T means temperature, E is the polarization component, and ℓ numbers the angular scales: larger ℓ correspond to smaller details. The spectra on the left side describe the power of these patterns and their mutual relationship. The Δ functions transfer the initial disturbances into the observed picture. The integral collects into one measurable number the contributions of many original scales. Therefore, the final set of measurements limits the raw spectrum, but does not reveal every detail of it: some changes cancel out after integration. The physical admissibility of two compensating spectra requires a separate proof - the mathematical possibility of compensation alone is not enough.

At the largest angles, cosmic variance is added. We have a limited number of single sky mods available; perfect elimination of noise does not create additional realizations of the same Universe. Polarization does add information, but the gain depends on the parameter and its correlation with

temperature. Therefore, an increase in the number of measured quantities does not mean an equal improvement in knowledge of the entire prehistory. [7]

Connections between different statistics help recovery, but they themselves need to be compared with competitors. In the chapter on the origin of the structure, we already encountered correlated features of power and bispectrum caused by changes in the speed of sound during inflation. They do not require a rebound. Such a combination would first indicate a certain type of early dynamics; a conclusion about a shrinking prehistory would require additional distinctions. [89]

The limit of knowledge here can be formulated precisely. If two models produce the same distribution of all observables available to us, processing the same data will not choose between them. The output may be a new observable that they predict differently, or an independently justified constraint on a class of models. A more detailed account of the hidden era does not in itself add information.

## How to check it

For a practical program, one fully specified rebound model and one specific non-rebound competitor should be selected. It is necessary to fix the law of gravity, fields, the initial state of disturbances and the transition to the hot stage. If the rebound precedes inflation, the overall calculation includes the dynamics of both stages and the duration of subsequent inflation: it determines what traces of history remain in the accessible range of scales. It is these models that are compared, and not the vague families “all beginnings” and “all cycles.”

First, the background dynamics and disturbances are integrated through the transition. The scalar power, tensor power, and bispectrum are then calculated from the matched action. The numerical solution is checked at known limiting modes, when changing the step and accuracy; the influence of disturbances on the background is assessed separately. If the calculation loses control precisely in the rebound region, it cannot be replaced by an arbitrary combination of two convenient solutions. The next result should then be proven transition dynamics.

The observational stage uses multi-frequency maps of temperature and polarization of the CMB. Scalar traces are checked in conjunction with available tensor component constraints. When connecting the galaxy distribution, the late gravitational bispectrum and object selection properties are calculated. The main competitors of the early feature are galactic radiation, calibration errors, random fluctuations and alternative early dynamics. Their parameters are evaluated together with the parameters of the history, and are not fixed in the most convenient values.

Before analyzing the real sky, artificial data are created for both models and the base smooth scenario. The entire search is repeated with the same masks, noises, and parameter ranges, measuring the frequency of the false rebound preference and the probability of detecting its trace. If the power-matching parameters inevitably require a detectable three-point signal, the absence of this signal precludes the corresponding implementation. You need to check the entire remaining valid range, not just one convenient point. If the difference is weaker than the overall uncertainty, both histories are preserved at the achieved accuracy.

A future installation should be designed for the specific difference that remains: the desired angular range, frequency purity, polarization accuracy, or number of available spatial modes. If the trace is beyond the causal boundary or is completely lost in the available distribution, reducing instrumental noise will not solve the problem. The next calculation is a map of distinguishability depending on the rebound parameters and the duration of subsequent inflation, with a re-evaluation of the remain-

ing parameters and interference. It will show where the trace has been preserved, but is still too weak, and where the selected observation channel no longer contains discriminating information.

**Chapter 14**

# Why does time have a direction?

A heated metal bar cools down in a colder room. Gas released from one half of the vessel fills the entire available volume. Light absorbed by the detector leaves a record that can then be read. These processes make it possible to distinguish the past from the future by their physical traces. Meanwhile, the equations of many mechanical models also allow an inverted sequence of movements. Why are inverse processes so unusual in the macroscopic world?

To pose the question, it is not necessary to consider all fundamental interactions as strictly symmetrical when reversing time. The difficulty already arises in those systems whose dynamics are reversible and whose behavior has a clear direction. Cosmology adds another problem to it: why did the early state of the world allow for a huge margin of subsequent irreversible changes? The answer depends on what kind of entropy we are discussing.

## Different states with the same macroscopic properties

Describing a gas by temperature, volume, and pressure leaves the positions and velocities of a huge number of molecules unspecified. One such macrostate—a state defined by collective measurable properties—is compatible with many different microstates. In statistical description, entropy is related to the size of this set. In the simplest Boltzmann notation:

$$S_{\mathrm{B}} = k_{\mathrm{B}} \ln \Omega.$$

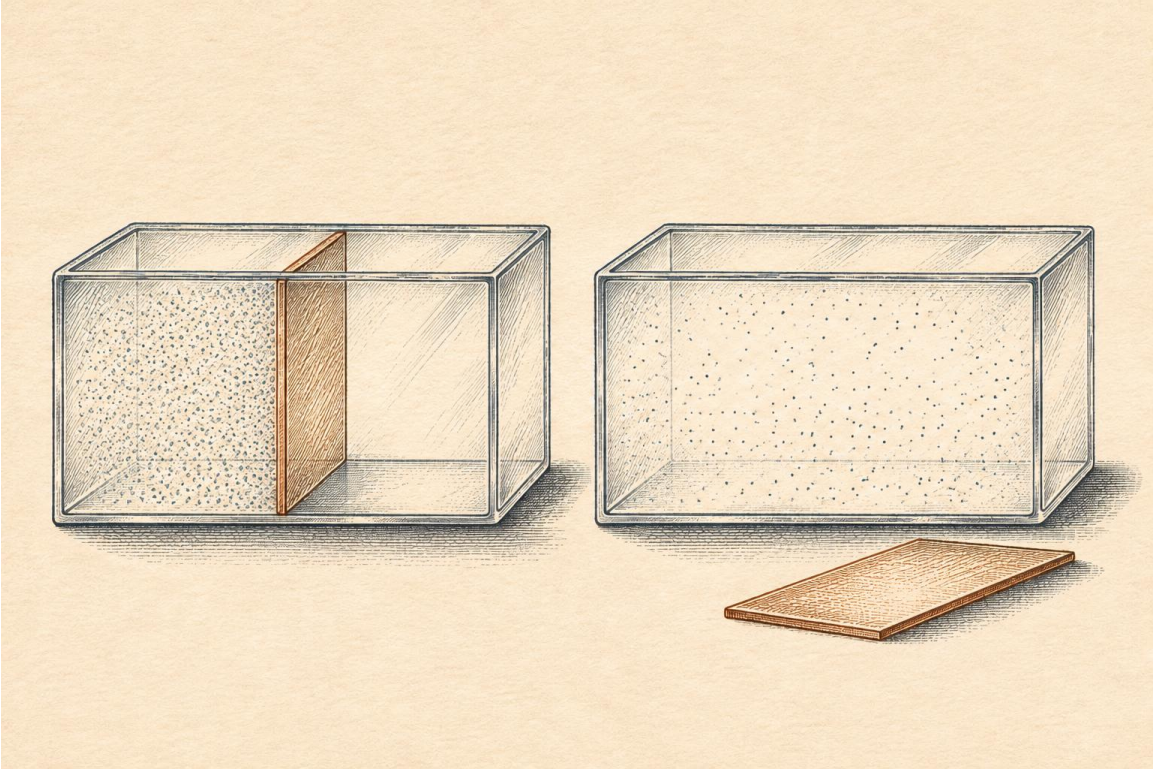
The quantity Ω denotes the number of microstates compatible with the selected macrostate, or the corresponding properly normalized volume in the state space. Boltzmann's constant converts logarithms into physical units. It is important what properties are fixed: energy, volume, number of particles and other restrictions determine what exactly is compared. The word “clutter” can serve as a household hint, but does not replace this definition.

Let an ideal gas be first contained by a partition in half of an insulated vessel. After its removal, the volume available to each molecule doubles. For N particles, the number of spatial variants increases by two to the power of N times, and the corresponding change in equilibrium entropy is equal to N Boltzmann constants times the logarithm of two. The effect is associated with the specific removal of the restriction. Gases don't have to look more chaotic for this calculation to make sense.

In this case, reversible microscopic movement does not have to destroy information about the original half of the vessel. They can be stored in complex correlations of coordinates and momenta that conventional pressure measurements cannot distinguish. If all the necessary movements and connections are reversed with incredible precision, the reverse process is permissible in the model under consideration. Typical macroscopic preparations do not provide such coordination. Therefore, practical irreversibility is compatible with the invertibility of the underlying equations.

However, the statistical argument has an initial condition: the gas was initially confined to half the container. If you choose the usual equilibrium state without special preparation, you will not get a story in which entropy increases noticeably all the time. Equilibrium fluctuations around typical values are expected. Therefore, explaining the tendency to move toward more probable macrostates and explaining the origin of a special initial macrostate are two related but separate problems.

This combination of microstates, which are not distinguished by the selected macroscopic quantities, is called coarsening of the description. The partition is chosen according to the interactions and observation time. Temperature is useful because many fast processes allow for a stable collective description. When conditions change, it is necessary to check whether its applicability remains. Particular care must be taken in transferring thermodynamic words from a gas in a vessel to the Universe as a whole.



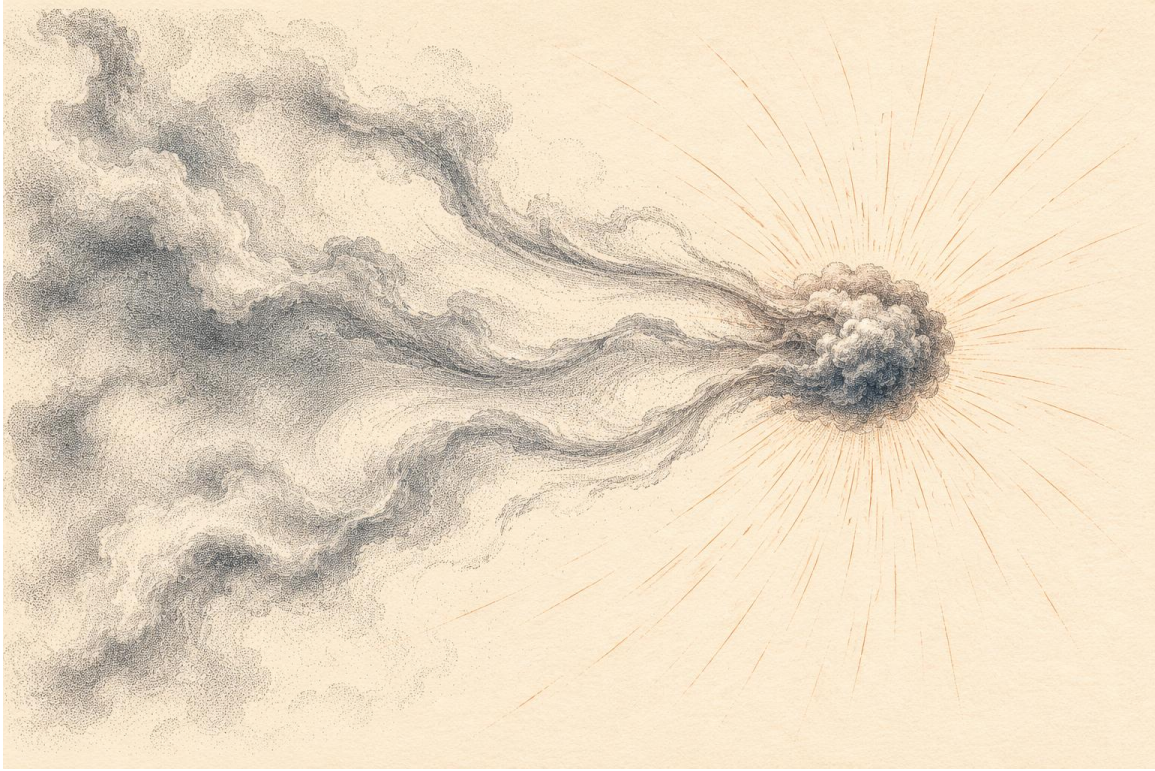
Engraving 17. Entropy and the removed constraint. The partition limits the available spatial states of the gas. After its removal, the number of valid options increases, although reversible microdynamics is not obliged to destroy information about the preparation. Molecules are shown as dots. The illustration refers to a gas in a container; transferring the same image to the Universe requires a separate definition of the system and restrictions.

## Why a hot start might be special

Early plasma was close to thermal equilibrium in many local processes. This can create the impression that it already had the highest possible entropy. But the local equilibrium of a certain set of particles is not equivalent to the equilibrium of the entire gravitating system. What matters is the spatial distribution of matter, geometry and degrees of freedom, which are not taken into account when describing a small area with a single thermometer.

Gravity has a peculiarity: a sufficiently large almost homogeneous system can evolve towards condensations, releasing energy. As the cloud contracts, the entropy of the matter itself may decrease, while the entrained radiation ensures an increase in the overall entropy. Therefore, a geometrically more assembled object is not necessarily a low-entropy outcome for the system together with its environment. It is fundamentally important to distinguish between the influence of gravity on the statistics of matter and the intrinsic degrees of freedom of the gravitational field. [106]

When they talk about the low initial entropy of the Universe, they mean the specialty of the early state relative to a wider set of permissible states and subsequent processes. Hot, nearly homogeneous matter could still form structures, release energy, and maintain large temperature differences. The number for the “entropy of everything” requires a definition of the system and a measure of comparison. There is no generally accepted universal formula that immediately assigns a single gravitational entropy to any cosmological space-time.



Engraving 18. Condensation of matter and outgoing energy. During gravitational compression, matter can be collected into a more compact structure, while simultaneously releasing energy to the environment. Therefore, the apparent orderliness of an object does not determine the entropy of the entire system. The engraving shows only this qualitative meaning; a universal measure of gravitational entropy for an arbitrary cosmological space-time is not assumed here.

Expansion itself is also not the definition of a thermodynamic arrow. During reversible expansion without heat exchange, the entropy of the selected comoving volume can be maintained, although its density and temperature decrease. In the compression model, irreversible processes can continue in the same direction of physical history. Changing the sign of H does not automatically turn heat flows back. It is up to the specific theory of states and transitions to reconcile the arrow with the rebound or cycle.

Inflationary smoothing is useful for explaining the properties of a particular area, but does not by itself establish the probability of its initial state. In reversible dynamics, the convergence of trajectories in a figure of several variables may be accompanied by the preservation of differences in other degrees of freedom. Carroll and Tam explored this problem through a measure of cosmological histories. Their reasoning emphasizes the dependence of the conclusions on the state space and the way it is measured; specific huge or small probabilities from such an analysis cannot be taken as the generally accepted probability of the birth of our Universe. [107]

A meaningful theory of initial conditions must tell what states are allowed, how they compare, and why the observed history receives the chosen weight. If low entropy is simply written into the boundary condition, this can be a fair and useful part of the model. But the explanation of its subsequent growth does not thereby become an explanation of the boundary condition itself. Promotion is possible when the latter receives additional physical motivation and distinct consequences.

## Decoherence and the direction of records

The quantum description adds another difference. The entropy of a complete closed state and the entropy of a selected subsystem refer to different objects. The density matrix ρ is a mathematical representation of a quantum state from which the probabilities of measurement results are derived. It allows you to describe both the entire system and its selected part. Von Neumann entropy is written through it as follows:

$$S_{\mathrm{vN}}(\rho) = -k_{\mathrm{B}}\,\mathrm{Tr}(\rho \ln \rho).$$

The symbol Tr means the sum of the diagonal elements of the matrix expression in parentheses. The usual evolution of a closed quantum system is reversible; it is called unitary. It preserves the eigenvalues of the density matrix, and hence the total entropy in this formula. The state of the subsystem is obtained by excluding environment variables from the description. Its entropy can increase when it becomes entangled with its surroundings, although the entropy of the whole remains the same. For an arbitrary system and an arbitrary initial state, such growth does not have to be monotonic.

A pure quantum state can be described by a single wave function; the mixed state of the selected system cannot be reduced to a single wave function. Moreover, purity does not mean low energy: a pure state can be highly excited. Measuring the power of disturbances does not reconstruct the entire density matrix. Therefore, excess small-scale power cannot automatically be called a measurement of excess initial entropy. To reach such a conclusion, the theory must relate the measured correlations to a specific definition of entropy.

Decoherence is the suppression of the observed interference between alternatives when they are connected with the environment. Different states leave different traces in the unobserved degrees of freedom. For an accessible subsystem, this can make the classical probabilistic description a good approximation. In Zurek's work, the interaction of the device with the environment determines which recording states are stable. Here the record means a physical correlation, such as the state of a measuring device, rather than the presence of any special observer. [108]

For early perturbations, decoherence helps explain why quantum statistics can be used as input to an approximately classical history. Computation begins with a given state and a specific interaction with the environment. It shows which correlations become inaccessible under the chosen description, and thereby explains part of the transition to the classical picture. The specialty of the initial state remains a separate condition for this calculation.

Nayeri's 2026 study examined the expanding and contracting semiclassical branches—roughly classical versions of cosmological history. In the adopted inflationary scheme, it is calculated how the differences in the associated environmental states suppress the interference between the branches. The author separates this process from the weights specified by the quantum boundary condition. The resulting arrow refers to a coarsened description within the branch and is based on a special initial

state. This is a quantitative result for given conditions, rather than an inference of low initial entropy from an arbitrary state. [109]

Verification of the cosmological proposal requires connecting these levels: the rule of initial conditions sets the statistics, the subsequent dynamics transfer it to the observed traces. The distinction between two boundary rules becomes available only where this transfer preserves the difference of signals. This is why a discussion of the arrow of time must lead us from general words about entropy to specific radiation that can be measured.

## Thermal history and access limits

Horizons develop their own thermodynamic structure. Gibbons and Hawking showed that in appropriate cosmological geometries with a positive cosmological constant, the horizon can be mapped to temperature and entropy, and the detector has a thermal response. This is a semiclassical result under certain conditions. It does not give the right to add up the entropy of the horizon, matter and entanglement as three obviously independent contributions without defining the system. [110]

The frequency spectrum of the CMB, discussed in the chapter on hot history, provides access to irreversible processes in the early plasma. The FIRAS measurements provide a reference test for its near-equilibrium form. Now the question can be narrowed down: what differences in the initial states could leave discernible traces in this spectrum? The observed quantity here is the frequency distribution of radiation energy. [111]

The energy of small-scale acoustic disturbances can be dissipated in the plasma and converted into heat. When the processes of restoring complete thermal equilibrium are no longer effective enough, such energy release leaves spectral distortions. They are usually described, in particular, by the μ and y components with different frequency shapes. At an earlier stage, a similar release of energy could only change the overall temperature, leaving almost no distinguishable remainder. Therefore, the spectrum explores a specific window of thermal history. [112]

Such measurements test the processes through which the selected initial state transferred energy from disturbances to radiation. A connection with the hypothesis of the origin of the arrow will appear if its boundary rule predicts the necessary amplitudes and shapes of disturbances. Without this, we are investigating the thermal history, but not yet testing the proposed explanation of the initial conditions. The next step is therefore to construct a limited example with a computable spectral trace.

## A map of the thermal imprint

Average spectral distortion tells you how much heat was retained in a particular history window. But the same average value does not require the same distribution of this trace across the sky. One might ask whether directions with slightly larger μ-distortion are related to large-scale temperature inhomogeneities in the CMB. This connection adds information about the ratio of long and short primary waves, which disappear with simple averaging of the spectrum.

The reason is that the μ-distortion from acoustic attenuation is related to the energy of small disturbances, that is, to a value quadratic in their amplitude. Temperature anisotropy also traces long waves. If the long wave modulates the power of the short ones, these two observed fields may be correlated. Payer and Zaldarriaga showed the relationship between μ–T and the primary bispectrum in a

highly elongated limit: one wave is long, the other two are short. This is an established theoretical proposal, not a new effect introduced by our book. [113]

Denoting the spherical harmonics of the distortion map by $\mu_{lm}$, and the temperature map by $a_{lm}^{T}$, we obtain the usual definition of the mutual angular spectrum:

$$C_\ell^{\mu T} = \frac{1}{2\ell+1} \sum_{m=-\ell}^{\ell} \left\langle \mu_{\ell m}\, a_{\ell m}^{T*} \right\rangle .$$

The angular index l determines the size of the pattern on the sky, the asterisk means complex conjugation, and the brackets indicate the average of the statistical ensemble. The actual estimator must additionally consider mask, noise, and angular mode mixing. A non-zero average μ does not by itself determine $C_l^{\mu T}$: two initial states can dissipate the same total energy and relate its spatial pattern to long waves differently.

Therefore, the previous project can be expanded with a certain pair of states. For the first one, almost Gaussian perturbations are specified; the second has a pre-selected weak pattern of communication between long and short waves. Their point-to-point power and average distortion are matched to a specified accuracy. The expected μ–T correlation is then derived from the full primary bispectrum and transfer. The coupling must have a finite number of fixed parameters and maintain the controllability of perturbation theory. Randomly drawing a correlation after viewing the data does not check the initial rule.

A simple artificial example is useful to test the computational chain. Let's take independent Gaussian long and short fields. In one case, we leave the short field unchanged; in the second, we multiply its amplitude by a value that weakly depends on the long field, and again normalize its average power. These two constructions can retain the same dispersion of short waves, but obtain different correlations of their local energy with the long wave. This explains why the equality of average spectral distortions does not close the question of spatial connection.

This construction serves as a controlled input to the program, rather than a replacement for the physical model of the initial state. First, the code should restore the specified connection in the ideal case and not create it when modulation is disabled. Then thermal transfer, angular resolution limitations, and real-world noise are introduced. For scientific inference, the artificial input is replaced by a bispectrum obtained from the selected dynamics and the initial rule; the correspondence between power and average μ is checked again with the same accuracy.

This proposal specifies a computable problem, but does not yet select a physical origin for the arrow of time. To obtain such a connection, the initial condition rule from the corresponding hypothesis must actually produce the chosen pattern. While this conclusion is not available, the distinguishability of statistical states is investigated. A positive result will show which properties are accessible to radiation; it will not measure the total entropy of the Universe and will not prove the uniqueness of its boundary condition.

The main experimental danger is the leakage of ordinary temperature anisotropy into the reconstructed μ map. Then its correlation with temperature contains a spurious contribution from a much stronger temperature field. Remazei and Hluba investigated component separation with explicit suppression of such leakage and showed the essential role of foregrounds in predictions. What is needed is a multi-frequency map, not just an accurate measurement of one average spectrum. [114]

One can also calculate the correlation of μ with the E-component of polarization. Its diagnostic capabilities were studied by Remazei, Ravenni and Hluba. However, the presence of a second plot does not automatically make the test independent: the temperature leakage in the μ map is correlated with E via the normal TE spectrum, and the frequency calibration and part of the foregrounds may be common. The benefit of the incremental channel must be assessed through joint covariance and realistic simulations of the entire processing. [115]

There are also physical alternatives: non-uniform energy release can generate its own spatial pattern of distortions. Therefore, competing late contributions and known carryover effects should be calculated separately for the selected primary template. The simple requirement that “correlation must be zero” is too crude. The specific amplitude and angular dependence of the additional component are checked after switching on the required base signal.

## How to check it

For a limited design, we can compare two specified initial states with the same dynamics: a basic one, giving a smooth spectrum, and a state with additional excitation in a predetermined small-scale band. These are not two ready-made theories of the arrow of time. This is a test of a specific consequence of the initial conditions. The amplitude, center scale, and bandwidth must follow from the selected state rule or have a predetermined range; The fit of the large-scale anisotropy model is checked simultaneously.

First, they calculate when and at what speed the energy of these disturbances is dissipated, then the final frequency spectrum, taking into account thermal processes. The basic forecast already includes standard sources of distortion: the additional contribution is checked, and not the absence of any deviation from the ideal black body. Different histories of energy release can give a similar final spectrum. Therefore, before designing observations, it is necessary to calculate which shape details actually distinguish between the selected states and competing energy sources.

The measuring circuit with an absolute spectrometer and a thermal standard is described in the chapter on hot history. For the current problem, the difference in initial states is translated into the difference in the signals of each frequency channel. The radiation temperature, calibration, and astrophysical components are then refitted in both models. The remaining difference is compared with the joint error matrix of the channels, which takes into account their total errors. This determines the required accuracy: similar primary states can become almost identical for the device after thermal transfer and noise adjustment.

The most dangerous are reference errors, temperature drift, frequency response inaccuracy and residual astrophysical radiation. In laboratory tests, it is necessary to check the response to small known differences in the spectra, and to introduce model signals along with noise into artificial data. Comparisons are made with alternative sources of energy release, including particle decay and gas heating. The set of frequencies and precision are chosen so that the residual difference after this assessment is not absorbed by the calibration.

If the chosen initial state inevitably produces distortion available to the device, the reliable absence of such a contribution limits its parameters. Detection requires testing the frequency form and competing processes; it does not determine the complete quantum purity of the early Universe. The closest calculation is a map of the probability of detecting additional excitation depending on its amplitude, central scale and width, after taking into account interference and thermal erasure. The false

detection threshold is set before the search. Such a map will allow you to select channel sensitivity and indicate where the spectral measurement will require another independent observable trace.

To expand the project spatially, a second, separate result is needed: a map of the distinguishability of two states with similar average distortions. After calculating μ–T, multi-frequency artificial maps are created, temperature leakage, calibration uncertainty and foregrounds are added, then the correlation is restored using the same algorithm that will be used on the data. Changing the frequency set and mask should not create the desired effect. If the observable correlation required for a fixed nonzero version of a state is not present at the sensitivity tested, that version fails the test. If both versions remain indistinguishable, the result sets the limit of a given observation channel and the requirements for an additional measurement.

**IV Underlying Structure**

**Chapter 15**

# What is the “where” made of?

The room seems to be the most reliable example of space. You can point to the door, measure the distance to the window, walk between the table and the wall. In such an experience, objects change position, but the “where” itself remains a ready-made container. Even when imagining empty space, we usually keep this room, just remove the furniture from it. But a physical theory does not have to start from an already built room. It may pose a more difficult question: what relationships make it possible to determine proximity, distance and direction in the first place?

In the previous chapter we asked why events develop into history with a certain direction in time. Geometry was already included in the description. Now the question changes: what makes it possible to attribute distances and proximity to events at all? The measured distances remain the original data; What remains to be explained is the stability of the very language in which they are written.

## From address to geometry

Three spatial dimensions mean that the local position of an event at a selected moment requires three independent coordinates. The coordinates can be changed: replace the Cartesian grid with a spherical one, select a different reference point. This does not increase the number of independent directions. In the theory of relativity, time coordinates are added to spatial coordinates, but time has a special role in the causal structure. Four-dimensional space-time cannot, without explanation, be depicted as a room with one more ordinary direction of motion.

The dimension of state space has a completely different meaning. To indicate the positions of two particles in ordinary space, six numbers are needed. If you also need to know their momenta, the number of parameters will double. The twelve directions available to man do not arise from this. We expanded the description of the system, rather than discovering new aspects of the room. Hilbert space is a mathematical space in which quantum states are written. Its dimension characterizes the possibilities of such a description and does not in itself tell anything about the number of spatial directions.

And the coordinates are not enough to define the geometry. The same difference in numbers on two parts of the map can correspond to different physical distances. We need rules that translate coordinate differences into readings of rulers and clocks—a metric. In general relativity, it is involved in dynamics: the distribution of energy affects geometry, and geometry affects the movement of matter and light. Already here the space ceases to be a motionless decoration. But geometric quantities are still included in the original language of the theory.

The emerging geometry means a stronger possibility. The initial variables of a certain theory may not describe points in familiar space, and smooth geometry appears only for certain states and scales. The analogy of temperature is useful. A molecule does not need its own temperature for a set of molecules to be thermodynamically described. The analogy shows the logical possibility of changing language, but does not establish what space is made of. Microscopic variables and the transition to geometry have yet to be presented.

Here the word "arises" does not necessarily mean an event in time. If large-scale language is derived from deeper language, it may be about the relationship between descriptions. We are not obliged to imagine an earlier era when the original elements were already waiting and the space had not yet come together. To talk about successive epochs, you first need to determine what variable is measuring the sequence. The question of the origin of time is therefore more difficult than simply replacing a three-dimensional picture with a multi-dimensional one.

## Description of the volume at the boundary

A concrete example of such a change in language is provided by holographic duality. In Juan Maldacena's proposal, certain quantum field theories are associated with theories containing gravity in anti-de Sitter space. The meaning of duality is the ability to translate physical states and observables between two descriptions. One uses bulk geometry and gravity, the other is structured as a theory without dynamic gravity on a lower-dimensional boundary. [116]

The “boundary” here is the mathematical part of a given structure. It is not glass that a spaceship can rest against, and it does not require placing the entire system inside another room. The word "holography" indicates the relationship of descriptions, but the usual optical hologram remains only an analogy. In it, light restores the image of an object; in duality, the correspondence of the complete physical dynamics in a certain model is discussed.

To appreciate the power of the idea, consider a problem involving difficult quantum interactions. In one language it is almost intractable, while in another a particular regime corresponds to relatively simple geometry. Translating between them makes previously inaccessible quantities calculable. The duality dictionary specifies which state and measurement on one side correspond to a state and measurement on the other. What is tested is the consistency of the predictions; asking which language is “real” does not, by itself, define a new experiment.

The anti-de Sitter geometry is significant. It has special asymptotic properties and is associated with a negative cosmological constant. The observed history of our Universe includes expansion and late acceleration; it cannot simply be renamed to the original AdS construct. In his research essay 2025, Tadashi Takayanagi explicitly identifies the transfer of holography to realistic cosmological spaces and the understanding of the emergence of time as open problems. This is a program guideline, and not an announcement of a completed model of our cosmos. [117]

The transfer to cosmology will require determining the initial variables, state and dynamics, and then reconstructing the expansion and observed perturbations. The similarity of geometric images is not enough for this. The next step is especially important: to obtain several related predictions from one design, so that its parameters cannot be independently reconfigured for each observation.

## Geometry in quantum connections

One of the most precise bridges between the two languages connects quantum entanglement with geometric area. An entangled joint state cannot be imagined even as a statistical mixture of products of the states of its parts. If the complete state is pure, the entropy of the selected part characterizes its entanglement with the rest. For a mixed complete state, the same entropy includes other sources of uncertainty. Ryu and Takayanagi proposed calculating the entropy of a region through the surface area in a gravitational description. In a suitable static formulation, the leading result has the form: [118]

$$S(A) = \frac{\text{Area}(\gamma_A)}{4G_N}$$

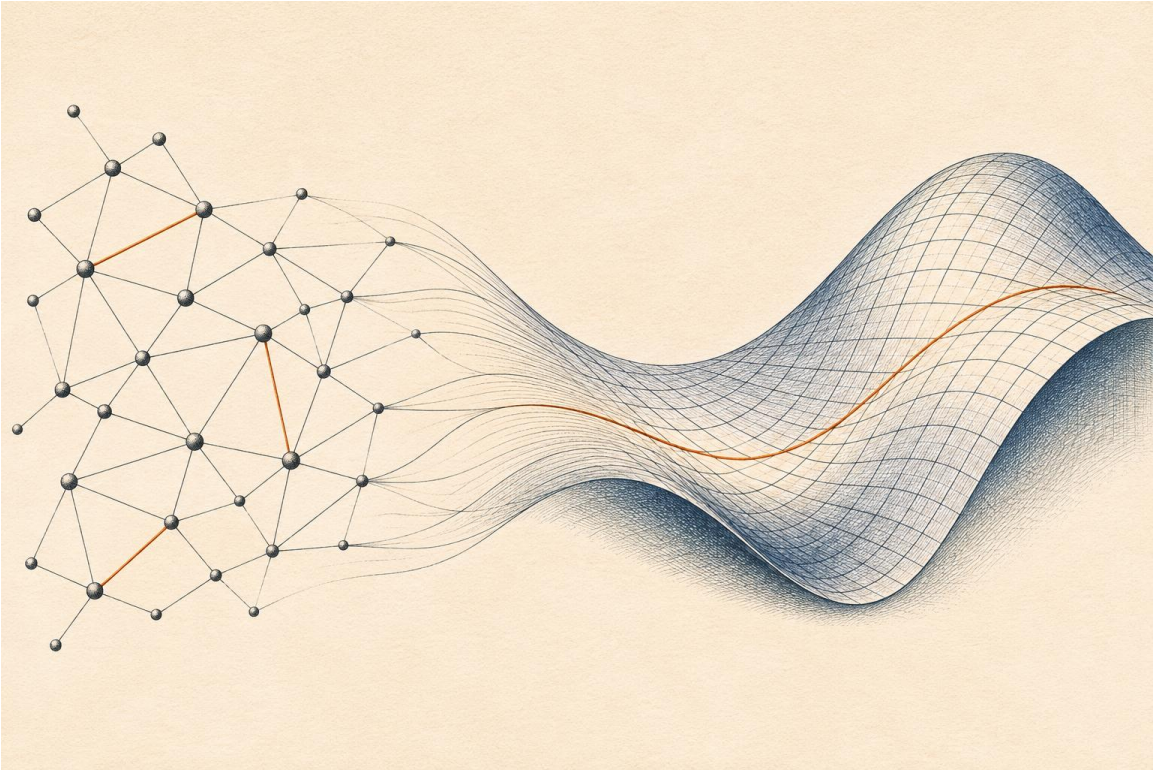
Here the speed of light, Planck's constant and Boltzmann's constant are taken to be equal to unity. A is the area of the boundary system. The surface $\gamma_A$ lies in the volume, ends at the edge A and has the minimum area among the surfaces that satisfy the required boundary and topological conditions. $G_N$ refers to the gravitational description of volume. Therefore, the numerator is not the area of the region A itself. We select a subsystem on one side of the correspondence and look for a geometric object on the other. Quantum corrections and non-stationary formulations require a generalization of this formula.

The connection between quantities is remarkable: the characteristic of a quantum state becomes a geometric object. Mark Van Raamsdonck's work explores how changes in entanglement between parts of the corresponding system are associated with changes in the connectivity of volumetric geometry. In the structures under consideration, the weakening of certain quantum connections is accompanied by the separation of geometric regions. This is an argument for the ability to recover spatial relationships from state structure. [119]

However, the statement “more entanglement - less distance” would be too rough a universal rule. Quantum states have many different correlations; Entropy alone does not determine all geometry, much less all dynamics. You need to know which subsystems are identified, which operators they correspond to, and for which family of states there is a smooth volumetric description. An arbitrary network of connected qubits does not yet become a small spatial Universe.

It is convenient to imagine the reconstruction of a map based on a set of measurements. Multiple distances between cities may allow for different locations; additional measurements eliminate some of the ambiguities. In the holographic problem, the role of the initial data is played by certain quantum characteristics, but the problem of compatibility remains. The resulting geometry must explain several observables at once. If you have to draw your own map for each correlation, there is no unified physical reconstruction.

The space reconstruction program must explain why certain quantum states allow stable distances, while others may not have a smooth geometric pattern at all. The test is the agreement of different methods to reconstruct the same geometry. This is a much more specific task than declaring any quantum state a “space of information.”



Engraving 19. From quantum connections to geometric description. In certain holographic designs, the quantum characteristics of the state are associated with geometric quantities. The transition from a network of connections to a smooth surface is an artistic analogy for a change in description. An arbitrary network of qubits does not automatically become a space: given dynamics, a correspondence dictionary, and the agreement of several ways to reconstruct one geometry are required.

## Evaporation and entropy of the subsystem

A black hole connects geometry with quantum information in a particularly tight way. Hawking's semiclassical calculation predicts the emission of quantum fields against the background of a black hole. If the flow carries away energy, the geometry parameters must change. At the same time, the thermality of an individual observed flow does not yet determine all the correlations of the complete state. It is the question of such correlations that makes evaporation a test of the consistency of quantum and geometric descriptions. [120]

Let's start with a purely quantum fact. If a closed system is in a pure state and is divided into two parts, their von Neumann entropies are equal. When one part is reduced, it cannot store arbitrarily more entanglement with the other: its capabilities are limited by the dimension of the state space. Don Page's work on typical pure states provides a quantitative basis for this assessment. This is a discussion about subsystems; it does not in itself determine the dynamics of a real black hole. [121]

It is also necessary to distinguish between two types of entropy. Thermodynamic entropy describes a variety of microstates consistent with the rough description. The exact entropy of a chosen quantum subsystem depends on its correlations with the rest. Therefore, reducing the second does not require negative heat production or violation of the usual law for the selected macroscopic process. Before drawing the “Page curve”, it is necessary to indicate which system has been identified and what entropy is being calculated.

The holographic approach uses generalized entropy: the gravitational contribution of the surface plus the entropy of quantum fields on the corresponding side. Engelhardt and Wall proposed to look for a quantum extremal surface that is stationary for this sum. First, admissible extrema with the required homology conditions are found; then the appropriate extremum with the lowest generalized entropy is selected. This is not minimization over any arbitrarily drawn surfaces. [122]

Let us choose a specific model by Almheiri, Engelhardt, Marolf and Maxfield: two-dimensional Jackiw-Teitelboim gravity with dilaton, associated with a conformal field in 1+1 dimensions. The initial two-sided black hole has two boundary quantum systems L and R; The auxiliary non-gravity bath B is initially in the ground state. The connection between R and B is turned on. We study the entropy of R with respect to the complement L∪B. This is significant: by definition, it is not equal to the entropy of the bath alone. [123]

For the dilaton normalization adopted in this work, candidate X has the generalized entropy:

$$S_{\mathrm{gen}}(X) = \frac{\phi_0 + \phi(X)}{4G_2} + S_{\mathrm{CFT}}(\Sigma_{RX}), \qquad \delta_X S_{\mathrm{gen}} = 0.$$

The units used here are $\hbar$=c=kB=1. The region ΣRX passes between X and the corresponding boundary point. The constant $\varphi_0$ specifies the topological contribution. The "area" in this two-dimensional description is represented by the dilaton; it cannot be read as the ordinary area of a two-dimensional surface. In the published calculation, the transition between branches of quantum extremal surfaces gives an increase, and later a decrease in the selected entropy after the initial transient processes. The authors separately emphasize: this is not a derivation of all the necessary radiation correlations and not a complete solution to the information problem. [123]

Penington's independent work also showed the essential role of quantum extremal surface changes in the description of an evaporating black hole and information recovery. The similarity of the results supports the study of this geometric instrument. However, the geometric procedure and the microscopic information recovery mechanism remain different levels of description; the agreement between them must be checked for a given model. [124]

The definition of a subsystem implies an important limitation of our illustration. You cannot replace R with B in the middle of the calculation, keeping the same curve by name. With this replacement, the reduced density matrix and the surface problem change. It is also impossible to demand that the shown entropy necessarily tend to zero: the initial correlations with the left system and the presence of a residual sector must be taken into account. This is checked by the formulation, even before the numerical solution of the equations.

To continue the research, we propose a very specific computational task. In the selected JT model, the temperature of the initial state, the central charge of the field, dilaton parameters and the protocol for turning on communication with the bath are fixed. Then the solutions for the geometry and the field are reproduced, and at each moment in time all admissible stationary points Sgen are independently searched. The program must preserve both dominant and non-dominant branches. Otherwise, a search started from one approach may miss the transition itself.

The next control is sensitivity to clipping and area of applicability. Short-wavelength contributions to field entropy and gravitational parameters must be reconciled in one procedure. It is verified that changing the computational resolution does not move the transition more than the stated error. The rate at which the connection is turned on is then varied: the physical transition is decoupled from

the brief state preparation effect. For each graph, a list of prerequisites is stored under which the semiclassical description is still reliable.

A stronger validation would require an independent microscopic characterization of the same model or a controlled analogue. In it, the entropy of a selected subsystem can be calculated directly from the density matrix and compared with a geometric forecast. The coincidence of one drawn curve is not enough: the same initial conditions, interactions and a rule for selecting a subsystem are needed. An experimental simulation would test this particular relationship of descriptions. It does not by itself turn the device into an astrophysical black hole.

For cosmology, the value of such a project lies in the method. The geometric boundary, the quantum subsystem, and the available information can be linked more precisely than the image of the finished room suggests. But transferring the result to the cosmological horizon requires redefining the state, boundaries and observer; the external bath does not appear there automatically. This book contains a statement of the following work. An independent calculation of the Page curve or an experiment to measure it was not performed here.

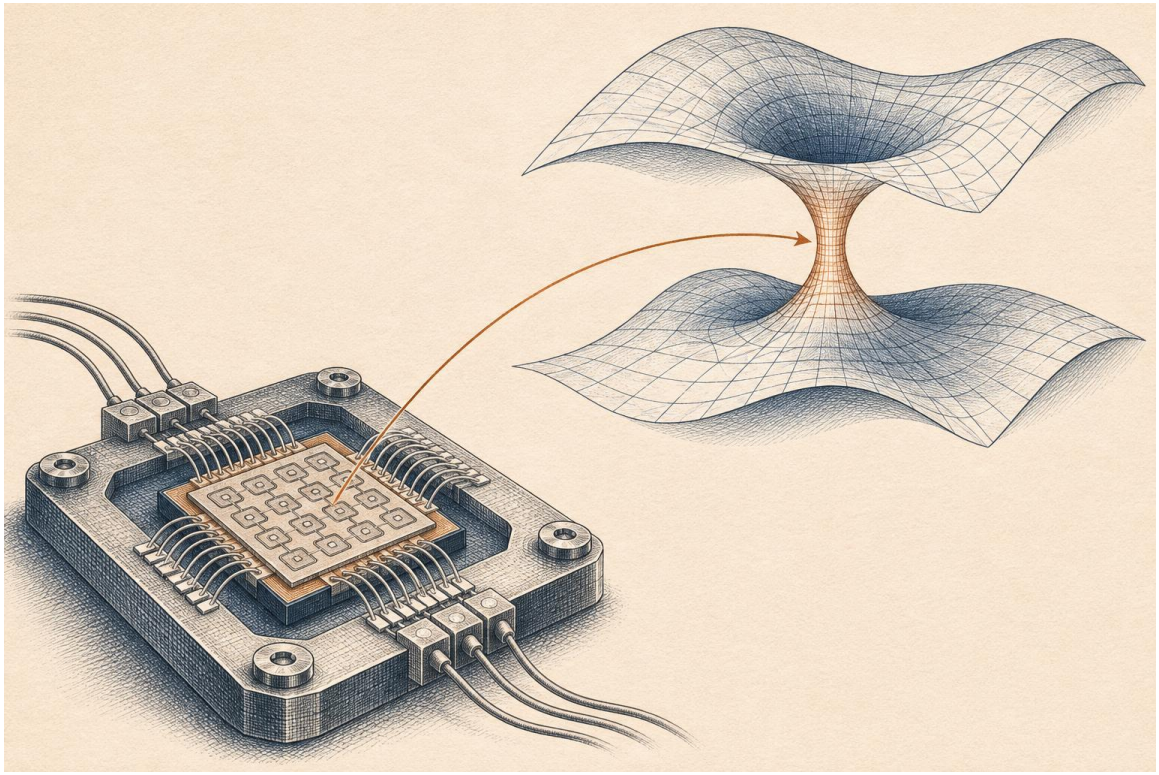
## Wormhole in the description of the experiment

In 2022, the work of Jafferis et al. was titled “Dynamics of a Traversable Wormhole on a Quantum Processor.” The experiment implemented a specially chosen quantum model and investigated the transfer of information in a protocol for which a gravitational interpretation was proposed. Quantum degrees of freedom were controlled on the processor. A spatial tunnel was not created between remote areas of the laboratory. [125]

The difference is significant: calculating fluid flow on an electronic device does not force water to flow through transistors. A quantum simulation can reproduce dynamics that are difficult to calculate classically, but moving to a geometric interpretation still requires a vocabulary of duality. It is this dictionary that defines what a laboratory result means in a gravitational description.

In July 2025, Nature published the critical work of Kobrin, Shuster and Yao and the response of the authors of the experiment. It was discussed which features of gravitational dynamics are actually preserved in a small, specially selected model and how stable they are when the operators being tested change. For the book, the very content of the disagreement is essential: the coincidence of the selected feature does not guarantee the reproduction of the entire physical mechanism. [126] [127]

The simulator allows control of the state and interactions, followed by changes to conditions that were not used in fitting the model. This creates a meaningful test: will the connection between the two descriptions hold for new measurements? Successfully tuning the selected process becomes the starting point for that experiment.



Engraving 20. Quantum simulator and geometric interpretation. The quantum processor allows you to prepare the state, control interactions and measure correlations. Geometric picture refers to the interpretation of the dynamics of a certain model. The device and its conventional mathematical representation are shown separately: the experiment does not create a spatial tunnel in the laboratory. The test is strengthened by new measurements not used in setting up the model.

## How to check it

For emergent geometry, you should start with a problem in which both sides of the correspondence are specified explicitly. We need a Hamiltonian—an energy operator that determines quantum evolution—a method for preparing the state, and a rule for converting observables. The connections between measurement results in different parts of the system or at different moments are described by correlation functions. They record in advance which of them are used when selecting a model, and which will remain testing. This way the geometric dictionary is able to predict data that has not yet been used.

The physical setup can be a quantum simulator with reproducible operations and reading correlations. The small system is first checked against a direct numerical solution. The degrees of freedom, interactions, and local perturbations are then varied, testing the predicted response times and correlations. If entropy is reconstructed from measurements, the errors in this reconstruction are also included in the comparison. The size dependence is significant: the pattern of several qubits may change before a smooth geometry regime appears. Therefore, we need to calculate how the verification effect should change as the system increases. The validation set includes new evolution times, not just new measurements at a single selected moment.

Test models without an accepted geometric interpretation must reproduce the features used in tuning and then compete on the validation data. This allows us to find out how distinctive the new feature is. Preparation, reading and control errors are included in both models in the same way.

Independent calibration of the device helps to separate the loss of the dynamics under study from the loss of sensitivity to its manifestation.

A positive result will support the specific match in the verified mode. A negative one will indicate an error in the chosen implementation, reconstruction, or stability assumption. In both cases, the conclusion refers to the quantum model examined. To make a statement about the structure of our cosmos, a separate physical bridge is needed.

The nearest necessary calculation is the prediction of test correlators with errors, dependence on the size of the system and pre-selected non-holographic competitors. The next, separate step towards cosmology requires the derivation of a measurable cosmic effect from the same construct: for example, a certain form of primary correlations with fixed parameter connections. Until such a bridge is built, we are checking the design of the model. This is enough for serious physics, if its result is named accurately.

Chapter 16

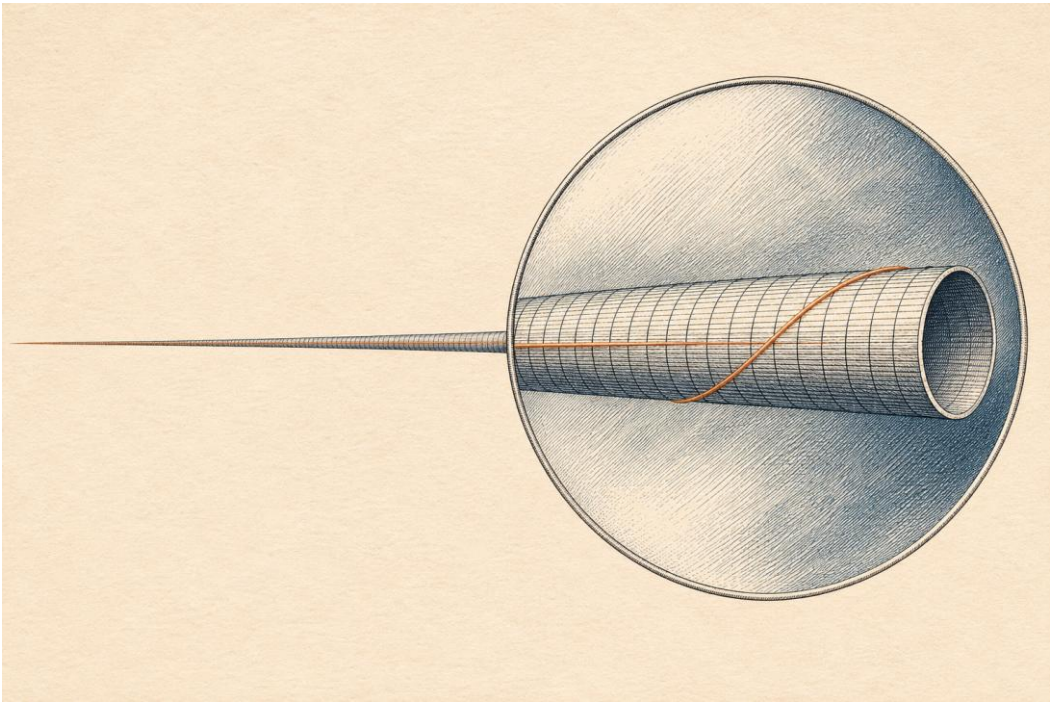
# Additional dimensions

An additional dimension is difficult to imagine precisely because we habitually try to place it next to already known directions. I want to turn my head and see another side of the world. But the physical hypothesis may be much less spectacular. A new direction can be detected as a subtle change in force, a certain sequence of particle masses, or a loss of energy in the stellar core. Geometry leaves traces in dynamics, even if it cannot be directly drawn.

After the chapter on emerging geometry, it is important to change the setting: now we will talk about additional physical directions, and not about the dimension of the space of quantum states. We will choose one simple example and trace its consequences from geometry to laboratory, accelerator and stellar core.

## Where did another direction go?

Let's imagine the surface of a very thin cylinder. For a creature capable of discerning its circumference, there are two directions: along the cylinder and around it. To an observer whose measurements are much coarser than the radius, the surface appears almost as a line. The second direction has not disappeared here. Sensitivity to movement on it has disappeared. This is a mental example of how the number of salient spatial directions can depend on the resolution of the experiment.



Engraving 21. Direction hidden by resolution. A thin cylinder serves as an analogy for a hidden direction: with coarse resolution, movement along it is discernible, and with a more detailed examination, also around it. The figure explains the dependence of the available description on the scale of measurement. It does not depict a proven arrangement of extra dimensions and does not require external space for their existence.

The compact dimension is designed according to a similar mathematical principle: movement along it can return you to the starting point. In this case, a cylindrical picture is not necessary. A

compact space is defined by its own distances and identifications; it does not require an external area in which its bend can be seen. Greater energy is needed not because the hidden door is locked, but because excitations along a small direction have a certain energy price.

In the Arkani-Hamed, Dimopoulos and Dvali scenario, usually abbreviated to ADD, conventional matter fields are localized on the brane, and gravitational degrees of freedom also extend in additional directions. The brane here denotes the lower-dimensional physical structure given by the model. This field distribution has been proposed to explain the large differences between the observed gravitational force and the scales of other interactions. [128]

This premise also answers the obvious question: why don't we go to extra dimensions? If the particles that make us up are localized, conventional bodies do not have arbitrary freedom of movement in the full space of the model. But the word "localized" must correspond to the mechanism. It is necessary to explain how the fields are contained, what excitations are allowed, and at what energies the approximation stops working. The name brane itself does not do this job.

Other designs are possible, including curved additional directions. They cannot be mixed in one forecast. The spectrum, particle coupling, and force variation depend on the geometry and boundary conditions. By choosing flat, compact directions, we make a specific commitment to data. The transition to another geometry is permissible, but along with it it is necessary to recalculate the observed consequences.

## A shared radius and its consequences

Let's take two additional spatial directions, each with a period $2\pi R$, and the same radius R. They form a square two-dimensional torus. Together with the three ordinary spatial directions and time, these are the six dimensions of space-time. The torus here refers only to the hidden part of geometry; the question of the closedness of the entire observed three-dimensional space will be a separate topic in the next chapter.

A wave traveling in a compact direction must agree with itself after a complete detour. Therefore, the allowed pulses form a discrete set. The energy of hidden motion is conserved even when the observer describes only ordinary coordinates; for him, it enters into the rest energy of the particle. This is how Kaluza–Klein modes arise—states with different four-dimensional masses. For an initially massless six-dimensional field and a selected torus in units $\hbar=c=1$:

$$m_{k_1,k_2}^2 = \frac{k_1^2 + k_2^2}{R^2}, \qquad k_1, k_2 \in \mathbb{Z}.$$

The zero mode corresponds to the absence of momentum in hidden directions. The first excitations have masses connected by an integer lattice. Levels can have the same mass: movements in opposite directions and along different axes give multiplicities. By decreasing the radius, we simultaneously increase the entire spectrum. It is impossible to independently choose a convenient radius for the laboratory force and a different first-mode mass for astrophysics while maintaining the same model.

The connection between gravitational scales arises from the same reduction of the theory to ordinary coordinates. Integration over two hidden directions gives a multiplier equal to their total volume. Let us denote the reduced four-dimensional Planck mass by $\bar{M}_{Pl}$, and set the coefficient of the

six-dimensional gravitational action by the mass $\bar{M}_6$. For this chapter, we also define $M_D=\sqrt{(2\pi)}\bar{M}_6$. Then:

$$\bar{M}_{\mathrm{Pl}}^2 = (2\pi R)^2 \bar{M}_6^4 = R^2 M_D^4.$$

This definition of $M_D$ must be remembered when reading other people's restrictions: different papers use different conventions about the factors 2π and the reduced Planck mass. Physics doesn't change, but the number in teraelectronvolts does. It is more reliable to first compare the radius, masses of states and magnitudes of bonds, and then convert the result to the chosen normalization. It is these parameters that are included in the measured process speeds.

At distances greater than R, ordinary long-range gravity predominates. Massive modes add rapidly decaying contributions. The easiest level might look like a Yukawa correction: an exponentially decaying addition to the Newtonian potential with a range inversely proportional to mass. Its strength is related to the multiplicity of the level and its interaction with the substance. When approaching the R scale, the following levels are significant. The full profile also depends on the spin and scalar degrees of freedom, so a freely chosen exponential is usually not enough for it.

There is a real example of such a measurement. In the experiment of Li et al., a stationary torsion detector interacted with a rotating attractor; the distances between them varied from 52 micrometers to 3 millimeters. The data was well described by Newtonian gravity. The micrometer limit 38.6 given by the authors with a confidence of 95 percent refers to the range of the Yukawa interaction with the gravitational relative force. It is not a universal limit of any compact radius. [129]

## Testing the illustrative ten-teraelectronvolt case

Let us substitute $M_D$=10 TeV and $\bar{M}_{Pl}=2.435\times10^{18}$ GeV into our normalization. The result will be R≈4.805 micrometer. The rest energy of the lightest non-zero mode, equal to ħc/R, will be about 0.041 eV. The difference in scales is huge, but there is no contradiction: ten teraelectronvolts characterize the coefficient of gravitational interaction in the selected record, and hundredths of an electronvolt characterize the spectrum step determined by the large compact radius.

This point is useful as a calculation example. It would be a mistake to immediately call it allowed by nature. At an accelerator, the creation of undetectable KK states can manifest itself as a missing transverse momentum along with a visible jet. A similar ATLAS search found no significant deviation from expected background processes. The translation of the result into the $M_D$ limit depends on the number of extra dimensions and the scope of applicability of the effective calculation. [130]

Different searches test different variations of ADD. For example, the CMS monophoton analysis published in 2026 looked at three to six additional dimensions. Its result cannot be directly written as a new limit for our two-dimensional hidden torus: the spectral density and predicted rates of processes change. [131]

A star can provide an even more sensitive test. Each individual KK mode interacts weakly, but many modes are accessible to the hot core, and their contributions to the energy loss add up. If they leave the core, the cooling changes. Hardy, Sokolov and Stubbs recalculated such processes by including additional channels for the production of KK gravitons. For two approximately equal toroidal dimensions, their conservative estimate from the supernova SN 1987A requires a first KK mass scale of approximately at least 0.6 eV. The limit depends on the properties of the hot substance and the conditions for energy loss. [132]

In the same conventions, this means R is approximately no more than 0.329 micrometer, and our $M_D$ is approximately no less than 38.2 TeV. These two numbers are derived from a translation of the original astrophysical estimate, rather than from a new analysis of observations. Therefore, the notional point 10 TeV fails this test where its premises apply. A possible future installation capable of measuring force at only a few microns does not automatically receive a new free search area for this particular minimal model.

Other restrictions use the capture of KK states and heating of neutron stars by their decay products. Stronger limits here require additional assumptions about lifetimes and decay channels. For the analysis of Hannestad and Raffelt, the author's corrected version is essential. Changing decays can weaken this channel while maintaining the cooling limitation; both processes need to be recalculated in one model. [133]

## Why the radius need not be fixed

Until now, R looked like a constant value printed in the problem statement. In a full-fledged multidimensional theory, the dimensions and shape of compact geometry can correspond to dynamical fields—moduli. Then you need to explain why the radius is kept around the selected value. If the corresponding field is light enough and connected to ordinary matter, it can create additional force. Geometry stabilization becomes part of the observational model rather than a technical note.

Therefore, the potential of the moduli, their masses and connections, excitation history and cosmological influence must be added to the KK spectrum. The ADD and Dark Dimension stabilization work propose concrete designs, but issues of scalar forces, moduli population, and correction control remain part of their validation. The phrase “extra scalars are suppressed” should be the result of the calculation, and not its replacement. [134]

Here there is a connection with the chapter 8. In the direction of Dark Dimension, they are trying to connect small dark energy with a tower of light states and one relatively large additional dimension. This connection is based on additional theoretical hypotheses. The evolving radius may link cosmological dynamics to changes in dark sector masses. But one radius and two equal radii are different models with different densities of available states. Our numerical constraint for n=2 cannot be transferred to n=1. [135] [63]

The strength of this approach is the coherence of the consequences. One radius defines the spectrum, which is involved in the laboratory force and in stellar cooling. An independent change in the spectrum for each experiment would destroy precisely this testable connection.

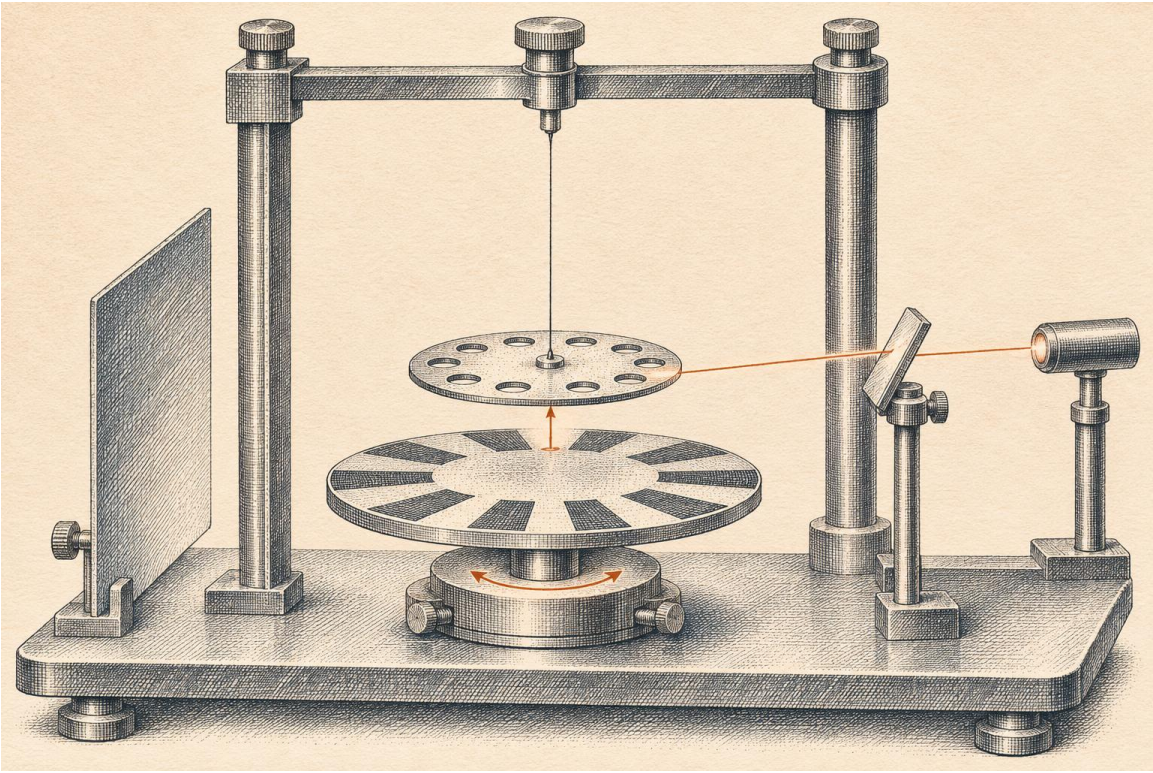
## How to check it

The object being tested should be completely defined: two equal compact radii, localization of the substance, spectrum of KK states, their connections and stabilization sector. First, a parameter range compatible with the chosen astrophysical and accelerator constraints is calculated. For each restriction, the conditions of applicability are written down separately. Thus, it becomes clear which area the laboratory can really further explore, and which can no longer be represented as free without changing the physical model.

Laboratory experiments use a torsion or micromechanical detector and an attractor of a known shape. The calculation of interaction is integrated according to the real densities of the bodies, taking

into account thickness, holes, gap and inclination. When the attractor rotates, its pattern sets the frequency of force changes; the amplitude and phase of the corresponding response can be compared. The mechanical response of the detector is then taken into account. This turns the spectrum prediction into a specific instrument signal that can be correlated across multiple distances and configurations.

Main competitors include electrical surface inhomogeneities, residual charges, magnetic moments, and quantum electromagnetic fluctuation forces. Independent measurement of the gap, change of materials or coatings, control of the screen and repetition with different attractor patterns are required. The signal frequency itself does not prove gravity: synchronous interference also follows the movement of the installation. The Newtonian model, one new massive field and a given KK tower are compared through the same hardware description.



Engraving 22. Measuring force at short distances. Conventional image of a torsion measurement: a suspended sensitive element interacts with a nearby attractor. The physical prediction depends on the gap, the geometry of the bodies and the properties of the surfaces. The illustration shows the principle of laboratory search for short-range contribution; the design is not a drawing of the installation, and its details do not indicate the achieved sensitivity or evidence of extra dimensions.

A positive signal with one characteristic length will not yet prove the existence of extra dimensions: a similar force can be created by an ordinary new field. A stronger test would be the consistent form of multiple contributions together with independent constraints on the same masses and couplings. Even it will require comparison of other spectral explanations. A zero result will exclude only the region of radii and connections for which the experiment had sufficient sensitivity. It will not establish that space is three-dimensional at any scale.

The next calculation should determine whether several KK levels and one exponential correction are distinguishable after averaging over bodies and taking into account the surface. The minimum

gap is especially important: at distances significantly larger than R, short-range contributions are strongly suppressed. If all the still resolved signal is below the noise, this will be a result of the capabilities of this installation. The next step then is to change its sensitivity or select another explicitly defined model.

**Chapter 17**

# Can space close on itself?

For space to have no edge, it does not have to continue indefinitely. This statement is easy to say and difficult to hold in your mind. We are accustomed to checking the finitude of an object by walking around it from the outside. But the entire geometry of space can be specified by internal distances and rules for the continuation of paths. External bypass is then simply not part of the task.

The previous chapter closed the hidden additional directions. Now the question relates to ordinary three-dimensional space: how are its parts connected into a whole? One may know the geometry of small triangles and the local rules of light propagation, but not yet know whether long enough paths can travel around the entire space and return to the original area. This is the difference between local geometry and cosmic topology.

## Finiteness without a wall

The surface of a sphere provides a familiar example of a finite area without an edge. For a creature living only on the surface, movement does not end with a cliff. It is convenient for us to see the sphere from the outside, but its internal geometry can be determined without such a view. In cosmology, the analogy refers to the possibility of finitude, rather than the literal statement that our Universe is a two-dimensional shell inside a larger ball.

There is an example that resists the usual picture even more. Let's imagine a flat square with identified opposite sides. Having reached the right edge of the picture, the path continues from the left; the top is connected to the bottom. The drawing itself has a boundary, but the space it describes has no boundary. The lines along the edges are a cut that we made for the convenience of the map. Inside the model there is no wall, no seam, no special physical event.

The three-dimensional version is obtained from a cubic region with opposite faces identified in pairs. This is a three-dimensional torus. In all sufficiently small neighborhoods it has the usual Euclidean geometry. There are directions along which movement returns to the starting point, although an arbitrary straight line does not have to close exactly. The cube visible on paper is not a cosmic container: its opposite sides represent the same places.

This separates curvature and topology. Curvature describes local geometric relationships. The topology defines the global connectivity of areas and the possible classes of paths. Zero spatial curvature is compatible with both infinite Euclidean space and a compact torus. Therefore, the result “the observed geometry is close to flat” does not in itself mean “the Universe is infinite.” Measuring one property should not be converted into an answer to another question.

Expansion also does not contradict compactness. If the coordinate size of a fundamental region is designated L, its physical size in a simple homogeneous model changes as aL. The total volume grows, although no walls move apart into the external void. All small measuring rulers are subject to the same local geometry as in the corresponding non-compact model. The difference is manifested in rather long paths and global properties of the fields.

A closed spatial path is not a journey into the past. Light takes time to travel, and the cosmos changes during this time. Moreover, the very fact of compactness does not guarantee that the light

has time to travel around the space within the available history. The size, expansion, and age of the observed stage determine whether global connections can leave a trace that is accessible to us.

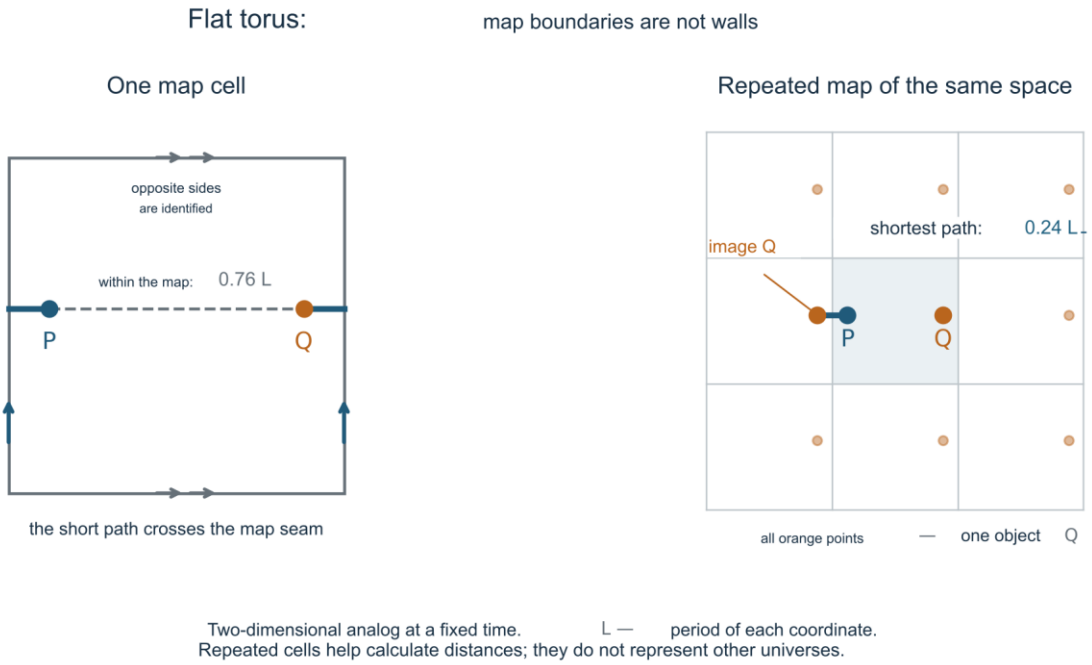



Figure 6. A two-dimensional flat torus as an analogue of a compact space: opposite sides of a square map are identified. A repeated map shows images of one object rather than new physical objects. For the selected points, the shortest path is 0.24L and intersects the coordinate seam. The diagram does not depict a surface embedded in external space.

## One source in several directions

If light from one object travels to us along different topological paths, the object can appear in multiple directions. This is similar to many images, but does not require mirrors. In a mathematical description, it is convenient to multiply the fundamental region and draw direct rays through its copies. The copies serve as a calculation: they are not additional physical galaxies or independent universes.

There is a difficulty in such a search. Different paths usually mean different emission times. One galaxy may appear in different stages of development, from a different angle and with a different observed brightness. Therefore, searching for identical photographs of the sky is a weak version of the idea. It is necessary to model the evolution of sources, catalog selection and light path geometry. The absence of obvious doubles does not allow one to immediately abandon the compact space.



Engraving 23. Two portraits from the same source. In a compact space, different light paths can produce multiple images of the same source. The different lengths of the path allow us to see it at different stages of evolution and from different directions. The two galactic portraits here are conditional: this is an explanation of the difficulty of the search, and not a found pair of topological images and not proof of the closedness of space.

A more rigorous possibility is provided by relict radiation. In the idealized picture we see a spherical surface of the last scattering. If, in identification space, this surface intersects with its topological counterpart, the intersection forms a circle. The same early regions are then observed along two circles in our sky. Cornish, Spergel, and Starkman proposed using such consistent patterns to search for cosmic topology. [136]

In the simple flat case, two spheres of the same comoving radius $\chi_{rec}$ intersect if the distance between their centers is less than $2\chi_{rec}$. This condition relates the size of space to the possibility of observing circles. However, light from the common early region arrives in different ways. The projection of the velocity of matter onto the line of sight, the late change in gravitational potentials, and the finite thickness of the last scattering layer change the patterns. Therefore, the test looks for predicted statistical agreement rather than requiring each temperature pixel to be equal.

Planck's analysis of 2015 data did not reveal the desired compact topology signal in the considered toroidal and layered models. For a cubic torus, a polarization search for coinciding circles yielded a lower bound on the radius of the sphere inscribed in the fundamental region: greater than 0.97 the distance to the last scattering with a confidence of 99 percent. This is a limitation of a certain geometry and method. It does not mean that the size of the entire Universe has been measured or that its infinity has been established. [2]

## From repetitions to allowed waves

Repeated images are not the only trace. Global geometry changes the set of oscillations allowed for physical fields. A string with fixed ends allows certain standing waves; periodic space also imposes consistency conditions. The analogy concerns the spectrum, not the material: outer space does not need to be an elastic string or have mechanical walls.

For a cubic torus with side L, the allowed wave vectors have the form following from periodicity. This is the same principle of wave matching after bypass that gave the KK spectrum in chapter 16; it now limits cosmological perturbations in three broad directions:

$$\mathbf{k_n} = \frac{2\pi}{L}\,\mathbf{n}, \qquad \mathbf{n} \in \mathbb{Z}^3.$$

In infinite flat space, directions and wavelengths form a continuous set. This is where the grate appears. Its orientation relative to our sky affects the statistical relationships of the observed patterns. At large L, the distance between the allowed wave vectors decreases, and in the accessible range the torus gradually approaches the usual continuous description. Therefore, a very large compact Universe can be practically indistinguishable from an infinite one.

For cosmic microwave background radiation, information should be sought not only in the average power of oscillations of a given angular size. The celestial map is laid out according to spherical harmonics - standard patterns on a sphere. The index ℓ specifies the angular scale, and m distinguishes patterns with one ℓ; their coefficients describe the contribution of each pattern to the map. Topology can relate coefficients that are not correlated in the original statistically isotropic model. Saving only the power averaged over m loses these connections and along with them part of the geometric information. [137]

The work of the COMPACT collaboration has shown with specific examples that the absence of coinciding temperature circles leaves room for searching for topology using intermodal correlations. This expands the set of tests, but does not turn any large unusual spot into evidence of finite space. It is necessary to calculate the entire correlation pattern of the selected manifold and check its compatibility with the observed sky. [138]

In more general spaces, identifications include rotations and other transformations. Additional parameters arise, and sometimes the position of the observer becomes important. Therefore, the calculated pattern of correlations belongs to a specific manifold. The cubic torus is convenient due to its transparent construction, but its limits do not cover all topologies.

## Polarization as a map check

Polarization describes the ordering of the directions of electrical oscillations of radiation. In relict light, it occurs when scattered by electrons, when the incoming radiation has a certain angular inhomogeneity. Its drawing is divided into E- and B-components with different transformation rules for mirror reflection. Temperature and polarization are related by common early disturbances, but depend differently on their evolution. Therefore, polarization can verify the temperature-matched geometry. [139]

The setup proposed here starts with a temperature map. It is used to estimate the permissible dimensions and orientations of the torus. But for each such geometry, it is necessary to take into account the measured temperature pattern itself: due to the connection between T and E, it already

predicts part of the polarization. The new test concerns the conditional distribution of E at this temperature map. It is not enough to simply take geometry from temperature analysis and generate a completely new sky for it, unrelated to the observed temperature.

For each fixed geometry with a Gaussian description, the conditional forecast is given by the expected polarization pattern and the covariance of the remainder—the magnitude of its scatter and connections between components. Predictions are then pooled across the entire feasible distribution of sizes and orientations, not just the best-performing geometry. The resulting mixture of distributions may no longer be Gaussian. Polarization adds information to this joint calculation; to regard it as a completely independent heaven would be to misjudge the power of the test.

The COMPACT 2025 study constructed correlation matrices also for tensor perturbations in the considered Euclidean topologies. Its discriminability estimates involve pure tensor signal analysis. For a real sky, we need to add scalar disturbances, noise, and foreground radiation. The found polarization connections relate to the chosen manifolds and are not required to be preserved in the cubic torus. [140]

What remains is cosmic variance: we observe one implementation of an early random field, and at the largest angular scales there are few available modes. Polarization expands the data set, but does not provide an infinite number of independent worlds. Even after removing instrumental noise, the accuracy of statistical model inference remains limited. [7]

## How to check it

The object of the first test will be a cubic three-dimensional torus with size L, orientation and a given model of primary disturbances. Temperature and polarization maps are used. For linear Gaussian perturbations, a joint theoretical covariance is constructed: relationships between temperature and temperature, polarization and polarization, and temperature and polarization. In the limit of very large L, the calculation should reproduce the original non-compact planar model. This limit tests both the physical structure and the program.

The synthetic maps are overlaid with instrument resolution, real masks, noise, and foreground frequency components. Removing the sky band itself couples the harmonics, so all competitors must go through the same observation and processing procedure. Frequency and time divisions help identify instrumental effects. Common temperature and polarization cleanup errors are included in joint covariance: consistent interference may otherwise appear to be a successful geometry prediction.

The distribution of geometric parameters is estimated from temperature, then the conditional prediction of E-polarization is checked. The same conditional forecast is built for each competitor: a non-compact model, acceptable primary anisotropy, calibration errors or physical polarization rotation. The very presence of a correlation between T and E is expected without topology; The advantage of the torus should be the correct prediction of its specific structure and residual scatter. Additionally, matching circles are taken into account if the selected size makes them available. The parameters of competitors, which are not limited by temperature, are integrated according to predetermined a priori distributions or independent external restrictions.

Searching through many sizes and orientations finds randomly successful options. Significance is therefore assessed by repeating the entire search on control simulations, including the polarization test step. A null result will limit the region of L and orientations with detectable effect, while maintaining the possibility of a much larger compact space. The torus will be favored by successful pre-

diction of the polarization not used in the choice of geometry, when compared with alternatives on the same data.

Upcoming work is a sensitivity map of this joint analysis. It should show where the predictions of the torus and its competitors differ, and where the difference is lost due to cosmic variance or geometry uncertainty. It is precisely this calculation that turns the admissibility of a finite space without an edge into a verifiable question about its structure.

**Chapter 18**

# Other universes

The expression “another universe” makes an impression even before we have explained what we consider to be one universe. If this word refers to the entire physical reality, by definition it does not have a second copy outside. If we are talking about a region with a common cosmological history, similar regions may be part of a larger pattern. A dispute about existence sometimes begins with an unspecified change in the scale of words.

In this chapter we will need precision. We will consider the mechanisms that can give rise to multiple cosmological regions, the difficulties of calculating their probabilities, and possible traces of interaction. The value of an idea will depend on the commitments it makes to observations. The increase in the number of unobservable worlds itself does not explain anything.

## Various tasks under a common name

The most moderate possibility is the continuation of our space beyond the region from which the light managed to come. In this case, we can talk about other galaxies and regions of matter in the same space-time, with the same low-energy physics. Horizon restricts access to data, and does not necessarily break the structure of the world. This is a continuation of the model; it does not require extra dimensions or other quantum laws.

The topological repetitions from the previous chapter are arranged differently. Multiple images may correspond to the same physical source. Computational copies of the fundamental region help trace rays, but do not multiply existing objects. By calling them parallel universes, we would turn the way of drawing a map into a new physical content that is not in the model.

The cosmological multiverse of eternal inflation suggests regions where early accelerated expansion ends in different ways or at different times. They are called pocket universes; in vacuum decay scenarios, bubbles appear. These are parts of a cosmological structure with given fields and dynamics of transitions. Not every pocket area is required to have the structure of a bubble with a separate wall.

Another problem relates to quantum theory. Everett's formulation of relative states uses universal quantum evolution without a separate collapse postulate. Modern expositions discuss decohered branches of the state with consistent records of different outcomes. Decoherence means that interaction with the environment distributes information about alternatives throughout it, suppressing the interference available when observing one subsystem. This explains the stability of the records, although this dynamics itself does not yet choose the interpretation of quantum mechanics. The branches are defined through the structure of the quantum state, and the bubbles through the cosmological dynamics of the fields. The relationship between these constructs would require a separate theory. [141] [142]

Discernment also determines verification. If two interpretations use the same rules for calculating probabilities, an experiment with those probabilities will not separate them. Changing the rules themselves, for example introducing physical collapse, already sets a different testable dynamic. The observation of interference does not certify the collision of cosmic bubbles, and the topological repetition does not select the quantum interpretation. Therefore, further we will talk specifically about the mechanism of the birth of cosmological regions.

## How space sustains inflation

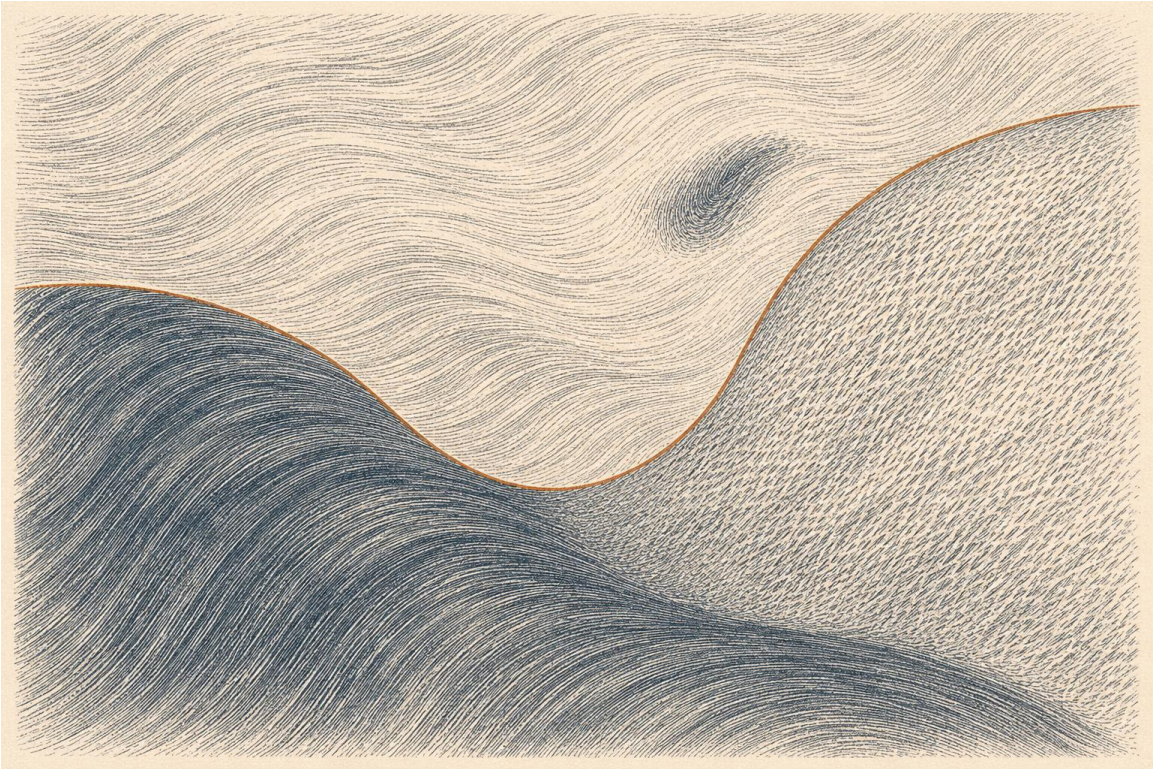
In Chapter 11, inflation was seen as a possible early stage, setting the stage for a hot history to follow. For our site it should be completed. But local termination does not necessarily mean termination of the process throughout the entire model space. Some areas may transition to normal evolution, while in others the inflationary regime persists and creates a new physical volume.

In stochastic self-reproduction scenarios, the classical movement of the inflation field competes with quantum fluctuations. During the characteristic expansion time, in some areas the field moves towards the end of inflation, while in others its change delays this exit. If the reproduction of areas that continue to expand is sufficiently effective, their total volume can grow, although many individual trajectories are already leaving the inflationary regime. Linde explored such a mechanism in work 1986. [143]

The presence of quantum fluctuations in itself does not guarantee eternal inflation. What is needed is a suitable form of the potential, a mode of applicability of the description, and a relationship of dynamic scales. Observations of that portion of the potential that could form disturbances accessible to us do not have to determine its distant region. The continuation of the field to where self-reproduction is assumed is an additional physical statement.

Another mechanism uses a metastable, or false, vacuum: a state that can persist for a long time, but has a decay channel. The transition occurs through the nucleation of regions of a new state while the remaining background continues to expand. If the expansion is fast enough compared to the loss of volume into bubbles, the transition may not be completed globally. Here, the birth of bubbles and the increase in the volume of a false vacuum compete; in the stochastic scenario - field drift and fluctuations. [144]

The word "bubble" here does not require ordinary gas and external air. It describes the region of a different state of the fields and the transition boundary. If the theory allows for multiple vacua, different regions may have different effective properties. However, the multitude of mathematically permissible vacua does not yet prove that they are all populated: dynamics must explain what transitions are possible, at what speeds and from what initial state.



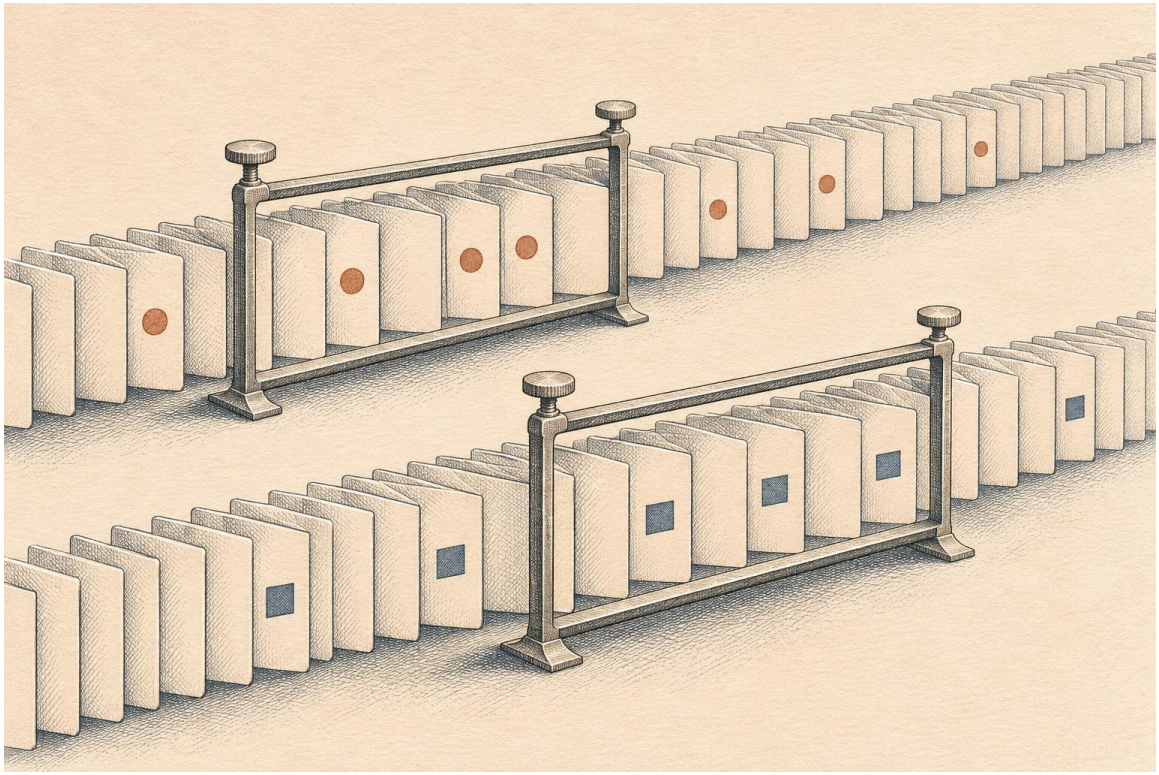
Engraving 24. Areas of different field states. In the bubble scenario we are talking about areas of different field states and transition boundaries. In the engraving they differ in texture and are not separated by external air. This is an image of hypothetical dynamics: the existence of several admissible states does not yet establish which of them arose and with what probability.

Finally, eternity in the future does not solve the question of the past. The Bordet-Guth-Vilenkin theorem establishes the past incompleteness of certain geodesics under its assumptions about mean expansion. It does not prove the emergence of everything from absolute nothing. Therefore, a self-perpetuating inflationary model may require a separate description of the past boundary, even if the production of new areas within it does not stop. [102]

## How to count infinity

Suppose the theory generates an infinite number of regions of two types. What is the probability of the first type? First you need to determine what makes up the sample: the areas themselves, equal physical volumes, or events of a certain kind. Then a rule for comparing them is required. In the final sample we count the frequencies; in an infinite ensemble, the ratio of two infinities does not yet determine the probability.

A simple mathematical example illustrates the problem. Suppose there are infinite numbered collections of red and blue cards. If we expand the sample, each time taking the first n cards of each color, the proportion of red ones is equal to half. If we take the first 2n red and the first n blue, it is equal to two thirds. In both cases, any given card will be included at some point. The order in which the infinite totality is exhausted varies.



Engraving 25. The order of counting the infinite. Two collections of cards stretching into the distance remind us that an infinite set does not determine the way it is counted. Different finite sample expansion rules may produce different proportions even when each card is included over time. The illustration conveys the meaning of the analogy; it does not specify numerical probabilities of cosmological regions and does not solve the problem of measure.

The cosmological problem of measure is more complex than this example. It is possible to truncate spacetime with a temporal surface, follow selected trajectories, or introduce other weightings. In a growing ensemble, the choice of rule changes the frequencies. For example, an event with a large registration delay may remain behind the cutoff, although its beginning has already been taken into account. Gut and Vanchurin studied this dependence at specific global cutoffs. Before calculating the typicality of our observation, it is necessary to choose a physical counting rule. [145]

The measure must be consistent with the dynamics and probabilistic requirements, produce certain results and withstand tests. Selecting a rule that makes an already known result typical does not complete the explanation. A new choice of measure changes the predictive structure and requires independent justification.

There is also an observation selection effect. Data are obtained under certain physical conditions; the distribution of recorded events may differ from the distribution of all model events. This selection should be taken into account, just as the sensitivity of a telescope is taken into account when counting galaxies. However, the selection condition does not replace the original distribution. To assess how expected our result is, we need a method for creating regions, a rule for weighing them, and an explicitly specified condition for inclusion in the sample under consideration.

The statement “everything is realized somewhere” bypasses this work. Even an infinite ensemble can contain only a limited class of states: an infinite sequence of even numbers does not contain odd ones. And the presence of our state among the admissible ones does not yet indicate its probability.

Explanatory power arises when the model constrains the distribution of outcomes and thereby risks being inconsistent with the data.

## Could another bubble leave a mark

The inaccessibility of most areas does not exclude the accessibility of individual tracks. In some bubble scenarios, the collision could affect the region from which our observed region later emerged. Then the calculation should relate the dynamics of the collision with the primary disturbances, and these with the temperature and polarization of the cosmic microwave background radiation. A specific chain of physical processes is checked.

The expected pattern depends on the potential, collision geometry, and subsequent evolution. Under suitable conditions, it has a characteristic angular region and a coupled temperature and polarization response structure. But a round spot in itself is not a distinctive feature. The random primordial field, late gravitational effects, and map contamination can create visually unusual regions without another cosmological bubble.

A historical example of meaningful testing is Feeney et al.'s analysis of seven years of WMAP data. The authors constructed a procedure for selecting candidates and comparing models, taking into account a search over the entire sky. The results obtained did not require adding bubble collisions to the original cosmology. This is an example of the limitations of specific patterns and parameters, not an observational refutation of any eternal inflation. [146]

Subsequent work by 2015 linked numerical models of the collision to temperature and polarization transfer functions. Such functions translate the initial spatial profile of disturbances into the observed sky pattern, taking into account its evolution and projection. The measurement gain is also limited by cosmic variance, and the derivation of fundamental parameters depends on the adopted cosmology. The numerical predictions of that paper require a new calculation before being applied to another setup. [147]

Two results are separated here. Based on the data, you can constrain the parameters of a predefined observed pattern. To turn this into a conclusion about the cosmological mechanism, you need to know how often and with what parameters it generates such traces. Even a convincing encounter would first certify an event in our accessible causal history. The infinite continuation of the ensemble would remain a separate inference about the global dynamics.

## How to check it

The work program begins with one model of the bubble transition: potential, initial state, collision parameters, and subsequent inflationary history. From these, disturbances and observed temperature and polarization profiles are calculated. The spatial and temporal resolution of the numerical calculation is increased until the shape of the template becomes stable at the required accuracy. Then they check which connections of the two channels are preserved when the parameters are allowed to change. Only such connections can become a prediction for a new dimension.

The main data will be multichannel maps of the cosmic microwave background radiation. The amplitude, angular size and spatial profile of the expected signal are measured along with the predicted polarization response. Comparisons are made with the usual cosmological realization, possible primary features of other origins, late structures and foreground models. Cosmological parameters

and calibration uncertainties vary coherently: a fixed convenient background can artificially enhance the preference for a new effect. For the candidate, frequency maps result in one angular sensitivity: resolution differences should not simulate spot shape changes. The mask and cleaning method are fixed until significance is assessed.

Artificial signals of known strength are added to the simulations and the detection completeness and false alarm rate for the entire algorithm are measured. A search of template positions, sizes, and families is included in this assessment. Polarization is checked conditionally using an already known temperature map, as in chapter 17. This uses the common physics of the two channels without re-counting the same information. Cosmic variance is preserved even when the device is improved.

The absence of a required detectable signal excludes the corresponding parameter range. But if visible collisions are rare or their traces are beyond the available scales, the absence of candidates weakly constrains the global model. A positive result should be maintained across changes in mask, observation frequency and processing method, and alternatives should be compared across the full profile, including polarization.

The closest calculation is the probability of detection as a function of the parameters of a particular collision. This is then combined with the predicted event frequency and amplitude distribution. If this second step depends on an unspecified measure, conditional sensitivity to observed patterns and results for the selected measures should be reported separately. Then the constraint actually obtained from the sky is not lost within the uncertainty of the global ensemble.

Chapter 19

# When Gravity Goes Quantum

Gravity acts on stone, atom and quantum system. But it does not follow from this that they all make it possible to study its nature equally well. The fall of an atom tests the effect of gravity on quantum matter. A more demanding question arises when the mass itself is in a superposition of different positions: what gravitational effect does it create and what happens to the other quantum system next to it? Here the familiar formula of force meets the need to describe several possible locations of the source simultaneously.

## Quantum question in a weak field

For this encounter, it is not necessary to start from the center of the black hole. Quantum properties of interaction can also manifest themselves in a weak field if the system is sufficiently well isolated and the observed quantity is sensitive to quantum correlations. The weakness of gravity then becomes the main experimental obstacle: its effect must be accumulated, maintaining a state that much stronger electric and magnetic forces can destroy or change.

The statement that the quantum theory of gravity is completely unknown is too harsh. General relativity can be used as a quantum effective theory at sufficiently low energies. This description separates effects determined by known degrees of freedom from unknown physics on extremely small scales. John Donohue showed how to extract leading long-range quantum corrections without having a definitive answer about the microscopic structure of space. This is a controlled area of calculation, not a complete theory for any energy. [148]

This leads to different experimental goals: to test the creation of entanglement, to find a correction to the force, or to test a change in quantum evolution. These problems are sensitive to different properties of the theory. Even discovered gravitational entanglement will not separate those variants of quantum gravity that have the same accessible low-energy limit.

In chapter 16 we looked for a change in the law of force. Here the question is different: can the leading Newtonian interaction itself quantumly act on two masses? Entanglement can arise from the ordinary energy of mutual attraction, when the positions of both sources are described quantumly. To do this, it is not necessary to first measure a small quantum correction to the potential. The effect of a known interaction on a joint state is significant.

## Two masses and four paths

Let us imagine two small masses, each in a superposition of two clearly distinguishable positions L and R. For a pair, four combinations arise: LL, LR, RL and RR. The distances, and therefore the energies of attraction, may differ between them. During the waiting time, the combination produces different quantum phases. Relative phase determines how the alternatives enhance or cancel each other in subsequent interference readout.

In the proposal by Sugato Bose et al., spatial branches are associated with spin states that help prepare the motion and then read the result. After convergence of the spatial branches, spin correlations are measured. Given a suitable sequence of operations, they carry information about the entanglement that arose during the interaction of the masses. The work describes an experimental

proposal; one cannot conclude from it that such gravitational entanglement has already been observed. [149]

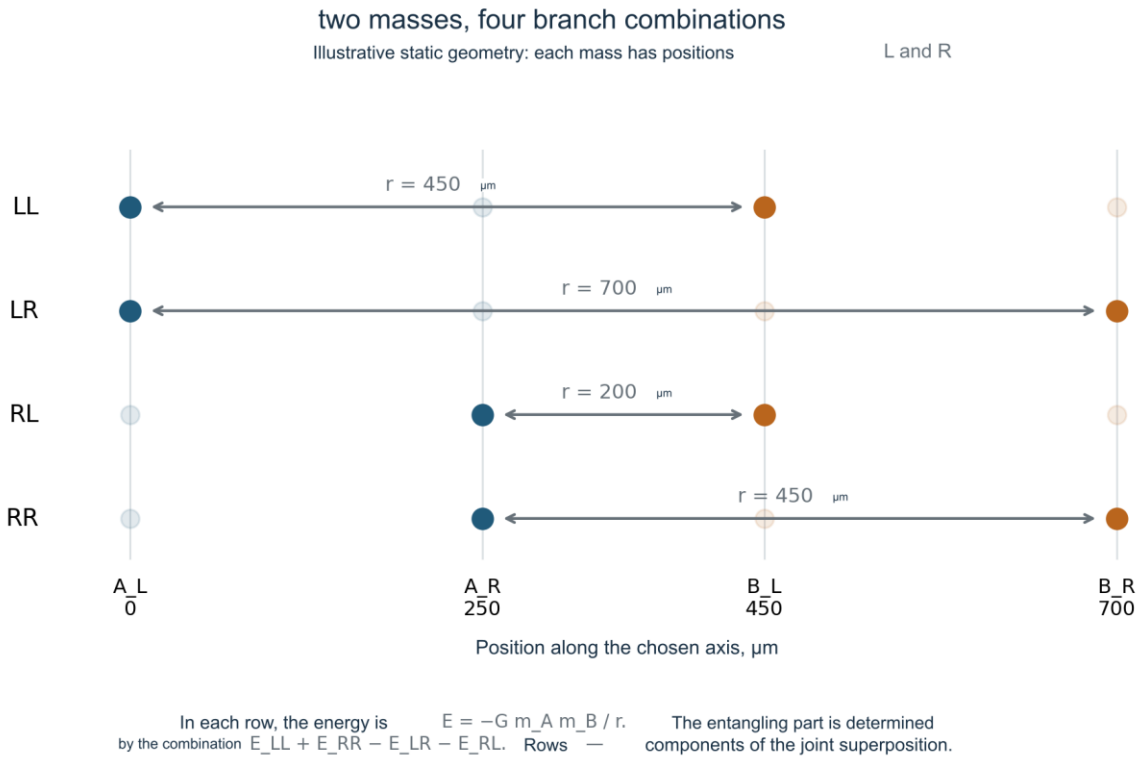



Figure 7. Four combinations of spatial branches of two masses in the conditional static geometry of the calculation example. Positions are shown in micrometers; the distances are 450, 700, 200 and 450 μm. These are components of a joint quantum state, and not four experiments with simultaneously localized particles. Preparation, bringing together branches and noise are not shown in the diagram.

Not every phase difference creates entanglement. If the phase of each branch can be represented as the sum of a separate action on the first mass and a separate action on the second, the initially independent states will remain independent. The entangling part describes the dependence of the influence on one mass on the position of the other. It is distinguished by a combination of four energies, in which independent local contributions are reduced. At constant distances:

$$H_{\text{int}} = \hbar g Z_A Z_B, \qquad g = \frac{E_{LL} + E_{RR} - E_{LR} - E_{RL}}{4\hbar}, \qquad E_{ij} = -\frac{G m_A m_B}{r_{ij}}.$$

$H_{int}$ is the interaction energy operator, and Z assigns plus and minus one to the two branches. Local terms have already been removed from the record: they change individual phases, but do not themselves entangle the masses. The g parameter is measured in inverse seconds and specifies the rate at which the entangling effect accumulates. The approach assumes narrow packets and known distances. For real trajectories, this combination of energies must be integrated over time, including the separation and convergence of branches.

Let's take a conventional calculation example: both masses are equal to $10^{-14}$ kilograms; the distances for LL and RR are 450 micrometers, for LR - 700, for RL - 200 micrometers. The absolute value of g is about 0.0314 $s^{-1}$. In an ideal model without noise, the first entanglement maximum is reached in about 25 seconds. These numbers show the scale of the task, but do not indicate the achieved ability to maintain precisely such superpositions for such a long time.

A static recording of potential also does not mean that the physical signal is transmitted instantly. This is a low-energy approximation for slowly changing configurations, in which some field variables are already excluded from the description. When the question concerns the role of mediation and causation, the conditions of this approximation must be reconstructed. You cannot first replace field dynamics with the direct interaction of two masses, and then consider the absence of a field in the abbreviated formula as proof of its physical uselessness. For the interpretation of the experiment, both the accuracy of the effective calculation and the theory from which it is derived are important.

The usual consistency of readings is not enough: general vibration also creates correlations. An entanglement witness is a combination of measurements that, for any admissible mixture of products of states, remains within a certain range. Going beyond its boundaries certifies entanglement. To see quantum phases, we need to measure spins in different directions. The frequencies of the positions LL, LR, RL and RR alone do not solve the problem: in an ideal phase interaction they can remain unchanged while the state becomes entangled.

## What does entanglement indicate?

Why does this result indicate a mediator? Local operations on each mass and transfer of classical results turn the mixture of products of states back into such a mixture. They may create ordinary correlations, but not entanglement. If gravitational mediation is completely reduced to this channel, it will not be able to entangle initially unentangled masses. The detected entanglement therefore excludes precisely this class of intermediaries if the prerequisites are met.

For the conclusion to be made, it is necessary to eliminate the entanglement introduced by the preparation, the general quantum element of the installation, or the residual electromagnetic interaction. It is also necessary to justify the identification of subsystems and the meaning of locality. The local operation in such an argument affects one of the selected subsystems. This is a more specific mathematical requirement than the general prohibition of faster than light transmission; The ban on superluminal communication alone is not enough for the mediator theorem.

This distinction has been the subject of detailed dispute. Andrea Di Biagio shows that the conclusion about the quantum nature of the gravitational field is not independent of the choice of theoretical description: the information locality required by some mediator arguments may be different from spatiotemporal locality. Therefore, the observed effect should be compared with quantitative predictions of specific alternatives, and not just with the general label "classical gravity". [150]

Tianfeng Feng, Vlatko Vedral and Chiara Marletto, in turn, defend the witness's inference under the explicit assumption of local mediation. They show why the state-collapse alternatives considered do not refute the argument when using nonlocal interaction in the appropriate sense. The disagreement cannot be resolved by choosing a more confident formulation. It is necessary to establish what assumptions the models being compared share and what measurements differentiate their predictions. [151]

There is also a subtlety in the very selection of independent subsystems. In gauge theories, the physical description of an object is related to the surrounding field; in gravity this is called, among other things, gravitational dressing. Nicolas Boule and Guilherme Franzman discuss how such connections complicate the decomposition of a complete state into independent factors. Their estimates provide negligible corrections for the experimental regimes under consideration. This means that it is

important here to quantitatively test the approximation of subsystems, and not to reject the experiment with just the name of the problem. [152]

The practical goal is to compare classes of dynamics based on phases, loss of coherence, and entanglement. A single experiment may eliminate a particular classical interaction model even if several other descriptions produce the same available results.

## Phase and loss of coherence

The entangling effect is counteracted by the loss of coherence—the stability of the relative phases on which interference depends. The density matrix ρ describes the joint quantum state, including statistical uncertainty and connections between alternatives. For the first calculation, we will accept independent local noise without memory, that is, without a significant influence of previous interactions with the environment on the current rate of state change:

$$\dot{\rho} = -ig[Z_A Z_B, \rho] + \sum_{i=A,B} \gamma_i (Z_i \rho Z_i - \rho), \qquad \gamma_i = \gamma_{\mathrm{env},i} + \eta|g|, \quad \eta \geq 0.$$

The first term on the right accumulates the interaction phase, and the sum describes the dephasing. In the chosen normalization, the coherence of one free system decays at a rate of 2γ. Part of $\gamma_{env}$ is attributed to the normal environment; addition η|g| is a testable assumption about the noise associated with the interaction force, with a dimensionless coefficient η. This is a family of models for sensitivity studies. A correlated noise or memory environment would require a different equation.

For the initial product of equal superpositions of two branches, this model gives a simple condition for the appearance of entanglement in the initial approximation in time:

$$g^2 > \gamma_A \gamma_B.$$

The threshold refers to the given equation, the initial states and the initial stage of evolution; it is not a universal boundary between quantum and classical gravity. It shows the competition between the accumulation of the entangling phase and the destruction of coherence. Therefore, increasing the latency only improves the result in the appropriate noise range.

For one fixed g, the uncertainty of the noise of the medium allows several expansions of the total dephasing into ordinary and additional contributions. The non-negativity of ordinary dephasing rates may provide a conservative upper bound for η, but does not uniquely determine it. Changing the distances will not eliminate this uncertainty if each configuration is allowed to have its own arbitrary environment correction. To isolate η, an independent calibration or a general physical model of interference that is simultaneously applicable to all series is needed.

There is also a meaningful classical alternative: continuously measure the position of one system and transmit the result to another through feedback. Kafri, Taylor and Milburn built a model of such a channel for mechanical resonators. In the design considered, the interaction is accompanied by noise and does not create entanglement. But it cannot be obtained from our equation by simply renaming η: the transition to the spatial branches of a particular interferometer requires a separate derivation. [153]

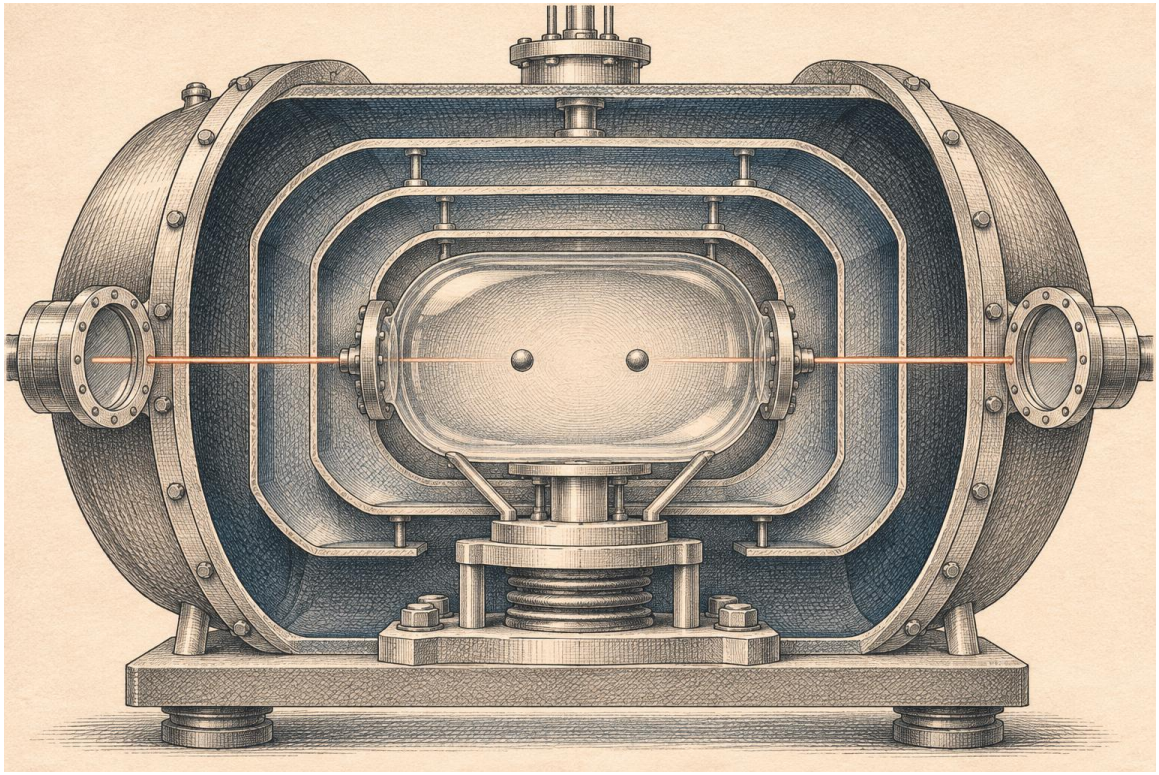
Residual electromagnetic interaction is dangerous in another way. It can create real entanglement and need not an additional noise parameter, but a separate coherent dynamics term. Therefore, detect-

ing entanglement and establishing the gravitational origin of the detected entanglement are two successive experimental tasks.

## How to check it

In the experiment, several geometries and times of interaction of two masses are compared. After the branches are brought together, individual coherence and spin correlations are measured along pre-selected directions. Local phases are also calibrated: they do not create entanglement, but rotate the correlations relative to the readout axes. The witness is assessed with preparation and measurement errors while testing the dependence of the accumulated phase on masses, distances and durations. This is a test of a joint state, not a single change in the visibility of the interference.

What is needed are control sequences with similar impulses and environmental conditions, but suppressed by the entangling combination of gravitational phases. Based on real trajectories, both the signal and the preserved sensitivity of the control to interference are calculated. Separately, particle charge, inhomogeneities in surface electric fields, magnetic gradients, vibrations, residual gas and thermal radiation are measured. The screen, if used, enters the model along with its movement, forces and noise. Changing the distance alone is not enough to establish the origin of the interaction.



Engraving 26. Save the quantum state. The conceptual setup emphasizes the challenge of isolating two small masses and controlling the environment. When testing gravitational entanglement, residual gas, heat, vibrations, and electromagnetic interactions are significant. The engraving does not depict the detection performed: a real experiment requires separate state preparation, branch convergence, and correlation measurement under a quantitatively validated interference model.

The coherent Newtonian potential with a calibrated medium, the same potential with a common addition $\eta$, the measurement and feedback channel derived for the installation, as well as the residual electromagnetic interaction are compared. Each model must simultaneously describe phase, visibil-

ity, and spin correlations. The interference parameters are related by a general physical dependence between the series; separate free adjustment for each experiment would make η indeterminable.

A statistically significant departure of the witness beyond the boundary of unentangled states will confirm entanglement under the accepted reading model. Establishing its gravitational origin will make it possible to exclude compared models that are unable to create such an effect. A stronger inference about a nonclassical mediator additionally requires a local mediation condition. A zero result may mean insufficient phase, destruction of coherence, and weak sensitivity of the witness; by itself it will not certify a classical field.

The next calculation is to derive the selected alternative dynamics for real trajectories and test the entire analysis on artificial data with known parameters and independently estimated noise. It must establish the required number of repetitions and the frequency of false attribution of ordinary noise to the parameter η. After this, the limitation of additional dephasing will have a certain physical meaning, and the dispute about the mediator will have comparable experimental consequences.

**V Open future**

**Chapter 20**

# Several futures of one Universe

By reconstructing the past from the light of distant objects, we gradually obtain the history of expansion. There is a natural desire to continue the found curve forward. Will space expand indefinitely? Will the acceleration continue? Which areas will someday be able to exchange signals? It is easy to continue the graph mathematically. Physically, this requires knowing which law determines the part of history that has not yet been completed.

A future forecast combines observations and assumptions about the continuation of the model. Sometimes this assumption is well founded and produces stable consequences. Sometimes several valid continuations describe the accessible past in the same way. The distinction can be made rigorous: construct two ordinary classical models that coincide in a certain past description, but have a different future causal structure. This example will show exactly what information cannot be extracted from one expansion history.

## What prerequisites determine fate

Spatial curvature is not enough to determine the fate of the universe. The connection between geometry and the future depends on the composition of energy and its pressure. With suitable properties of dark energy, a spatially closed model can expand indefinitely, and an open one can go into compression. Krauss and Turner emphasized this dependence after the return of the cosmological constant to observational cosmology. Geometry informs an important part of the structure of the world, but further movement requires the law of dynamics. [154]

If the positive cosmological constant persists and eventually dominates, the expansion approaches exponential. If the density of the accelerating component begins to decrease quickly enough, the acceleration may end. In other models, a return to compression is possible. There are also Big Rip scenarios: with a constant pressure-to-density ratio less than minus one, in the corresponding model of general relativity, the density and scale factor diverge in a finite proper time. This is a conditional consequence of a given continuation, and not an established ending of the observable Universe. [155]

Observational estimates of the equation of state refer to available epochs. Combinations of BAOs, CMBs, and supernovae test distance and expansion histories within selected models. Even a convincing detection of the evolution of dark energy would not determine all of its future properties. What matters is the range where the data actually constrains the dynamics. [8]

Convenient parameterizations also have a scope. For example, describing the equation of state in terms of several coefficients helps to compare recent expansion history. But the continuation of such a formula to arbitrarily large future scales becomes a new assumption. A function that describes the observed interval well can behave beyond it completely differently than the physical field for which it was used to approximately describe. [156]

In the chapter on acceleration we already encountered a similar difficulty: the bell-shaped deviation of the equation of state gave an acceptable trajectory at the late observed interval, but its infinite continuation led to an unlimited curvature of the potential - its second derivative with respect to the field - at a finite value of the field. This example tested the suitability of a particular extrapolation.

Now more control is required: both future models must have smooth potentials over the entire range traversed, and the difference in their horizons must be derived from asymptotics. Then the uncertainty of the forecast cannot be explained by a mathematical defect in one of the models.

## Dependence of the horizon on the future

The particle horizon limits the region from which signals could have arrived to us during the accepted history of the Universe. The event horizon answers another question: what signals will ever arrive. For a spatially flat model with an infinite proper future, the corresponding comoving distance is determined by the integral:

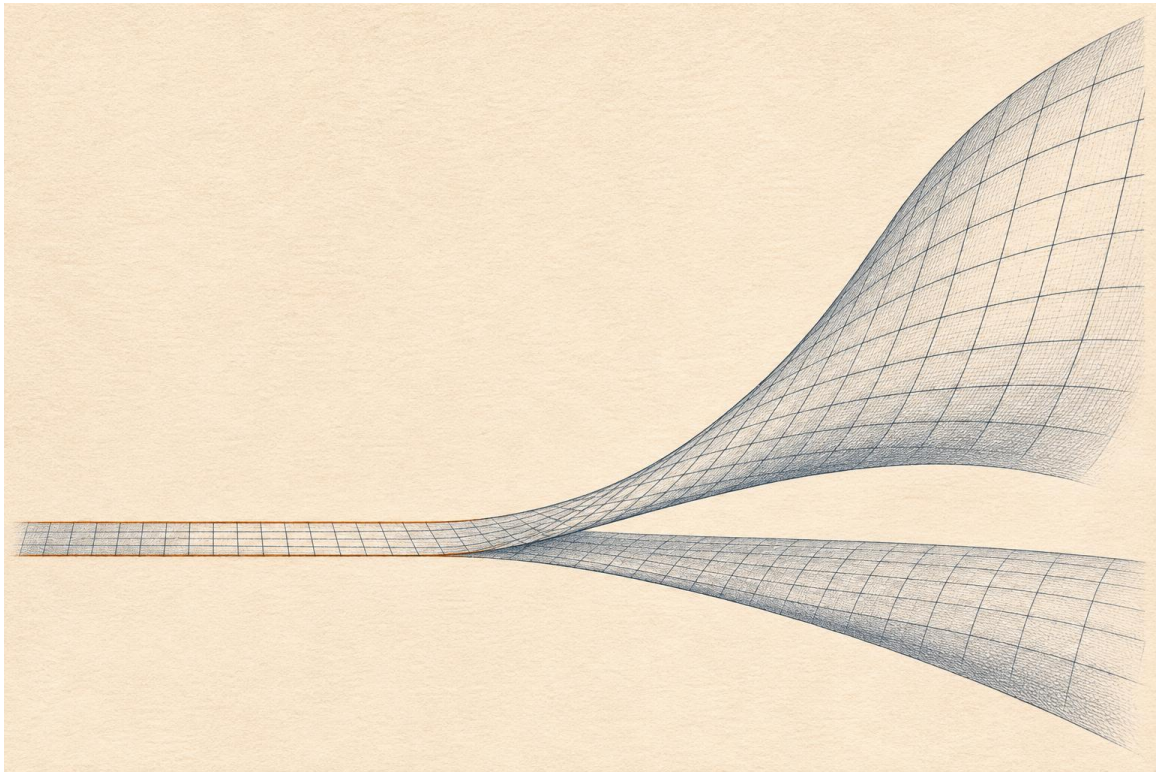
$$\chi_{\mathrm{e}}(t) = c \int_t^{\infty} \frac{dt'}{a(t')}.$$

The speed of light is denoted c, and a is the scale factor. If the integral is finite, there is a limit to the comoving distance that the light sent at a given moment can travel. If it diverges, there is no such limit in the unbounded plane geometry under consideration. We are talking about the causal availability of events. Even in the absence of a future horizon, infinite space does not become entirely observable in a finite time.

With exponential expansion, the denominator grows so quickly that the integral converges. With the power-law expansion characteristic of the dust model, it diverges. Therefore, the observed acceleration in a particular epoch does not yet prove the existence of an eternal horizon: the entire future function of the scale factor is needed. The Hubble sphere, determined by the current expansion rate, does not contain this information.

The presence of a horizon is also related to the thermodynamics discussed earlier. In de Sitter space, semiclassical theory assigns temperature and entropy to the cosmological horizon. But transferring this description to the future of our Universe presupposes a corresponding future geometry. Changing the law of evolution can also change the causal boundary to which the thermodynamic calculation relates. [110]

This creates a particularly accurate test of the strength of the forecast. Is it possible to build two worlds that expand equally into the present, but only one of which has a future horizon? The answer is positive in a fairly wide class of smooth scalar models. This requires neither negative kinetic energy nor the destruction of space in a finite time.



Engraving 27. General story and different sequels. An identically depicted section of the story leads into two possible continuations. This is a metaphor for comparing different laws of dynamics consistent with a common past; branching does not mean the physical division of the Universe. The presence of a future horizon in the considered models is determined by the entire subsequent evolution, and not by one observed period of acceleration or by the appearance of this engraving.

## Two potentials with a common past

Let us consider general relativity, a spatially flat homogeneous background, ordinary dust matter, and one minimally coupled canonical scalar field. The standard positive kinetic term is called canonical. We do not introduce additional terms directly relating the field to curvature and energy exchange with dust. Let us take today's scale factor equal to one. Positive constants Λ, S and M have the dimension of energy density; The dust density decreases as M divided by the cube of the scale factor. For simplicity, we omit radiation: this is a demonstration model, and not a complete description of the hot history.

Let's introduce the variable N - the natural logarithm of the scale factor - and a smooth switching function. Then we define two possible histories of the density of the scalar component itself:

$$N = \ln a, \qquad g(N) = \begin{cases} 0, & N \le 0, \\ e^{-1/N^2}, & N > 0, \end{cases} \qquad F(N) = \int_0^N g(u)\,du,$$

$$\rho_A(a) = \Lambda + Sa^{-3},$$

$$\rho_B(a) = (\Lambda + Sa^{-3})e^{-3F(\ln a)}.$$

Up to the present N is non-positive, the function F is equal to zero and the two densities coincide exactly. All their derivatives at today's point also coincide. After it, the multiplier in model B begins to smoothly decrease the density. The switch is unusual in that it does not have a sharp edge in any derivative. This is an infinitely differentiable function of class $C^\infty$.

So far we have only two dependences of density on expansion. For them to become a physical counterexample, it is necessary to present the dynamics of the field. The law of conservation of energy determines the ratio of pressure to density w. For each history, you can restore the field motion and its potential:

$$w_A = -\frac{\Lambda}{\Lambda + Sa^{-3}}, \qquad w_B = w_A + g(N),$$
$$\frac{d\phi_i}{dN} = M_{\rm Pl}\sqrt{3\Omega_{\phi,i}(1+w_i)},$$
$$V_i = \frac{1-w_i}{2}\rho_i, \qquad i \in \{A, B\}.$$

Here Ω denotes the fraction of the energy of the corresponding field in the total density, $M_{Pl}$ is the reduced Planck mass, and the speed of light in the field formulas is taken as unity. The expansion rate is obtained from the Friedmann equation with a common dust component. This restoration of potential from cosmological dynamics has a well-known scientific basis. Its physical meaning is limited by the accepted assumptions about gravity, matter and the kinetic term. [157]

For all finite values of N, the densities are positive, and w of both models lies strictly between minus one and one. This means that the kinetic energy and potential are positive. We choose the origin of the field in the same way: for N = 0 we set φ = 0 in both models, taking the shown positive branch of motion. The speed of the field and the rate of expansion will also coincide. The derivative of the field with respect to N does not vanish, so N can be expressed in terms of φ and obtain the autonomous potential V(φ). It is not switched by an external clock: the moving field itself reaches new values. In the area traversed, both potentials coincide; on the one that has not yet been completed, they differ.

The positive S is significant here. Thanks to it, the field is already moving at today's point. We do not cause the field to suddenly move from exact rest to a smooth potential. In each model, its own law of motion and initial data determine a unique solution. Different futures result because different potentials lie ahead, not because the same equation arbitrarily selects an outcome.

So, a homogeneous background history coincides. For identical initial perturbations, their linear evolution also coincides, in which the first order in small amplitude is preserved: the potential and its derivatives along the common background are identical. Finite inhomogeneities can enter the region of potential differences before the background field. Therefore, the exact nonlinear equivalence is not established here; Complete quantum equivalence, including non-perturbative processes, has not been established. Positive kinetics and canonical propagation velocity also do not replace a complete stability analysis.

## Where futures diverge

In model A, the field density tends to positive Λ. The dust thins out, H approaches a constant positive value, and the expansion becomes asymptotically exponential. The integral of the future light path is finite. This model has an event horizon, although proper time continues indefinitely.

In model B, the function g tends to unity, and the difference between F and N tends to a finite constant. This follows from the fact that the deviation of g from unity decreases as the inverse square of N and has a finite integral in the distant future. Therefore, the additional factor in the density asymptotically behaves like the inverse cube a with a constant coefficient. The density A multiplied by it tends to Λ. This means that the density B itself, and along with it the total density, decreases as in

the dust model. The scale factor increases as time to the power of two-thirds, and the integral of the future light path diverges.

The field in model B grows unlimitedly: its derivative with respect to N tends to a positive constant. Consequently, the reconstruction does not rest on the final future point of the field, through which it would be necessary to separately continue the potential. For A there is a smooth analytical continuation of the potential near its positive minimum. In both models, the future is infinite in its own time. The difference between horizons is established by asymptotics, and not by the appearance of the final section of the drawn curve.

For illustration, we can take $\Lambda = 0.699$, $S = 0.001$ and $M = 0.300$ in units of today's critical density. Then both models are now accelerating, and the ratio of the field pressure to its density is close to minus one. These numbers are chosen for demonstration purposes and are not obtained by fitting to the data. The field density term decreasing like dust also does not make its disturbances dusty: the canonical field retains its own propagation rules.

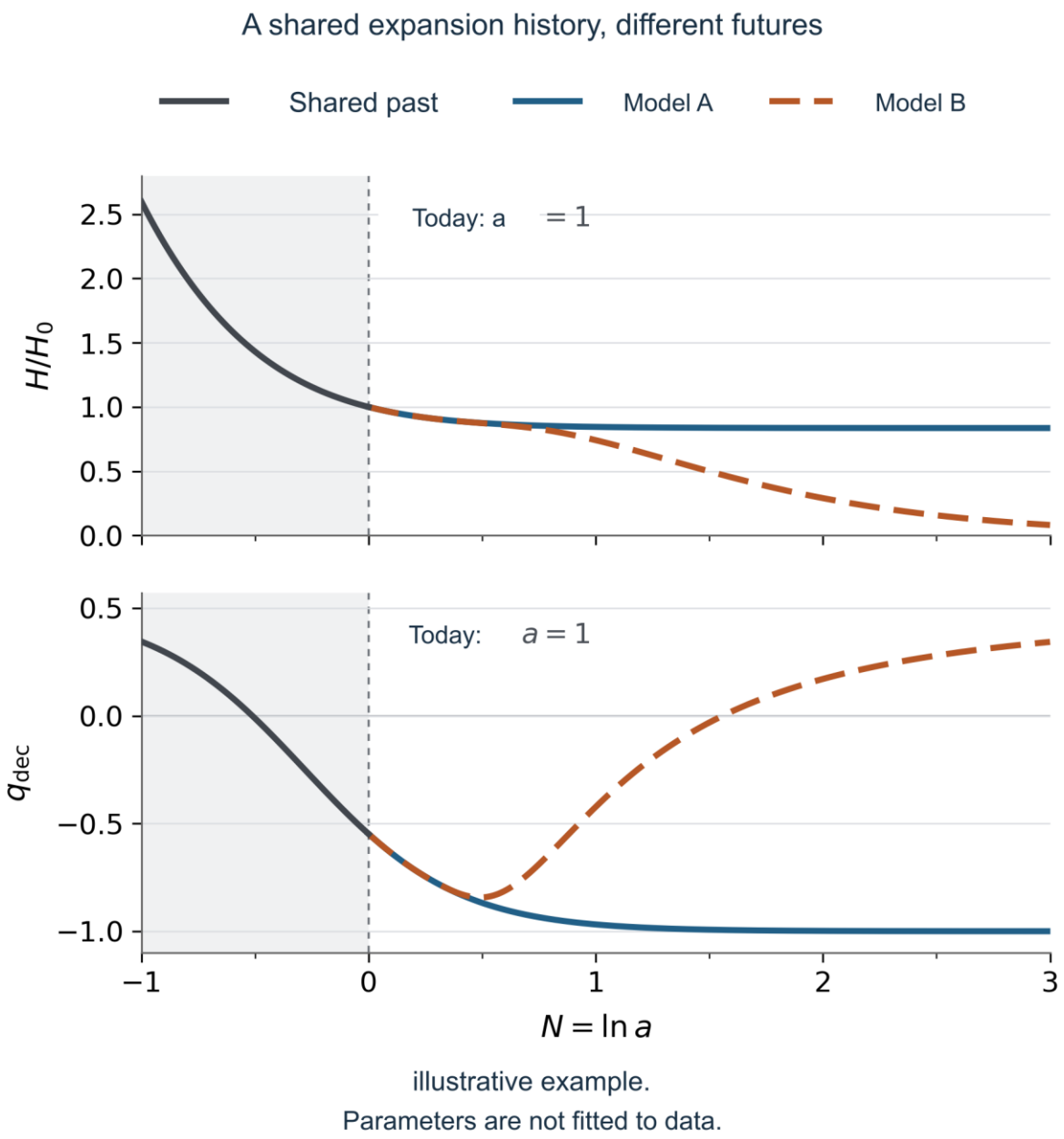



Figure 8. General past background story and two future sequels. The expansion rate $H/H_0$ and the deceleration parameter are shown as functions of $N = \ln a$. Model A approaches exponential expansion, Model B returns to deceleration. The parameters are for demonstration purposes and are not adjusted to observations.

Exact gluing has an important mathematical condition. Potential B is smooth, but is not real-analytic at the junction. For analytic functions, a match on an open interval of a connected domain would cause the continuations to coincide. Two functions of class $C^\infty$ can have the same value and all derivatives at a point, although the functions themselves differ to the right of it: the Taylor series is not required to restore a smooth function. If we require in advance that both potentials be globally analytic, this counterexample will be excluded by this additional requirement.

Thus, the construction verifies a certain statement: the general past background history, together with the coinciding linear dynamics, does not define a single future in the specified class of smooth models. It is not a new theory of dark energy and does not establish what continuation is realized by

nature. Even in a narrower analytical class, the ultimate accuracy of real data remains a separate problem: observations do not report the exact values of all derivatives.

## How to check it

The counterexample itself is first checked mathematically: from the reconstructed potentials, the field and Friedmann equations should be reintegrated with common initial data, the solutions with given densities should be compared, and the future asymptotics should be checked. This numerical reconciliation is for illustrative purposes; the exact coincidence of the past follows from the definition of the function, and the presence of a horizon follows from the convergence of the integral. Observations of the general past in the accepted background and linear description will not be able to choose between these two potentials.

For physical research, a given family of models is taken, which already differ over the available period of history. One set of parameters should describe the distances, rate of expansion and growth of the structure. It is tested against spectroscopic redshifts and BAOs, standardized supernova luminosities, and gravitational lensing. Calibrations, subject selection, material distribution, and early standard scale uncertainties are assessed together. It then calculates which future properties are stable across the remaining range of models.

An additional route is to re-measure the spectra of the same distant sources after a large time interval. The slow drift of the cosmological redshift tests the expansion dynamics over time for the observer. Loeb proposed to use, in particular, absorption in the spectra of quasars. This is a way to differentiate between models with different available expansion histories. For our exact pair A and B, the instantaneous drift calculated at today's point from the general history is the same. Future re-observations will be able to separate them only after a measurable discrepancy has arisen. [10]

What is needed is a long-term stable spectrograph, a reproducible wavelength scale, and comparison of multiple sources. Changes in spectral profiles, observer movement, local accelerations and instrumental drift are monitored. The idea is included in the scientific program of the ANDES spectrograph being created; there is no assumption here of a measurement already achieved or a guaranteed time frame for the result. Artificial shifts in the data and independent benchmarks should show how much drift is actually being recovered. [11]

If consistent observations rule out the behavior required by the model, its future prediction will lose basis. agreement will keep the forecast conditional on the continuation of the law. For an exact pair A and B, it is necessary to wait for an accessible discrepancy or to justify a narrower class of potentials by independent physics. The following calculation for a different family should show the residual signal difference after adjusting the interference and the probability of its detection at a given false signal threshold. In a drift measurement program, this is a function of observation duration, number of sources, and calibration stability. This calculation will separate achievable verification from future speculation.

Chapter 21

# How to pose a question to nature

At the beginning of the book, the question of a place for the world seemed almost geographical. It would be enough to move further away and see where its outer border is. It gradually became clear that behind this image were hidden various tasks: to determine the structure of space, to restore early history, to understand the composition of space and to establish the limit of available information. Each problem requires its own way of obtaining an answer.

Now you can assemble the research program. Its result should be a difference between predicted observations that remains after taking into account the actual equipment and alternative explanations. Some of the required data already exists. Other tasks will require new installations. In terms of questions, the first limitation remains the theory itself: it has not yet been brought to a computable consequence.

## When an idea becomes a task

The phrase “dark energy is changing” denotes a large class of possibilities. To carry out the test, you need to specify the field, its dynamics, connections with matter and initial conditions. The expansion history, disturbances, and possible laboratory effects can then be calculated. Narrowing the statement makes the conclusion limited in scope, but gives it certainty.

It is useful to write down four things: what model we are testing, what parameters should remain common, what exactly the instrument measures, and what results the model cannot explain. In the future, a description of the errors and the range of applicability are added to this. Such a document allows another researcher to repeat the analysis and check whether the original commitments remain after exposure to the data.

The conditions for failure of the calculation are also important. A model may become unstable, fall outside the bounds of an effective theory, or lose predictive power due to too many free functions. These are meaningful results. They occur before the sky comparison and show what additional physics is needed to continue working.

One should also distinguish between a successful description and a new prediction. If a function with a large number of parameters is fitted to a measured curve, the mere proximity to this curve does not test the explanation. A stronger test occurs where the parameters found determine another effect that was not used in the selection. That is why the requirement for common parameters for different observations runs through the book.

## One mechanism across several measurements

Let's take a scalar field that varies over cosmological times. If it is associated with the electromagnetic sector, its movement can influence atomic transitions. Distance history, clock comparison, and astrophysical spectroscopy then potentially explore different aspects of the same model. But clocks usually limit a combination of coupling strength and the rate of change of the field, rather than one universal constant that is the same for all possible theories. [158] [60]

This is where a specific research question emerges. Is there one region of potential and interaction parameters that reconciles cosmological background, irregularity growth, local frequency measure-

ments, and free fall tests? To answer, it is necessary to derive the corresponding connections, take into account the possible difference between the local field and the cosmological one, and calculate the composite dependence of the additional force. Otherwise, combining data will only create the appearance of a stricter restriction. [61]

A similar logic applies to early disturbances. A short change in environmental properties can leave features in the power spectrum and more complex correlations. We must compute both forms from one action or one selected state. Arbitrarily adding a squiggly curve to each statistic does not test the overall mechanism. There must be mandatory relationships between features that can be independently refuted. [89] [90]

For dark matter, a common parameter can connect completely different objects. The velocity dependence of self-scattering should work for ensembles of galaxies and dark clumps in lenses. The mass of the ultralight field and its cosmological fraction must coordinate the early suppression of structure and the late internal dynamics of stellar systems. Astrophysical histories vary, so overall microphysics is tested along with the distribution of these histories, rather than by requiring all objects to have the same profiles.

In the program for the origin of matter, one set of masses and interactions of new neutral particles must simultaneously pass laboratory restrictions and generate the desired asymmetry in a given early history. If the observed asymmetry is not included in the entire feasible set of allowed parameters, the chosen scenario fails. The discrepancy between one convenient point does not give such a conclusion. [51]

## What does it mean to distinguish between two models?

Suppose a device measures the speed of some process. Part of the result is due to the unknown background, and part is due to the new interaction, the magnitude of which we want to determine. The conditional model can be written as follows:

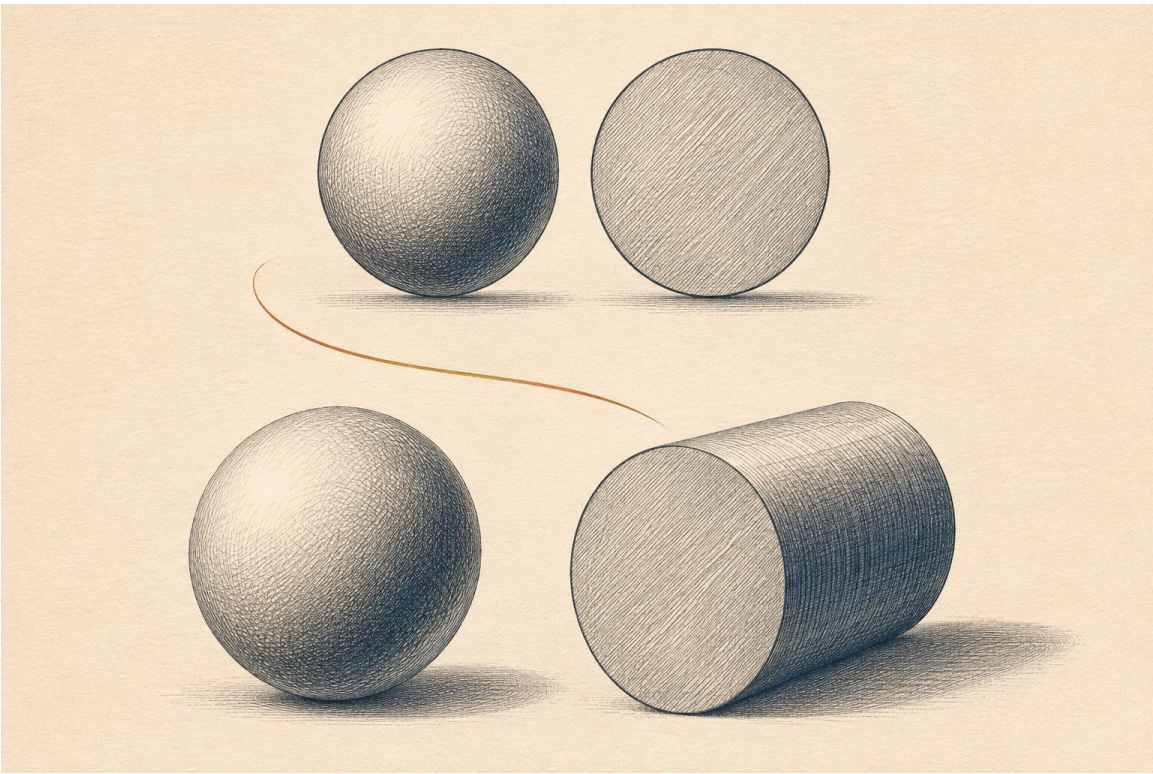
$$R_i = b_i + \eta s_i$$

R denotes the measured speed, b is the background, s is the calculated response to the selected setting, and η is the unknown strength of the effect. If each measurement is allowed its own unknown background, different values of η can be compensated for by varying b within the allowed parameter range. The instrument is capable of measuring R very accurately, but this accuracy alone will not separate the cause of the signal. The condition of non-negativity of individual contributions sometimes allows us to obtain a conservative upper bound for the effect, while maintaining the uncertainty of its actual magnitude.

Now add a physical control. Let two settings change s while the background remains the same to an independently established precision. Subtracting the results isolates the contribution of η because the shared background cancels. The real difficulty lies in that shared-background assumption. It is necessary to check whether switching settings changes the temperature, electrostatic coupling, readout efficiency, or another relevant factor.

This example shows the difference between a weak signal and an unidentifiable parameter. In the first case, additional precision can help. In the second, it is necessary to change the setup of the experiment, measure the background independently, or introduce a reasonable connection between the settings. The free unknown contribution cannot be eliminated by simply increasing the acquisition time.

For cosmological data, the same thing happens, although instead of counting rates, spectra, distances, and correlation functions are considered. Different physical parameters can compensate for each other's influence. Additional observation is useful when it depends differently on these parameters. Two very precise measurements of almost the same combination can leave the main question unanswered.



Engraving 28. New measurement angle. Two different shapes can produce a similar projection from the same viewing direction. The additional angle reveals a difference that is not eliminated by the sharpness of the previous image alone. This geometric analogy explains the degeneracy of parameters: the usefulness of a new experiment depends on what combination of physical causes it allows to test.

The redshift drift calculation in chapter 8 gives a numerical example. For the same $H_0$ and matter fraction, the scalar field noticeably changes the predicted shift. But the model with the cosmological constant approaches the same curve if we allow it to have different values for these parameters. This is not a reason to select new values of $H_0$ according to the illustrative plot. This is an indication of what independent data should be included in the overall analysis. Once they are added, the compensating adjustment must pay for its disagreement with measurements of the distances and composition of the Universe.

## What measurement should you take next?

Once degeneracy is found, the next question concerns a new observation. You need to understand what part of the uncertainty it removes. If two measurements are sensitive to the same combination of parameters, an increase in accuracy may make little difference in model comparisons. Another measurement, quite crude in itself, can limit precisely the freedom thanks to which a competitor reproduces previous data.

The computational supplement clarifies which independent measurements could constrain compensating parameter adjustments. At eight selected redshifts, we profile the cosmological-constant model over $H_0$, $\Omega_{m0}$, and a common velocity offset B, using the fully specified covariance. Over a twenty-year interval, with an independent error of 1 cm/s and a correlated mode of 0.5 cm/s, the profiled discrepancy Q is 0.316615. A hypothetical external constraint $H_0 = 70 \pm 1$ km/s/Mpc raises it to 1.565071; a separate constraint $B = 0 \pm 0.1$ cm/s yields only 0.331525. Applying both gives 3.420077. This demonstrates how constraints complement one another within this setup; it does not rank actual instruments.

Q here measures the residual dissimilarity of two predictions without added noise after adjusting the allowed parameters and taking into account conditional external constraints. It cannot be converted to sigma without separately defining the statistical criterion, generating the data, checking the false decision rate and power. To select the next real experiment, one will also need cost, achievable accuracy, dependencies of systematic errors, and the possible dependence of external estimates of $H_0$ on the cosmological model itself being tested.

In this calculation, the external constraints are specified as independent Gaussian measurements centered on the input values. The random noise is not playing out yet. Therefore, the Q gain speaks to the geometry and weight of the constraints, but does not establish the error rate in real data. Before transferring the result to an observational project, it is necessary to create ensembles of artificial catalogs from both models and test the procedure with a pre-selected decision rule.

The usefulness of a project can also be determined through the expected change in model probabilities. This Bayesian test is described in the mathematical appendix, but it will require parameter distributions, competitor probabilities, and a complete data model. It does not coincide with the profiled divergence of the average curves. Separating these two tasks allows you to gradually increase the complexity of the study while maintaining clear control over each step.

The map obtained from the hypothetical example gives direction for the next work. One may ask what is more beneficial in the announced budget: a new redshift range, a longer interval, an independent absolute scale, or better calibration. The answer cannot be chosen in advance. It depends on the sources available and on how errors change with the experimental design. In the next chapter, we will look at what part of this calculation can be transferred to AI and how to check its result.

## Three research problems

The first problem concerns a brief event in the early Universe. It is necessary to choose two fully defined models: for example, a short change in the speed of propagation of disturbances and a specific excited initial state. The first step is to establish a region where their normal spectra are close within the limits of available accuracy. After this, calculate the differences in bispectra and polarization predictions, transfer them through further cosmic evolution and the observation model. The result should be a range of parameters within which the additional statistics actually differentiate mechanisms.

In such a project, it is necessary to fix in advance the control forms and the method of taking into account frequencies, phases and other parameters being sorted out. The feature found after extensive search requires appropriate statistical calibration. Even successfully distinguishing this pair of models will not prove the uniqueness of the explanation among all conceivable theories. It will give a narrower, but reproducible result about the two declared mechanisms.

The second problem connects the microphysics of dark matter with two populations of objects. Having chosen the dependence of the self-scattering cross section on velocity, one should construct the distribution of halo histories and simultaneously calculate the kinematic and lens characteristics. Some objects are used to determine parameters, and some are used for independent verification. The most important result here is the ability to predict the distribution of new observations, including the scatter, and not just the average success curve.

If the distribution of stories turns out to be too loose, you need to find out what additional observations are limiting it. Data about the stars, gas and environment can reduce this uncertainty. An increase in the number of parameters is permissible only together with an assessment of how many new observed connections are retained. Otherwise, the hypothesis of a unified microphysics will remain a formal superstructure over the independent fits of each object.

The third problem continues the calculation of the scalar field from chapter 8. The restored potential should be included in a complete model of perturbations and connections with ordinary matter. Distances, structure growth, frequency relationships, and expected violations of free-fall universality must then be jointly calculated. For a connected dark sector, it is necessary to take into account the energy exchange already at the level of background equations and disturbances. You cannot automatically use unrelated field formulas for it.

The same problem includes the following calculation for the redshift drift. We need to replace the notional eight measurements from the app with a real list of absorbers and spectral transitions, determine the accuracy for each of them, and relate the calibration errors between epochs. The maximum difference between the two fixed curves was about z=0.78; conventional ground-based optical spectroscopy of the Lyman-α forest operates at substantially higher redshifts. Therefore, you cannot simply order more time on one device. Combinations of optical and radio measurements, the benefits of independent constraints $H_0$, and those directions for improving accuracy that actually reduce degeneracy should be compared. [14] [13]

A separate part of this work will be checking physical stability and acceptable continuation of potential. Our Gaussian illustration shows why a locally successful history does not guarantee regular continuation over the entire range of the field. A good result will be either a consistent model domain with a declared scope of applicability, or a proven inability to fulfill its obligations. The complete program and mathematical conventions are collected in the appendices.

All three tasks require, first of all, calculations and analysis of already available data types. More distant programs are associated with new measurement modes. For gravitational entanglement it is necessary to combine a sufficiently large gravitational phase with control of non-gravitational interactions and loss of coherence. For redshift drift, maintain a comparable frequency scale between time-separated observations. To search for topology, calculate the total covariance of signals with real masks and noise. In each case, the technical goal is determined by the shape of the expected signal.

## How to check it

The research procedure itself needs to be checked. First, a set of artificial data is created in which the true model is known. It includes noise, selection, observation mask, and realistic systematic effects. The analysis is performed in the same way that it is intended to be applied to the real data. Such an experiment shows how often the method declares an effect where there is none, and how often it misses a signal that is actually present.

Testing on an erroneously specified background model is especially useful. One can add a controlled calibration error, change the distribution of astrophysical histories, or introduce unplanned noise correlation. If the procedure confidently calls each such effect new physics, its sensitivity is not meaningful enough. It is necessary to either expand control observations or honestly limit the scope of inference.

Next, part of the observations is saved for verification, which was not involved in the selection of parameters. The division rule is selected before viewing the desired effect. For coupled cosmological data, simple random division of catalog rows may not be sufficient: general calibrations and large-scale modes preserve the dependence. The actual statistical structure of the data must be taken into account.

The null result should be accompanied by a sensitivity map. It indicates which amplitudes and parameter ranges could be detected and which remained virtually indistinguishable from the background. A positive result must withstand independent processing, changes in valid taxonomy models, and testing of additional mandatory implications. A single convenience value of statistical significance does not replace this work.

Finally, you need to make the result reproducible: save model versions, normalizations, input data, selection conditions and code. The computational package contains programs for redshift drift, uniform wave transfer and oscillatory control. Additional programs test background reconstructions, growth, phase dynamics, and scale translations. For the remaining examples, the mathematical appendix specifies formulas, inputs, and output boundaries. The kit allows you to repeat the listed checks and distinguish them from observations that have not yet been analyzed.

This is what a small step beyond the edge of knowledge looks like. First, the formulation of the question changes: new variables appear, a different relationship between observations, or a previously unexplored class of models. This step is then given a form in which it can encounter data resistance. The most valuable continuation of the book will begin where one of these calculations provides an answer that we did not foresee in advance.

Chapter 22

# Cosmology with AI

A research book can pass on more than a set of ideas to the next generation. It is able to leave problems with defined inputs, scope, control answers, and clear failure conditions. Then the scientist working with the artificial intelligence starts with a testable foundation. He can change the assumption, see which conclusion disappears, and decide what calculation or measurement really needs to be done next. Such a foundation allows you to accumulate results without turning each new attempt into a repetition of all previous work.

In this chapter we take a first limited step. For the redshift drift, a discriminability map of two given cosmological models was made. For early disturbances and dark matter, the following problems have been formulated, but have not yet been brought to the analysis of observations. The artificial intelligence was not trained on these tasks within the scope of the book; assessments of the accuracy of neural networks and claims about the discovery of new physics are absent here. A research design is proposed in which each subsequent improvement can be compared with an open benchmark calculation.

## Three different roles of artificial intelligence

The first role is that of a research assistant. The system searches for the required definition, suggests a transformation of the equation, writes a program, lists possible degeneracies and selects a counterexample. The useful result of this work should exist separately from the dialogue: in the form of output, code, a table, or a document indicating the underlying assumptions. If the text seems convincing, but the calculation cannot be reconstructed from it, it has not yet become a scientific result. The speed of preparation of such a text does not say anything about the correctness of the physical model.

A simple check procedure is needed here. First, the question and acceptable approximations are fixed. Dimensions, signs, limiting cases, and conservation of general parameters are then independently checked. The program is then compared with the answer obtained by another method. AI can suggest all these actions, but the test should not consist of asking the same system again whether it agrees with its own answer. A more reliable computable commitment: when a new interaction is turned off, the known limit must be restored with a given numerical accuracy.

The second role is the emulator. The full numerical solver receives the physical parameters and calculates the observed quantity; the emulator learns to quickly approximate this display. Its input can be the component densities and parameters of the initial spectrum, and the output can be a set of power spectra. Acceleration is especially useful when the same type of calculation needs to be repeated many times. However, a new theory, a new parameter range, or a different instrument model may move the problem beyond the training set. agreement within the former area does not automatically transfer there.

The third role is solving the inverse problem of simulations, simulation-based inference, or SBI. The simulator creates possible observations given the given parameters; the trained model approximates the connections between parameters and data necessary for inference. It can estimate the posterior distribution, likelihood function, or likelihood ratio when direct calculation of the desired value

is difficult. This family of methods is associated with a specific data generator and a set of assumptions. An overview by its developers explains which inverse problems open up this possibility. [159]

Confusing these roles creates false expectations. Well-written code does not yet test the emulator; an accurate emulator does not yet check the physics of the original solver; A careful restoration of the parameters of the artificial Universe does not yet show that the real Universe is structured the same way. In our problem set these levels are separated. For each, the required inputs, the controlled error and the result, which can be considered completion of the work, are indicated. This allows the use of different AI systems without changing the meaning of the research task itself.

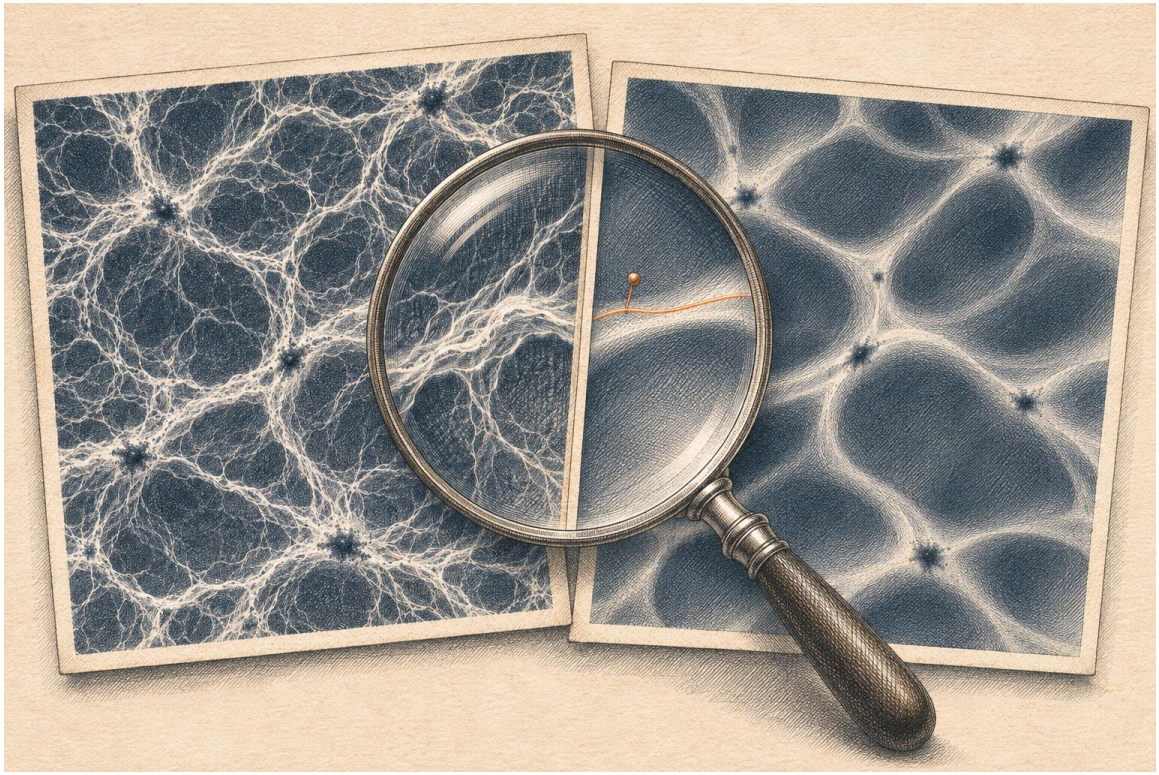
## Speed up calculations and preserve physics

A practical example of emulation is given by CosmoPower. The paper on the complete cosmological emulation and inference process discusses the preparation, packaging, and testing of approximate solvers for specific models and parameter ranges. A useful principle for our book here is that along with a fast predictor, information about what it approximates and where it has been tested should be shared. Using a ready-made emulator does not mean that an arbitrary new scalar field is already included in its training. Such an extension will require new reference calculations and separate verification. [160]

The control we propose begins with a selected sample of points that the training did not see. On it, you need to measure the error in the predicted observations, and then check how much this error shifts the conclusion about the physical parameters. A rare large error near the boundary of the allowed region may be more significant than a small average error over the entire volume. Therefore, the distribution of errors and specific cases of failure should be published. If the emulation accuracy is insufficient, the disputed point must be recalculated by the original solver and the difference must be stored in the verification log.

Another useful example is the CAMELS project, in which simulations relate changes in cosmological parameters to changes in astrophysical prescriptions. The original work compares hydrodynamic realizations with different descriptions of the processes of galaxy formation and evolution. This shows the practical possibility of studying the dependence of the output on cosmology and astrophysics simultaneously. For the program proposed here, such sets serve as a model for organizing an experiment. We did not train the algorithm on CAMELS and did not obtain new restrictions on dark matter from this project. [161]

In future work, some of the implementations should remain entirely outside the scope of training. It is important to separate samples not only by random initial numbers, but also by physical requirements, if it is the resistance to them that is being tested. An algorithm that works successfully with new implementations of the previous simulator may make errors after changing feedback from stars or active cores. This transfer should be checked separately. However, several consonant simulators do not cover all possible errors: they may use the same approximation, which is not present in nature.



Engraving 29. Fast calculation and accurate standard. Two conventional images of the structure are compared as a reference calculation and its fast approximation. The highlighted area reminds you to check for local errors, including rare cases of failure. The engraving does not represent the results of AI training in the book: it explains the future procedure for comparing the emulator with the original computer.

## Why proper calibration is not enough

Bayesian inference connects the selected model, data, and prior information. If the physical parameters are denoted by θ and the observation by x, then its usual notation is:

$$p(\theta \mid x, M) = \frac{p(x \mid \theta, M)\, p(\theta \mid M)}{p(x \mid M)}$$

The M symbol is significant here. It includes a physical description, an observation generator, and error conventions. Even a perfect calculation of the right-hand side remains conditional with respect to M. For a new cosmological hypothesis, it is necessary to separately study the computational accuracy of the method and the sufficiency of the model itself. Otherwise, a narrow parameter interval may express confidence within an overly restricted family of artificial worlds. The suspicion of such an effect is verified by expanding the setup and independent observations, and not just by increasing the training sample.

Simulation-based calibration, SBC, proposes to control the algorithm on parameters and data generated from a declared joint distribution. It is checked whether the position of the parameter that generated the data among the posterior samples is consistent with the expected rank distribution. The method is useful for finding computational errors. But successful calibration against a given simulator does not establish the physical truth of that simulator and does not guarantee good behavior in every small parameter range. It is the boundaries of this conclusion that should accompany the result of the test. [162]

The work of Alokda, Porciani and Eggemeier on the derivation of primary non-Gaussianity examines a specific example where average coverage testing alone is not sufficient. The authors compare the neural network method with explicit likelihood inference and consider the behavior of distributions for fixed parameters. In the cases studied, combining the power spectrum and bispectrum could produce wider neural network distributions than the explicit likelihood inference used, although the usual average test did not reveal the problem. This is the result of a certain comparison of methods; it is not evidence of the overall failure of SBI, nor does it constitute a test of transfer between different simulators. [163]

For our purposes, this implies a specific requirement for the future protocol. It is necessary to separately check the recovery of parameters in different areas, sensitivity to the boundaries of the prior distribution, and behavior when combining statistics. Predictive tests should also be performed on features that were not used during training. Finally, testing on a different error model or a different physical generator is required. Such a test examines resistance to a declared nonconformity; even its success leaves the possibility of an unknown common error among all selected generators.

## Map of distinguishability of two worlds

Before training a complex system, it is useful to solve a simpler problem: is there a difference in the selected observations that cannot be absorbed by parameter tuning? In the chapter on dark energy, an example of a scalar field with a brief deviation of the equation of state from the cosmological constant is constructed. Its drift prediction without added noise is now compared with the ΛCDM family of models. Eight points are located at z = 0.25; 0.5; 0.75; 1; 1.5; 2; 2.5 and 3. This is a fictitious grid and not a list of actual spectroscopic targets.

In the competing model, $H_0$, the fraction of matter $\Omega_{m0}$, and the total additional shift B vary freely. The parameter B represents the unknown constant component of the velocity displacement. In addition to the independent error of each point, one correlated mode is introduced, depending on the redshift. Its shape and amplitude are announced in advance. Therefore, you can reproduce the result and then see how much it changes with a different covariate. The assumption of correlations is part of the problem, not a hidden setup of the calculation.

$$C_{ij} = \sigma^2 \delta_{ij} + \tau^2 u_i u_j, \qquad u_i = \frac{z_i - \bar{z}}{\max_j |z_j - \bar{z}|}, \qquad \tau = 0.5 \ \mathrm{cm/s}$$

The independent error σ refers to the accumulated velocity shift and is the same for all eight points. A correlated mode describes a random amplitude with zero mean and a Gaussian distribution. Its effect is already included in C. Free B acts equally on all points; it differs from the centered non-uniform mode u. The covariance is considered known and does not change when selecting cosmological parameters. A real instrument will require a more complex description, which must be derived from the characteristics of the spectra and control of the stability of the measurements.

Let y be the vector of shifts without the added noise of the scalar model, and fΛ the prediction of the model with the cosmological constant. For each combination of accuracies, the minimum squared discrepancy is calculated. Additionally, you can specify a conditional independent external Gaussian constraint $H_0$ with center 70 km/s/Mpc and width sH:

$$Q_* = \min_{H_0,\Omega_{m0},B} \left[ \left(\mathbf{y} - \mathbf{f}_\Lambda - B\mathbf{1}\right)^\mathsf{T} C^{-1} \left(\mathbf{y} - \mathbf{f}_\Lambda - B\mathbf{1}\right) + \frac{(H_0 - 70)^2}{s_H^2} \right]$$

Without an external constraint, the last term is missing. This formula uses a well-known profiling method, and the novelty of the exercise lies in the specific formulation and calculated results. Q shows how much dissimilarity remains after adjustment. It is not a sigma number, probability of detection, or expected information gain. For such conclusions, another calculation is needed: random data from both models, a predetermined decision rule and a check of the frequency of its errors. Here only the deterministic stage is performed.

For twenty years at σ = 1 cm/s, Q = 0.316615 was obtained. The fitted Λ-model selects $H_0$ around 55.66 km/s/Mpc, $\Omega_{m0}$ around 0.3232 and B around 0.2403 cm/s. These numbers are not estimates of the parameters of the real Universe. They show how, by changing the allowed parameters, the alternative model approximates the selected curve. The conditional limitation $H_0 = 70 \pm 1$ km/s/Mpc increases the minimum to Q = 1.565071: the previous compensation becomes too expensive for the accepted functionality.

The result of joint verification is especially useful. If we separately limit B to the value $0 \pm 0.1$ cm/s, we only get Q = 0.331525. If we add the same constraint to the external $H_0$, we get Q = 3.420077. This means that the effect of calibration depends on what other freedom of adjustment has already been eliminated. In this problem, two constraints complement each other. This behavior cannot be inferred from a list of precisions in isolation; it has to be calculated for the joint model and the general error system.

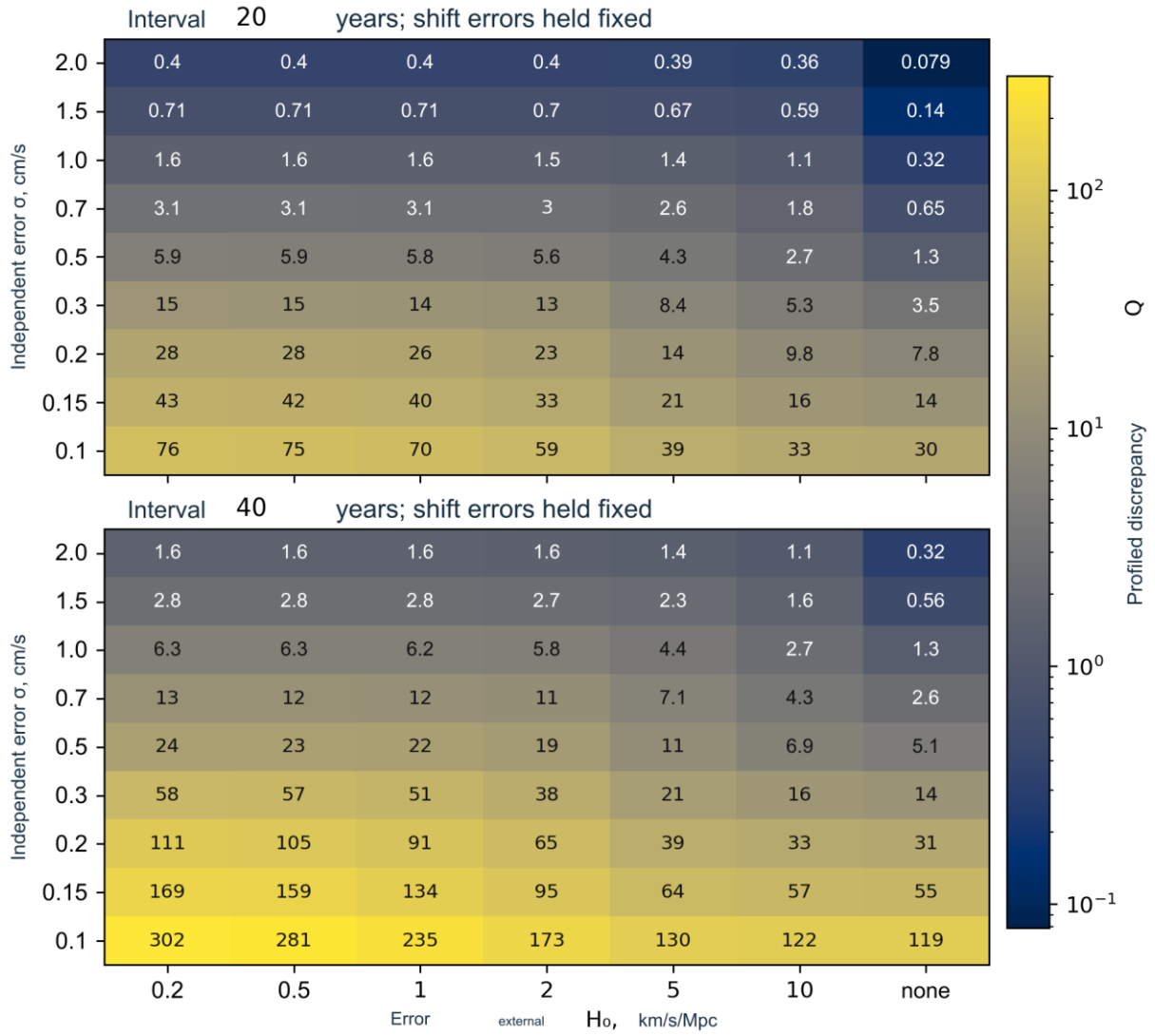



Figure 9. Profiled divergence map Q: two observation durations, nine independent σ errors, seven external constraint options $H_0$. The correlated amplitude τ = 0.5 cm/s is fixed; "no" means no external limit $H_0$. When moving from 20 to 40 years, the errors in the accumulated velocity shift are preserved. This is a conditional map, not a forecast of the device; Q is not statistically significant. Full values and assumptions are available in the computational appendix.

A total of 126 combinations are calculated, and additional comparisons also include the conditional constraint $\Omega_{m0} = 0.3 \pm 0.01$. When moving from twenty to forty years, the covariance of the velocity shift is artificially preserved. Without external restrictions, Q therefore increases exactly fourfold: the signal and the optimal B double, the quadratic measure increases fourfold. This is a useful check of the program. The actual benefit of long-term observation may differ due to instrument aging, sampling changes, error correlations, and costs of repeat spectroscopy.

With σ = 0.2 cm/s, a twenty-year calculation without external restrictions gives Q = 7.795838, and with the specified limitation $H_0$ - 26.349304. The numbers are useful as a control of playback and an indication of the production's sensitivity to accuracy. They do not determine the required accuracy of the future telescope. To do this, we need to include spectral lines, accessible objects, the sources' own accelerations, the calibration procedure, and the likelihood of obtaining different results. The real outer measurement of $H_0$ may also depend on cosmology and share systematic errors with the underlying data.

## How to choose the next experiment

The discrepancy map helps to find directions, but does not select the optimal experiment. It considers one given scalar prediction and does not average over unknown parameters, candidate data, or observation costs. The next step is to identify a variety of feasible plans: for example, improving instrument stability, expanding the redshift range, or independently constraining a parameter. For each plan, errors, resources, and acceptable physical models must be described in the same way. Otherwise, the comparison will be reduced to the advantage of arbitrarily chosen assumptions.

One well-known way of making this choice is through expected information gain. If the goal is to distinguish between models, the utility of a design can be defined as the average change in the probability distribution of their index after an eventual measurement. Bayesian planning requires prior model probabilities, parameter distributions, and predictive distributions of the data. Methods for approximate calculation of such utility are explored, in particular, by Foster et al. In our code this value is not calculated; the calculated map Q does not replace it. [164]

## Three tasks for an open continuation

The first task already has a working narrow standard: to reproduce the drift map and its control values. Its next level is the same analysis of noise implementations for each competing model. The accelerator can then be trained, compared to the direct calculation, and tested for transfer to new covariances. The physical layer will require realistic spectra and accessible objects. An AI system is considered useful if it reduces computational costs with a pre-declared acceptable error or finds a specific previously missed degeneracy that can be confirmed by an independent calculation.

The second challenge concerns early features. It is necessary to select a completely defined pair of mechanisms and find the region where their power spectra are close after an acceptable adjustment. Bispectra and observed polarization consequences are then calculated from the same parameters. You cannot allow each statistic to have its own independent form of singularity: then the test of single origin disappears. In an open set this is still a specification. We need a correct generator of primary disturbances, transfer to observable quantities and general covariance; The book does not contain such a full-fledged analysis.

The third problem connects populations of objects with the general microphysics of dark matter. For the chosen law of self-scattering, it is necessary to simultaneously predict the properties of ensembles of galaxies and clumps detected by gravitational lenses. The comparison must take into account the distribution of formation histories and astrophysical feedback. Part of the population is left for independent testing, and the interaction parameters are kept common. This task is also written as a specification. It cannot be turned into a constraint on the scattering cross section until a proven generator, selection model, and suitable observations are obtained.

## Checking Mathematical Sense

Another possible AI assistance is to translate individual statements into a form that can be verified by a proof system. The HepLean project shows examples of formalizing the definitions and derivations of high energy physics in Lean. FormalScience's work examines automated formalization with human participation and specifically focuses on preserving the meaning of the original task. For a book, a reasonable first step is limited: formally verify the chosen algebraic lemma or corollary of the

stated assumptions. A complete formalization of cosmological models has not been completed here. [165] [166]

Even a successful formal test operates within the written definitions. If during translation the condition of positive energy has disappeared or the meaning of the observed quantity has changed, the proof may be logically correct and physically inapplicable. Therefore, along with the formal statement, it is necessary to store the original record, the correspondence of notations and the scope of applicability. Numerical verification of limiting cases and formal proof have different objectives. Numerical checks were performed in the drift calculation; to call them a machine proof of the entire physical structure would be incorrect.

## How to check it

The test begins with reproducing the standard. An independent researcher runs the published code, obtains the Q table, and compares it to the benchmark numbers. Then it checks the profile with another optimizer, turns off the correlated mode and restores the previous independent case. For our implementation, such a comparison has been made: at four control points the difference in minimums is less than $3 \times 10^{-13}$. An exact quadruple change in Q without external constraints when doubling the interval tests the adopted scaling model. These results refer to calculation, not to nature's confirmation of a scalar hypothesis.

The next level requires pre-announced tests on artificial data. A rule for distinguishing models must be defined, observations must be generated from both sides of the comparison, and the rates of mis-selection and omission of differences must be measured. For trained methods, accuracy relative to the direct solver, behavior in different parameter ranges, and results under modified physical prescriptions are separately checked. The training, validation, and final test sets must have fixed boundaries; learning the last set to tweak the method turns it into another part of the training.



Engraving 30. Checking on deferred data. Separate sets of conventional cosmological maps represent training, intermediate testing and final testing. The last set remains closed to configure the method. This is an image of a research discipline, and not a ready-made protocol for dividing a real catalog: common calibrations and physical dependencies of data require separate consideration, even when the sheets are depicted separately.

At the physical level, a measurement with a verifiable instrument model and independent control of significant uncertainties is required. For drift, this means a stable spectroscopic scale and a description of the sources; for early features - joint analysis of statistics with transfer and foregrounds; for dark matter - accounting for populations and selection. The next researcher can start at any level, but must name it. A scientific contribution occurs where a new test is performed, a persisting difference is discovered, or a limitation is proven that the previous formulation had hidden.

# Epilogue

The world does not have to take up space inside another world. Spatial geometry can be determined by internal dimensions, and questions about its origin require physical models and observable consequences. Our research began with this change in the usual setting. By the end of the book, it made it possible to connect distant problems: the shape of space, the properties of particles, the direction of time and the fate of cosmic expansion.

Some answers turned out to be more reliable than the initial impression of an unusual topic. The hot history has several independent supports. The distinction between horizon and edge is given by precise definitions. Mathematics allows for finite spaces without walls. These results don't disappear just because other questions in cosmology remain open.

Elsewhere it has become clear how much depends on the continuation of the pattern. Based on the observed past, one cannot arbitrarily assign a single future. A successful geometric design in a certain theoretical regime still requires a bridge to our Universe. A possible trace of an early event needs to be compared with mechanisms that are capable of producing similar data. Each such limit shows a specific place for the next study.

The general parameters were especially useful. The same field mass must act in early space and in late stellar systems. One radius of hidden space defines several physical scales. One model of the new particles must withstand laboratory constraints and produce a valid cosmic history. The more independent commitments a hypothesis makes, the more meaningful its success or failure.

However, failure does not necessarily mean an error in the very design of the study. The lack of a common parameter range, the inability to distinguish between two mechanisms with a given device, or the instability of a convenient solution are certain results. They free further work from false certainty and show which condition needs to be changed in a meaningful way. The new version of the model receives new commitments, which are checked again.

This logic persists even in the most daring questions. Possible other cosmological regions, emergent space, or the quantum structure of gravity become part of the physical program once the dynamics and effect available have been determined. Before this, they can direct the thought, but the power of the conclusion remains different. The more unusual the idea, the more useful it is to be able to name a specific observation after which you will have to abandon it or significantly change it.

We tend to picture the advance of knowledge as an expanding map: another object, a more distant galaxy, an earlier epoch. Sometimes progress does take that form. At other times, the very quantities used to construct the map change. It becomes possible to connect different measurements, or we discover that an earlier question combined incompatible definitions. A new result may then begin with a small mathematical correction that changes the meaning of a large, familiar claim.

Computational examples make this boundary tangible. Two models that differ markedly for fixed parameters become closer after fitting them. Calibration, almost useless on its own, becomes important when combined with independent measurement. Quantum and classical systems can coincide in the initial distribution and diverge in its development. Each result tells what assumption held the previous conclusion and where to look for the next meaningful test.

Some of the tasks proposed in the book can be continued now: to calculate the distinguishability of two early mechanisms, to test the general model of dark matter on an independent sample, to con-

nect the cosmological field with precise laboratory restrictions. Others require a lot of work on instruments and theory. For all of them, one criterion of progress remains: whether it becomes clearer which possible arrangements of the world are compatible with what nature allows us to measure.

Perhaps the next picture of the universe will use concepts that seem irrelevant today. Perhaps familiar space and time will remain as an extremely accurate approximation. The decision will depend on what connections can be derived and verified. The place required for research is primarily between the formulated hypothesis and the as yet unobtained result of experiment.

**Appendix A**

# Calculations and limits of their applicability

This appendix covers computational examples of the main text: assumptions, formulas, inputs, and output bounds. The numbers are not a new treatment of observational catalogs. The parameters of the illustrative models are chosen explicitly; Agreement with a particular value does not mean agreement with all the data. The procedure for launching programs is given in the accompanying instructions for the calculations.

The field formulas use units c=$\hbar$=1 and the reduced Planck mass $M_{pl}$. Distance formulas retain the speed of light c explicitly. Today's scale factor is set to unity, N=ln a; a prime denotes differentiation with respect to N unless otherwise stated. Identical letters in different examples do not imply a shared physical model: each example begins with its own assumptions.

## Age and three different distances

Let's take a flat model with a non-compact spatial topology $R^3$, non-relativistic matter, an effective radiation component and a cosmological constant. Here $H_0$=67.4 km/s/Mpc, $\Omega_m$=0.315, $\Omega_r$=0.000092 and $\Omega_\Lambda$=0.684908. The extension function looks like:

$$E(a) \equiv \frac{H(a)}{H_0} = \sqrt{\Omega_r a^{-4} + \Omega_m a^{-3} + \Omega_\Lambda}.$$

This is a convenient analytical model, and not an exact reproduction of the Planck calculation. In particular, the transition of massive neutrinos from relativistic to non-relativistic behavior is not modeled here. The age and radial comoving distance are obtained from different integrals: the first sums up the proper time of the cosmological observer, the second - the path of the light signal in the comoving coordinate. [4] [6]

$$t(a) = \frac{1}{H_0}\int_0^a \frac{d\tilde{a}}{\tilde{a}E(\tilde{a})}, \qquad D_C(z) = \frac{c}{H_0}\int_{1/(1+z)}^1 \frac{d\tilde{a}}{\tilde{a}^2 E(\tilde{a})}.$$

The lower limit of zero means the selected continuation of the hot model. It does not prove that such a description applies to an absolute beginning. At z=1, the travel time of light is 7.950 billion years, today's comoving distance is 11.092 billion light years. The proper distance at the moment of emission is 5.546 billion light years; in this flat model it coincides with the distance along the angular diameter. The luminosity distance is 22.185 billion light years. Different values correspond to different ways to specify the distance.

$$D_A = \frac{D_C}{1+z}, \qquad D_L = (1+z)D_C.$$

For a model continuing indefinitely into the future, the present radii of the particle horizon and the future event horizon are written as follows. The event horizon exists only if the corresponding integral converges. [1]

$$R_{\mathrm{p},0}=\frac{c}{H_0}\int_0^1\frac{da}{a^2E(a)},\qquad R_{\mathrm{e},0}=\frac{c}{H_0}\int_1^\infty\frac{da}{a^2E(a)},\qquad R_{H,0}=\frac{c}{H_0}.$$

Numerical integration gives an age of 13.791 billion years and radii 46.133, 16.679 and 14.507 billion light years, respectively. Each number has its own question. Hubble's radius depends on today's expansion rate; the event horizon is also from the future that we assumed. Changing the future expansion law can change the second integral, preserving all available past history.

## Reconstructing the scalar-field potential

The reconstruction begins with the function q=1+w, positive for the canonical field under consideration. Let $u=\varphi/M_{pl}$, $S=\rho_\varphi/(3M_{pl}^2H_0^2)$, $U=V/(3M_{pl}^2H_0^2)$. For a flat model with dust $\Omega_{m0}=0.3$, without radiation, we set a smooth profile:

$$q(N)=A\exp\left[-\frac{(N+b)^2}{2s^2}\right],\qquad A=0.25,\quad s=0.2,\quad b=\ln 1.5.$$

When S(0)=0.7, the law of conservation of energy and the Friedmann equation allow us to find the density, field trajectory and potential energy. The positive sign of the field velocity is chosen. This reconstruction method has known previous applications; its use in the book is not claimed to be a new method. [157] [59]

$$S'=-3qS,\qquad E^2=0.3e^{-3N}+S,\qquad u'=\sqrt{\frac{3qS}{E^2}},\qquad U=S\left(1-\frac{q}{2}\right).$$

The resulting parametric dependence U(u) is then checked by inversely solving the equation of motion. Substituting a given w back into the identity would be too weak a test. Therefore, the Klein–Gordon equation with the restored potential is separately integrated:

$$u''+\left(3+\frac{E'}{E}\right)u'+\frac{3U_{,u}}{E^2}=0.$$

During the numerical verification, the potential was restored on grids of 12 001 and 24 001 points, after which the Klein-Gordon and Friedman equations were separately integrated. In the area $0\le z\le 3$, the maximum absolute difference w did not exceed $2\times10^{-11}$, the relative difference H - $4\times10^{-12}$. The minimum potential was found at $z\approx0.199002$; Today the field is already rising along a small section of it, consuming kinetic energy. Negative potential curvature in a different range does not in itself mean negative kinetics or gradient instability.

Testing for small changes in homogeneous initial data is useful, but does not replace the analysis of all spatial disturbances. There is also a more serious limit: the literal continuation of the same Gaussian profile into an unlimited future leads to a finite limiting value of the field and divergent curvature of the potential. When $N\to\infty$ it turns out:

$$\frac{V_{,\phi\phi}}{H^2}=-\frac{(N+b)^2}{4s^4}+\frac{3(N+b)}{2s^2}+\frac{1}{2s^2}+o(1).$$

The limit point is reached only at infinite time. This is not a prediction of a catastrophe tomorrow, but a defect in the exact global continuation of the chosen function: a potential with a continuous second derivative cannot be drawn through this end. In the book, such a result is used to select suitable hypotheses, rather than hiding behind a good match on a finite interval.

If the field is linearly related to electromagnetism, we set $\Delta\alpha/\alpha=\zeta(u-u_0)$. Then the laboratory clock limits the product of the coupling ζ and the current field velocity:

$$\frac{\dot{\alpha}}{\alpha} = \zeta H_0 \sqrt{3\Omega_{\phi 0} q_0}.$$

With $H_0$=70 km/s/Mpc and $\zeta=10^{-6}$, the selected profile gives about $1.86\cdot10^{-17}$ per year. This is a specific example forecast. From the drift constraint α it is impossible to obtain a universal constraint w without additional assumptions: the coupling ζ may be smaller, and the local dynamics may differ from the cosmological one. Transfer to equivalence experiments also requires a model of the composition of bodies and possible shielding. [167] [60] [168]

## Degrees of freedom and stability conditions

The restored extension does not yet define a workable theory. What is needed is action, physical variables, and a region of energies in which they can be trusted. For the example of the book, the initial action is general relativity, the canonical scalar field and separately conserved cold matter. With signature −+++ it looks like:

$$S = \int d^4x\sqrt{-g}\left[\frac{M_{\rm Pl}^2}{2}R - \frac{1}{2}g^{\mu\nu}\partial_\mu\phi\partial_\nu\phi - V(\phi)\right] + S_m[g,\psi_m].$$

First, we consider the degrees of freedom of gravity and field, separately from matter. In the spatial decomposition of the metric, six components of the spatial metric and one scalar field give seven configuration variables. The time function and the three shift components act as constraint multipliers. Four first-class constraints, together with coordinate freedom, remove eight out of fourteen phase variables. Three propagating degrees of freedom remain: two tensor polarizations and one scalar. The material sector adds its own disturbances.

This calculation cannot be transferred to an arbitrary action with higher derivatives. Additional terms sometimes introduce new modes, sometimes bound by degeneracy and additional restrictions. Therefore, the study begins with a variation of the full action. If you choose a gauge first and mistakenly lose the constraint equation, the resulting “stable” set of equations may not describe the original theory at all. In case of automatic inference, the preservation of the dynamics constraints should be independently verified.

## What does a quadratic action test?

After eliminating non-dynamic variables, the quadratic action isolates the main part of the equations of small perturbations. For one diagonalized scalar mode ζ, normalization without an additional factor 1/2 is convenient:

$$S_\zeta^{(2)} = \int dt\, d^3x\, a^3 Q_s \left[\dot{\zeta}^2 - \frac{c_s^2}{a^2}(\partial_i\zeta)^2 + \cdots\right].$$

Here the ellipsis includes mass and other less derivative terms, and, in the presence of other dynamic modes, connections with them. The correct sign of the kinetic coefficient $Q_s>0$ and positive $c_s^2$ are required for the propagating mode in the regime under consideration. Negative $Q_s$ means ghost kinetics; negative $c_s^2$ causes a rapid increase in fairly short waves within the range of applicability.

These conditions test for certain dangers, but do not prove nonlinear stability or quantum completeness.

Bellini and Savitsky gave a useful parameterization of the linear dynamics of scalar-tensor models of the Horndesky class. In their notation $Q_s=2M^{*2}D/(2-\alpha_B)^2$, where $D=\alpha_K+3\alpha_B^2/2$. The tensor sector also requires positive kinetics and acceptable propagation speed. Formulas refer to a given class of actions and a selected system of variables. In particular, a variable containing a division by $\dot{\varphi}$ may become unusable when the field is stopped; Its singular coefficient alone does not yet establish a physical catastrophe. [169]

If multiple scalar modes are present, the kinetic matrix K is considered instead of a single $Q_s$, and the gradient terms are given by the matrix G. After correct removal of constraints, K should be positive definite on the physical dynamic modes; the squared velocities are determined by the generalized eigenvalue problem $Gv=c^2Kv$. For ideal dust, zero speed of sound is acceptable and is not equivalent to negative. Its gravitational increase in density must be assessed based on its full dynamics, and not declare each growing mode a pathology.

The negative effective squared mass also requires growth time analysis. Slow evolution on the cosmological scale may be a physical part of the model, while explosive growth in the range used would destroy the chosen background. Therefore, checking the signs should be accompanied by solving equations and comparing characteristic times. Analysis of the short-wavelength main part and analysis of the long-term evolution answer different questions.

## Checking a book's canonical profile

For the Lagrangian $P(X,\varphi)$, where $X=-g^{\mu\nu}\partial\mu\varphi\partial\nu\varphi/2$, the density is equal to $2XPX-P$, and the speed of small scalar perturbations in the local comoving description is determined by the relation below. Such a general class was studied by Garriga and Mukhanov. For $P=X-V$ we obtain the canonical result $c_s^2=1$. [170]

$$c_s^2=\frac{P_X}{P_X+2XP_{XX}}=1\quad(P=X-V).$$

This can be seen directly: the main part of the field perturbation action contains $a^3[(\delta\varphi)^2-(\nabla\delta\varphi)^2/a^2]/2$. In particular, the derivative of the potential does not change the relative sign of these two terms. Gravitational constraints and interaction with matter perturbations remain in the complete problem. This derivation tests the canonical propagating mode and does not replace the integration of the entire cosmological system.

We use the same notation $N=\ln a$, $q=1+w$, $S=\rho_\varphi/(3M_{Pl}^2H_0^2)$, $u=\varphi/M_{Pl}$. In the example $q=0.25$ $\exp[-(N+\ln1.5)^2/(2\times0.2^2)]$, $S(0)=0.7$, $\Omega_{m0}=0.3$. The conservation law implies $S'=-3qS$ and $u'^2=3qS/E^2$, where $E=H/H_0$. On the interval $0\le z\le3$ the profile q is strictly positive; positive S is preserved. Consequently, the reconstructed background kinetic energy $q\rho_\varphi/2$ does not change sign.

In the Bellini-Sawicki parametrization for this minimally coupled canonical field, $\alpha_B=\alpha_M=\alpha_T=0$, and $\alpha_K=\varphi^2/(H^2M_{Pl}^2)=u'^2$. Therefore, their scalar kinetic coefficient takes a particularly simple form:

$$Q_s = \frac{M_{\rm Pl}^2}{2}u'^2 = \frac{3M_{\rm Pl}^2qS}{2E^2} > 0.$$

This is a substitution of the canonical action into a known parameterization, and not a new stability formula. $Q_s$ refers to the scalar sector in this parameterization; the dust remains a separate dynamical system, and its connections with the field must be preserved in the complete equations. The limit of very small q requires care: the field becomes a bad clock, and a variable normalized to its speed may poorly describe the usual small perturbation $\delta\varphi$. Therefore, the numerical code must control the conditioning of the variables and, if necessary, proceed to regular calibration. The smallest $Q_s$ in such a choice of coordinates does not yet determine the scale of the strong coupling of the physical field.

Separately, we calculate the adiabatic derivative $c_a^2=\dot{p}\varphi/\dot{\rho}\varphi$. Substituting $p\varphi=(q-1)\rho_\varphi$ and $\rho_\varphi'=-3q\rho_\varphi$, we obtain by ordinary differentiation:

$$c_a^2 = q - 1 - \frac{q'}{3q} = q - 1 + \frac{N + \ln 1.5}{3(0.2)^2}.$$

This is a ratio of background changes, not a physical speed of propagation. In the numerical check performed for the book, $c_a^2$ varies approximately from −9.1736 to 2.4109 and becomes zero at $z\approx0.36668$. Meanwhile, $c_s^2$ of the canonical mode is equal to unity over the entire interval. Excluding this model only based on the sign of $c_a^2$ would be a mistake: for a scalar field, the connection between pressure and density disturbances depends on the chosen reference frame and contains a nonadiabatic part.

The test used the 24 001 point along N. The independent ratio of the numerical derivatives $p\varphi$ and $\rho_\varphi$ is consistent with the derived $c_a^2$ with the maximum absolute discrepancy being less than $9\times10^{-6}$. The minimum q is about $1.50\times10^{-6}$, the minimum $u'^2$ is $2.25\times10^{-7}$; both are positive. These numbers apply only to the specified interval and parameters. They do not prove the stability of all continuations of the potential or its behavior under large perturbations.

## Application to two different futures

The same control applies to constructing two smooth futures with a common past. Let us keep its notation: $\rho A=\Lambda+Sa^{-3}$, $\rho B=\rho A\exp(-3F)$, $F'=g\geq0$. Here S is the positive dimensional constant of this structure, rather than the normalized density function from the previous example. With positive Λ, S and M for any finite N we obtain:

$$q_A = \frac{Sa^{-3}}{\Lambda + Sa^{-3}} > 0, \qquad q_B = q_A + g(N) > 0, \qquad H_i^2 = \frac{Ma^{-3} + \rho_i}{3M_{\rm Pl}^2} > 0.$$

The densities are positive, so the restored kinetic energies $q_i\rho_i/2$ are also positive. Both actions are canonical, and their scalar principal part has $c_s^2=1$. Consequently, on the selected trajectories there is no defect in the sign of the canonical kinetics and its short-wave gradient term. This is an analytical test using design formulas; Separate numerical integration of disturbances from future models has not been performed here.

For A in the distant future, qA tends to zero. The field, like a clock, becomes a degenerate choice of variable, although this is not yet a physical instability. Tested signs do not rule out all nonlinear

effects and do not establish the admissibility of quantum corrections to the non-analytic coupling of the B potential. Therefore, the statement of different horizons retains the status of a controlled background example with specified limitations, rather than a complete audit of its microscopic origins.

## Where does reliable calculation end?

An effective theory allows a controlled low-energy description without knowing all the microscopic details. Donohue showed how to use this approach to make computable low-energy quantum corrections to gravity. The mere presence of unknown physics at high energies therefore does not prohibit verifiable calculations. But the order of expansion and the magnitude of the discarded terms must be determined. [148]

For a new cosmological action, physical frequencies, H and wave numbers k/a should be compared with the scale of applicability $\Lambda$EFT. It may depend on the background; with weak kinetics, after canonical normalization, the interactions sometimes become stronger. The conditions $H \ll \Lambda EFT$ and $k/a \ll \Lambda EFT$ are useful, but insufficient without checking the coefficients of the operators and the loop expansion. You cannot assign $\Lambda$EFT equal to the Planck mass just because it is already present in the notation.

Radiative stability requires one more step. When adding all allowed interactions, one must calculate corrections to the potential and kinetic terms, determine the protecting symmetry, or honestly specify the setting. For the restored profile, such a calculation was not carried out here. Its microscopic continuation and the full set of connections with matter are not specified, so it is not yet possible to numerically prove the smallness of all quantum corrections. The background reconstruction does not contain this information in a hidden way.

It is useful to require in advance that the result does not depend on the arbitrary precision of the potential interpolation. Its derivatives are included in the dynamics of disturbances and interactions, so almost identical background curves can give different errors in differentiation. Multi-resolution testing and independent derivative recovery should evaluate this specific uncertainty. Their success will confirm the computational implementation, but will not replace the physical verification of the selected action.

The next specific task is to select these connections, derive the quadratic action of the complete system, check its spectrum, and integrate the disturbances over the range used. Then perform the first quantum correction in the explicitly chosen effective theory and estimate the residual error. The report should separate three results: the verified canonical main part, the performed background control and the still open question of radiative stability. This format allows you to build up the proof without presenting one successful graph as a ready-made fundamental theory.

## Redshift drift and parameter freedom

Let's take the same Gaussian profile q(N) and compare it with the cosmological constant. In both initial models, $H_0$=70 km/s/Mpc, $\Omega_{m0}$=0.3 and $\Omega_{\varphi 0}$=0.7; radiation in the interval 0≤z≤3 is not taken into account. For a comoving absorber observed for $\Delta t_0$=20 Julian years, the time-linear approximation gives the spectroscopic equivalent of the velocity change:

$$\Delta v(z) = \frac{c\,\Delta z}{1+z} \simeq cH_0\Delta t_0 \left[1 - \frac{E(z)}{1+z}\right].$$

This is a kinematic consequence of FLRW and the definition of redshift. The value Δv describes a small shift in the spectrum; it is not a change in the Newtonian speed of a distant galaxy. A cosmological model is needed when calculating E(z). Self-accelerations, movement of the observer and changes in the scale of the device are so far excluded from the average signal. [10] [14]

At z=0.5, the model with the cosmological constant gives +5.476 cm/s, the scalar model gives +3.996 cm/s. At z=1 the values are +5.136 and +3.448 cm/s, at z=3 - −4.946 and −5.319 cm/s. The maximum difference modulus at the selected interval is 1.823 cm/s around z=0.777. A nontrivial zero crossing occurs at z≈2.089 for a constant and z≈1.945 for a scalar. All numbers refer to specified parameters and not estimates from observations.

Let's check what part of the difference is preserved after selecting other cosmological parameters. Let's set eight conditional measurements at z=0.25; 0.5; 0.75; 1; 1.5; 2; 2.5; 3. Their averages are equal to the scalar forecast; no random noise is added. Each is assigned an independent error $\sigma_i$=1 cm/s specifically for the difference between the two epochs. Such accuracy and coverage do not follow from the characteristics of a particular device. Initially, they are needed to separate the mathematical distinguishability of the curves from the problem of constructing the installation.

A flat model with a cosmological constant is fitted to the conditional averages. Additionally, we resolve the residual calibration shift B, common to the eight measurements, in units of cm/s. It differs from the dimensionless b in the Gaussian profile. The sum of squares of normalized residuals is minimized:

$$Q(H_0, \Omega_{m0}, B) = \sum_{i=1}^{8} \frac{\left[\Delta v_\phi(z_i) - \Delta v_\Lambda(z_i; H_0, \Omega_{m0}) - B\right]^2}{\sigma_i^2}.$$

If $H_0$=70, $\Omega_{m0}$=0.3 and B=0 are fixed, Q=11.007. After free selection of $H_0$ and $\Omega_{m0}$ with B=0, we obtain Q=0.333; the minimum is located around $H_0$=57.106 km/s/Mpc and $\Omega_{m0}$=0.31760. With free B, the minimum decreases to Q=0.317 with $H_0$≈55.696 km/s/Mpc, $\Omega_{m0}$≈0.32336 and B≈0.246 cm/s. The main part of the original difference is absorbed by the freedom of cosmological parameters. An additional global shift in this particular grid changes the result much less.

Here Q is not the measured statistic $\chi^2$, the probability of detection, or the number of standard deviations. Conditional data contains no random noise, no external constraints on parameters, and no real error covariance. The low $H_0$ found cannot be declared acceptable based on the totality of cosmological observations: such observations were not used at all in this comparison. Adding them would require a joint likelihood function and would change the cost of the compensating adjustment.

One general B also does not cover all spectroscopy errors. Different installations may have individual offsets and wavelength-dependent distortions. If each point is allowed a completely independ-

ent unknown shift, any difference in the means will be absorbed by these free parameters. The next calculation must include physically calibrated covariance, real spectra, and source selection. Comparing only the maximum distance between two fixed curves to design an experiment is not enough.

The numerical result is further verified through two light paths. First, the change in receiver time is integrated, then the condition of equality of the comoving photon path between the same absorber and the observer is solved anew. The calculation is carried out in small scale factor increments to avoid subtracting nearly equal redshifts. For z=0.5 and z=3 of both models, the difference from the linear twenty-year formula is less than $4 \cdot 10^{-8}$ cm/s. This is a check of the calculation and the smallness of the final time step, and not a check of the selected scalar field by nature.

## Profile and local direction of indistinguishability

$$C_{ij} = \sigma^2 \delta_{ij} + \tau^2 u_i u_j, \qquad u_i = \frac{z_i - \bar{z}}{\max_j |z_j - \bar{z}|}, \qquad \tau = 0.5 \text{ cm/s}$$

C is fixed and positive definite for $\sigma > 0$. The random amplitude of the mode u, which is non-uniform in z, has zero mean and Gaussian dispersion $\tau^2$; its integration gives the recorded covariance. The free common shift B is a different parameter: its vector is equal to one, while the sum of the components u is equal to zero. You cannot simultaneously add the same random contribution to C independently and count it again as a separate uncertainty.

$$Q_* = \min_{H_0, \Omega_{m0}, B} \left[ \mathbf{r}^\mathsf{T} C^{-1} \mathbf{r} + \frac{(H_0 - 70)^2}{s_H^2} + \frac{(\Omega_{m0} - 0.3)^2}{s_m^2} + \frac{B^2}{s_B^2} \right], \qquad \mathbf{r} = \mathbf{y} - \mathbf{f}_\Lambda(H_0, \Omega_{m0}) - B\mathbf{1}$$

A member is missing if a corresponding outer constraint is not specified. All three conditional external constraints are assumed to be independent and centered on the input values of the scalar model. Units $s_H$ - km/s/Mpc, $s_B$ - cm/s; $s_m$ is dimensionless. For a fixed $\Omega_{m0}$, the drift depends linearly on $H_0$, so $H_0$ and B are found from weighted linear normal equations with appropriate penalties. Then a one-dimensional search for the minimum was performed using $\Omega_{m0}$. This is the profile of the quadratic functional, not the marginal probability of the model.

$$\mathbf{d} = C^{-1/2}(\mathbf{y} - \mathbf{f}_0), \quad A = C^{-1/2} G, \quad P_\perp = I - AA^+, \quad Q_{\text{lin}} = \mathbf{d}^\mathsf{T} P_\perp \mathbf{d}$$

G contains local derivatives of predictions with respect to the adjusted parameters; $A^+$ is the pseudo-inverse Moore-Penrose matrix. This is the known linear projection after reducing the covariance to unit form. It removes those difference components that are absorbed in the first order by changing parameters. Gaussian external constraints are enabled by adding rows to the residual vector and response matrix. The local result cannot be replaced by a global nonlinear profile. In the tested case of twenty years, $\sigma = 1$ cm/s and without external restrictions $Q_{\text{lin}} = 0.3177280257$, while the nonlinear minimum is equal to 0.3166149159.

## Measurement selection as a separate problem

$$U(d) = \mathbb{E}_{\mathbf{y}|d}[D_{\text{KL}}(p(M \mid \mathbf{y}, d) \,\|\, p(M))]$$

This is the standard Bayesian utility for distinguishing models: d denotes the experimental design, M is the model index, and the expectation is taken from the predictive distribution of possible data averaged across the models and their parameters. We need normalized prior probabilities of models,

parameter distributions, a noise model, and a certain set of plans. Utility taking into account cost should be specified separately. This value has been studied in the experimental design literature; it is not calculated in the attached code. The Q map serves as a preliminary diagnostic and does not replace U(d). [164]

## Why does growth normalization change the conclusion?

In the general theory of relativity for a smooth canonical field and one nonrelativistic component on sufficiently small scales compared to the horizon, the linear increase in the density contrast is described by the equation:

$$D'' + \left(2 + \frac{E'}{E}\right) D' - \frac{3}{2}\Omega_m(N) D = 0.$$

In our simplified comparison, with a=0.01, both models have D=D′=0.01. Emission and scale dependence of massive neutrino transport are not included. For the Gaussian scalar model we get D(1)=0.75127, for the model with a cosmological constant - 0.77898. The ratio is 0.96443. This is the difference in growth with the same early normalization in the stated approximation.

For z=0.5, the forecast ratio fσ₈ is equal to 0.92691, if we keep the general early normalization. If we instead manually equate today's σ₈, the ratio becomes 0.96110. Both operations are mathematically valid, but answer different experimental questions. The first test tests the joint prediction of late growth from early conditions; in the second, part of the difference is removed in advance by renormalization. The equality of early D here serves as an approximate proxy for the overall primary amplitude, and not a full calculation of the transfer of disturbances.

This equation cannot be used without modification for a model in which dark matter exchanges energy with a scalar field. There the background and disturbance equations change. This limitation is especially significant when discussing the dark dimension scenario: the general shape of the expansion graph does not allow the dynamics of another theory to be transferred to it. [63]

## Two smooth futures with a common past

Let's build a separate logical example. The Universe is flat, there is dust and a canonical field; radiation not included. The dust density is M $a^{-3}$. Positive Λ, S and M have the dimension of energy density. Let us choose the general normalization $\varphi_A(0)=\varphi_B(0)=0$. Let us introduce a function that, together with all its derivatives, vanishes in the previous section:

$$g(N) = \begin{cases} 0, & N \le 0, \\ e^{-1/N^2}, & N > 0, \end{cases} \qquad F(N) = \int_0^N g(x)\,dx.$$

Two field densities and two equations of state are given as follows:

$$\rho_A = \Lambda + S e^{-3N}, \qquad \rho_B = \rho_A e^{-3F}, \qquad w_A = -\frac{\Lambda}{\Lambda + S e^{-3N}}, \qquad w_B = w_A + g.$$

The conservation law is satisfied for both models. At each finite N we have 1+w>0, so the trajectory and potential can be restored in the usual way. The term S $a^{-3}$ ensures a non-zero field velocity at the moment of connection, due to which the inverse function N(φ) is smooth. Such a term in the scalar density does not turn its perturbations into dust. [157]

$$\frac{d\phi}{dN} = M_{\rm Pl}\sqrt{3\Omega_\phi(1+w)}, \qquad V = \frac{1-w}{2}\rho, \qquad H^2 = \frac{Me^{-3N}+\rho}{3M_{\rm Pl}^2}.$$

For A we can write the potential explicitly. Let us choose φ(0)=0, denote C=2√[S/(3(M+S))] and $\varphi_\infty = M_{pl}C\ \mathrm{arsinh}\sqrt{[(M+S)/\Lambda]}$. Then:

$$V_A(\phi) = \Lambda + \frac{\Lambda S}{2(M+S)}\sinh^2\left(\frac{\phi_\infty - \phi}{M_{\rm Pl}C}\right).$$

Potential A is analytic and allows continuation through the limiting value of the field. The potential B obtained by the second reconstruction is infinitely differentiable, but is not real analytic at the junction point. This is an essential prerequisite. Two analytic functions in a common connected region could not exactly coincide on an open past interval and then diverge in this way.

For positive N, the integral F has an explicit expression and asymptotic behavior:

$$F = Ne^{-1/N^2} - \sqrt{\pi}\ \mathrm{erfc}(1/N) = N - \sqrt{\pi} + \frac{1}{N} + O(N^{-3}).$$

For model A, the density tends to a positive constant, so its future is asymptotically de-Sitter. At B, the field density behaves as a positive constant multiplied by $a^{-3}$; asymptotically $a \propto t^{2/3}$. The future conformal integral converges in A and diverges in B. It is the asymptotics that establishes the difference between the horizons: a finite numerical graph is not enough for such a conclusion.

The numerical illustration uses Λ=0.699, S=0.001 and M=0.300 in units of today's critical density. With independent control, separate integration of the field equation reproduced the density A with a relative error less than 10−14. For B on two potential grids, the maximum relative error did not exceed 2 × 10−9 in the section 0≤N≤8. Both results are given in the computational kit. The example does not violate the uniqueness of the Cauchy problem: after the connection, different potentials act, that is, different physical models.

The coincidence has been proven for a homogeneous background and linear disturbances with common initial data in a common past section. A finite inhomogeneity can penetrate into the region of differing potentials before the background field. Complete nonlinear, nonperturbative quantum or global observational equivalence has not been proven. Nevertheless, the example shows the exact limit of the inference about the infinite future from the reconstructed past in the indicated approximation.

## An independent test with dependent maps

For a fixed cosmology and topology, we consider together the Gaussian vectors of temperature T and E-polarization with zero averages. Polarization cannot be considered an independent re-realization of the temperature map. Its conditional mean and conditional covariance have the form:

$$\mu_{E|T} = C_{ET} C_{TT}^{-1} T, \qquad \Sigma_{E|T} = C_{EE} - C_{ET} C_{TT}^{-1} C_{TE}.$$

The matrices here should describe the observed data: with a sky mask, instrument noise and appropriate foreground modeling. Temperature data first constrains θ parameters including size, orientation, and cosmological parameters; the polarization forecast is then averaged over the remaining uncertainty:

$$p(E|T) = \int p(E|T,\theta)\, p(\theta|T)\, d\theta.$$

This is the point of testing on another channel: to use it as a prediction of the same model, taking into account general physical information. Substituting a single best orientation may inflate confidence. The book formulates a program for such an analysis for the selected topology, but a new numerical limit on the size of the space is not obtained. [138] [140] [137]

## Phase and noise in gravitational experiment

For two systems with two branches, each difference of four Newtonian energies determines an interaction that can entangle their states. Local phase terms are omitted because they do not change entanglement:

$$E_{ij} = -\frac{G m_A m_B}{r_{ij}}, \qquad g = \frac{E_{LL} + E_{RR} - E_{LR} - E_{RL}}{4\hbar}, \qquad H_{\mathrm{int}} = \hbar g Z_A Z_B.$$

With masses $10^{-14}$ kg and distances $r_{LL}=r_{RR}=450$ μm, $r_{LR}=700$ μm, $r_{RL}=200$ μm, we obtain $|g|\approx 0.0314$ $s^{-1}$. For an initial product of equal superpositions, the ideal measure of entanglement, called negativity, is $|\sin(2gt)|/2$. The first maximum occurs after approximately 25 seconds. This is an assessment of the phase scale of the selected geometry, and not a design of an already operating device. [149]

The noise considered in the materials is given by a separate Markov equation. His convention is essential: the coherence of one qubit decays at a rate of 2γ, not γ.

$$\dot{\rho} = -ig[Z_A Z_B, \rho] + \sum_{j=A,B} \gamma_j (Z_j \rho Z_j - \rho), \qquad \gamma_j = \gamma_{\mathrm{env},j} + \eta |g|.$$

For this dynamics and this initial state, the early appearance of entanglement requires $g^2 > \gamma_A \gamma_B$. If each experiment is allowed a separate unknown background, the different decompositions of the total γ into the usual and hypothetical components may coincide. The non-negativity of the contributions sometimes gives a conservative upper bound for η, but does not itself determine its value. Controlled geometry changes and independent noise calibration are needed. Inference about mediator properties also depends on the explicitly adopted interaction structure and locality. [150] [151] [152]

## Particle scales and additional directions

For wave dark matter, it is necessary to distinguish between the de Broglie length with constant h and the reduced length with $\hbar$. The following expressions define the accepted dimensional estimates; the exact correlation scales depend on the wave distribution:

$$\lambda_{\mathrm{dB}} = \frac{h}{mv}, \qquad \ell_{\mathrm{coh}} = \frac{\hbar}{mv}, \qquad \tau_{\mathrm{coh}} = \frac{\hbar}{mv^2}.$$

For $mc^2=2\cdot10^{-20}$ eV and v=20 km/s, the first two estimates are equal to 30.115 and 4.793 pc. The coefficient 2π changes the comparison of the field scale with the size of the star system. But length alone does not determine its heating: spatially uniform acceleration moves the entire system, therefore, internal heating requires inhomogeneities of force and their temporal correlations. The cosmological fraction of such matter also does not have to automatically equal the fraction at the center of a particular halo. [45]

In a separate example with two equal plane complementary directions, the normalization of the fundamental scale is fixed as follows:

$$M_{\mathrm{Pl}}^2 = (2\pi R)^2 \overline{M}_6^4 = R^2 M_D^4, \qquad M_D = \sqrt{2\pi}\,\overline{M}_6.$$

At $M_D$=10 TeV, the radius is 4.805 μm, and the energy of the first mode is 0.0411 eV. The stellar limit of about 0.6 eV for the first mode considered in the literature in the corresponding two-dimensional case would mean R≤0.329 μm and $M_D$≥38.2 TeV in this convention. Therefore, the original example with 10 TeV is conditionally excluded if the cooling calculation assumptions apply. This conclusion does not automatically transfer to one additional dimension or to arbitrary geometry. [171] [132]

## Why frequency is not a ready-made thermometer

For the selected phase transition acoustic gravitational wave source calibration, the characteristic bubble size and peak frequency are related as follows. Here $v_{\mathrm{wall}}$ is the wall velocity in units of c, $c_s=1/\sqrt{3}$ is the speed of sound in relativistic plasma, $\beta/H_*$ is the inverse transition duration in units of the expansion rate, $g_*$ is the number of effective relativistic degrees of freedom. $T_*$ denotes the temperature after the transition and the associated reheating. The estimate assumes a fast transition $\beta/H_* \gg 1$ and a standard radiative redshift without additional late entropy input. The $z_p$ parameter describes the shape of the spectral peak and is not the cosmological redshift. [54]

$$H_* R_* \simeq (8\pi)^{1/3} \frac{\max(v_{\mathrm{wall}}, c_s)}{\beta/H_*}.$$

$$f_0 \simeq 2.6 \times 10^{-5}\,\mathrm{Hz}\, \frac{T_*}{100\,\mathrm{GeV}} \left(\frac{g_*}{100}\right)^{1/6} \frac{z_p/10}{H_* R_*}.$$

For $v_{\mathrm{wall}}$=0.6, $g_*$=106.75, and $z_p$=10, a transition with $T_*$=100 GeV and $\beta/H_*$=100 produces the same peak near 1.496 mHz as a transition with $T_*$=1000 GeV and $\beta/H_*$=10. A single frequency cannot determine the temperature without constraints on the source dynamics. This example does not calculate the signal amplitude, the lifetime of the acoustic waves, or the detection probability. The next physical step requires a joint calculation of the transition, baryon asymmetry, laboratory constraints, and wave spectrum using one common set of model parameters.

## An illustrative example of gravitational-wave propagation

Only the uniform tensor mode transport from the gravity testing chapter is calculated here. The wavelength is much smaller than the scale of the background change; its speed is c, there is no additional mass and no conversion to other fields. We assume consistent source normalization and the absence of local screening transitions that change the $M_*$ values at the ends of the path. Under these conditions, the envelope is proportional to $1/(aM_*)$, therefore:

$$\Xi(z) = \frac{M_*(0)}{M_*(z)} = \exp\left[\frac{1}{2}\int_0^z \frac{\alpha_M(\tilde{z})}{1+\tilde{z}}\, d\tilde{z}\right].$$

The sign of the integral can be checked without a numerical solver. From $\alpha_M = d \ln M_*^2 / d \ln a$ and $a = 1/(1+z)$ it follows $d \ln M_*/dz = -\alpha_M/[2(1+z)]$. Integration from the source to today's observer gives a positive sign in the expression for $M_*(0)/M_*(z)$. With $\alpha_M = 0$ we obtain $\Xi = 1$; at $z = 0$ the ratio is also equal to one. This check prevents the distance from being confused with its inverse amplitude factor.

For a computational example that does not claim to be a complete theory, we assign $\alpha_M = \alpha_{M0}\, a^s$ for $s > 0$. Then:

$$\Xi(z) = \exp\left\{\frac{\alpha_{M0}}{2s}\left[1 - (1+z)^{-s}\right]\right\}.$$

With $\alpha_{M0} = 0.1$ and $s = 1$ for $z = 0.5$; 1; 2; 3 are obtained accordingly 1.016806; 1.025315; 1.033895; 1.038212. The adaptive quadrature of the original integral reproduces the analytical expression with an absolute discrepancy less than $10^{-13}$. The relative effect at $z = 1$ is equal to approximately 2.53 percent in distance. It is not an estimate of achievable sensitivity: source distribution, orientation error, and instrumentation were not calculated here.

The function $\alpha_M(a)$ does not yet define scalar perturbations, stability and local tests. They require a complete consistent set of equations. In addition, in the shielded models indicated in the main chapter, the value of the amplitude ratio may change or return to unity. Therefore, this result is used as a control of the transport formula and an example of normalization, and not as proof of the existence of an admissible new gravity. Inputs, table and comparison of methods are given in the computational kit.

**Appendix B**

# Research programs

These programs turn the book's questions into a sequence of calculations and measurements. They use published mechanisms and the general method of Chapter 21: define a model in advance, link different observables with common parameters, and name a result that will force the rejection of the version being tested. The current status is listed separately from the next required step.

## Program 1 Dark energy field in space and laboratory

The program develops chapters 3, 8 and 10. We consider a canonical scalar field with a potential $V(\varphi)$ and a linear relationship between the change in the fine structure constant and the field: $\Delta\alpha/\alpha = \zeta\Delta\varphi/M_{Pl}$. One potential, one trajectory and one $\zeta$ coupling must explain the cosmological and laboratory data. The local model is fixed without screening and without compensating changes in other constants. The clock limits the product of coupling and field velocity, so these quantities cannot be separated without additional assumptions. [60]

The frequency ratios of different optical clocks, the spectral lines of distant absorbers, and cosmological distances are physically compared. Repeat spectra of the same absorbers verify the change in redshift; this channel is sensitive to the history of expansion and at $\zeta=0$. For free fall experiments, the scalar charges of the materials are first calculated. They monitor standard drift, magnetic and temperature shifts, and spectra calibration. Competitors include instrument errors and other changing constants. The limit of violation of the equivalence principle is translated into a limitation $\zeta$ through the same interaction model. [61] [172]

The version with the declared potential range and non-zero connection is excluded if the valid areas of all channels do not overlap. For the head profile 8, the potential was restored, the homogeneous dynamics were checked, and the redshift drift was calculated; the last example revealed strong degeneracy with $H_0$ and the matter fraction. The next calculation should combine real spectral errors and external cosmological constraints, connect the local field with the cosmological trajectory and derive the charges of the bodies. There is no joint fitting of observations and protection of low mass field yet. The Gaussian profile is applicable on the stated interval; its exact infinite continuation has the defect described in chapter 8. [59] [62]

The development of the first program is a completed map of the profiled drift divergence under conditional correlated errors and external constraints. It shows the complementarity of independent $H_0$ and calibration. To actually select observations, we still need the instrument model, cost, and testing on random implementations from both cosmologies; they are separate from the performed calculation in the computational appendix.

## Program 2 Expansion, growth and transport of waves

Chapters 3, 8, and 10 examine distance and structure as different consequences of the same dynamic. The version being tested uses general relativity, separately conserved matter, and a canonical field. The primary amplitude and slope are set in a common early epoch; transfer functions are calculated from the matched history. It is impossible to adjust the current amplitude anew for each channel. The smooth field approximation is permissible only where the smallness of its disturbances has been verified, primarily in the corresponding subhorizontal regime.

Spectroscopic surveys measure BAO and the anisotropy of galaxy distributions, galaxy images provide weak lensing, supernovae provide relative distances. The general model predicts each observed signal along with the selection of objects. The constant Λ and specific changes in gravity are compared with it. Nonlinear evolution, baryon feedback, redshift distribution, galaxy-matter coupling, and neutrino mass are taken into account together. Overlapping review volumes require common covariance. [58] [73] [74]

The version is rejected if the range of parameters explaining the distances requires a growth that is inconsistent with the data after matching the initial conditions and noise. The next step is to implement the background and perturbations in one cosmological code and test the remaining sample without new normalization. The book has verified the illustrative background dynamics; There is no complete joint analysis yet. Formulas for separately conserved matter and a smooth field cannot be transferred to the interacting dark sector of the 11 program.

An additional check of the second program is the gravitational wave distance. In the chosen theory, it is derived together with growth and lensing, including wave generation and possible screening. The general parameter area must support all channels. A comparison is not considered a test of one theory if each channel is independently assigned a convenient free function. The conditional transfer example in the appendix only tests the analytic relationship when the background is declared.

## Program 3 One early episode and several statistics

For questions in chapters 11–14, two specific competitors are selected against the general inflationary background. The first contains a brief reduction in the speed of sound disturbance; the time, width and amplitude of the episode are included in the fixed action. The second specifies a Gaussian excited state in a certain scale band with zero initial three-point correlations. Cubic interactions and the subsequent bispectrum are derived from each description. It is unacceptable to independently select the phase of the bispectrum after adjusting the power. These mechanisms have known previous studies. [89] [91] [90]

Using multi-frequency maps of the CMB, temperature and E-polarization power and three-point correlations of different configurations are measured. Instrumental implementation requires control of the beam, polarization angle, noise and galactic radiation. Artificial maps of both models and the smooth base scenario are passed through the same masks and processing. Temperature and polarization are analyzed together; Iterating over the position and width of the feature is included in the significance calibration. Galactic data is added only after nonlinear transport has been calculated.

A non-zero realization is excluded if the parameters explaining the power require a measurable bispectrum that is rejected by the data. The next calculation must first determine whether the selected pair has virtually the same two-point statistics, and then determine the payoff of the remaining observables. The specification has now been prepared, but its discriminability has not been calculated. The preference for the excited state does not yet prove the rebound: for such a conclusion, an independent model of its origin is needed.

The third program adds spatial correlation of μ-distortions with CMB temperature. Two models may have similar average energy released during the decay of small disturbances, and different coupling of long and short modes. First, their total bispectrum and carryover are derived, then spectral clearing, temperature leakage, and total covariance are modeled. The primary mechanism remains the same; The individual amplitudes of each channel cannot be independently assigned after viewing the result.

## Program 4 Topology through conditional polarization forecast

The continuation of chapters 1, 15, and 17 tests a cubic three-dimensional torus with a common side length L, an orientation, and a specified primordial spectrum. These parameters determine the discrete spatial modes and the full temperature-polarization covariance. Temperature data yield a distribution over geometries; the conditional distribution of E-polarization is then calculated given the temperature already measured. Averaging over admissible geometries preserves predictive uncertainty. A single best-fitting orientation cannot replace that distribution. [2] [140]

The measuring material is CMB temperature and polarization maps. The theoretical covariance is carried out through the real beam, pixelation and sky mask; adds noise and correlated clearing errors to both cards. In artificial data, the entire L and orientation search is repeated. Competitors include the non-compact planar model, primary anisotropy, polarization calibration, and permissible physical polarization rotations. Coincident circles are used where the selected geometry actually predicts them. A tensor forecast by itself does not describe the full observed sky.

A particular range of sizes and orientations is ruled out if the required correlation pattern is absent and the test has sufficient power. The next deliverables are a computed covariance with a verified large-L limit and a calibrated conditional polarization test. So far, a protocol has been prepared; no new size bound has been obtained. Non-detection of a pattern too weak to observe does not establish that space is infinite and does not automatically test the other-world scenarios in Chapter 18. Cosmic variance remains even with an ideal instrument. [7]

## Program 5 Two additional directions and a common scale

In chapter 16 a model of two equal flat compact directions with period $2\pi R$ is specified. With the accepted normalization $\bar{M}_{Pl}^2 = R^2 M_D^4$ the radius, the first KK-energy $\hbar c/R$ and the fundamental scale are related. It is also necessary to set the stabilization of the geometry and interaction of the entire tower of states. Illustration $M_D = 10$ TeV gives $R \approx 4.805$ micrometer and first energy about 0.041 eV; it is a calculated point whose viability is tested separately. [128]

A torsion detector with a moving attractor measures the deviation of the force from the Newtonian dependence; the signal is calculated for real body sizes. Surface charges, vibrations and other non-gravitational forces are controlled. The astrophysical channel checks the birth of KK states and the loss of energy by hot matter. The supernova profile, pion interactions, free escape conditions, and possible decays are important here. Competitors to the laboratory effect include new forces without additional dimensions. [129] [132]

The conservative astrophysical requirement of the first KK energy not lower than approximately 0.6 eV translates into $R \lesssim 0.329$ micrometer and $M_D \gtrsim 38.2$ TeV in this normalization. Consequently, the original 10-TeV point is conditionally excluded where the assessment premises apply; you cannot silently replace it with another model. The next calculation is to highlight the jointly permissible range and collapse its force prediction with the installation geometry. Currently only scale translations have been verified. There is no full joint fit, including cooling and stabilization; Decay restrictions require their own model of the population of states. [133] [132] [134]

## Program 6 Gravitational phase and additional loss of coherence

In the program of chapter 19, two masses are prepared in spatial superpositions. One geometry defines the entangling Newtonian interaction g. In the local equation without memory of the dephasing rate $\gamma_i = \gamma_{env,i} + \eta|g|$ for $\eta \geq 0$. The parameter η is common for series with different distances and waiting times. Ordinary noise is specified by the environment model being tested. The competing classical measurement and feedback channel requires a separate output for the selected interferometer. [149] [153]

Measure relative phases, interference contrast, and correlations required to witness entanglement. Control sequences with suppressed gravitational contribution and similar impulses are carried out. Independently limit charges, surface electrical irregularities, magnetic gradients, vibrations, gas and thermal radiation. The electromagnetic channel is capable of creating real entanglement, so it cannot be replaced by additional noise. Interpretation of the result requires explicit assumptions about the locality and properties of the mediator. [150] [151]

Specified dynamics are excluded if the distribution of phases and correlations is inconsistent with the data and controls. With arbitrary independent noise of each series, η is not uniquely restored. However, the non-negativity of $\gamma_{env,i}$ allows us to obtain a conservative upper bound on η from the full dephasing taking into account errors. The next step is to derive the overall noise response and test the discriminability of the models on artificial data. There are now illustrative dynamics and analyzes of this ambiguity; there is no new experimental limit on η.

## Program 7 Self-scattering of matter in galaxies and lenses

Continuing from chapter 6, it is assumed that all dark matter elastically scatters on itself. A well-known two-parameter angular model with normalization $s_0$ and characteristic velocity ω is selected. One scattering law should describe the sparse centers of some halos and the dense centers of others through different evolutions. The masses, concentrations, ages, and baryon histories of objects follow general population distributions; a separate section for each galaxy is not allowed. [43] [42]

Radio interferometry of neutral hydrogen and spatially resolved optical spectroscopy provide velocity fields of small galaxies. Images of highly lensed arcs constrain the masses, profiles, and numbers of perturbing halos. Artificial disturbances are introduced into images to measure detection probability. The competitor is cold, collisionless matter with baryon feedback; both models should be given the same freedom of storytelling. Monitor disc tilt, non-circular motion, primary lens, background source, and structures along the line of sight. [44]

The two-parameter version fails if the common region of $s_0$ and ω does not describe both ensembles or requires a detectable fraction of dense halos that is not present. The next calculation is to calibrate heat transfer and collapse on evolutionary simulations, and then predict the delayed sample. The total, transport and heat transfer sections cannot be replaced with each other. The book contains illustrations of physical scale only; There is no general population analysis of kinematics and lenses yet.

## Program 8 Wave matter from quasars to stars

The second program of the chapter 6 specifies a free ultra-light field interacting gravitationally, and a possible admixture of ordinary cold dark matter. The general parameters are mass m and cos-

mological fraction of the field f. The initial spectrum and transfer functions are calculated in a consistent manner. The local density of the wave component in each halo is derived from the same mixture model; it cannot be independently selected to save any stellar object. Early smoothing of the structure and late dynamics must have the same physical cause.

High-resolution spectrographs measure the transmittance of distant quasars in the Lyman-α forest. Repeated stellar spectroscopy and deep imaging reveal the internal velocities, sizes and ages of old cold systems. Competitors are warm matter and changes in the primary spectrum in the early channel, tides and double stars in the late channel. The thermal history of the gas, ionizing background, metals, initial compactness and orbits are monitored. The overall acceleration of the entire stellar system is not considered its internal heating. [45] [46]

The selected region of m and f is excluded if the parameters satisfying the early data do not allow the observed cold systems to persist under acceptable histories. The next step connects the hydrodynamic prediction of the spectra with the evolution of the wave field, stellar self-gravity and coherent tidal forces. The remaining population is tested, including the selection of objects. So far, only characteristic lengths and frequencies have been calculated: a new joint mass limit has not been obtained. The observational indistinguishability of the weak effect does not support the field.

## Program 9 Two heavy neutrinos and a baryon excess

For chapters 4 and 7, a minimal model of two HNLs with a coupling matrix F and masses $M_1$, $M_2$ is fixed. The heating temperature is pre-selected quite high, then radiation dominance takes effect. The initial HNL populations and asymmetric charges are zero; there is no later dilution by entropy. F and M alone determine light neutrino masses, production of heavy states, decays and baryon yield of $Y_B$. A third HNL or a given previous asymmetry would mean a different hypothesis being tested. [48] [51]

At accelerators, they look for the birth of HNL in the decays of mesons and W, and measure distant vertices, lifetimes, and lepton channels. They are compared with neutrino oscillations and double beta decay without neutrinos. In the latter, light and heavy exchange and their interference are taken into account. Major uncertainties relate to particle production, detector sensing region geometry, vertex reconstruction efficiency, and nuclear matrix elements. The cosmology part additionally tests primordial nucleosynthesis and late decays. [50] [173]

The model is excluded if the observed $Y_B$ interval with the correct sign is not included in the achievable set of laboratory acceptable parameters. The next calculation is to reproduce the control points of matrix quantum kinetics, including coherence, thermal rates, charge redistribution, and sphalerons; then construct the $Y_B$ range at fixed measurable masses and mixings. Kinetics approximations must have an estimated error. A specification of the known mechanism has now been compiled; new scan was not performed. Detection of HNL alone is not enough to reconstruct the origin of a substance.

## Program 10 Singlet transition and common source of CP violation

Another test in Chapter 7 considers the Standard Model extended by one real scalar S, a fixed renormalizable potential, and a CP-violating operator of dimension five that couples S, the Higgs field, and the top quark with coefficient $c_t/\Lambda$. The masses, mixing, and potential coefficients are shared by all calculations. The transition must complete, and the generated charge must survive. The

profile, thickness, and velocity of the bubble wall enter both the particle-transport calculation and the calculation of a possible gravitational-wave source. [52]

The accelerators test the properties of scalars and CP-sensitive correlations of top quarks. Field inversion molecular spectroscopy limits electric dipole and other CP-violating interactions. The frequency offset may depend on several operators, so one EDM limit cannot be applied to an arbitrary combination without recalculation. The gravitational wave spectrum is compared with interferometer noise and astrophysical backgrounds. Competitors include a transition without sufficient baryon output, another source of CP violation, and waves from the hidden sector. [53] [54]

The scenario is rejected if no laboratory permissible completed transition gives the required $Y_B$ without subsequent erasure of the asymmetry and leaving the area of effective theory. The next step is a consistent scan of the potential, bubble birth, walls and quantum transport with the output of all laboratory signals. For waves, the same wall speed is used. So far, only illustrative frequency calibration has been performed, and $Y_B$ has not been calculated. The frequency itself does not determine the temperature; the absence of weak waves does not exclude the entire mechanism.

## Program 11 One radius and interacting dark sector

A bunch of chapters 6, 8, 15 and 16 select a specific implementation of Dark Dimension with one big compact direction. The radius R(u), field potential, KK spectrum and dark matter connections come from the same geometry. In the published example, the potential and mass of dark matter depend exponentially on the field. The variable mass causes an exchange of energy, so the background and disturbances are output together. This is a different object than the two-dimensional torus of program 5. [135] [63]

They measure cosmological distances and structure growth, short-range force in the laboratory, astrophysical energy losses and possible decays. Clocks and free fall are connected if the chosen compactification predicts corresponding bonds with ordinary matter. One set of radius, its field dependence, potential and population of KK states must pass through all channels. Supernova calibrations, baryon feedback, neutrinos, surface forces, and properties of hot stellar matter are monitored. The competitors are unrelated fields and separate new forces.

A constrained implementation is ruled out if there is no general feasible region after accounting for these uncertainties. The next product is an independent implementation of the selected action, the associated background and linear equations, and the power signal of the actual plant. Radius stabilization and applicability require their own verification. A published cosmological analysis exists, but it is not reproduced in the book program. Known results on the stabilization of different geometries cannot simply be glued together into a complete model; the intrinsic connections between field and matter must be preserved in all calculations. [134]

## Program 12 Vacuum gravity without re-setting

The task is to check whether the small gravitational contribution of the vacuum is preserved when the description of matter changes. Two formulations are fixed: general relativity with a given renormalized constant term and the original global model for separating the vacuum contribution of Kaloper and Padilla. They cannot be mixed with later local versions without a new action definition and conditions. The space-time region, boundary conditions, matter fields, and order of quantum correc-

tions are indicated. First, it is checked whether the selected solution allows the required global averaging.

The first calculation adds a constant shift to the Lagrangian of matter and produces a change in the gravitational equation while maintaining the other premises. The second introduces a given phase transition with an explicit history of the vacuum contribution. A mechanism that eliminates a permanent part is not required to eliminate a temporarily changing remainder. Therefore, the expansion reaction is separately calculated and the conservation law is checked. Free parameters are not adjusted again after viewing each result.

The next physical step arises after obtaining a specific H(z) and perturbations: comparison with hot history, distances and structure growth. The useful result is the permissible area of transitions and amendments, or the exact place where the mechanism ceases to perform the stated task. The laboratory cannot change the constant vacuum term of the entire Universe at will. The current status of the program is a consistent comparison; a new calculation of the cosmological phase transition and proof of complete radiative stability have not been performed here.

## Program 13 Two origins of deficiency of small structures

We compare cold dark matter with a modified primordial spectrum and one specific version of warm dark matter with a smooth primordial spectrum. The warm component is specified by its mass, momentum distribution, and density fraction. The primordial modification has a finite set of parameters fixed before the analysis. Both models are fitted to similar spectra of 21-cm inhomogeneities at a selected reference epoch. This creates a meaningful test: the additional channel must distinguish causes that already look similar in the first measurement.

The next step calculates multiple epochs, line-of-sight direction dependence, and admissible nonlinear statistics. Physically, multi-frequency radio maps will be required before the strong influence of stars. The model observations include the antenna frequency pattern, foreground, calibrations, lost modes, and hydrogen thermal history. Many epochs do not guarantee success: if after the reference time both models have the same transfer functions and growth, the additional linear observation may not contain a new difference.

The required product is a map of discriminability in the space of scale, redshift and error, with repeated selection of acceptable competitor parameters. There must also be regions where the inverse problem remains ambiguous. Before transferring to a specific project, the map is translated into requirements for array area, bases, bandwidth and calibration stability. The book calculates the correspondence between frequencies and epochs; joint simulation of the two cosmologies with the instrument remains an open part.

## Program 14 Neutrino medium and its acoustic trace

One microscopic neutrino interaction with given masses and coupling constants is selected. It yields a collision term rather than an arbitrary correction to the CMB spectrum. The competitor is standard free propagation at a similar total density of relativistic particles. If the interaction transfers energy between components or changes the number of particles, this change is included in the background equations and the initial distribution.

Computational verification begins with conservation of energy and proper transition between strongly interacting media and free propagation. The joint temperature and polarization spectra are

then calculated by varying the baryon density, primary spectrum, and calibrations. The physical criterion is a mandatory consistent phase and amplitude structure, which cannot be removed by permitted retuning. A single $N_{eff}$ value does not describe all of these properties.

After the cosmological analysis, we can continue the neutrino distribution to the present day and calculate the capture by tritium, taking into account masses, mixing and local condensation. Energy resolution, beta decay background, and target properties are included in the event model. The result should link early parameters to both channels or show why this link is not clearly defined. The book provides a standard temperature reference and test route; new Boltzmann calculation of the interacting medium and laboratory sensitivity are not declared.

## Program 15 Quantum dynamics and classical competitor

The initial control is already given in the book: quantum and classical systems with a coinciding positive Gaussian distribution in phase space can develop higher moments differently during nonlinear interaction. It checks the code and the meaning of the initial mapping. The open cosmological part begins with one given interaction of inflationary perturbations, a finite initial time, and an explicitly chosen class of classical statistical states.

First, those initial symmetrized correlations that must be identical are coordinated. The subsequent development, including the order of approximation and renormalization, is then calculated using independent methods. For each difference, the observed statistics are indicated: for example, the specific configuration of the bispectrum after transfer to CMB or the distribution of matter. The numerically small quantum contribution is compared with the approximation error and accuracy of the classical integrator before with the accuracy of the instrument.

Physical verification requires a mask model, noise, nonlinear evolution, and possible classical simulators. The classic competitor is allowed only pre-announced freedom. If the difference disappears after taking it into account, the chosen statistic does not solve the problem. If retained, it is the tested family that is excluded; a universal denial of all classical explanations would require another proof. The oscillatory control performed is not a measurement of the quantum origin of the Universe. The purpose of the sequel is to establish whether a similar difference survives physical transfer and realistic observational precision.

## Program 16 History of expansion in gravitational wave transport

Two early post-inflation histories are recorded, valid before the start of the verified hot phase. In one, the selected radiation history begins immediately, in the other there is an intermediate epoch with a certain equation of state and completion mechanism. Both histories must satisfy the constraints of nucleosynthesis and the conservation law. The primary tensor spectrum receives a preliminarily limited family of forms; for an arbitrary spectrum function, the inverse problem may remain unidentifiable.

The wave equations are integrated through transitions with convergence checked, and then today's spectral density is calculated. Pairs of models are matched to a close signal in the same frequency band. The next band and CMB polarization test the prediction of the same set of parameters. Sources such as phase transitions and cosmic strings are considered separately, since they change the very mechanism of wave production.

The physics program includes detector calibration, correlated noise, and residual astrophysical background. Its product is the regions of frequencies and errors where the selected histories necessarily differ, and the regions where a change in the initial spectrum masks them. Such a comparison cannot be replaced with the promise of determining the heating temperature from a single peak. The book has already illustrated the degeneracy of the phase transition frequency; a complete new multi-band analysis remains a challenge.

## Program 17 Information from an evaporating black hole

A specific two-dimensional Jackiv-Teitelboim gravity model is selected, associated with a conformal field and an external reservoir. The action, state, boundary trajectory, connection with the reservoir and the semi-classical approximation mode are fully specified. The first study reproduces the extrema of generalized entropy and the transition between admissible branches. A graph similar to the Page curve is not enough: you need to show the origin of each branch from the same equations.

Then they change one physical element - the initial state or communication mode - and check whether the output is maintained. An independent calculation must distinguish between subsystem entropy, thermal entropy, and the entropy of the entire closed system. The accuracy of the approximation and possible changes in the area that the algorithm assigns to the radiation subsystem are taken into account. The non-smoothness of the approximate minimum of two branches does not in itself mean a physical singularity.

The closest test here is mathematical and computational. A possible laboratory simulation tests the mapping of a selected system onto a model, rather than astrophysical evaporation per se. Transferring the result to a four-dimensional black hole or cosmological horizon requires a separate conclusion. The book explains the theoretical route; new Page curve calculation not performed. A useful extension is a reproducible set of conditions under which the inference is robust, and a precise bound on its applicability.

**Appendix C**

# Computational tasks and reproduction

This appendix distinguishes between performed calculations, method tests, and future studies. For task D1, programs, input data and control values are given. Objectives D2 and D3 remain specifications for studies of early-Universe features and dark matter populations. A ready-made generator, neural network training, or a new physical limit are not announced for them.

## How to reproduce a completed calculation

Launch commands and requirements for the software environment are given in the accompanying instructions for the calculations. Differences in the last decimal places between platforms are acceptable; they must not change the declared test results within the specified tolerance.

## Task D1: specification of the model and input data

The target model is a flat homogeneous cosmology with conserved nonrelativistic matter and a canonical scalar field. The input parameters $H_0 = 70$ km/s/Mpc and $\Omega_{m0} = 0.3$ are specified by the author. The equation of state has the profile $1 + w = A \exp[-(\ln(1 + z) - b)^2/(2s^2)]$, where $A = 0.25$, $s = 0.2$ and $b = \ln(1{,}5)$. The field density follows from the continuity equation. This is an existing calculation example of a book; it is not adjusted to observations.

Vector z is equal to [0.25; 0.5; 0.75; 1; 1.5; 2; 2.5; 3]. The mean drift calculation assumes co-occurring sources and neglects emission at this redshift range. Internal accelerations of absorbing systems are not included. The velocity shift over the interval $\Delta t$ is calculated as $c\Delta t[H_0 - H(z)/(1 + z)]$ with consistent conversion of units. 20 and 40 Julian years are considered. This definition of an average signal is not a model for measuring actual spectral lines.

The independent error $\sigma$ takes the values 0.1; 0.15; 0.2; 0.3; 0.5; 0.7; 1; 1.5 and 2 cm/s. The total covariance is given by $C_{ij} = \sigma^2\delta_{ij} + \tau^2 u_i u_j$, where $\tau = 0.5$ cm/s and u = [−0.76; −0.6; −0.44; −0.28; 0.04; 0.36; 0.68; 1]. The correlated amplitude has zero mean. The free general shift B changes the mean prediction and does not coincide with this mode. When the interval changes, both components of the covariance are artificially preserved.

The competing family is a flat model with a cosmological constant. $H_0$, $\Omega_{m0}$ and B are profiled. In the external conditional constraint $H_0$, the center is always equal to 70 km/s/Mpc, the width sH takes the values 0.2; 0.5; 1; 2; 5; 10 km/s/Mpc or there is no restriction. Nine errors, seven variants $H_0$ and two intervals form 126 lines of the main scan. External assessment is considered to be independent of drift; the applicability of such an assumption to the present data has not been separately examined.

Another 14 lines compare seven combinations of conditional constraints for each interval at $\sigma = 1$ cm/s. The widths used are sH = 1 km/s/Mpc, $s\Omega = 0.01$ and sB = 0.1 cm/s with centers 70; 0.3 and 0. For a fixed $\Omega_{m0}$, the parameters $H_0$ and B are solved linearly. The minimum for $\Omega_{m0}$ is searched using a grid of points 1201 with refinement of the found local minima. The search ranges $H_0$ from 20 to 140 and $\Omega_{m0}$ from 0.01 to 0.99 are numerical delimiters; not a single final minimum reaches them.

## Benchmark results and limits of inference

For twenty years and σ = 1 cm/s without external restrictions, Q = 0.31661491586716844. With the constraint $H_0$ the width 1 results in 1.5650711955566339; with a separate restriction B of the width 0.1, the result is 0.33152500553204495; with both - 3.4200771730750636. When adding all three constraints, Q = 5.694309749083916. These numbers measure the residual divergence of the curves without added noise after adjustment and the addition of conditional penalties. They are not statistical significance, probability of detection, Bayesian evidence, or expected information gain.

A separate three-parameter optimization tests four combinations of constraints: the maximum absolute divergence Q is equal to 9.77 × 10−15. When the correlated mode is turned off, 0.31681625152981635 is obtained. Without external constraints, going from twenty to forty years gives Q40/Q20 = 4 for all nine σ. Throughout the main scan, increasing the constraint H0 does not reduce the minimum. The positive definiteness of C and the coincidence of two realizations of the local linear projection are verified. Nonlinear profile and local projection have different meanings. These checks are specific to this computational example.

With independent control, the scalar field density is recalculated by quadrature over the redshift, and H0, Ωm0 and B are selected jointly. The signal and profile functions from the module being tested are not imported. For seven combinations of constraints of the twenty-year example, the maximum absolute difference Q was 1.42 × 10−14 with the established tolerance 10−8. The report is provided in the computational kit. Implementation agreement verifies the calculation under common physical assumptions; it does not exclude the error of the assumptions themselves.

## Problem D2 and early features

The goal is to find the region of discriminability of two given early mechanisms after they admit a similar power spectrum. The input should be actions or states, initial conditions, acceptable parameters, general transfer to observations, and an error model. It is required to calculate the power spectrum and bispectrum from one set of parameters, then estimate how much difference remains after joint adjustment. Initial control - restoration of the smooth limit when the feature is turned off and independent confirmation of normalizations. The next result is a reproducible region of degeneracy, not just one selected beautiful curve.

The available illustrations of early features can serve as an initial diagnosis of the form, but do not replace the derivation of joint statistics from a particular mechanism. There is no ready-made launch command in the specification, since the complete generator has not yet been created. Completion requires a robust solution to the perturbations, a chosen order of approximation, translation, foregrounds, and joint covariance. You can then test emulation and SBI on separate sets. Success will be determined by a reproducible difference under stated conditions and a calibrated error rate, as well as an explicit indication of the area where there is no difference.

## Problem D3 and the dark matter population

The goal is to test one given self-scattering velocity dependence on several populations, comparing it with a selected model of cold dark matter and astrophysical feedback. Microphysical parameters remain general; formation histories and observation parameters vary among objects within a given hierarchical model. The inputs will be ensembles of simulations, a selection model, measured

characteristics of galaxies and lenses, and error estimates. Training and testing should be separated by objects, stories, and, in a separate trial, by the physical prescriptions of the simulator.

The book so far provides a formulation of this problem. A simple illustration of a density profile is not a sufficient population generator. Independent benchmark implementations, tests of transfer between astrophysical descriptions, and prediction for a delayed population without retuning the general microphysics are needed. A possible meaningful outcome is the discovery of an irremovable disagreement in part of the parameter space or the establishment of remaining degeneracy. A numerical limit on the interaction cross section will require real observations and a validated derivation procedure. Until this point, the result field in the machine-readable task remains blank.

## Three levels of task completion

The first level is a computational standard: fixed inputs, a working command, control results and a certain tolerance. At this level is D1. The second level is checking the output on simulated data: noise implementations of both models, a pre-announced selection rule, error rates, calibration checks and robustness to the specified generator mismatch. This level has yet to be completed for all three tasks. The third level is the physical study: data, hardware characteristics, selection model, and independent tests of main systematic effects.

The transition between levels is accompanied by a new recorded result. The program speedup is taken into account along with the error; expansion of the model - along with a change in the scope of applicability; adding an observation - along with the dependencies of its uncertainties. Lack of discriminability is also a useful answer if it is established for a clearly defined class of models and measurements. This arrangement allows scientists and AI systems to continue working on a single problem ticket, preserving the origin of each output and not attributing capabilities to the precalculation that it does not already have.

## Additional control calculations

An additional program repeats age and distance integrals, scalar potential reconstruction with a separate solution to the field equation, adiabatic derivative testing, simplified linear growth, and physical scale conversions. A computational suite contains inputs, results, and errors. The numbers correspond to the teaching assumptions of Appendix A; there is no complete solution of spatial disturbances and fitting of observations.

A separate program checks the two background reconstructions from chapter 20. For A, an explicit potential is used, for B, a parametric reconstruction on two grids is used. The general past history follows from the definition of the switching function; different horizons - from its analytical asymptotics. The final grid checks the implementation on the selected interval and does not replace these arguments. The results are shown in the computational kit.

Another program calculates an entangling combination of four Newtonian energies, tests for ideal negativity through partial transposition of the density matrix, and several cases of early thresholding under local dephasing. The oscillatory program repeats the oscillatory control of chapter 12. These programs do not describe a complete setup or provide a new experimental constraint.

# Glossary

Entries follow the order of the Russian edition. Latin and Greek abbreviations follow the main terms. Definitions refer to the sense in which concepts are used in the book.

Baryonic asymmetry. The excess of baryons over antibaryons remaining in the Universe. It is convenient to express it relative to the photon density or entropy for a specified thermal history. The explanation must reproduce the magnitude of the excess and its conservation; electrical neutrality of matter does not mean equality of matter and antimatter.

Bispectrum Three-point correlation statistics. For a statistically homogeneous field, the wave vectors of the triple are closed into a triangle. For Gaussian perturbations with mean zero, the bispectrum is equal to zero. A nonzero signal may reflect early interactions or late nonlinear evolution; these sources must be distinguished.

Parameter degeneracy. A situation where different combinations of parameters give the same or similar predictions for selected observations. A more accurate measurement of one combination does not always allow us to determine each value separately. Additional observations with different dependences on parameters and independent calibration help.

Geodetic incompleteness. A property of space-time in which some geodesic does not continue within a given model at a finite value of its natural parameter. For a massive particle, this parameter is its own time. Incompleteness indicates the limit of description, but does not itself determine the physics of the continuation or creation of the world.

Holography. The idea of describing a gravitational system through equivalent degrees of freedom in a lower-dimensional space. The implementations studied relate to certain theories and geometries. They do not prove that the visible world is a projection onto a physical screen, and they do not provide a ready-made description of our Universe.

Event horizon. A causal boundary that separates events from which signals can ever reach the observer from events that will not be available to him in the future. In cosmology, its presence depends on further expansion. Measuring today's acceleration alone is not enough to set such a boundary forever.

Particle horizon. The boundary of the region from which signals could have reached the observer during the accepted past history of the Universe. It is defined by this history of expansion. The particle horizon is not a material wall and does not automatically match the depth of a particular telescopic view.

Gravitational lensing. Changing the directions and shapes of light beams under the influence of gravitational geometry. It allows you to study the distribution of mass, including invisible mass, from images of background objects. Mass recovery requires a lens model and geometry; multiple distributions sometimes produce similar observed effects.

Gravitational waves. Propagating perturbations of gravitational geometry capable of transferring energy and changing the mutual distances of free test bodies. They are created by astrophysical and supposed early cosmic processes. The frequency of the signal depends on the mechanism and subsequent expansion, so it is not a unique thermometer of the era.

Gradient instability. The growth of small spatial disturbances associated with the inappropriate sign of the gradient term in the region of applicability of the theory. Differs from the slow gravitational growth of matter.

Decoherence. Suppression of available interference between quantum alternatives due to their correlations with the environment. For a subsystem, this can make the classical probabilistic picture a good approximation. The process does not require the fundamental disappearance of information from the complete state and does not explain the specialty of the initial conditions.

Redshift drift. Slow change in redshift of a single cosmological source between observation epochs. For an comoving source in FLRW, it relates the rate of expansion at the moments of reception and emission of light. Its isolation requires control of its own accelerations and long-term stability of the spectral calibration.

Inflation. The hypothesized stage of accelerated expansion of the early Universe, during which the comoving Hubble length decreased. Various implementations are capable of creating primary disturbances and explaining the properties of the observed region. Successful predictions do not establish a single field potential or an absolute beginning of existence.

Quantum extremal surface. A surface on which the generalized entropy is stationary in a given gravitational formulation. Its use requires defining the subsystem and the approximation mode.

Compactification. The assumption that spatial directions are closed or have a finite characteristic size and are therefore not perceived as large directions of movement. Their geometry influences the spectrum of available excitations. Small size alone does not guarantee that the model will agree with all experiments.

Cosmic variance. Statistical uncertainty associated with the finite number of available cosmic modes and realizations of the observed field. Eliminating instrument noise does not remove it. Its influence depends on the parameter being measured, the volume being examined, and the sharing of correlated observables.

Cosmological rebound. The transition from compression to expansion, at which the scale factor reaches a non-zero minimum. It requires a certain geometry, matter composition, or changes in gravitational dynamics. The smoothness of a homogeneous solution does not yet prove the stability of the perturbations, full geodesic continuability, or the realism of the rest of the story.

Cosmology. The branch of physics that studies the Universe as a whole: its composition, geometry, expansion, history and origin of structure. Cosmological models connect measurements of different eras by general laws. The observed area does not necessarily coincide with all existing space.

Redshift. An increase in the observed wavelength compared to the length at emission; denoted by z. In cosmological expansion, it is related to the ratio of scale factors between the reception and emission of light. The movement of the source and gravitational effects can also change the observed frequencies.

Page Curve. Dependence of the entropy of the radiation subsystem on time during evaporation in the selected model. Its expected decrease at a later stage is associated with the redistribution of information in the complete system. In a specific calculation, you need to explicitly indicate the subsystem: the entropies of the external bath and the boundary system do not coincide by definition.

Curvature. A property of geometry that expresses deviation from the plane and manifests itself in the relative motion of nearby free bodies. The spatial curvature of the slice and the curvature of spacetime are different. Zero spatial curvature establishes neither the infinity of the world nor the absence of global identifications.

Scale factor. Function a(t), describing the change in distances between participants in the general cosmological expansion. Its absolute normalization is conditional; today's value is taken as one. An increase in the scale factor does not mean an equal expansion of related systems, such as atoms, planetary systems, or galaxies.

Metric. An object that specifies intervals between close events through changes in their coordinates. In space-time, it determines proper time, spatial distances and light directions. Different coordinate records can describe the same metric, so changing formulas does not always mean new physical geometry.

Multiverse. The name of various assumptions about the many cosmic regions or worlds among which ours is located. The scenarios differ in mechanisms, causality, and test status. The cosmological multiverse and the many-worlds interpretation of quantum mechanics are not the same statement.

Neutrino cosmological background. Relic neutrino population of the early hot Universe. Its indirect cosmological traces and the direct capture of individual particles are different measurement tasks.

Generalized entropy. In semiclassical gravity, the sum of the geometric contribution of the area and the consistently renormalized entropy of quantum fields in the chosen formulation.

Inverse problem. Reconstruction of causes, parameters or initial conditions from measured consequences. In cosmology, it requires a description of signal transfer and observational selection. Several models may produce the same data; discrimination requires additional observables or independently justifiable constraints on admissible explanations.

Field potential. A function describing the potential part of the field energy in theory. Its shape affects movement, equilibrium and disturbance properties. Observations limit only the accessible range of dynamics; continuation of the potential to untraveled values requires additional physical prerequisites.

Space-time. General geometric description of events with spatial and temporal coordinates. In the general theory of relativity, its metric depends on matter and energy and determines the movement of free bodies and light. Time differs from spatial directions in its role in causal structure.

Profiling parameters. Minimization of the measure of disagreement with respect to interfering parameters with fixed tested values. Differs from Bayesian averaging in the distribution of parameters.

Radiative stability. Preservation of the declared property of the model while taking into account quantum corrections in the declared scheme without repeated arbitrary adjustment of the parameters at each step.

Dimension. The number of independent coordinates required to locally specify a position in the space under consideration. The usual model of space-time has three spatial and one time coordinates. The large dimension of the space of quantum states does not mean additional physical directions of motion.

Reheating. Transition from the energy of the fields that supported inflation to particles and radiation of the hot stage. The process may include several nonequilibrium stages. Its duration and dynamics influence the relationship between the scale of observations and the time of their origin in the early model.

Free streaming of particles. A regime in which collisions do not have time to maintain local equilibrium at the scale under consideration. The perturbations of such a component differ from the perturbations of a tightly coupled fluid.

Systematic error. Bias or distortion of the result due to instrumentation, calibration, data selection, or inaccuracy of the processing model. Increasing the number of observations does not necessarily eliminate it. Evaluation requires independent testing, response modeling, and benchmark measurements; a common source can link errors from different methods.

Scalar field. A quantity specified by a single number at each point in space-time and transformed as a scalar when changing coordinates. Its dynamics are determined by the kinetic term, potential and interactions. A scalar field can model processes; the name itself does not establish its existence.

Power spectrum. Statistical description of the amplitude of inhomogeneities at different spatial or angular scales. It is associated with point-to-point field correlation and does not determine the specific location of objects. Different mechanisms can produce similar power, but differ in higher order correlations.

Spin temperature. Parameter of the ratio of populations of two hyperfine levels of the ground state of hydrogen. Does not have to coincide with the kinetic temperature of the gas or the temperature of the cosmic microwave background radiation.

Standard candle. A source whose absolute luminosity can be estimated or standardized by attributes. Comparing this luminosity with the resulting flux gives the distance. The method requires calibration, taking into account absorption, selection of objects and the possible evolution of their properties; a candle is not the same lamp.

Standard siren. A source of gravitational waves for which the signal shape allows one to estimate the luminosity distance for a given propagation theory. Measuring expansion usually also requires redshift. Accuracy is limited by system orientation, calibration, host galaxy selection, and selection of detected events.

Statistical significance. A characteristic of how unusual the result obtained is given a given hypothesis being tested and a statistical model. It is not equal to the probability of the new theory being true. Interpretation is influenced by noise assumptions, analysis options, biases, and the set of explanations being compared.

Hubble sphere. A surface with a characteristic radius c/H in a homogeneous expanding model, where the cosmological receding velocity is equal to the speed of light. Its position is determined by the current expansion rate. It is not a universal causal horizon: the possibility of receiving a signal also depends on subsequent evolution.

Dark matter. A component whose presence in the standard cosmological interpretation is inferred from the gravitational influence on motion, lensing and structure growth. Its microscopic nature has not been established. A negative result of the search for one particle limits the corresponding model, and not automatically any explanation to dark matter.

Dark energy. The component that accounts for the late acceleration of expansion in the standard gravitational description. They can serve as a cosmological constant or a dynamic system of fields. Conclusions about properties depend on the adopted geometry, the composition of the Universe and the law of gravity.

Dark Ages. The period after the formation of neutral atoms and before the significant influence of the first luminous objects. The exact boundaries depend on the history of the sources' formation.

Topology. The global structure of space: its connectivity, closed paths and identification of points. The same local curvature allows different topologies. A compact space may have a finite volume without a physical edge; it does not require the outer room in which it is located.

Equation of state. Relationship between pressure, density and other characteristics of a component. The book uses the parameter w - the ratio of pressure to energy density. For the cosmological constant $w = -1$, for nonrelativistic dust - 0. The effective value recovered by dividing the interacting components differently may differ from each field's own parameter.

Falsification. A test in which the prediction of a hypothesis may be confronted with an observational result that is inconsistent with it under the given conditions. Probabilistic models require criteria and uncertainties. The absence of a signal refutes those versions that required its detection at the achieved sensitivity.

Frequency comb. A light source with many precisely related spectral lines. When linked to an atomic frequency standard, it serves as a calibration tool for the spectrograph. The presence of a comb alone does not eliminate all errors: light transfer, detector response, and instrument changes between observations must be taken into account.

Emulator. Fast computational approximation to a given physical solver. Its error relative to the solver and the error of the physical description itself are assessed separately.

Entropy. A quantitative characteristic of a state, the definition of which depends on the description used: macrostate, quantum density matrix, subsystem or horizon. These quantities cannot be automatically identified. The entropy of a closed quantum state is preserved during unitary evolution, while the entropy of a selected subsystem can change.

Effective field theory. Description of physical processes in a limited range of energies and scales, taking into account the influence of inaccessible parts through permissible interactions. Its predictions require verification of the range of applicability. A successful effective theory does not have to remain true at any energy.

BAO—baryon acoustic oscillations. Traces of sound waves of early plasma in the spatial distribution of matter. The characteristic scale is used as a standard ruler for measuring geometry and extension. Its physical length is calculated from early history, so absolute calibration requires assumptions about the composition and dynamics of the Universe.

BBN - primordial nucleosynthesis. Formation of light nuclei in the first minutes of hot history. Calculations relate the amounts of deuterium, helium and other light elements to the density of ordinary matter, nuclear reactions and the rate of expansion. Observational verification requires taking into account subsequent stellar processing and systematic errors.

CMB - cosmic microwave background radiation. Radiation retained from the hot early Universe and reaching us after matter became sufficiently transparent. Its spectrum, temperature inhomogeneities and polarization carry various information. The observed pattern contains both primary disturbances and the consequences of subsequent evolution.

CP symmetry. The joint symmetry of the replacement of particles by antiparticles, denoted C, and spatial reflection P. Its violation means the difference in the corresponding processes. It is part of the usual conditions for the dynamic creation of baryon asymmetry, but the magnitude of the observed effect and its cosmological effectiveness depend on the specific mechanism.

EDM—electric dipole moment. Characteristics of separation of positive and negative electrical charge. The constant moment of an elementary particle along its spin is sensitive to the violation of spatial reflection and time reversal. Experiments with particles, atoms and molecules limit the interactions, but translating the result into parameters requires a microscopic model.

HNL is a heavy neutral lepton. A hypothetical neutral fermion, heavier than light neutrinos and capable of interacting through mixing with them. In some models, such particles explain the neutrino masses and participate in the creation of baryon asymmetry. The discovery of a particle does not yet confirm the cosmological mechanism.

$H_0$ is the Hubble constant. The current value of the cosmological expansion rate H. For nearby objects, it relates the distance to the cosmological part of the recession velocity after taking into account proper motions. Typically expressed in kilometers per second per megaparsec; the name does not imply that H is constant over time.

KK - Kaluza-Klein modes. A set of excitations arising when the field is expanded in an additional compact direction. In an effective description with fewer dimensions, modes appear as particles with different masses. Their spectrum and interactions depend on geometry, boundary conditions and theory.

SBI. Simulation-based inference - restoration of parameter distributions or comparison of models using simulations. Robustness depends on training models, statistics, inference procedures, and calibration checks.

$S_8$ is the matter-clustering amplitude. The combination $S_8 = \sigma_8\sqrt{(\Omega_m/0.3)}$ used when comparing structure measurements. Here $\Omega_m$ is the current fraction of matter, and $\sigma_8$ characterizes the root-mean-square linear density fluctuations in spheres of radius 8/h megaparsecs; h specifies $H_0$ in units of 100 kilometers per second per megaparsec. This is a model parameter.

ΛCDM. Basic cosmological model including the cosmological constant Λ, cold dark matter, ordinary matter and radiation. The abbreviation CDM stands for cold dark matter. The analysis specifies the geometry, initial disturbances, and a set of free parameters; extensions of the model may change the conclusions.

μ–T correlation. Statistical connection of the spatial map of μ-distortion of the spectrum with temperature inhomogeneities of the cosmic microwave background radiation. In given models, it is sensitive to the coupling of long and short primary modes.

# References

Sources are listed in order of first reference. Numbers in the text lead to the corresponding entries.

[1] Tamara M. Davis; Charles H. Lineweaver. Expanding Confusion: common misconceptions of cosmological horizons and the superluminal expansion of the Universe. 2004. https://doi.org/10.1071/AS03040. https://arxiv.org/abs/astro-ph/0310808

[2] Planck Collaboration. Planck 2015 results. XVIII. Background geometry & topology. 2016. https://arxiv.org/abs/1502.01593

[3] Chris Clarkson; Bruce A. Bassett; Teresa Hui-Ching Lu. A general test of the Copernican Principle. Physical Review Letters 101, 011301 (2008). https://doi.org/10.1103/PhysRevLett.101.011301. https://arxiv.org/abs/0712.3457

[4] David W. Hogg. Distance measures in cosmology. 2000. Preprint. https://arxiv.org/abs/astro-ph/9905116

[5] D. J. Fixsen. The Temperature of the Cosmic Microwave Background. 2009. https://doi.org/10.1088/0004-637X/707/2/916. https://arxiv.org/abs/0911.1955

[6] Planck Collaboration. Planck 2018 results. VI. Cosmological parameters. Astronomy & Astrophysics 641, A6 (2020). https://doi.org/10.1051/0004-6361/201833910. https://arxiv.org/abs/1807.06209

[7] Douglas Scott; Dagoberto Contreras; Ali Narimani; Yin-Zhe Ma. The information content of cosmic microwave background anisotropies. JCAP 06 (2016) 046. https://doi.org/10.1088/1475-7516/2016/06/046. https://arxiv.org/abs/1603.03550

[8] DESI Collaboration. DESI DR2 Results II: Measurements of Baryon Acoustic Oscillations and Cosmological Constraints. Physical Review D 112, 083515 (2025). https://doi.org/10.1103/tr6y-kpc6. https://arxiv.org/abs/2503.14738

[9] S. Blondin et al. Time Dilation in Type Ia Supernova Spectra at High Redshift. 2008. https://doi.org/10.1086/589568. https://arxiv.org/abs/0804.3595

[10] Abraham Loeb. Direct Measurement of Cosmological Parameters from the Cosmic Deceleration of Extragalactic Objects. 1998. https://doi.org/10.1086/311375. https://arxiv.org/abs/astro-ph/9802122

[11] European Southern Observatory. ANDES instrument for the Extremely Large Telescope. Official description of the project; verified 9 November 2026. https://elt.eso.org/instrument/ANDES/

[12] ANDES Consortium; INAF. ANDES Calibration Unit. Official description of the project; verified 9 November 2026. https://andes.inaf.it/calibration-unit/

[13] A. Trost; C. M. J. Marques; S. Cristiani et al. The ESPRESSO Redshift Drift Experiment III — The Third Epoch of QSO J052915.80-435152.0. arXiv:2603.02318 (2026); accepted into Astronomy & Astrophysics. https://arxiv.org/abs/2603.02318

[14] J. Liske; A. Grazian; E. Vanzella et al. Cosmic dynamics in the era of Extremely Large Telescopes. Monthly Notices of the Royal Astronomical Society 386, 1192–1218 (2008). https://doi.org/10.1111/j.1365-2966.2008.13090.x. https://arxiv.org/abs/0802.1532

[15] P. Noterdaeme; P. Petitjean; R. Srianand; C. Ledoux; S. Lopez. The evolution of the Cosmic Microwave Background Temperature: Measurements of TCMB at high redshift from carbon monoxide excitation. 2011. https://doi.org/10.1051/0004-6361/201016140. https://arxiv.org/abs/1012.3164

[16] B. D. Fields; P. Molaro; S. Sarkar. Big Bang Nucleosynthesis. In: Review of Particle Physics 2025. https://pdg.lbl.gov/2025/reviews/rpp2025-rev-bbang-nucleosynthesis.pdf

[17] Ryan Cooke; Max Pettini; Charles C. Steidel. One Percent Determination of the Primordial Deuterium Abundance. 2018. https://doi.org/10.3847/1538-4357/aaab53. https://arxiv.org/abs/1710.11129

[18] Julien Froustey; Cyril Pitrou; Maria Cristina Volpe. Neutrino decoupling including flavour oscillations and primordial nucleosynthesis. Journal of Cosmology and Astroparticle Physics 12, 015 (2020). https://doi.org/10.1088/1475-7516/2020/12/015. https://arxiv.org/abs/2008.01074

[19] Sergei Bashinsky; Uros Seljak. Signatures of Relativistic Neutrinos in CMB Anisotropy and Matter Clustering. Physical Review D 69, 083002 (2004). https://doi.org/10.1103/PhysRevD.69.083002. https://arxiv.org/abs/astro-ph/0310198

[20] Brent Follin; Lloyd Knox; Marius Millea; Zhen Pan. A First Detection of the Acoustic Oscillation Phase Shift Expected from the Cosmic Neutrino Background. Physical Review Letters 115, 091301 (2015). https://doi.org/10.1103/PhysRevLett.115.091301. https://arxiv.org/abs/1503.07863

[21] Francis-Yan Cyr-Racine; Kris Sigurdson. Limits on Neutrino-Neutrino Scattering in the Early Universe. Physical Review D 90, 123533 (2014). https://doi.org/10.1103/PhysRevD.90.123533. https://arxiv.org/abs/1306.1536

[22] David Camarena; Francis-Yan Cyr-Racine. Strong constraints on a simple self-interacting neutrino cosmology. Physical Review D 111, 023504 (2025). https://doi.org/10.1103/PhysRevD.111.023504. https://arxiv.org/abs/2403.05496

[23] Andrew J. Long; Cecilia Lunardini; Eray Sabancilar. Detecting non-relativistic cosmic neutrinos by capture on tritium: phenomenology and physics potential. Journal of Cosmology and Astroparticle Physics 08, 038 (2014). https://doi.org/10.1088/1475-7516/2014/08/038. https://arxiv.org/abs/1405.7654

[24] PTOLEMY Collaboration; M. G. Betti et al. Neutrino physics with the PTOLEMY project: active neutrino properties and the light sterile case. Journal of Cosmology and Astroparticle Physics 07, 047 (2019). https://doi.org/10.1088/1475-7516/2019/07/047. https://arxiv.org/abs/1902.05508

[25] PTOLEMY Collaboration / Laboratori Nazionali del Gran Sasso, INFN. The Experimental Challenges. Official page of PTOLEMY; verified 8 November 2026. https://ptolemy.lngs.infn.it/the-experimental-challenges/

[26] V. Mossa et al. LUNA Collaboration. The baryon density of the Universe from an improved rate of deuterium burning. 2020. https://doi.org/10.1038/s41586-020-2878-4.

[27] A. Kogut et al. The Primordial Inflation Explorer (PIXIE): A Nulling Polarimeter for Cosmic Microwave Background Observations. 2011. https://doi.org/10.1088/1475-7516/2011/07/025. https://arxiv.org/abs/1105.2044

[28] Abraham Loeb; Matias Zaldarriaga. Measuring the Small-Scale Power Spectrum of Cosmic Density Fluctuations Through 21 cm Tomography Prior to the Epoch of Structure Formation. Physical Review Letters 92, 211301 (2004). https://doi.org/10.1103/PhysRevLett.92.211301. https://arxiv.org/abs/astro-ph/0312134

[29] Antony Lewis; Anthony Challinor. The 21cm angular-power spectrum from the dark ages. Physical Review D 76, 083005 (2007). https://doi.org/10.1103/PhysRevD.76.083005. https://arxiv.org/abs/astro-ph/0702600

[30] Rajesh Mondal; Rennan Barkana. Prospects for precision cosmology with the 21 cm signal from the dark ages. Nature Astronomy 7, 1025–1030 (2023). https://doi.org/10.1038/s41550-023-02057-y. https://arxiv.org/abs/2305.08593

[31] Yacine Ali-Haïmoud; P. Daniel Meerburg; Sihan Yuan. A new light on 21 cm intensity fluctuations from the dark ages. Physical Review D 89, 083506 (2014). https://doi.org/10.1103/PhysRevD.89.083506. https://arxiv.org/abs/1312.4948

[32] Julian B. Muñoz; Yacine Ali-Haïmoud; Marc Kamionkowski. Primordial non-gaussianity from the bispectrum of 21-cm fluctuations in the dark ages. Physical Review D 92, 083508 (2015). https://doi.org/10.1103/PhysRevD.92.083508. https://arxiv.org/abs/1506.04152

[33] Paul Bode; Jeremiah P. Ostriker; Neil Turok. Halo Formation in Warm Dark Matter Models. Astrophysical Journal 556, 93–107 (2001). https://doi.org/10.1086/321541. https://arxiv.org/abs/astro-ph/0010389

[34] UC Berkeley Space Sciences Laboratory. LuSEE-Night. Official project page; verified 8 November 2026. https://www.ssl.berkeley.edu/projects/lusee-night/

[35] Stuart D. Bale et al. LuSEE 'Night': The Lunar Surface Electromagnetics Experiment. arXiv:2301.10345 (2023); paper presented at URSI GASS 2023. https://doi.org/10.48550/arXiv.2301.10345. https://arxiv.org/abs/2301.10345

[36] Adrian Liu; Aaron R. Parsons; Cathryn M. Trott. The Epoch of Reionization Window: I. Mathematical Formalism. Physical Review D 90, 023018 (2014). https://doi.org/10.1103/PhysRevD.90.023018. https://arxiv.org/abs/1404.2596

[37] Douglas Clowe; Marusa Bradač; Anthony H. Gonzalez; Maxim Markevitch; Scott W. Randall; Christine Jones; Dennis Zaritsky. A direct empirical proof of the existence of dark matter. Astrophysical Journal Letters 648, L109–L113 (2006). https://doi.org/10.1086/508162. https://arxiv.org/abs/astro-ph/0608407

[38] J. Aalbers et al. (LZ Collaboration). Dark Matter Search Results from 4.2 Tonne-Years of Exposure of the LUX-ZEPLIN (LZ) Experiment. 2025. https://doi.org/10.1103/4dyc-z8zf. https://arxiv.org/abs/2410.17036

[39] G. Carosi et al. (ADMX Collaboration). Search for Axion Dark Matter from 1.1 to 1.3 GHz with ADMX. 2025. https://doi.org/10.1103/d7mg-6sqq. https://arxiv.org/abs/2504.07279

[40] Daniel C. Brotherton et al. (ALPS II). Any Light Particle Searches with ALPS II: first science results. 2026. https://doi.org/10.1103/61sw-k3bc. https://arxiv.org/abs/2512.14110

[41] D. S. Akerib et al. (LZ Collaboration). Searches for Light Dark Matter and Evidence of Coherent Elastic Neutrino-Nucleus Scattering of Solar Neutrinos with the LUX-ZEPLIN (LZ) Experiment. 2026. https://doi.org/10.1103/jvqf-njpj. https://arxiv.org/abs/2512.08065

[42] Ethan O. Nadler; Daneng Yang; Hai-Bo Yu. A Self-interacting Dark Matter Solution to the Extreme Diversity of Low-mass Halo Properties. 2023. https://doi.org/10.3847/2041-8213/ad0e09. https://arxiv.org/abs/2306.01830

[43] Zixiang Jia; Fangzhou Jiang; Shubo Li; Ran Li; Jing Wang; Ling Zhu. An Enhanced Isothermal Jeans Approach to Constraining Dark Matter Self-Interactions from Galactic Kinematics. 2026. The version used was arXiv v2 from 3 November 2026, section 4.2 and conclusion. https://doi.org/10.1093/mnras/stag969. https://arxiv.org/abs/2601.17118

[44] Alexandres Lazar et al. A dark matter profile to model diverse feedback-induced core sizes of ΛCDM haloes. 2020. https://doi.org/10.1093/mnras/staa2101. https://arxiv.org/abs/2004.10817

[45] Keir K. Rogers; Hiranya V. Peiris. Strong bound on canonical ultra-light axion dark matter from the Lyman-alpha forest. 2021. https://doi.org/10.1103/PhysRevLett.126.071302. https://arxiv.org/abs/2007.12705

[46] Andrew Eberhardt; Mateja Gosenca; Lam Hui. Heating and scattering of stellar distributions by ultralight dark matter. 2026. https://doi.org/10.1103/zngx-f8pz. https://arxiv.org/abs/2510.17079

[47] A. D. Sakharov. Violation of CP invariance, C asymmetry, and baryon asymmetry of the universe. JETP Letters 5, 24–27 (1967); Russian original Pisma ZhETF 5, 32–35 (1967); reprint UFN 161(5), 61–64 (1991). https://www.ufn.ru/ru/articles/1991/5/h/

[48] E. Kh. Akhmedov; V. A. Rubakov; A. Yu. Smirnov. Baryogenesis via neutrino oscillations. Physical Review Letters 81, 1359–1362 (1998). https://doi.org/10.1103/PhysRevLett.81.1359. https://arxiv.org/abs/hep-ph/9803255

[49] M. D'Onofrio; K. Rummukainen; A. Tranberg. The Sphaleron Rate in the Minimal Standard Model. Physical Review Letters 113, 141602 (2014). https://doi.org/10.1103/PhysRevLett.113.141602. https://arxiv.org/abs/1404.3565

[50] ATLAS Collaboration. Search for heavy neutral leptons in decays of W bosons using leptonic and semi-leptonic displaced vertices in sqrt(s)=13 TeV pp collisions with the ATLAS detector. Journal of High Energy Physics 07 (2025) 196. https://doi.org/10.1007/JHEP07(2025)196. https://arxiv.org/abs/2503.16213

[51] J. de Vries; M. Drewes; Y. Georis; J. Klarić; V. Plakkot. Confronting the low-scale seesaw and leptogenesis with neutrinoless double beta decay. Journal of High Energy Physics 05 (2025) 090. https://doi.org/10.1007/JHEP05(2025)090. https://arxiv.org/abs/2407.10560

[52] J. Ellis; M. Lewicki; M. Merchand; J. M. No; M. Zych. The scalar singlet extension of the Standard Model: gravitational waves versus baryogenesis. Journal of High Energy Physics 01 (2023) 093. https://doi.org/10.1007/JHEP01(2023)093. https://arxiv.org/abs/2210.16305

[53] T. S. Roussy et al. An improved bound on the electron's electric dipole moment. Science 381, 46–50 (2023). https://doi.org/10.1126/science.adg4084. https://arxiv.org/abs/2212.11841

[54] C. Caprini et al.; LISA Cosmology Working Group. Detecting gravitational waves from cosmological phase transitions with LISA: an update. Journal of Cosmology and Astroparticle Physics 03 (2020) 024. https://doi.org/10.1088/1475-7516/2020/03/024. https://arxiv.org/abs/1910.13125

[55] D. E. Kaplan; M. A. Luty; K. M. Zurek. Asymmetric dark matter. Physical Review D 79, 115016 (2009). https://doi.org/10.1103/PhysRevD.79.115016. https://arxiv.org/abs/0901.4117

[56] Adam G. Riess et al. Observational Evidence from Supernovae for an Accelerating Universe and a Cosmological Constant. Astronomical Journal 116, 1009–1038 (1998). https://doi.org/10.1086/300499. https://arxiv.org/abs/astro-ph/9805201

[57] DESI Collaboration. DESI DR2 Results IV: Alcock-Paczynski Measurements from the Lyman Alpha Forest and Cosmological Constraints. 2026. Preprint. https://arxiv.org/abs/2607.27410

[58] DES Collaboration. Constraints on Dynamical Dark Energy from Multiple Probes in the Full Dark Energy Survey. 2026. Preprint. https://arxiv.org/abs/2605.27221

[59] Y. Park; M. Raveri; B. Jain. Reconstructing quintessence. Physical Review D 103, 103530. https://arxiv.org/abs/2101.04666

[60] P. P. Avelino. Avoiding unrealistic priors: the case of dark energy constraints from the time variation of the fine-structure constant. Physical Review D 93, 083501. https://arxiv.org/abs/1602.04501

[61] T. Damour; J. F. Donoghue. Equivalence Principle Violations and Couplings of a Light Dilaton. Physical Review D 82, 084033. https://arxiv.org/abs/1007.2792

[62] S. M. Carroll. Quintessence and the Rest of the World: Suppressing Long-Range Interactions. Physical Review Letters 81, 3067 (1998). https://doi.org/10.1103/PhysRevLett.81.3067. https://arxiv.org/abs/astro-ph/9806099

[63] A. Bedroya; G. Obied; C. Vafa; D. H. Wu. Evolving dark sector and the dark dimension scenario. Physical Review D 114, 103506, published 4 November 2026; DOI 10.1103/1rsq-cv2m. https://journals.aps.org/prd/abstract/10.1103/1rsq-cv2m

[64] Stephen P. Martin. Two-loop effective potential for a general renormalizable theory and softly broken supersymmetry. Physical Review D 65, 116003 (2002). https://doi.org/10.1103/PhysRevD.65.116003. https://arxiv.org/abs/hep-ph/0111209v2

[65] R. L. Jaffe. The Casimir Effect and the Quantum Vacuum. Physical Review D 72, 021301 (2005). https://doi.org/10.1103/PhysRevD.72.021301. https://arxiv.org/abs/hep-th/0503158

[66] Nemanja Kaloper; Antonio Padilla. Sequestering the Standard Model Vacuum Energy. Physical Review Letters 112, 091304 (2014). https://doi.org/10.1103/PhysRevLett.112.091304. https://arxiv.org/abs/1309.6562v2

[67] Nemanja Kaloper; Antonio Padilla; David Stefanyszyn; George Zahariade. A Manifestly Local Theory of Vacuum Energy Sequestering. Physical Review Letters 116, 051302 (2016). https://doi.org/10.1103/PhysRevLett.116.051302. https://arxiv.org/abs/1505.01492v2

[68] $H_0$DN Collaboration. The Local Distance Network: a community consensus report on the measurement of the Hubble constant at 1% precision. A&A 708, A166 (2026). https://doi.org/10.1051/0004-6361/202557993. https://arxiv.org/abs/2510.23823

[69] Wendy L. Freedman et al. Status Report on the Chicago-Carnegie Hubble Program (CCHP): Measurement of the Hubble Constant Using the Hubble and James Webb Space Telescopes. 2025. https://doi.org/10.3847/1538-4357/adce78. https://arxiv.org/abs/2408.06153

[70] TDCOSMO Collaboration. TDCOSMO 2026: A 3% measurement of the Hubble constant from strong lensing and stellar kinematics. 2026. Preprint. https://arxiv.org/abs/2610.14781

[71] George Efstathiou. Evolving Dark Energy or Supernovae Systematics? MNRAS 538(2), 875 (2025). https://arxiv.org/abs/2408.07175

[72] M. Vincenzi et al. (DES Collaboration). Comparing the DES-SN5YR and Pantheon+ SN cosmology analyses: Investigation based on Evolving Dark Energy or Supernovae systematics? MNRAS 541(3), 2585 (2025). https://arxiv.org/abs/2501.06664

[73] DES Collaboration. Dark Energy Survey Year 6 Results: Cosmological Constraints from Galaxy Clustering and Weak Lensing. 2026. https://doi.org/10.1103/nnlj-gyr2. https://arxiv.org/abs/2601.14559

[74] Angus H. Wright et al. KiDS-Legacy: Cosmological constraints from cosmic shear with the complete Kilo-Degree Survey. 2025. https://doi.org/10.1051/0004-6361/202554908. https://arxiv.org/abs/2503.19441

[75] Jay R. Krishnan; Kevork N. Abazajian. Statistics meet systematics: Resolution of the massive early JWST galaxy tension. Physical Review D 113, 083007 (2026). https://doi.org/10.1103/gjf5-3r89.

[76] Leonardo Comini; Sunny Vagnozzi; Abraham Loeb. Dark energy, spatial curvature, and star formation efficiency from JWST photometric and spectroscopic high-redshift galaxies. Journal of High Energy Astrophysics 53, 100626 (2026). https://doi.org/10.1016/j.jheap.2026.100626. https://arxiv.org/abs/2604.13866

[77] Enis Belgacem; Yves Dirian; Stefano Foffa; Michele Maggiore. Modified gravitational-wave propagation and standard sirens. Physical Review D 98, 023510 (2018). https://doi.org/10.1103/PhysRevD.98.023510. https://arxiv.org/abs/1805.08731

[78] LIGO Scientific Collaboration; Virgo Collaboration; Fermi Gamma-Ray Burst Monitor; INTEGRAL. Gravitational Waves and Gamma-rays from a Binary Neutron Star Merger: GW170817 and GRB 170817A. The Astrophysical Journal Letters 848, L13 (2017). https://doi.org/10.3847/2041-8213/aa920c. https://arxiv.org/abs/1710.05834

[79] Macarena Lagos; Maya Fishbach; Philippe Landry; Daniel E. Holz. Standard sirens with a running Planck mass. Physical Review D 99, 083504 (2019). https://doi.org/10.1103/PhysRevD.99.083504.

[80] Charles Dalang; Lucas Lombriser. Limitations on Standard Sirens tests of gravity from screening. Journal of Cosmology and Astroparticle Physics 10, 013 (2019). https://doi.org/10.1088/1475-7516/2019/10/013. https://arxiv.org/abs/1906.12333

[81] Charles Dalang; Pierre Fleury; Lucas Lombriser. Horndeski gravity and standard sirens. Physical Review D 102, 044036 (2020). https://doi.org/10.1103/PhysRevD.102.044036. https://arxiv.org/abs/1912.06117

[82] B. P. Abbott et al. A gravitational-wave standard siren measurement of the Hubble constant. 2017. https://arxiv.org/abs/1710.05835

[83] Alan H. Guth. Inflationary universe: A possible solution to the horizon and flatness problems. 1981. https://doi.org/10.1103/PhysRevD.23.347.

[84] James M. Bardeen; Paul J. Steinhardt; Michael S. Turner. Spontaneous creation of almost scale-free density perturbations in an inflationary universe. 1983. https://doi.org/10.1103/PhysRevD.28.679.

[85] Planck Collaboration. Planck 2018 results. X. Constraints on inflation. 2020. https://doi.org/10.1051/0004-6361/201833887. https://arxiv.org/abs/1807.06211

[86] Thibaut Louis et al.; ACT Collaboration. The Atacama Cosmology Telescope: DR6 Power Spectra, Likelihoods and LambdaCDM Parameters. The arXiv entry indicates acceptance into JCAP. https://arxiv.org/abs/2503.14452

[87] BICEP/Keck Collaboration. BICEP/Keck XIII: Improved Constraints on Primordial Gravitational Waves using Planck, WMAP, and BICEP/Keck Observations through the 2018 Observing Season. 2021. https://doi.org/10.1103/PhysRevLett.127.151301. https://arxiv.org/abs/2110.00483

[88] Planck Collaboration. Planck 2018 results. IX. Constraints on primordial non-Gaussianity. Astronomy & Astrophysics 641, A9 (2020). https://doi.org/10.1051/0004-6361/201935891. https://arxiv.org/abs/1905.05697

[89] Ana Achucarro; Jinn-Ouk Gong; Gonzalo A. Palma; Subodh P. Patil. Correlating features in the primordial spectra. Physical Review D 87, 121301 (2013). https://doi.org/10.1103/PhysRevD.87.121301. https://arxiv.org/abs/1211.5619

[90] Ana Achucarro; Vicente Atal; Pablo Ortiz; Jesus Torrado. Localized correlated features in the CMB power spectrum and primordial bispectrum from a transient reduction in the speed of sound. Physical Review D 89, 103006 (2014). https://doi.org/10.1103/PhysRevD.89.103006. https://arxiv.org/abs/1311.2552

[91] R. Holman; Andrew J. Tolley. Enhanced Non-Gaussianity from Excited Initial States. JCAP 05 (2008) 001. https://doi.org/10.1088/1475-7516/2008/05/001. https://arxiv.org/abs/0710.1302

[92] Latham A. Boyle; Paul J. Steinhardt. Probing the early universe with inflationary gravitational waves. Physical Review D 77, 063504 (2008). https://doi.org/10.1103/PhysRevD.77.063504. https://arxiv.org/abs/astro-ph/0512014

[93] Yuki Watanabe; Eiichiro Komatsu. Improved Calculation of the Primordial Gravitational Wave Spectrum in the Standard Model. Physical Review D 73, 123515 (2006). https://doi.org/10.1103/PhysRevD.73.123515. https://arxiv.org/abs/astro-ph/0604176

[94] Sachiko Kuroyanagi; Christophe Ringeval; Tomo Takahashi. Early Universe Tomography with CMB and Gravitational Waves. Physical Review D 87, 083502 (2013). https://doi.org/10.1103/PhysRevD.87.083502. https://arxiv.org/abs/1301.1778

[95] David Polarski; Alexei A. Starobinsky. Semiclassicality and Decoherence of Cosmological Perturbations. Classical and Quantum Gravity 13, 377–392 (1996); version v2 used. https://doi.org/10.1088/0264-9381/13/3/006. https://arxiv.org/abs/gr-qc/9504030v2

[96] Jérôme Martin; Vincent Vennin. Quantum Discord of Cosmic Inflation: Can we Show that CMB Anisotropies are of Quantum-Mechanical Origin? Physical Review D 93, 023505 (2016). https://doi.org/10.1103/PhysRevD.93.023505. https://arxiv.org/abs/1510.04038

[97] Elliot Nelson. Quantum Decoherence During Inflation from Gravitational Nonlinearities. Journal of Cosmology and Astroparticle Physics 03 (2016) 022. https://doi.org/10.1088/1475-7516/2016/03/022. https://arxiv.org/abs/1601.03734

[98] J. E. Moyal. Quantum mechanics as a statistical theory. Mathematical Proceedings of the Cambridge Philosophical Society 45(1), 99–124 (1949). https://doi.org/10.1017/S0305004100000487.

[99] Daniel Green; Rafael A. Porto. Signals of a Quantum Universe. Physical Review Letters 124, 251302 (2020). https://doi.org/10.1103/PhysRevLett.124.251302. https://arxiv.org/abs/2001.09149

[100] Guillermo Ballesteros; Jesús Gambín Egea; Alejandro Pérez Rodríguez. Classical and quantum evolution of inflationary fluctuations. 2026. https://doi.org/10.1103/w7y3-gxbr. https://arxiv.org/abs/2604.18416v2

[101] Juan Maldacena. A model with cosmological Bell inequalities. Fortschritte der Physik (2016), first online 2015. https://doi.org/10.1002/prop.201500097. https://arxiv.org/abs/1508.01082

[102] Arvind Borde; Alan H. Guth; Alexander Vilenkin. Inflationary Spacetimes Are Incomplete in Past Directions. Physical Review Letters 90, 151301 (2003). https://doi.org/10.1103/PhysRevLett.90.151301. https://arxiv.org/abs/gr-qc/0110012

[103] Abhay Ashtekar; Tomasz Pawlowski; Parampreet Singh. Quantum Nature of the Big Bang: Improved dynamics. Physical Review D 74, 084003 (2006). https://doi.org/10.1103/PhysRevD.74.084003. https://arxiv.org/abs/gr-qc/0607039

[104] Jerome Quintin; Zeinab Sherkatghanad; Yi-Fu Cai; Robert H. Brandenberger. Evolution of cosmological perturbations and the production of non-Gaussianities through a nonsingular bounce: Indications for a no-go theorem in single field matter bounce cosmologies. Physical Review D 92, 063532 (2015). https://doi.org/10.1103/PhysRevD.92.063532. https://arxiv.org/abs/1508.04141

[105] James B. Hartle; Stephen W. Hawking. Wave function of the Universe. Physical Review D 28, 2960 (1983). https://doi.org/10.1103/PhysRevD.28.2960.

[106] David Wallace. Gravity, Entropy, and Cosmology: In Search of Clarity. 2010. https://doi.org/10.1093/bjps/axp048. https://arxiv.org/abs/0907.0659

[107] Sean M. Carroll; Heywood Tam. Unitary Evolution and Cosmological Fine-Tuning. 2010. Preprint. https://doi.org/10.48550/arXiv.1007.1417. https://arxiv.org/abs/1007.1417

[108] Wojciech H. Zurek. Pointer basis of quantum apparatus: Into what mixture does the wave packet collapse? 1981. https://doi.org/10.1103/PhysRevD.24.1516.

[109] Ali Nayeri. Inflationary branch decoherence and the cosmological arrow of time. Physical Review D 113, 126030 (2026). https://doi.org/10.1103/1k1w-c7vd. https://arxiv.org/abs/2602.21263

[110] G. W. Gibbons; S. W. Hawking. Cosmological event horizons, thermodynamics, and particle creation. Physical Review D 15, 2738 (1977). https://doi.org/10.1103/PhysRevD.15.2738.

[111] D. J. Fixsen; E. S. Cheng; J. M. Gales; J. C. Mather; R. A. Shafer; E. L. Wright. The Cosmic Microwave Background Spectrum from the Full COBE/FIRAS Data Set. 1996. https://doi.org/10.1086/178173. https://arxiv.org/abs/astro-ph/9605054

[112] Jens Chluba; Adrienne L. Erickcek; Ido Ben-Dayan. Probing the inflaton: Small-scale power spectrum constraints from measurements of the Cosmic Microwave Background energy spectrum. 2012. https://doi.org/10.1088/0004-637X/758/2/76. https://arxiv.org/abs/1203.2681

[113] Enrico Pajer; Matias Zaldarriaga. A New Window on Primordial non-Gaussianity. Physical Review Letters 109, 021302 (2012). https://doi.org/10.1103/PhysRevLett.109.021302. https://arxiv.org/abs/1201.5375

[114] Mathieu Remazeilles; Jens Chluba. Extracting foreground-obscured μ-distortion anisotropies to constrain primordial non-Gaussianity. Monthly Notices of the Royal Astronomical Society 478, 807–824 (2018). https://doi.org/10.1093/mnras/sty1034. https://arxiv.org/abs/1802.10101

[115] Mathieu Remazeilles; Andrea Ravenni; Jens Chluba. Leverage on small-scale primordial non-Gaussianity through cross-correlations between CMB E-mode and μ-distortion anisotropies. Monthly Notices of the Royal Astronomical Society 512, 455–470 (2022). https://doi.org/10.1093/mnras/stac519. https://arxiv.org/abs/2110.14664

[116] Maldacena, J. M. The Large N Limit of Superconformal Field Theories and Supergravity. Advances in Theoretical and Mathematical Physics 2, 231–252 (1998) (1999). https://doi.org/10.1023/A:1026654312961. https://arxiv.org/abs/hep-th/9711200

[117] Tadashi Takayanagi. Emergent Holographic Spacetime from Quantum Information. Physical Review Letters 134, 240001 (2025). https://arxiv.org/abs/2506.06595

[118] Shinsei Ryu; Tadashi Takayanagi. Holographic Derivation of Entanglement Entropy from the anti–de Sitter Space/Conformal Field Theory Correspondence. Physical Review Letters 96, 181602 (2006). https://doi.org/10.1103/PhysRevLett.96.181602. https://arxiv.org/abs/hep-th/0603001

[119] Mark Van Raamsdonk. Building up spacetime with quantum entanglement. General Relativity and Gravitation 42, 2323–2329 (2010). https://doi.org/10.1007/s10714-010-1034-0. https://arxiv.org/abs/1005.3035

[120] S. W. Hawking. Particle creation by black holes. Communications in Mathematical Physics 43, 199–220 (1975). https://doi.org/10.1007/BF02345020.

[121] Don N. Page. Average Entropy of a Subsystem. Physical Review Letters 71, 1291–1294 (1993). https://doi.org/10.1103/PhysRevLett.71.1291. https://arxiv.org/abs/gr-qc/9305007v2

[122] Netta Engelhardt; Aron C. Wall. Quantum Extremal Surfaces: Holographic Entanglement Entropy beyond the Classical Regime. Journal of High Energy Physics 01 (2015) 073. https://doi.org/10.1007/JHEP01(2015)073. https://arxiv.org/abs/1408.3203v3

[123] Ahmed Almheiri; Netta Engelhardt; Donald Marolf; Henry Maxfield. The entropy of bulk quantum fields and the entanglement wedge of an evaporating black hole. Journal of High Energy Physics 12 (2019) 063. https://doi.org/10.1007/JHEP12(2019)063. https://arxiv.org/abs/1905.08762v3

[124] Geoffrey Penington. Entanglement Wedge Reconstruction and the Information Paradox. 2020. https://arxiv.org/abs/1905.08255v3

[125] Jafferis, D. et al. Traversable wormhole dynamics on a quantum processor. Nature 612, 51–55 (2022). https://doi.org/10.1038/s41586-022-05424-3.

[126] Kobrin, B.; Schuster, T.; Yao, N. Y. Experiments implementing small commuting models lack gravitational features. Nature 643, E17–E19 (2025). https://doi.org/10.1038/s41586-025-08939-7.

[127] Jafferis, D. et al. Reply to: Experiments implementing small commuting models lack gravitational features. Nature 643, E20–E23 (2025). https://doi.org/10.1038/s41586-025-08995-z.

[128] Arkani-Hamed, N.; Dimopoulos, S.; Dvali, G. The Hierarchy Problem and New Dimensions at a Millimeter. Physics Letters B 429, 263–272 (1998). https://doi.org/10.1016/S0370-2693(98)00466-3. https://arxiv.org/abs/hep-ph/9803315

[129] Lee, J. G.; Adelberger, E. G.; Cook, T. S.; Fleischer, S. M.; Heckel, B. R. New Test of the Gravitational $1/r^2$ Law at Separations down to 52 μm. Physical Review Letters 124, 101101 (2020). https://doi.org/10.1103/PhysRevLett.124.101101. https://arxiv.org/abs/2002.11761

[130] ATLAS Collaboration. Search for new phenomena in events with an energetic jet and missing transverse momentum in pp collisions at sqrt(s)=13 TeV with the ATLAS detector. Physical Review D 103, 112006 (2021). https://doi.org/10.1103/PhysRevD.103.112006. https://arxiv.org/abs/2102.10874

[131] CMS Collaboration. Search for new physics in the final state with a single photon and large missing transverse momentum in proton-proton collisions at sqrt(s)=13 TeV. Physical Review D 113, 072020 (2026). https://doi.org/10.1103/f9r8-styj. https://arxiv.org/abs/2511.17310

[132] E. Hardy; A. Sokolov; H. Stubbs. Stellar cooling limits on KK gravitons and dark dimensions. JHEP 03 (2026) 029; preprint arXiv:2510.18975v2 (2025). https://arxiv.org/abs/2510.18975

[133] S. Hannestad; G. G. Raffelt. Supernova and neutron-star limits on large extra dimensions reexamined. Physical Review D 67, 125008; erratum 69, 029901; author's version corrected 2 April 2025 (2003). https://doi.org/10.1103/PhysRevD.67.125008. https://arxiv.org/abs/hep-ph/0304029

[134] A. P. Braun; M. Cicoli; R. Milioli; R. Valandro. Moduli stabilisation for ADD and the Dark Dimension scenario. JHEP 10 (2026) 112, published October 9, 2026. https://link.springer.com/article/10.1007/JHEP10(2026)112

[135] M. Montero; C. Vafa; I. Valenzuela. The dark dimension and the Swampland. JHEP 02 (2023) 022. https://arxiv.org/abs/2205.12293

[136] Neil J. Cornish; David N. Spergel; Glenn D. Starkman. Circles in the Sky: Finding Topology with the Microwave Background Radiation. Classical and Quantum Gravity 15, 2657–2670 (1998). https://doi.org/10.1088/0264-9381/15/9/013. https://arxiv.org/abs/astro-ph/9801212

[137] Johannes R. Eskilt et al.; COMPACT Collaboration. Cosmic topology. Part IIa. Eigenmodes, correlation matrices, and detectability of orientable Euclidean manifolds. JCAP 03 (2024) 036. https://doi.org/10.1088/1475-7516/2024/03/036. https://arxiv.org/abs/2306.17112

[138] Yashar Akrami et al.; COMPACT Collaboration. Promise of Future Searches for Cosmic Topology. Physical Review Letters 132, 171501 (2024). https://doi.org/10.1103/PhysRevLett.132.171501. https://arxiv.org/abs/2210.11426

[139] Wayne Hu; Martin White. CMB Anisotropies: Total Angular Momentum Method. Physical Review D 56, 596–615 (1997). https://doi.org/10.1103/PhysRevD.56.596. https://arxiv.org/abs/astro-ph/9702170

[140] Amirhossein Samandar et al. (COMPACT Collaboration). Cosmic topology. Part IIIb. Eigenmodes and correlation matrices of spin-2 perturbations in orientable Euclidean manifolds. JCAP 08 (2025) 015. https://doi.org/10.1088/1475-7516/2025/08/015. https://arxiv.org/abs/2503.08671

[141] Hugh Everett III. “Relative State” Formulation of Quantum Mechanics. Reviews of Modern Physics 29, 454–462 (1957). https://doi.org/10.1103/RevModPhys.29.454.

[142] Wojciech H. Zurek. Environment-induced superselection rules. Physical Review D 26, 1862 (1982). https://doi.org/10.1103/PhysRevD.26.1862.

[143] Andrei D. Linde. Eternally existing self-reproducing chaotic inflationary universe. Physics Letters B 175, 395–400 (1986). https://doi.org/10.1016/0370-2693(86)90611-8.

[144] Alan H. Guth. Eternal inflation and its implications. Journal of Physics A 40, 6811–6826 (2007). https://doi.org/10.1088/1751-8113/40/25/S25. https://arxiv.org/abs/hep-th/0702178

[145] Alan H. Guth; Vitaly Vanchurin. Eternal Inflation, Global Time Cutoff Measures, and a Probability Paradox. 2011. Preprint. https://arxiv.org/abs/1108.0665

[146] Stephen M. Feeney; Matthew C. Johnson; Daniel J. Mortlock; Hiranya V. Peiris. First Observational Tests of Eternal Inflation: Analysis Methods and WMAP 7-Year Results. Physical Review D 84, 043507 (2011). https://doi.org/10.1103/PhysRevD.84.043507. https://arxiv.org/abs/1012.3667

[147] Stephen M. Feeney; Franz Elsner; Matthew C. Johnson; Hiranya V. Peiris. Forecasting constraints from the cosmic microwave background on eternal inflation. Physical Review D 92, 083515 (2015). https://doi.org/10.1103/PhysRevD.92.083515. https://arxiv.org/abs/1506.01716

[148] John F. Donoghue. General relativity as an effective field theory: The leading quantum corrections. Physical Review D 50, 3874–3888 (1994). https://doi.org/10.1103/PhysRevD.50.3874. https://arxiv.org/abs/gr-qc/9405057

[149] Bose, S. et al. A Spin Entanglement Witness for Quantum Gravity. Physical Review Letters 119, 240401 (2017). https://doi.org/10.1103/PhysRevLett.119.240401. https://arxiv.org/abs/1707.06050

[150] A. Di Biagio. Gravity-induced entanglement is not a theory-independent witness of nonclassicality of the gravitational field. Physical Review D 114, 084050 (2026). https://doi.org/10.1103/r8ry-sp35. https://arxiv.org/abs/2511.02683

[151] Tianfeng Feng; Vlatko Vedral; Chiara Marletto. Collapse-based models for gravity do not violate the entanglement-based witness of non-classicality. Physical Review D 113, 104055 (2026). https://doi.org/10.1103/83rl-nygv. https://arxiv.org/abs/2503.19774

[152] Nicolas Boulle; Guilherme Franzmann. Subsystems independence in gravitationally induced entanglement proposals. Physical Review D 114, 025015 (2026). https://journals.aps.org/prd/abstract/10.1103/tgjx-y7hl

[153] Kafri, D.; Taylor, J. M.; Milburn, G. J. A classical channel model for gravitational decoherence. New Journal of Physics 16, 065020 (2014). https://doi.org/10.1088/1367-2630/16/6/065020. https://arxiv.org/abs/1401.0946

[154] Lawrence M. Krauss; Michael S. Turner. Geometry and Destiny. General Relativity and Gravitation 31, 1453–1459 (1999). https://doi.org/10.1023/A:1026757718530. https://arxiv.org/abs/astro-ph/9904020

[155] Robert R. Caldwell; Marc Kamionkowski; Nevin N. Weinberg. Phantom Energy: Dark Energy with $w < -1$ Causes a Cosmic Doomsday. 2003. https://doi.org/10.1103/PhysRevLett.91.071301. https://arxiv.org/abs/astro-ph/0302506

[156] Eric V. Linder. Exploring the Expansion History of the Universe. Physical Review Letters 90, 091301 (2003). https://doi.org/10.1103/PhysRevLett.90.091301. https://arxiv.org/abs/astro-ph/0208512

[157] A. A. Starobinsky. How to determine an effective potential for a variable cosmological term. JETP Letters 68, 757–763 (1998). https://doi.org/10.1134/1.567941.

[158] M. Martinelli et al.; Euclid Collaboration. Euclid: constraining dark energy coupled to electromagnetism using astrophysical and laboratory data. Astronomy & Astrophysics 654, A148 (2021). https://arxiv.org/abs/2105.09746

[159] Kyle Cranmer; Johann Brehmer; Gilles Louppe. The frontier of simulation-based inference. Proceedings of the National Academy of Sciences 117, 30055–30062 (2020). https://doi.org/10.1073/pnas.1912789117. https://arxiv.org/abs/1911.01429

[160] H. T. Jense; I. Harrison; E. Calabrese; A. Spurio Mancini; B. Bolliet; J. Dunkley; J. C. Hill. A complete framework for cosmological emulation and inference with CosmoPower. arXiv:2405.07903v1 (2024); used for methodological discussion. https://arxiv.org/abs/2405.07903

[161] Francisco Villaescusa-Navarro; Daniel Anglés-Alcázar; Shy Genel et al. The CAMELS project: Cosmology and Astrophysics with MachinE Learning Simulations. The Astrophysical Journal 915, 71 (2021). https://doi.org/10.3847/1538-4357/abf7ba. https://arxiv.org/abs/2010.00619

[162] Sean Talts; Michael Betancourt; Daniel Simpson; Aki Vehtari; Andrew Gelman. Validating Bayesian Inference Algorithms with Simulation-Based Calibration. arXiv:1804.06788v2, corrected 21 October 2020. https://arxiv.org/abs/1804.06788

[163] Toka Alokda; Cristiano Porciani; Alexander Eggemeier. Coverage is not enough: Frequentist tests of simulation-based inference for primordial non-Gaussianity. Astronomy & Astrophysics 714, A66 (2026). https://doi.org/10.1051/0004-6361/202660668. https://arxiv.org/abs/2605.00980

[164] Adam Foster; Martin Jankowiak; Eli Bingham; Paul Horsfall; Yee Whye Teh; Tom Rainforth; Noah Goodman. Variational Bayesian Optimal Experimental Design. Advances in Neural Information Processing Systems 32 (2019); arXiv:1903.05480v3. https://arxiv.org/abs/1903.05480

[165] Joseph Tooby-Smith. HepLean: Digitalising high energy physics. arXiv:2405.08863v1 (2024); the author's version was used. https://arxiv.org/abs/2405.08863

[166] Jordan Meadows; Lan Zhang; Andre Freitas. FormalScience: Scalable Human-in-the-Loop Autoformalisation of Science with Agentic Code Generation in Lean. ACL 2026; arXiv:2604.23002v1. https://arxiv.org/abs/2604.23002

[167] M. Filzinger et al. Improved limits on the coupling of ultralight bosonic dark matter to photons from optical atomic clock comparisons. Physical Review Letters 130, 253001 (2023). https://doi.org/10.1103/PhysRevLett.130.253001. https://arxiv.org/abs/2301.03433

[168] G. Dvali; M. Zaldarriaga. Changing alpha with time: implications for fifth-force-type experiments and quintessence. Physical Review Letters 88, 091303. https://arxiv.org/abs/hep-ph/0108217

[169] Emilio Bellini; Ignacy Sawicki. Maximal freedom at minimum cost: linear large-scale structure in general modifications of gravity. Journal of Cosmology and Astroparticle Physics 07 (2014) 050. https://doi.org/10.1088/1475-7516/2014/07/050. https://arxiv.org/abs/1404.3713v3

[170] Jaume Garriga; V. F. Mukhanov. Perturbations in k-inflation. Physics Letters B 458, 219–225 (1999). https://doi.org/10.1016/S0370-2693(99)00602-4. https://arxiv.org/abs/hep-th/9904176

[171] Particle Data Group; Y. Gershtein and A. Pomarol (section authors). Extra Dimensions, Review of Particle Physics 2025. 2025. https://pdg.lbl.gov/2025/reviews/rpp2025-rev-extra-dimensions.pdf

[172] MICROSCOPE Collaboration; P. Touboul et al. MICROSCOPE Mission: Final Results of the Test of the Equivalence Principle. Physical Review Letters 129, 121102. https://arxiv.org/abs/2209.15487

[173] KamLAND-Zen Collaboration; S. Abe et al. Search for Majorana Neutrinos with the Complete KamLAND-Zen Dataset. Physical Review Letters 135, 262501 (2025). https://doi.org/10.1103/jkf6-48j8. https://arxiv.org/abs/2406.11438

# Author and projects

Email: info@brenev.com

Author website: brenev.com

Mira website: mira.technology

Other projects: haraizen.tech

Telegram: https://t.me/Eudgenee